

Electronic Thesis and Dissertation Repository

8-12-2011 12:00 AM

Design and Syntheses of Novel Quenchers for Fluorescent Hybridization Probes

Mohamed Moustafa
The University of Western Ontario

Supervisor
Prof. Robert Hudson
The University of Western Ontario

Graduate Program in Chemistry
A thesis submitted in partial fulfillment of the requirements for the degree in Doctor of Philosophy
© Mohamed Moustafa 2011

Follow this and additional works at: <https://ir.lib.uwo.ca/etd>

 Part of the [Nucleic Acids, Nucleotides, and Nucleosides Commons](#)

Recommended Citation

Moustafa, Mohamed, "Design and Syntheses of Novel Quenchers for Fluorescent Hybridization Probes" (2011). *Electronic Thesis and Dissertation Repository*. 259.
<https://ir.lib.uwo.ca/etd/259>

This Dissertation/Thesis is brought to you for free and open access by Scholarship@Western. It has been accepted for inclusion in Electronic Thesis and Dissertation Repository by an authorized administrator of Scholarship@Western. For more information, please contact wlsadmin@uwo.ca.

DESIGN AND SYNTHESSES OF NOVEL QUENCHERS FOR FLUORESCENT
HYBRIDIZATION PROBES

(Spine title: Design and Syntheses of Novel Quenchers for Fluorescent Hybridization
Probes)

(Thesis format: Monograph)

by

Mohamed E. Moustafa

Graduate Program in Chemistry

A thesis submitted in partial fulfillment
of the requirements for the degree of
Doctor of Philosophy

The School of Graduate and Postdoctoral Studies
The University of Western Ontario
London, Ontario, Canada

© Mohamed Moustafa 2011

THE UNIVERSITY OF WESTERN ONTARIO
School of Graduate and Postdoctoral Studies

CERTIFICATE OF EXAMINATION

Supervisor

Examiners

Dr. Robert H.E. Hudson

Dr. Kim Baines

Supervisory Committee

Dr. Michael Kerr

Dr. Kim Baines

Dr. Brian Shilton

Dr. Michael Kerr

Dr. Ibrahim M. Abdou

The thesis by

Mohamed El-sayed Moustafa

entitled:

**Design and Syntheses of Novel Quenchers for Fluorescent
Hybridization Probes**

is accepted in partial fulfillment of the
requirements for the degree of
Doctor of Philosophy

Date

Chair of the Thesis Examination Board

Abstract

Since most of human diseases are related to genetic mutations, during the past two decades, identification of such mutations has attracted much attention. Detection of these mutations is mainly based on hybridization with the complementary reporter probes.

Nucleic acid detection takes place by changing either the reporter's fluorescence intensity or the colour of its fluorescence. The use of fluorescent probes for nucleic acid detection has attracted much attention due to its efficiency, the ease of synthesis and availability of commercial reporters that facilitate the probe synthesis. Nowadays, most of nucleic acid detection using fluorescent probes relies on quenching of fluorescence by energy transfer from one fluorophore to another or to a nonfluorescent molecule (quencher). The most common, widely used, quencher in fluorescent probes is 4-(*N,N*-dimethylamino)azobenzene-4'-carboxylic acid (DABCYL).

The goal of this thesis was to introduce new quenchers which structurally mimic the universal quencher DABCYL into peptide nucleic acid (PNA), DNA and RNA probes. These quenchers are also characterized by their ability to undergo photoisomerization upon illumination with light.

Chapter 2 describes the synthesis of a novel azobenzene-PNA quencher; incorporation of the PNA quencher into PNA-molecular beacon probe and demonstration of efficient quenching ability upon hybridization with the complementary DNA sequence.

Chapter 3 describes the synthesis of a new modified azo-based uracil PNA monomer and evaluation of its quenching ability by incorporation of the PNA monomer in a dual peptide sequence that is amenable to enzymatic degradation. The modified azo-based uracil moiety has shown the ability to quench the fluorescein emission; upon enzymatic cleavage of the peptide, fluorescent signal was recovered.

Chapter 4, based on the proven quenching ability of the modified azo-based uracil, this modification was introduced into deoxyribo- and ribonucleosides. The photoisomerization and halochromic behavior has been investigated on the synthesized compounds.

The advantages of this nucleobase modification are: 1) introduction of novel quencher, 2) potential duplex stabilization by retaining the ability of formation of hydrogen bond between the modified nucleobase and the complementary nucleobase, 3) potential photoregulation ability of azo-based modified nucleobase containing oligomers with responding to incident light.

Chapter 5 describes the synthesis of modified acridine-based uracil PNA monomer and evaluation of its fluorescence property.

Keywords

Dimethylaminoazobenzene, peptide nucleic acid PNA, DNA, photochromic nucleosides, quencher, fluorescent probes and acridine

Acknowledgments

First of all, I thank God almighty for giving me the courage, strength and ability to continue my graduate studies and finish this dissertation with all kind of stress, pressure and difficulties that I faced throughout my study period.

I would like to express my deep gratitude and thanks to my supervisor Prof. Hudson for his encouragement, scholastic guidance, suggestions and improving my presentation skills through giving me the opportunity to attend many conferences. Thanks Dr. Hudson

I want to express my deep thanks and appreciation to my country Egypt for the financial support that gave me the opportunity to be here in Canada to learn and develop my research skills, thanks Egypt.

I would like to thank lab members past and present for their friendship. Dr. Fil, Dr. Dave Mark, André, Kirby, Mojmir, Melissa, McKenry and Adam. Special thanks to Mark and André for helping me to run mass analysis for my oligomer samples. Kirby and McKenry, thanks for the sense of humor environment that you have spread at the lab. I love you all.

I would like to thank my committee members for taking the time to read my thesis and their helpful discussions and guidance through my thesis preparation.

Last but not least, during my study period there was a lot of struggling, stress, depression, difficult times and challenges. Certainly this work never be done without support that I had from my beloved wife Amira and my kids Ahmed, Youssef and Adam. Special thanks to my soul mate my wife Amira for her love and well taking care of our kids (huge responsibility!!!). I want to thank my father and my mother for their support even they are in Egypt, but they were so supportive to continue my doctoral studies. I knew that all of you had difficult and lonely times, really I appreciate what all of you have done to me and I wish I can make you up. Thanks my lovely family.

Dedication

To My lovely family

Wife Amira

Sons, Ahmed, Youssef and Adam

Table of Contents

CERTIFICATE OF EXAMINATION	ii
Acknowledgments	v
Dedication.....	vi
Table of Contents.....	vii
List of Tables	xi
List of Figures.....	xii
List of Schemes.....	xvii
List of Abbreviations	xviii
CHAPTER 1	1
AZOBENZENE AND ITS APPLICATION IN NUCLEIC ACID CHEMISTRY	1
1.1 Nucleic acid overview	1
1.2 Automated DNA synthesis	3
1.3 Control of DNA's functions by light	6
1.4 Azobenzene.....	8
1.4.1 The UV/Vis spectroscopy of azobenzene.....	8
1.4.2 Photoisomerization of azobenzene	10
1.4.3 Utility of azobenzene as quencher	13
1.4.4 Some of biological applications based on azobenzene photoswitching ...	14
1.4.5 Photoregulation of enzymatic activities by azobenzene	17
1.4.6 New properties of azobenzene.....	20
1.5 Goal of this thesis.....	22
1.6 References.....	23
Chapter 2	30
SYNTHESIS AND PHOTOPHYSICAL STUDIES OF AZO-BASED QUENCHER FOR PNA-MOLECULAR BEACON	30

2.1	Fluorescence	30
2.2	Fluorescence resonance energy transfer (FRET) theory and fluorescent hybridization probes a.....	31
2.2.1	Examples of fluorescent hybridization probes using FRET mechanism..	33
2.3	Peptide nucleic acid (PNA).....	37
2.3.1	PNA binding modes with nucleic acids (NAs).....	38
2.3.2	PNA modifications	41
2.3.3	Synthesis of PNA oligomers.....	42
2.4	PNA applications	48
2.5	Results and discussion	49
2.5.1	Synthesis of the backbone.....	50
2.5.2	Synthesis of the dimethylaminoazobenzene PNA monomer.....	51
2.5.3	Photoisomerization studies	52
2.5.4	Effect of acid on dimethylaminoazobenzene PNA monomer	51
2.5.5	Quenching ability of dimethylaminoazobenzene PNA monomer	52
2.5.6	Design and synthesis of dual-labeled PNA molecular beacon	56
2.6	Conclusion	59
2.7	Experimental.....	60
2.8	References.....	65
CHAPTER 3.....		72
SYNTHESIS AND PHOTOPHYSICAL STUDIES OF NOVEL QUENCHER FOR PNA		72
3.1	Introduction.....	72
3.2	Results and discussion	73
3.2.1	Photoisomerization of azo-based uracil derivative and solvent effect on its absorption spectrum.....	75
3.2.2	pH-Sensitivity of azo-based uracil.....	76

3.2.3	Design and synthesis of dual peptide for quenching study.....	81
3.3	Conclusion	87
3.4	Experimental.....	88
3.5	References.....	94
CHAPTER 4	97
SYNTHESIS AND PHOTOPHYSICAL STUDIES OF NOVEL PHOTOCHROMIC PHOSPHORAMIDITE FOR DNA AND RNA	97
4.1	Introduction.....	97
4.2	Result and discussion.....	99
4.2.1	Photoisomerization studies	101
4.2.2	pH-Sensitivity	103
4.3	Conclusion	105
4.4	Experimental.....	106
4.5	References.....	112
CHAPTER 5	115
SYNTHESIS OF ACRIDINE-BASED PNA MONOMER SUITABLE FOR PNA-FLUORESCENT PROBES	115
5.1	Hydrogen bonding	115
5.2	Base-stacking.....	116
5.3	Fluorescent nucleobases	117
5.4	Acridine	121
5.5	Results and discussion	123
5.5.1	Photophysical properties.....	124
5.5.2	Fluorescence properties of acridine-based monomer	125
5.5.3	Future work.....	125
5.5.4	Conclusion	125
5.6	Experimental.....	126

5.7 References...	130
CHAPTER 6	136
FUTURE OUTLOOK	136
APENDICES (Selected NMR and MS spectra)	138
CURRICULUM VITAE	158

List of Tables

Table 2-1: Melting Temperature	59
Table 3-1: Selected bond distances (Å) and angles (°) for III-2	74
Table 3-2: Maximum absorption wavelength and molar extinction coefficient of III-3	75
Table 3-3: Effect of addition of 3 mM HCl on absorption maximum wavelength (λ_{\max}) of III-3	77
Table 3-4: X-ray crystallographic structural parameters for compound III-2	92
Table 5-1: Photophysical properties of V-6	124

List of Figures

Figure 1-1: The central dogma of molecular biology.	2
Figure 1-2: Watson-Crick base pairing between T:A and G:C.....	3
Figure 1-3: DNA duplex structure.	3
Figure 1-4: Composition of commercial available phosphoramidite monomers.....	4
Figure 1-5: Traditional solid-phase phosphoramidite oligonucleotide synthesis cycle.....	5
Figure 1-6: Release of the oligomer from the universal support by NH_4OH	6
Figure 1-7: Photocleavable moieties for photoregulation of biological activity.	7
Figure 1-8: Different classes of photochromic molecules.	8
Figure 1-9: Different examples of azobenzenes.	9
Figure 1-10: a) Molecular orbital diagram for azobenzene system, b) UV-Vis spectrum of azobenzene in ethanol at room temperature.....	9
Figure 1-11: Photoisomerization of azobenzene in response with UV/Vis light.....	10
Figure 1-12: Excitation and relaxation routes of <i>trans</i> and <i>cis</i> azobenzene isomer.	11
Figure 1-13: The proposed mechanisms for the isomerization of <i>trans</i> to <i>cis</i> azobenzene...	12
Figure 1-14: Proposed mechanism for <i>cis</i> to <i>trans</i> thermal isomerisation in azobenzene	13
Figure 1-15: Structure of the universal quencher DABCYL.	14
Figure 1-16: Photoisomerization azobenzene-based cyclic peptides.....	16
Figure 1-17: Structure of azobenzene monomer used in photoregulation of DNA.....	18
Figure 1-18: Photoswitching of transcription using T7 RNA polymerase.	19

Figure 1-19: Photoregulation of RNase H activity.	20
Figure 1-20: Fluorescent azobenzene due to B-N interaction.....	21
Figure 1-21: Bridged azobenzene	21
Figure 2-1: Jablonski diagram illustrated luminescence origin.	31
Figure 2-2: Resonance energy transfer Jablonski diagram and spectral overlap donor emission spectra with acceptor absorption spectra.	33
Figure 2-3: Schematic representation for adjacent probes.....	33
Figure 2-4: Schematic representation for 5`-nuclease probes.....	34
Figure 2-5: Schematic representation for strand-displacement probes.....	34
Figure 2-6 : Schematic representation for molecular beacon.	35
Figure 2-7: Examples of fluorophores and quenchers have been used in fluorescent.....	36
Figure 2-8: Comparison between DNA and PNA structures.	38
Figure 2-9: Binding modes of PNA with double-stranded DNA.....	39
Figure 2-10: Triplex invasion of double helix DNA by homopyrimidine PNA oligomers. .	40
Figure 2-11: Double duplex invasion of DNA by pseudo complementary PNAs.....	41
Figure 2-12: Selected examples of modified PNA backbone.....	42
Figure 2-13: Selected examples of modified PNA nucleobases.....	42
Figure 2-14: Side reactions in PNA synthesis.....	44
Figure 2-15: Structures of commercially available <i>t</i> Boc/Z PNA monomers.....	46
Figure 2-16: Structures of commercially available Fmoc/Bhoc monomers.	46
Figure 2-17: General strategy for solid phase peptide nucleic acid synthesis.....	46

Figure 2-18: Examples of various protecting groups in PNA synthesis.....	47
Figure 2-19: Comparison between the structure of GPNA and <i>aeg</i> -PNA.....	49
Figure 2-20: Changes in the UV-Vis absorption spectrum of II-5 in EtOH.....	53
Figure 2-21: UV-Vis spectral change of II-5 in dichloromethane.....	52
Figure 2-22: The effect of increasing amounts of II-5 on the emission spectra of A) fluorescein and B) pyrene.....	55
Figure 2-23: The effect of increasing amounts of II-5 on the fluorescence emission spectra of sulforhodamine 640 dye.	55
Figure 2-24: Structures of the fluorophores have been used in the study.....	56
Figure 2-25: Mass spectrum of azo-based PNA oligomer II-6	57
Figure 2-26: Mass spectrum of PNA-MB II-7	57
Figure 2-27: Fluorescence emission spectra of 4-(<i>N,N</i> -dimethylamino)azobenzene based PNA-MB and PNA-MB-cDNA.....	58
Figure 2-28: Schematic representation for formation of triplex PNA ₂ :DNA	59
Figure 3-1: Examples of azo-based PNA monomers.....	72
Figure 3-2: Similarity in structure between DABCYL and the modified uracil.....	73
Figure 3-3: The X-ray crystal structure of III-4	74
Figure 3-4: Photoisomerization of 4-(<i>N,N</i> -dimethylamino)phenylazouracil derivatives.	75
Figure 3-5: Absorption spectrum of III-3 in CH ₃ CN.....	76
Figure 3-6: Schematic representation of azonium and ammonium ions.....	76
Figure 3-7: Spectral change of III-3 in CH ₃ COCH ₃	77
Figure 3-8: Effect of TFA on III-3 in a) CH ₃ CN, b) in EtOH.....	78

Figure 3-9: Compound III-3 in a) various solvents, b) after addition of TFA., c) after basification.....	79
Figure 3-10: Compound III-3 in CH ₂ Cl ₂ with haloacids.....	79
Figure 3-11: Fluorescence changes of 8 μM fluorescein upon addition of various amount of III-3 in EtOH	80
Figure 3-12: Fluorescence spectra of 5 μM concentration of pyrene in ethanol recorded upon addition of varied amount of III-3 in EtOH	80
Figure 3-13: Schematic representation on the mechanism of FRET-Peptide.....	81
Figure 3-14: Designed FRET Peptide having azo-based PNA monomer as quencher and FITC as fluorophore.....	82
Figure 3-15: UV-Vis spectra of FRET-Peptide	84
Figure 3-16: Schematic representation of the modified dual labelled peptide design.	84
Figure 3-17: Fluorescence emission spectrum of dual peptide	85
Figure 3-18: Mass spectrum of FRET-peptide	86
Figure 3-19: Mass spectrum of FRET-peptide after digestion	86
Figure 4-1: Modified oligonucleotides carrying azobenzene a) in the side chain, b) as linker.....	98
Figure 4-2: Schematic representation of <i>trans-cis</i> photoisomerization of IV-2 and IV-6 ..	101
Figure 4-3: Absorption spectra of A) IV-2 in CH ₂ Cl ₂ , B) IV-6 in CH ₃ CN	102
Figure 4-4: Structure of 4-(<i>N,N</i> -dimethylaminoazo)phenyl(deoxy)uridine and its protonated forms	103
Figure 4-5: Changes in UV-Vis spectra of A) IV-2 and C) IV-6 upon addition of increasing concentrations of TFA.	105

Figure 5-1: Base pairing between DAP:T comparing to A:T	115
Figure 5-2: Hybridization of cytosine and its modification moPhpC with guanine	116
Figure 5-3: Representation of hybridization of 2AP with thymine and cytosine	118
Figure 5-4: Structure of some pteridine derivatives.....	118
Figure 5-5: Examples of expanded nucleobases.....	119
Figure 5-6: Examples of hydrocarbons and heterocycle DNA base replacement.	120
Figure 5-7: Structures of some conjugated base analogues used in DNA and RNA probes	121
Figure 5-8: Structure of acridine, m-AMSA and acridine orange (AO).....	122
Figure 5-9: UV-Vis spectrum of V-6 in neutral and acidic form.....	124
Figure 6-1: Structures of phenylazo derivatives	136
Figure 6-2: Structures of azo-based uracil derivatives.....	137

List of Schemes

Scheme 2-1: Synthesis of 2-Fmoc(<i>aeg</i>)- <i>t</i> -butyl ester backbone.....	50
Scheme 2-2: Synthesis of azo-based PNA monomer.	51
Scheme 2-3: Ammonium/azonium protonated ions of 4-(<i>N,N</i> -dimethylamino)azobenzene.	52
Scheme 3-1: Synthesis of 4-(<i>N,N</i> -dimethylamino)phenylazouracil PNA monomer.....	73
Scheme 3-2: Degradation mechanism of FITC labelled peptide by the effect of TFA.....	83
Scheme 4-1: Synthesis of phosphoramidite possesses phenylazo moiety for photoswitching	100
Scheme 4-2: Synthesis of photochromic riboside.	101
Scheme 5-1: Synthesis of acridine-based PNA monomer V-6	123

List of Abbreviations

A	adenine
ADP	adenosine diphosphate
<i>aeg</i>	aminoethylglycine
EDANS	5-((2-aminoethyl)amino)naphthalene-1-sulfonic acid
Bhoc	benzhydryloxy carbonyl
BSA	bovine serum albumin
calc.	calculated
ROX	6-carboxy-x-rhodamine
Cat D	cathepsin d
δ	chemical shift in parts per million downfield from tetramethylsilane
CD	circular dichroism
cDNA	complementary deoxyribonucleic acid
CPG	controlled-pore glass
<i>J</i>	coupling constant in Hz
C	cytosine
°C	degrees Celsius
dA	deoxyadenosine
dC	deoxycytosine
dG	deoxyguanosine
DNA	deoxyribonucleic acid
dT	deoxythymidine
DCC	dicyclohexyl carbodiimide
DCU	<i>N,N'</i> -dicyclohexylurea
DIEA	<i>N,N</i> -diisopropylethylamine
DMF	<i>N,N</i> -dimethylformamide
DMT	4,4'-dimethoxytrityl
DMSO	dimethyl sulfoxide
DAN	dimethylamino-2-acetyl naphthalene
Dde	1-(4,4-dimethyl-2,6-dioxacyclohexyl)ethylidene
JOE	2',7'-dimethoxy-4',5'-dichloro-6-carboxyfluorescein
DMTCI	4,4'-dimethoxytrityl chloride
DABCYL	4-(<i>N,N</i> -dimethylamino)azobenzene-4'-carboxylic acid
DCA	dodecylammonium chloride
d	Doublet
ESI	electrospray ionization
EtOH	Ethanol
EDTA	ethylenediaminetetraacetic acid disodium
Fmoc	fluorenylmethoxycarbonyl
FITC	fluorescein isocyanate

FISH	fluorescence <i>in situ</i> hybridization
Φ_F	fluorescence quantum yield
FRET	fluorescence resonance energy transfer
Fmoc-OSu	<i>N</i> -(9-fluorenylmethoxycarbonyloxy) succinimide
FDA	food and drug administration
G	guanine
HF	hydrogen fluoride
HRMS	high resolution mass spectrometry
HOBt	<i>N</i> -hydroxybenzotriazole
MALDI-TOF	matrix assisted laser desorption-ionization time-of-flight
mRNA	messenger ribonucleic acid
MB	molecular beacon
MmT	monomethoxytrityl group
m	multiplet
NVOC	nitroveratryloxycarbonyl
ONs	oligonuclotides
ONB	<i>ortho</i> -nitrobenzyl
PNAs	peptide nucleic acids
PSS	photostationary phase
PCR	polymerase chain reaction
RP-HPLC	reversed phase high pressure liquid chromatography
RNA	ribonucleic acid
RNAP	RNA polymerase
SNPs	single-nucleotide polymorphisms
s	singlet
<i>t</i> Boc	<i>tert</i> -butyloxycarbonyl
THF	tetrahydrofuran
T	thymine
tRNA	transfer ribonucleic acid
TAMRA	<i>N,N,N',N'</i> -tetramethyl-6-carboxyrhodamine
EtN ₃	triethylamine
TLC	thin layer chromatography
TFA	trifluoroacetic acid
TFMSA	trifluoromethane sulphonic acid
TMP	trimethyl phosphate
TMS	trimethylsilyl
t	triplet
Trp	tryptophane
UV	ultra violet
U	uracil
Vis	visible
λ	wavelength

Chapter 1

Chapter 1

1 Azobenzene and Its Application in Nucleic Acid Chemistry

1.1 Nucleic acid overview

Since the discovery of the three dimensional structure of DNA double-helix in 1953 by Watson and Crick,¹ nucleic acids have been recognized as key components of life. This discovery encouraged many scientists to devote effort to explore the emerging science of molecular biology. Without a doubt, all living organisms need to reproduce. To ensure the continuation of their species, genetic information must be transferred from a generation to the next. This idea led scientists to question how these biological processes took place.

In 1958, Francis Crick² was the first to propose the concept of "the central dogma of molecular biology". Simply, it describes the flow of information via biological processes involving transcription of DNA to RNA which is then translated to protein. Protein is never back-translated to RNA or DNA, DNA is never created from RNA except in case of retroviruses. Furthermore, DNA is never directly translated to protein.

As shown in (Fig.1-1), the central dogma of molecular biology is represented in three stages: Firstly, replication of DNA which involves the copying of DNA. Secondly, transcription involves the formation of mRNA, a single stranded ribonucleic acid that carries the genetic code from the DNA in the nucleus to the sites of protein synthesis in the cytoplasm. Thirdly, translation of mRNA to proteins which are responsible to perform all of the body's essential functions as growth, repair, metabolizing food, fighting infections and much more.

If a mutation occurs in a gene, this can lead to production of a completely distorted protein that is unable to carry out its function or it may change the amount of a protein being produced. To control the effect of mutations, unique strategies were established based on oligonucleotides (ONs) namely antigene and antisense. In the antigene strategy, nucleic acid analogues are designed to recognize and bind to the complementary

sequence in a particular gene (DNA) and thereby interfere with the transcription of that particular gene (thus inhibit the formation of mRNA). While in the antisense strategy the nucleic acid analogues are designed to recognize and hybridize to a complementary sequence in mRNA and thereby stop its translation to protein and therefore effectively turn that gene "off".

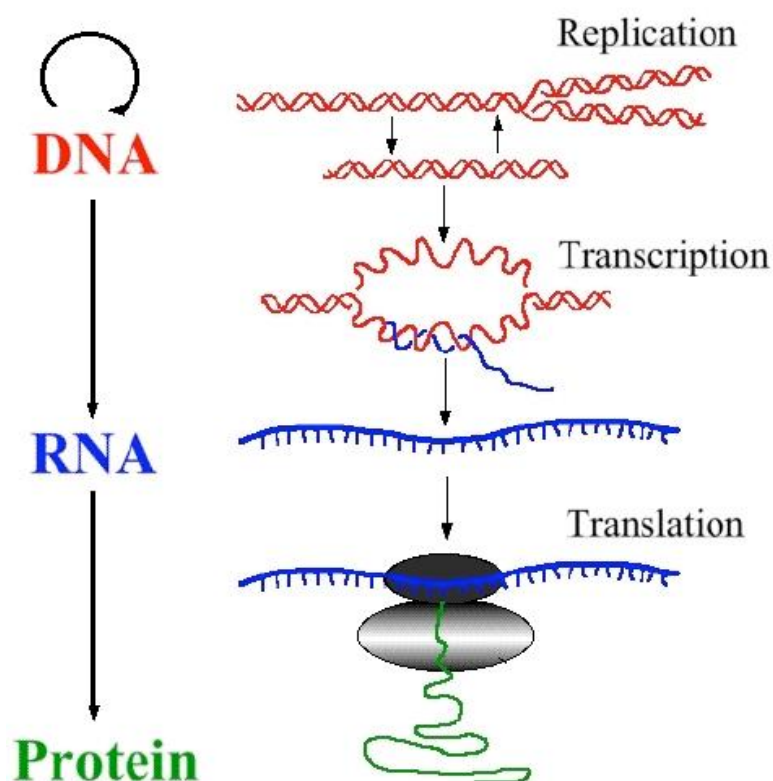


Figure 1-1: The central dogma of molecular biology. Adapted from <http://www.accessexcellence.org/RC/VL/GG/central.php>.

Oligonucleotides have also been shown to be of particular value as diagnostic agents that are easily labeled with reporter groups as fluorophores and bind with its complementary nucleic acids with high and specific affinities.

Hybridization between nucleic acids to form DNA:DNA or DNA:RNA duplexes is ascribed to the specific binding between the nitrogenous nucleobases in each strand. It is known that guanine (G) pairs with cytosine (C) and thymine (T)/(uracil (U) in case of RNA) pairs with adenine (A) via the hydrogen bonding interactions shown in (Fig. 1-2).

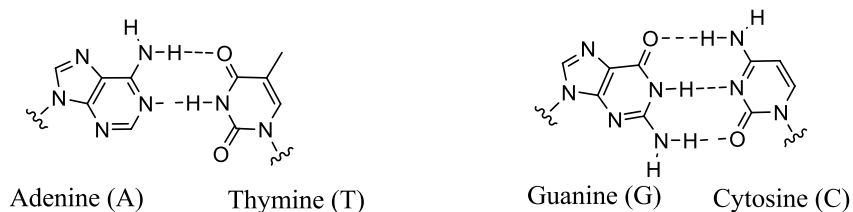


Figure 1-2: Watson-Crick base pairing between A: T and G:C.

A typical DNA duplex is formed by two strands that run in opposite directions to yield a helical structure (Fig. 1-3). These strands are composed of deoxynucleosides dA, dC, dG and dT which is connected together via negatively charged phosphate groups. The stability of the DNA duplex is determined by the composition of the DNA sequence and the ionic conditions of the aqueous environment.

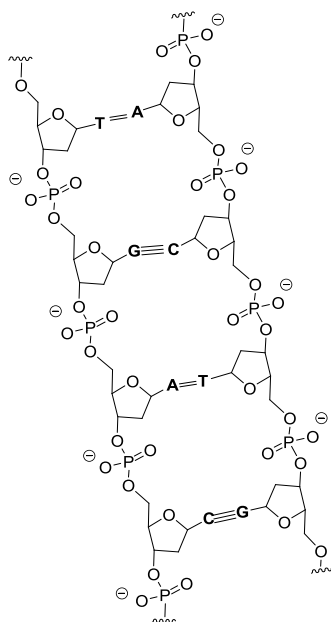


Figure 1-3: DNA duplex structure.

1.2 Automated DNA synthesis

Nucleic acids are naturally synthesized within the biological environment via bioreactions that are catalyzed by enzymes. However, there is a huge need for millions of DNA assays to be able to examine antigene and antisense probes. Currently, nucleic acids can be synthesized in laboratory with sequences similar to the naturally occurring DNA

strands. In addition, synthesis of DNA strands bearing chemically modified nucleobases that possess novel functions and unique properties is possible. This innovation leads to production of numerous DNA oligonucleotides with potential biological applications.

Currently, a well established methodology called "solid support synthesis of oligonucleotides"³ is widely used for the synthesis of DNA sequences using an automated instrument, the "DNA synthesizer". This technique is extremely useful because it provides a rapid and inexpensive access to custom-made oligonucleotides of the desired sequence. The phosphoramidite protocol is the most common strategy for DNA synthesis, this protocol is characterized by using nucleotide phosphoramidite units bearing different bases as illustrated in (Fig. 1-4). Each phosphoramidites is composed of nucleobase with suitable protecting group for the exocyclic amine, deoxyribo sugar with dimethoxytrityl (DMT) group protect the 5'-OH and phosphate with diisopropylamine and 2-cyanoethyl groups which are very essential to order the synthesis direction.

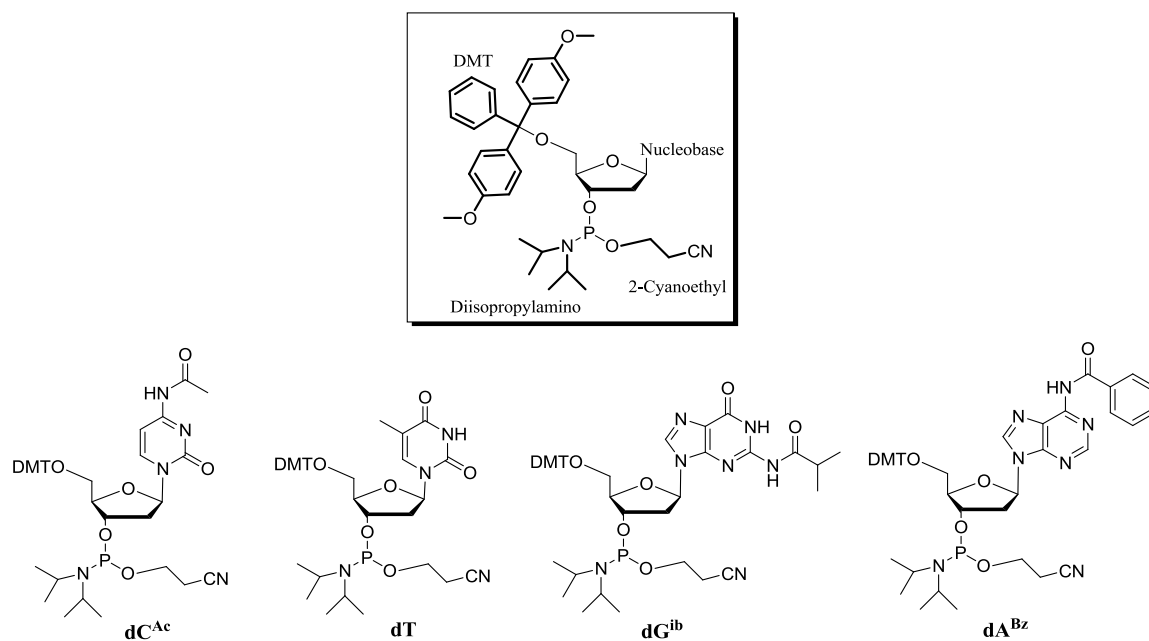


Figure 1-4: Composition of commercial available phosphoramidite monomers.

Automated DNA synthesis is carried out by using controlled-pore glass (CPG) support, the phosphoramidite with the different nucleobases are loaded into the commercially available DNA synthesizer and simply by choosing the desired DNA sequence through a program, the synthesis can be achieved in few hours based on the length of the DNA sequence. As illustrated in (Fig. 1-5), the DNA synthesis cycle consists of four stages namely detritylation, coupling, capping and oxidation. For every synthesis cycle, one nucleotide is added at a time for the growing oligonucleotide through the four steps until the desired sequence is built. In fact, the desired sequence may be accompanied with undesired oligonucleotide species in different length due to incomplete synthesis during the process. After synthesis completion, the oligonucleotide is released from the support under basic conditions, generally with ammonium hydroxide, is purified by reversed-phase high pressure liquid chromatography (RP-HPLC) to afford the desired sequence. The pathway to release the oligonucleotide from the solid support is shown in (Fig. 1-6).

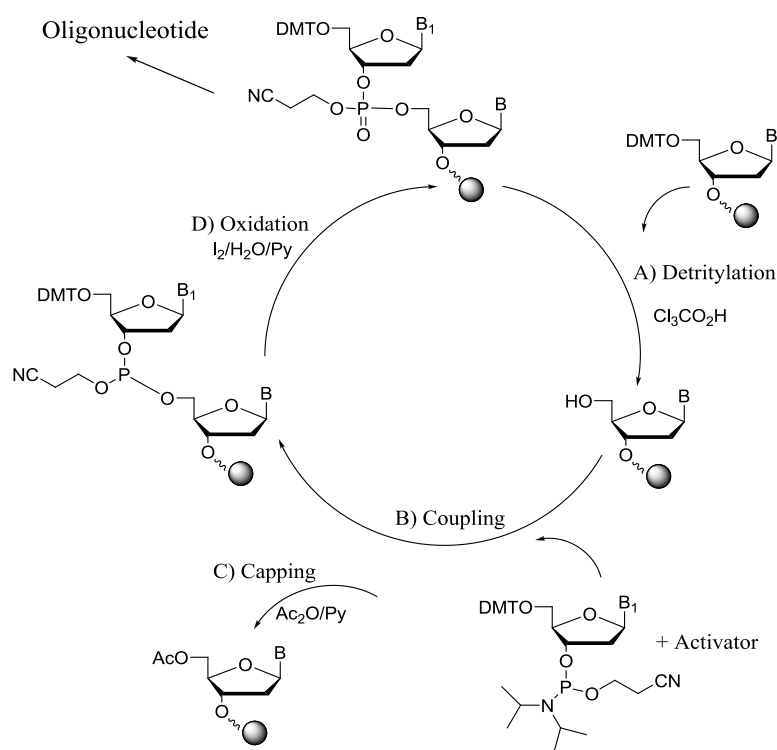


Figure 1-5: Traditional solid-phase phosphoramidite oligonucleotide synthesis cycle.

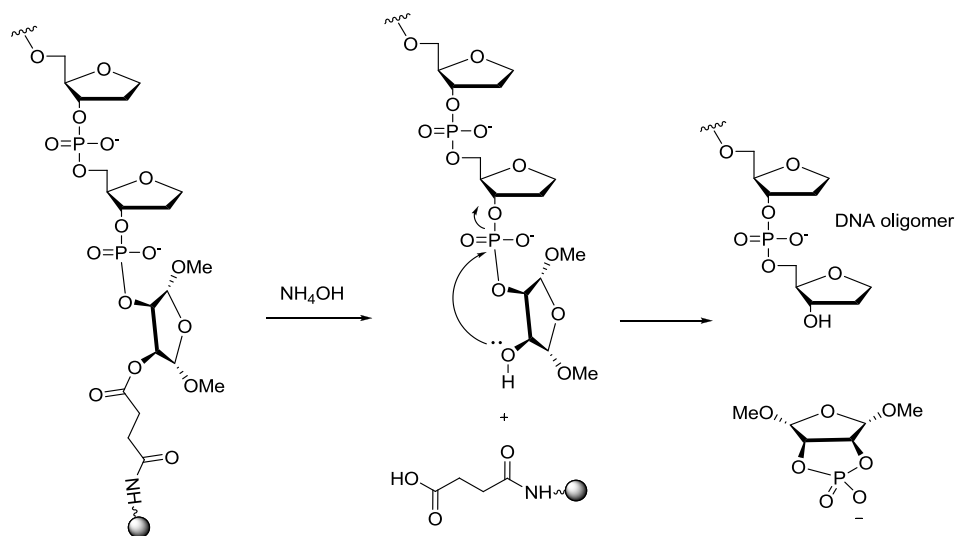


Figure 1-6: Release of the oligomer from the universal support by NH_4OH .

Although the utility of the phosphoramidite methodology for oligonucleotide synthesis for several biological uses is satisfactory, its usage for production of large-scale oligonucleotide synthesis was accompanied with side-reactions, which were tolerated in small-scale synthesis. These side reactions are depurination of protected bases due to repetitive acid treatment at detritylation step, and missing one or more of the correct nucleotides in the desired sequence by the effect of acid treatment leading to formation of sequences with mutations; thusly, the presence of such mutations limits its applications.

1.3 Control of DNA's functions by light

There exists a large effort directed to develop biomolecular tools to control biological processes using external stimuli. Over the last two decades several external stimuli were investigated to regulate the replication, transcription and translation processes of genes.

Amongst the variety of stimuli such as light, pH, electric field and heat, light is the most promising. This is due to many reasons such as using light is efficient, clean and does not produce any contaminants that could affect the biological system and the facile synthesis of various photoresponsive molecules which provide a wide range of excitation wavelengths.

Photoresponsive molecules are defined as molecules that undergo predictable changes in response to light. They are classified as photocleavable and photoswitchable molecules, also known as photochromic molecules. Examples of photocleavable moieties are hydroxyphenylacetyl, coumarin and *o*-nitrobenzyl derivatives (Fig. 1-7). *o*-Nitrobenzyl derivatives have been widely used due to its stability in synthetic and biological environments. Because the photocleavable processes are irreversible, photoswitchable molecules are preferable. Photochromic molecules are molecules that undergo structural rearrangement between two or more isomeric forms in response to irradiation. The direction of this arrangement is determined by the wavelength of the incident light.

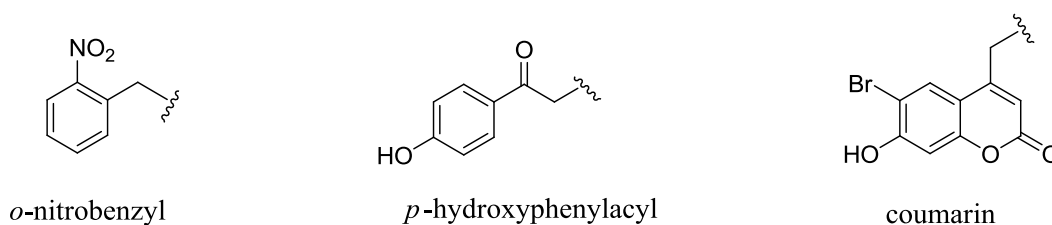


Figure 1-7: Photocleavable moieties for photoregulation of biological activity.

There are several classes of photochromic molecules as azobenzenes, stilbenes,⁴ diarylethenes,⁵ thioindigo derivatives,⁶ fulgides⁷ and spiropyrans.⁸ The structures are illustrated in (Fig. 1-8). In all cases, the photoisomerization process is reversible; while after repeated isomerization cycles a fatigue can set. In our work we are interested in azobenzene as photochromic molecule.

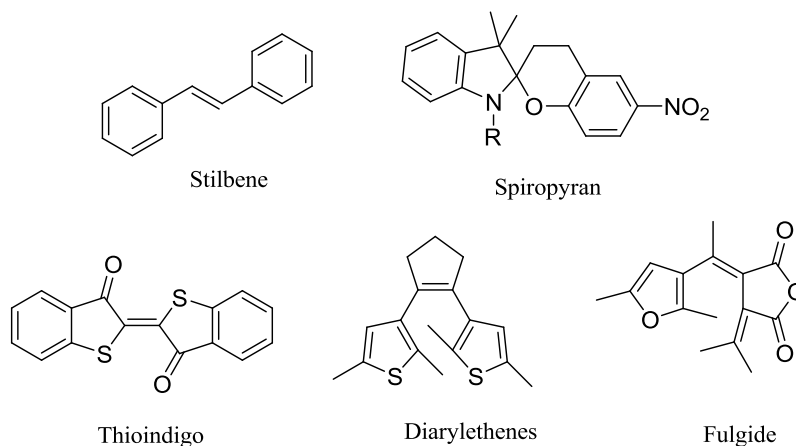


Figure 1-8: Different classes of photochromic molecules.

1.4 Azobenzene

Azobenzene, is an organic molecule consisting of two phenyl rings linked together with azo group (N=N) in which each nitrogen atom carries a non-bonding pair of electrons. Azobenzene was used for the first time in 1879,^{9a-b} and initially was used as a dye. It is currently employed in 60-70 % of the dye industry.¹⁰

Recently, the isomerization properties of azobenzenes were rediscovered and have been exploited in many applications such as optical data storage,¹¹ liquid crystal display,¹² molecular machines design¹³ and many biochemical activities.^{14-a-b} All these applications are based on its ability to undergo geometrical *trans-cis* isomerization in response with light.

1.4.1 The UV/Vis spectroscopy of azobenzene

To have a full understanding of the spectroscopy of azobenzene, knowledge of its excited states is essential. *Cis*- and *trans* azobenzene have three excited single states attributed to three absorption bands that appear in the visible and near UV regions as shown in (Fig. 1-10a and 1-10b).^{15a-b} In the azobenzene system, there are three types of electronic transitions: 1) The lowest-energy transition is that obtained due to the forbidden $n_s \rightarrow \pi_1^*$ transition which corresponds to the $S_0 \rightarrow S_1$, this transition appears in the visible region at approximately 430 nm and 440 nm for *cis* and *trans* isomers, respectively. 2) Transition

that occurs due to symmetry-allowed $\pi_1 \rightarrow \pi_1^*$ transition corresponding to the $S_0 \rightarrow S_2$ which appears in the UV region at 280 nm and 314 nm for *cis* and *trans* isomers respectively and 3) the highest-energy transition due to $\sigma \rightarrow \sigma^*$ transition that occurs at the region 230-244 nm are for *cis* and *trans* isomers. The presence of an electron donating substituent in *ortho* or *para* positions as (OH or NH₂) to the azo group leads to decrease the energy of $\pi\text{-}\pi^*$ transition and consequently the $\pi\text{-}\pi^*$ absorption band shifts to longer wavelength. Generally, the greater the electron donating substituent the greater the bathochromic shift. For example, the presence of dimethylamino group in *para* position of azobenzene ring decreases the $\pi\text{-}\pi^*$ energy more than *p*-amino group and thusly appearing at longer wavelength. Another example of azobenzene analogues is pseudostilbene (Fig. 1-9), an azobenzene system which contains an electron donating and electron accepting group in resonance at the *para* positions. The presence of the donating and accepting groups leads to a reduction of the energy of $\pi\text{-}\pi^*$ transition and consequently its appearance at longer wavelengths.

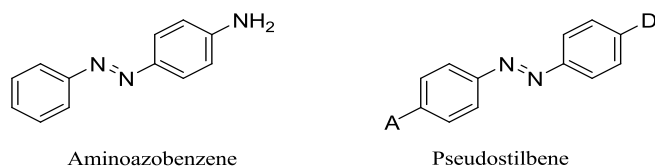


Figure 1-9: Different examples of azobenzenes and effect of substituents on the absorption bands. D and A represent donor and acceptor groups substituted.

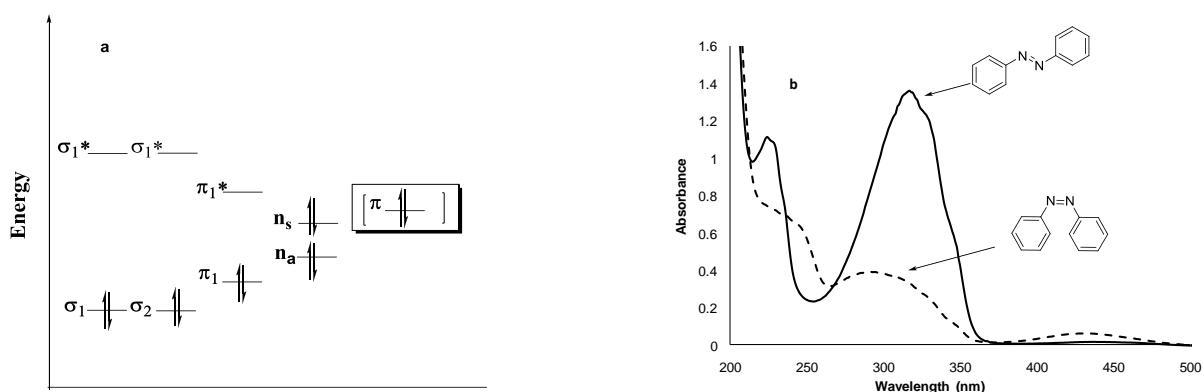


Figure 1-10: a) Molecular orbital diagram for azobenzene system, adapted from ref.^{15b} b) UV-VIS spectrum of *trans* and *cis* azobenzene in ethanol at room temperature.

1.4.2 Photoisomerization of azobenzene

Azobenzene can undergo geometrical structural change from *trans* to *cis* isomer, and reverse, in response to optical excitation with light at suitable wavelength. As shown in (Fig. 1-11), *trans* to *cis* isomerization takes place via excitation with UV light at ($300 < \lambda < 400$ nm), while upon excitation of *cis*-form with visible light ($\lambda > 400$ nm), or thermally, the *trans* isomer is recovered. The *trans* isomer is a conjugated planar molecule and its π electrons can be delocalized over the entire molecule therefore it is thermally stable while in the *cis* isomer there is a steric clash between the two phenyl rings which forces the molecule to have a skewed conformation and consequently it is less stable than the *trans* isomer. The *trans*-to-*cis* photoisomerization process is seen to be accompanied by a structural change in which the distance between *para* carbon atoms in azobenzene decreased from 9 Å in *trans* isomer to 5.5 Å in the *cis* isomer.¹⁶ This change in geometry is the cornerstone for various azobenzene applications.

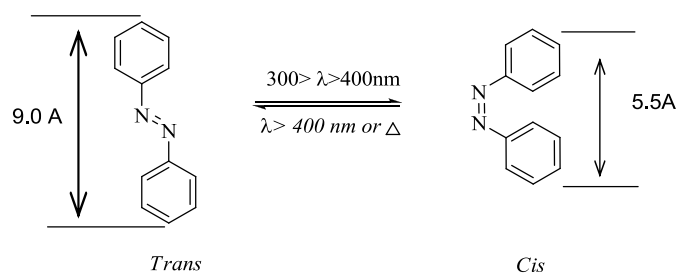


Figure 1-11: Photoisomerization of azobenzene in response with UV/Visible light.

As shown in (Fig. 1-12), after excitation of the *trans* isomer with light of suitable wavelength, it will decay to either the ground state (S_0) of *trans* or that of *cis* isomer. Similarly, upon excitation of the *cis* isomer a relaxation to either the ground state (S_0) of *cis* or *trans* occurred. The decaying of the *cis* isomer may take place thermally to the *trans* isomer. A photostationary state (PSS), an equilibrium state between the rates of excitation and relaxation of the *cis* and *trans* isomers, can be reached when both *cis* and *trans* isomer absorb radiation of the same frequency. Due to the absorbance spectra of *trans* and *cis* azobenzene are quite different, the photoisomerization process can be followed by UV/Vis spectroscopy. The ground state energy of *trans* isomer at room temperature was found to be lower than the *cis*-azobenzene by an estimate 11.8-13.8

kcal/mol.^{17a-b} and the energy barrier to reach *cis* isomer was found to be 36.9 kcal/mol.¹⁸ Consequently, in the dark the more thermally stable *trans* isomer is found to predominate.

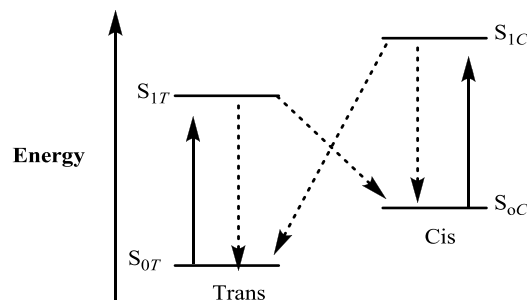


Figure 1-12: Excitation and relaxation routes of *trans* and *cis* azobenzene isomer.

1.4.2.1 The photoisomerization mechanism

The mechanism of the photoisomerization of azobenzene has been a longstanding debate in the literature. There are two proposed pathways for this process to take place either by a rotation or inversion mechanism^{19a-e} as illustrated in (Fig. 1-13). Rotation mechanism involves a torsion of the N=N bond around the dihedral angle (ϕ , CN-NC), while inversion mechanism involves an in-plane inversion of the angle (θ) around the azo group and one of the attached carbon of the benzene ring (NN-C). Despite the numerous reports investigating the photoisomerization mechanisms of azobenzene, there has been no agreement on which pathway the photoisomerization takes.

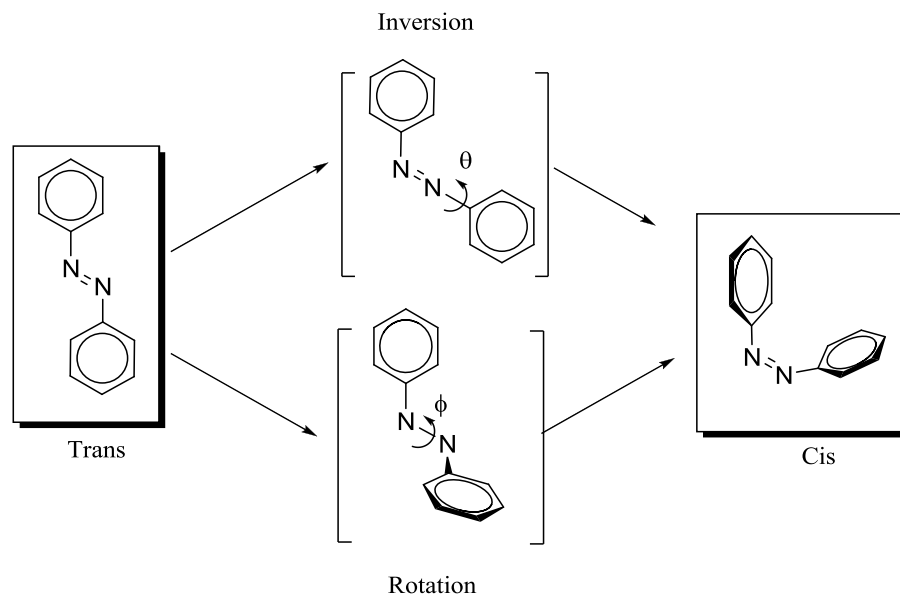


Figure 1-13: The proposed mechanisms for the isomerization of *trans* to *cis* azobenzene.

1.4.2.2 Thermal *cis* to *trans* isomerization.

Similar to the photoisomerization, the thermal isomerization *cis* to *trans* is agreed to take place via rotation mechanism or inversion mechanism as shown in (Fig. 1-14). Although both mechanisms are viable,²⁰ more studies support the rotation mechanism.^{21a,b} Thermal isomerization of azobenzenes is dependent on various factors as solvent polarity, substitution on the aromatic ring and pH of the medium. Subjecting azobenzene to acidic condition catalyzes the thermal isomerization via formation of an azonium protonated intermediate and thus the π -bond of N=N is ruptured and consequently facilitates the rotation around the N-N via rotation mechanism.²²

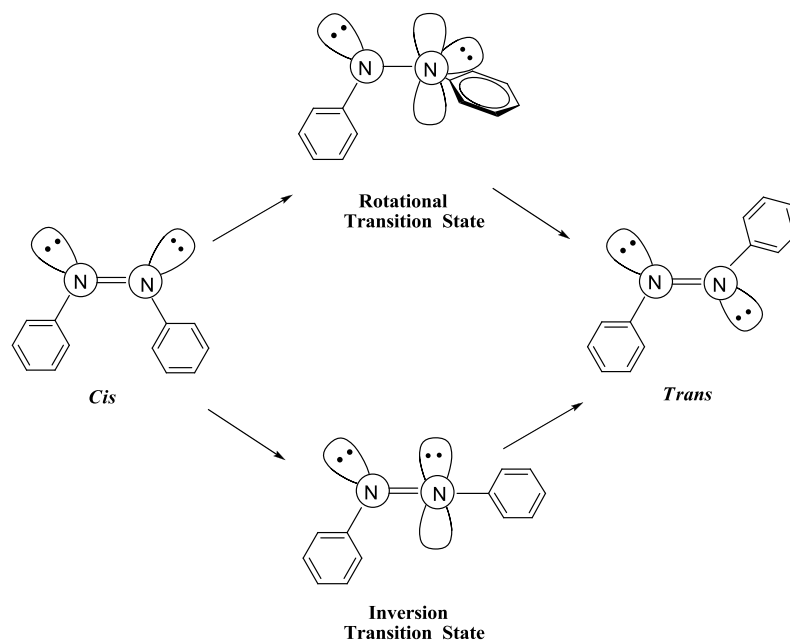


Figure 1-14: Proposed mechanism for *cis* to *trans* thermal isomerisation in azobenzene adapted from ref. ^{21b}

1.4.3 Utility of azobenzene as quencher

During the last two decades DNA detection has attracted much attention due to its potential applications in disease treatment. The most common method for DNA hybridization detection is molecular beacon technology²³ (MB) which involves labeling of DNA probes with fluorescent dyes and quenchers. This approach relies on the design of the labeled probes.

One example of an azobenzene derivatives used as a quencher is *p*-aminoazobenzene. It has been tested for quenching the fluorescence signal of Bovine Serum Albumin (BSA) protein,²⁴ a protein that responsible in the transport and disposition of endogenous and exogenous compounds present in blood. It is known that BSA has two tryptophan residues Trp-212 and Trp-314 which possess intrinsic fluorescence. At physiological pH, it was found that the fluorescence intensity of BSA was quenched gradually with the increase of *p*-aminoazobenzene concentrations accompanied with blue shift of the maximum emission wavelength up to 7 nm.

4-(*N,N*-Dimethylamino)azobenzene-4'-carboxylic acid (DABCYL) is another example of an azobenzene-based quencher (Fig.1-15). It is characterized by an absorption maximum at 475 nm and it has quenching range from 400-550 nm. This property has allowed its use to quench a wide range of common fluorescent dyes such as 5-((2'-aminoethyl)amino)naphthalene-1-sulfonic acid (EDANS) (λ_{em} = 490 nm), carboxy-fluorescein (FAM) (λ_{em} =520 nm), tetrachlorofluorescein (TET) (λ_{em} = 535 nm), 2',7'-dimethoxy-4',5'-dichloro-6-carboxyfluorescein (JOE)(λ_{em} = 548 nm) and hexachlorofluorescein (HEX) (λ_{em} = 550 nm). The quenching ability of DABCYL molecule was intensively investigated in numerous biological systems with oligonucleotides (for nucleic acid detection or peptide for monitoring enzymatic activity).²⁵

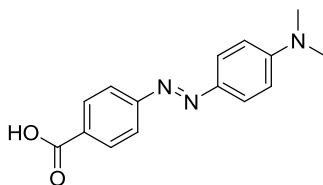


Figure 1-15: Structure of the universal quencher DABCYL.

1.4.4 Some of biological applications based on azobenzene photoswitching

Azobenzene has proven to be a useful tool for switching activities in biological systems. This is mainly due to three reasons: azobenzene chemistry is well established, photoisomerization of azobenzene is reversible and photoisomerization can easily be achieved by shining light on the azobenzene-based biological system to be regulated. Azobenzene photoregulation was extensively investigated in various biological systems as peptides, enzymes, ion channels and oligonucleotides.

1.4.4.1 Photoregulation of peptides by azobenzene

Azobenzene derivatives were employed to photo-induce random/ α -helix transitions in polypeptides. The first example of polypeptides containing photoisomerizable azobenzene chromophore were reported by Goodman,^{26a,b} who used phenylazophenyl alanine for photoregulation of polypeptides.

To follow the variation of polypeptide structures corresponding to the photoisomerization of tethered azobenzene, circular dichroism (CD) was used. It was the most effective technique since the various polypeptide structures, random coil, α -helix and β -structure have a characteristic circular dichroism spectra. Pieroni and coworkers^{27a,b} reported the incorporation of azobenzene into the side chain of poly(L-glutamic acid). In organic solvents as trifluoroethanol or trimethyl phosphate (TMP), the azo-based polypeptide has been confirmed by CD to exist in α -helix structure. Upon illumination at 350 nm to produce *trans*-to-*cis* photoisomerization, no change in CD spectrum was observed. This indicates, under these solvents, light does not induce any variation in the main-chain structures. While in water at critical pH values,²⁸ 20% azo-modified poly(L-glutamic acid) exhibited CD spectra attributed to random coil structure and upon irradiation no change in the CD was observed. By the addition of surfactant dodecylammonium chloride (DAC)^{27b} at its critical micelle concentration, the CD spectrum confers the random coil structure. Upon exposure to light at 350 nm, CD spectrum confirms switching of the azo-modified polypeptide from random coil to up to 30% α -helix structure. A complete conversion from α -helix to random coil transition was obtained by irradiation of the sample at 450 nm or thermally in the dark.

The effect of *trans*-to-*cis* isomerization of azobenzene derivatives has been investigated by photoinducing the helical sense of poly(L-aspartate).^{29a-c} In 1,2-dichloroethane, the poly(L-aspartate) with high content of azo units has been confirmed to exist in left-handed helical structure and upon irradiation with uv-light at 350 nm, a transition to right-handed helical structure was observed. It was found that using solvent mixtures as 1,2-dichloroethane: trimethyl phosphate (TMP) (75:25%) induces a large photoresponsive effect even at a low content of azo units.

Another example of photoregulation of cyclic peptide by azobenzene was reported by Vollmer and coworkers,³⁰ they designed a peptide system composed of two cyclic octapeptides with alternating D- and L- α -amino acids linked by an azobenzene linker as shown in (Fig. 1-16). Azobenzene is known to exist in the more thermally stable *trans* isomer and thus the peptides were assembled in high-order oligomers due to

intermolecular hydrogen bonding between the peptides. Upon irradiation with UV light at 366 nm, a conversion from intermolecular assemblies into single intramolecular hydrogen bonded species was observed due to *trans*-to-*cis* isomerization and recovery of *trans* isomer was obtained via irradiation with visible light. The photoisomerization of the azobenzene-based cyclopeptide was completely reversible in both directions.

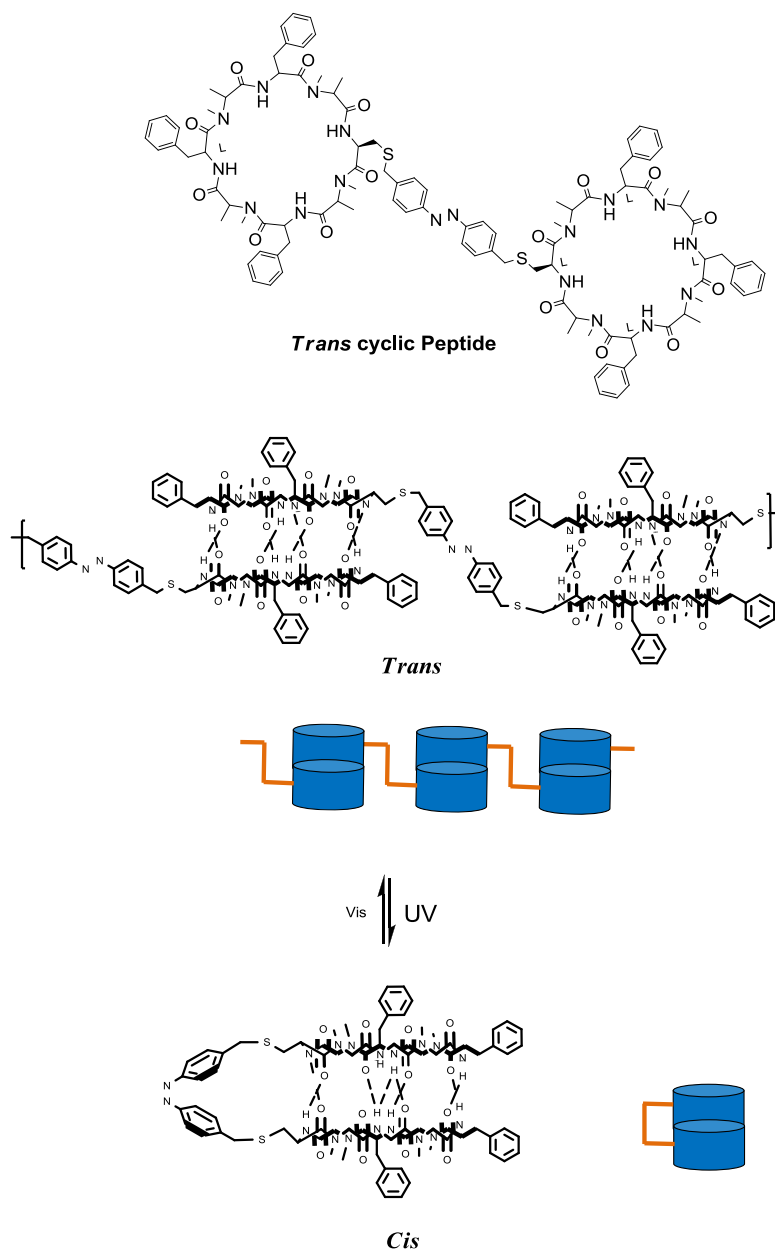


Figure 1-16: Photoisomerization of azobenzene-based cyclic peptides. Upon UV irradiation, a conversion from intermolecular assemblies (*trans* form) into single intramolecular hydrogen bonded species (*cis* form) was obtained.

1.4.5 Photoregulation of enzymatic activities by azobenzene

Azobenzene has been widely used for reversible switching by light between alternative conformations of peptides and proteins. Different approaches have been used to introduce azobenzene into peptides and proteins such as, incorporation during peptide synthesis,^{31a,b} incorporation during in vitro translation,³² incorporation in vivo by utilizing an orthogonal tRNA/aminoacyl-tRNA synthetase pair (specific for phenylalanine-4'-azobenzene³³) and through chemical modification of peptides and proteins.³⁴ Photoregulation of enzyme activities has been achieved for numerous kinds of enzymes as phospholipase,³³ papain, α -chymotrypsin, RNase S.³⁵

α -Chymotrypsin and papain catalyze the cleavage of peptide bonds, controlling the enzymatic activity of α -chymotrypsin and papain by azobenzene was found to take place in different mechanisms. α -Chymotrypsin³⁶ activity was controlled by photoisomerization of azobenzene through immobilizing the α -chymotrypsin inside a copolymer matrix containing azobenzene moieties. In other words, there was no need to directly attach azobenzene unit to the enzyme. Willner and coworkers³⁷ have shown that photocontrol of papain activity can be achieved in a different way, through photoisomerization of covalently attached azobenzene moieties to the lysine residues in the enzyme backbone. They believed that the photoisomerization of *trans*-azobenzene units to *cis* isomers is accompanied with structural changes in the protein backbone and consequently affects the binding properties of the enzyme toward the substrate.

Schierlinga and coworkers³⁸ were able to control the activity of restriction enzyme PvuII for gene targeting DNA genome at specific sites in *vivo*. To accomplish this purpose, 4,4'-bis(maleimido)azobenzene has been used as azobenzene analogue. Azobenzene moieties were attached through two cysteine residues between the two halves of the enzyme PvuII and thereby cross-linking them. Upon illumination with blue light (450 nm), an increase in DNA cleavage activity up to 16 fold was observed by changing the configuration of azobenzene units from *cis* to *trans*.

1.4.5.1 Incorporation of azobenzene to oligonucleotides

The first example of reversibly photoswitchable oligonucleotides was introduced by Yamana and co-workers.^{39a,b} They were able to bind two oligonucleotides via azobenzene as a linker, upon irradiation with light at around 350 nm the azobenzene linkers efficiently undergo *trans*-to-*cis* isomerization. Later, Komiyama's group incorporated azobenzene (Fig. 1-17) to the side chain of DNA oligonucleotides using phosphoramidite chemistry. In this study, a short DNA oligomer was synthesized (homothymidine-8mer) whereas azobenzene was introduced as a replacement of one nucleoside. In case of *trans* isomer, the melting temperature between the azobenzene containing homothymidine and homoadenosine was found to be slightly different from that between unmodified homothymidine and homoadenosine by 0.9 °C. Upon photoisomerization to *cis* isomer, a reduction of 8.9 °C in the melting curve was observed. On the basis of these results Komiyama investigated the ability of azobenzene-photoisomerization on the regulation of DNA duplex⁴⁰ and triplex.⁴¹

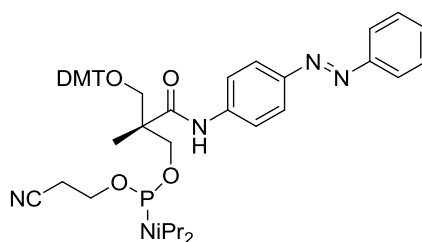


Figure 1-17: Structure of azobenzene monomer used in photoregulation of DNA.

1.4.5.1.1 Photoregulation of DNA transcription by azobenzene

Asanuma and coworkers⁴² were able to utilize azobenzene in photoregulation of the transcription through controlling T7 RNA polymerase reaction (T7 RNAP). At the first study, a 20-mer containing the azobenzene residue at different locations as an insertion without replacement of any nucleotide was synthesized and a 39-mer was used to form the double stranded T7 promoter (Fig. 1-18). It was found that upon illumination with visible light, the azobenzene units exist in the *trans* isomer, the transcription rate was suppressed by 10% relative to the control reaction. While by irradiation with UV light the *cis* isomer was generated and consequently the transcription rate was increased. They

explained the effect of *trans* to *cis* photoisomerization on the transcription by that when azobenzene exist as *trans* configuration can intercalate between the DNA double strands and thus maintain the DNA duplex. By switching *trans* to *cis* isomer, the azobenzene disturbed the DNA duplex and thus facilitates the transcription reaction. The regulation of transcription was found to be dependent on the azobenzene unit location. The highest efficiency of transcription photoregulation was achieved when azobenzene unit was located between the 10th and 11th nucleotides of the non template strand. The T7 promoter has two functional regions known as "loop binding region" and "the unwinding region". Later, it was found that the introduction of two azobenzene residues into the nontemplate strand of the T7 promoter whereas one at position-9 (in the loop binding region) and at position-3 (in the unwinding region) afforded 7.6 fold increase in transcription rate after irradiation with UV light (Fig.1-18b).⁴³

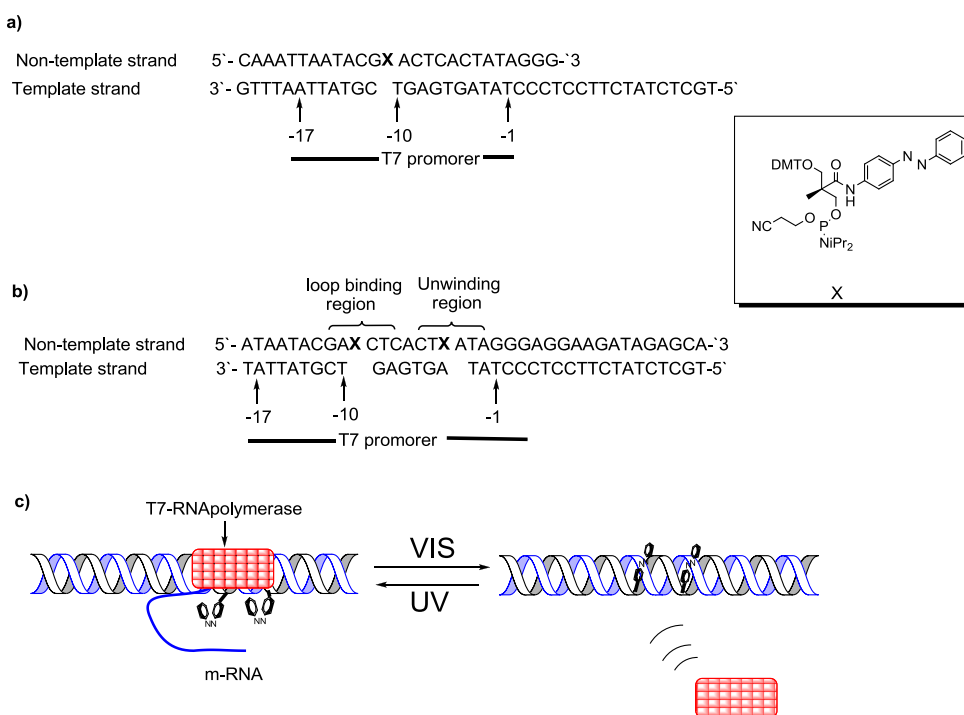


Figure 1-18: Photoswitching of transcription using T7 RNA polymerase.

1.4.5.1.2 Control RNase H activity by azobenzene

RNase H, is an enzyme which hydrolyzes RNA only when it is hybridized to the complementary DNA. Komiyama and coworkers⁴⁴ have investigated the control of

RNase H activity through the photoisomerization of azobenzene. In their study, a model of a 20-mer sense RNA strand was designed to hybridize to 20-mer native antisense DNA strand and another 20-mer sense DNA strand containing five azobenzene residues as extra residues. As illustrated in (Fig. 1-19), at the beginning the azobenzene containing antisense DNA strands was hybridized with DNA sense forming a stable duplex ($T_m = 60.8\text{ }^\circ\text{C}$ in the *trans* form). Upon illumination with UV light, the *cis* isomer was produced and thus the duplex was destabilized ($T_m = 42.6\text{ }^\circ\text{C}$) and consequently the antisense DNA strand is released due to the instability of the sense/antisense duplex and is hybridized to the RNA strand, thusly RNA strand was subjected to digestion by RNase H. It was found that the RNase H activity was increased by 3 fold after UV irradiation.

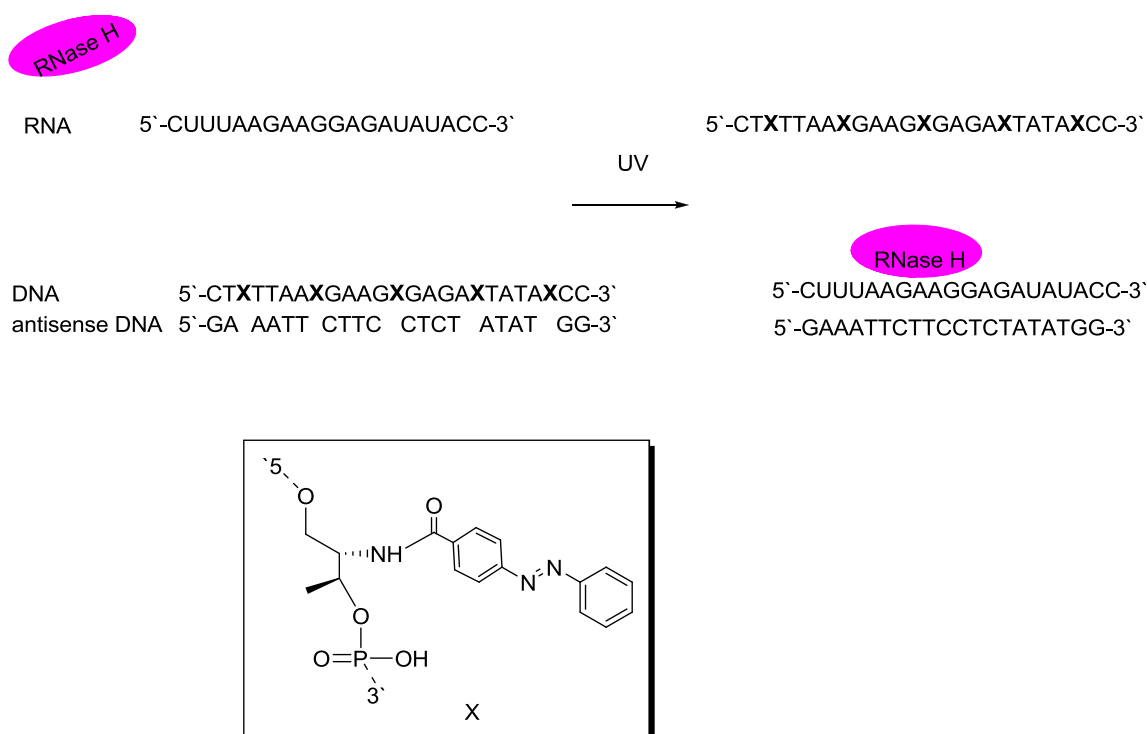


Figure 1-19: Photoregulation of RNase H activity.

1.4.6 New properties of azobenzene

It is well known that azobenzene derivatives are not inherently fluorescent which is ascribed to the high efficiency of *trans-cis* photoisomerization. Kawashima and coworkers^{45a,b} reported the synthesis of an azobenzene fluorescent molecule by

incorporating bis-pentafluorophenyl borane moiety at an *ortho* position of azobenzene as shown in (Fig1-20). With varying donor/acceptor groups at *para* positions of azobenzene led to azobenzenes characterized by its ability to emit green, yellow, orange and red fluorescence. The fluorescence property of boron-based azobenzene derivatives is due to the coordination of boron atom with the lone pair of azo nitrogen atom and thusly, the isomerisation around the azo bond is restricted and consequently upon excitation of boron-based azobenzene derivatives, the photoisomerization pathway is less favoured.

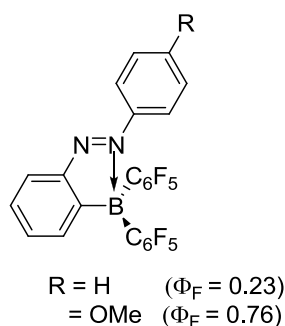


Figure 1-20: Fluorescent azobenzene due to B-N interaction.

Furthermore, Siewersten and coworkers^{46a,b} were able to tune the photoswitching wavelength of azobenzene. They have designed an azobenzene derivative with unexpected properties characterized by an ethylene bridge which connects the two phenyl rings at the *ortho* position. As shown in (Fig. 1-21), this design strains and disrupts the *trans* isomer, therefore, the *cis* isomer become the more thermally stable. They were able to obtain the *trans*-to-*cis* photoisomerization with green light irradiation (480-550 nm) with efficiency close to 100% due to the effect of ethylene bridge, while *cis* -to-*trans* photoisomerization occurs with near UV light (380-400 nm).

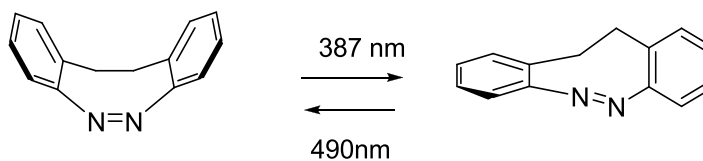


Figure 1-21: Bridged azobenzene

1.5 Goals of this thesis

The aim of this thesis was to develop novel quenchers for labeling fluorescent hybridization probes that may be used for the detection of DNA mutations.

Since 4-(*N,N*-dimethylamino)azobenzene-4'-carboxylic acid (DABCYL) is a common quencher that is used for labeling fluorescent probes, we aimed to introduce it into peptide nucleic acid (PNA). The 4-(*N,N*-dimethylamino)azobenzene moiety may be introduced into PNA as a nucleobase replacement and evaluation of its quenching and photoresponse abilities can be done. The quenching efficiency of the 4-(*N,N*-dimethylamino)-azobenzene moiety was evaluated in a PNA molecular beacon design.

Furthermore, because the azobenzene molecule is not able to participate in the hydrogen bond network with nucleobases, we aimed to introduce a novel uracil-based quencher that mimics the structure of the universal quencher DABCYL. The modified uracil is designed to have a 4-(*N,N*-dimethylamino)phenylazo moiety at C5 which does not interfere with hydrogen bonding sites of uracil and therefore retain the base pairing ability with adenine.

There are several advantages of the synthesis of modified uracil analogue with intrinsic quenching ability such as it may be used as a quencher in molecular beacon probes, possibility to attach the modified uracil at any position of the designed oligomer and therefore may lead to increase the stability of the formed duplex with the complementary nucleic acid and finally, the presence of phenylazouracil moiety that can undergo configurational change upon excitation with light at certain wavelength may lead to its use in photoregulation of the formed duplex between oligomer that contains the modified uracil and the complementary nucleic acid sequence.

1.6 References

1. a) Watson, J.D.; Crick, F.H.C. Molecular structure of nucleic acids; A structure for deoxyribose nucleic acid, *Nature*, **1953**, 171, 737-738. b) Watson, J.D.; Crick, F. H.C. Genetical implications of the structure of deoxyribosenucleic acid, *Nature*, **1953**, 171, 964-967.
2. Crick, F.H.C. Central dogma of molecular biology, *Nature*, **1970**, 227, 561-563.
3. Beaucage, S.L.; Iyer, R.P., The synthesis of modified oligonucleotides by the Phosphoramidite approach and their applications, *Tetrahedron*, **1993**, 49, 6123-6194.
4. Imaio, M.; Arai, T. Synthesis and photochemical properties of polyphenylene dendrimers with photoreactive stilbene core, *Tetrahedron Lett.*, **2002**, 43, 5265-5268.
5. Masahiro, I.M. Diarylethenes for memories and switches, *Chem. Rev.*, **2000**, 100, 1685-1716.
6. Quemina, D.; Preat, J.; Wathélet, V.; Fontaine, M.; Peréte, A. E. Thioindigo dyes: highly accurate visible spectra with TD-DFT, *J. Am. Chem. Soc.*, **2006**, 128, 2072-2083.
7. Orlandi, G.A.; Garavelli, M. Significance of a zwitterionic state for fulgide photochromism: implications for the design of mimics, *Angew. Chemie. Int. Ed.*, **2010**, 49, 2913-2916.
8. Wang, S.; Songa, Y.; Jiang, L. Photoresponsive surfaces with controllable wettability, *J. Photochem. Photobio. C: Photochem. Rev.*, **2007**, 8, 18-29.
9. a) Meister, L.; Bruning, H. Preparation of red, brown and yellow colors by the action of the disulfo acids of β naphthal on diazo compounds, *J. Am. Chem. Soc.*, **1879**, 1, 120. b) James, H.; Stebbins, Jr. New azo colors belonging to the so-called tetrazo group, *J. Am. Chem. Soc.*, **1881**, 3, 20-23.
10. Zollinger, H. *Color chemistry, syntheses, properties and applications of organic dyes and pigments*; 3rd revised Ed.; Wiley-VCH; Weinheim, **2003**.
11. Pedersen, T.G.; Johansen, P.M.; Pedersen, H. C. Characterization of azobenzene chromophores for reversible optical data storage: molecular quantum calculations. *J. Opt. A: Pure Appl. Opt.*, **2000**, 2, 272-278.

12. Wu, Y.; Kanazawa, A.; Shiono, T.; Ikeda, T.; Zhang, Q. Photoinduced alignment of polymer liquid crystals containing azobenzene moieties in the side chain. 4. dynamic study of the alignment process. *Polymer*, **1999**, 40, 4787-4793.
13. Harada, A. Cyclodextrin-based molecular machines, *Acc. Chem. Res.*, **2001**, 34, 456-464.
14. a) Ulysse, L.; Cubillos, J.; Chmielewski, J. Photoregulation of cyclic peptide conformation, *J. Am. Chem. Soc.*, **1995**, 117, 8466-8467. b) James, D.A.; Burns, D.C.; Woolley, G.A. Kinetic characterization of Ribonuclease S mutants containing photoisomerizable phenylazophenylalanine residues, *Protein Eng.* **2001**, 14, 983-991.
15. a) Rau, H. *Photochromism: molecules and systems*. Elsevier: Amsterdam, **1990**. b) Griffiths, J. Photochemistry of azobenzene and its derivatives, *J. Chem. Soc. Rev.*, **1972**, 1, 481-493.
16. Hampson, G.C.; Robertson, J.M. Bond lengths and resonance in the *cis*-azo-benzene molecule, *J. Chem. Soc.*, **1941**, 409-413.
17. a) Dias, A.R.; Dapiedade, M.E.M.; Simoes, J.A.M.; Simoni, J.A.; Teixeira, C.; Diogo, H.P.; Yang, M.Y.; Pilcher, G. Enthalpies of formation of *cis*-azobenzene and *trans*-azobenzene, *J. Chem. Thermodyn.*, **1992**, 24, 439-447. b) Schulze, F.W.; Petrick, H. J.; Cammenga, H.K.; Klinge, H.Z. *Phy. Chem.,(Wiesbaden)*, **1977**, 107, 1-19.
18. Talaty, E.R.; Fargo, J.C. Thermal *cis-trans* isomerization of substituted azobenzenes, *Chem. Comm.*, **1967**, 65-66.
19. a) Rau, H. Further evidence for rotation in the π - π^* and inversion in the n - π^* photo isomerization of azobenzenes, *J. Photochem.* **1984**, 26, 221-225. b) Monti, S.; Orlandi, G.; Palmieri, P. Features of the photochemically active state surfaces of azobenzene, *Chem. Phys.*, **1982**, 71, 87-99. c) Olbrich, G. INDO-SCF and CI calculations on the *trans-cis* isomerization of azomethane in the ground state and in excited states, *Chem. Phys.* **1978**, 27, 117-125. d) Baird, N.C.; Swenson, J.R. Quantum Organic Photochemistry. IV. The photo-isomerization of diimide and azoalkanes, *Can. J. Chem.* **1973**, 57, 3097-3101. e) Camp, R.N.; Epstein, I.R.; Steel, C. Theoretical studies of the photochemistry of acyclic azoalkanes, *J. Am. Chem. Soc.* **1977**, 99, 2453-2459.

20. Xie, S.; Natansohn, A.; Rochon, P. Recent developments in aromatic azo polymers research, *Chem. Mater.*, **1993**, 5, 403-411.
21. a) Whitten, D.G.; Wildes, P. D.; Pacifici, J. G.; Irick, G.; Solvent and substituent on the thermal isomerization of substituted azobenzenes. Flash spectroscopic study. *J. Am. Chem. Soc.*, **1971**, 93, 2004-2008. b) Haberfield, P.; Block, P. M.; Lux, M. S. J. Enthalpies of solvent transfer of the transition states in the *cis-trans* isomerization of azo compounds. Rotation vs. the nitrogen inversion mechanism, *J. Am. Chem. Soc.*, **1975**, 97, 5804-5806.
22. Dunn, N.J.; Humphries IV, W.H.; Offenbacher, A. R.; King, T.L.; Gray, J.A. pH-dependent *cis*→*trans* isomerization rates for azobenzene dyes in aqueous solution, *J. Phys. Chem. A*, **2009**, 113, 13144-13151.
23. Youngmi, K.; Dosung, S.; Weihong, T. Molecular beacons in biomedical detection and clinical diagnosis, *Int. J. Clin. Exp. Pathol.*, **2008**, 1, 105-116.
24. Zhang, Y.Z.; Liu, Y.X.; Zhou, C.X.; Liu, Y.; Zhou, B.; Ding, X.L. ; Liu, Y. Fluorescence study on the interaction of bovine serum albumin with *p*-aminoazobenzene, *J. Fluoresc.*, **2008**, 18, 109-118.
25. Felderbauer, P.; Schnekenburger, J.; Lebert, R.; Bulut, K.; Parry, M.; Meister, T.; Schick, V.; Schmitz, F.; Domschke, W.; Schmidt E. W.; A novel A121T mutation in human cationic trypsinogen associated with hereditary pancreatitis: functional data indicating a loss-of-function mutation influencing the R122 trypsin cleavage site, *J. Med. Genet.* **2008**, 45, 507-512.
26. a) Goodman, M.; Kossoy, A. Conformational aspects of polypeptide structure. xix. azoaromatic side-chain effects, *J. Am. Chem. Soc.* **1966**, 88, 5010-5015. b) Goodman, M.; Falxa, M.L. Conformational aspects of polypeptide structure. XXIII. Photoisomerization of azoaromatic polypeptides, *J. Am. Chem. Soc.* **1967**, 89, 3863-3867.
27. a) Pieroni, O.; Houben, J.L.; Fissi, A.; Costantino, P., Reversible conformational changes induced by light in poly(L-glutamic acid) with photochromic side-chains, *J. Am. Chem. Soc.*, **1980**, 102, 5913-5915. b) Pieroni, O.; Fabbri, D.; Fissi, A.; Ciardelli, F., Photomodulated conformational-changes of azo-modified poly(L-glutamic acid) in micellar systems., *Makromol. Chem., Rapid Commun.* **1988**, 9, 637-640.

28. Ciardelli, F.; Pieroni, O.; Fissi, A.; Houben, J.L., Azobenzene-containing polypeptides-photoregulation of conformation in solution. *Biopolymers* **1984**, *23*, 1423-1437.
29. a) Ueno, A.; Anzai, J.; Osa, T.; Kadoma, Y. Light-induced conformational changes of polypeptides. photoisomerization of azoaromatic polypeptides. *Bull. Chem. Soc. Jpn.* **1979**, *52*, 549-554. b) Ueno, A.; Takahashi, K.; Anzai, J.; Osa, T. Photocontrol of polypeptide helix sense by *cis-trans* isomerization of side-chain azobenzene moieties. *J. Am. Chem. Soc.* **1981**, *103*, 6410-6415. c) Ueno, A.; Adachi, K.; Nakamura, J.; Osa, T. Photoinduced conformational changes of azoaromatic polyaspartes containing octadecyl side chains. *J. Polym. Sci., Polym. Chem.* **1990**, *28*, 1161-1170.
30. Vollmer, M.S.; Clark, T.D.; Steinem, C.; Ghadin, M. R. Photoswitchable hydrogen-bonding in self-organized cylindrical peptide systems, *Angew. Chem. Int. Ed.* **1999**, *38*, 1598-1601.
31. a) Liu D, Karanicolas, J; Yu, C.; Zhang, Z.; Woolley, G.A. Site-specific incorporation of photoisomerizable azobenzene groups into ribonuclease S, *Bioorg. Med. Chem. Lett.*, **1997**, *7*, 2677-2680. b) Ueda, T.; Murayama, K.; Yamamoto, T.; Kimura, S.; Imanishi, Y. Photoregulation of hydrolysis activity of semisynthetic mutant phospholipases A2 replaced by non-natural aromatic amino acids. *J. Chem. Soc. Perk. T.*, **1994**, *1*, 225-230.
32. Muranaka, N.; Hohsaka, T.; Sisido, M. Photoswitching of peroxidase activity by position-specific incorporation of a photoisomerizable non-natural amino acid into horseradish peroxidase. *FEBS Lett.*, **2002**, *510*, 10-12.
33. Bose, M.; Groff, D.; Xie, J.; Brustad, E.; Schultz, P.G. The incorporation of a photoisomerizable amino acid into proteins in E. coli. *J. Am. Chem. Soc.*, **2006**, *128*, 388-389.
34. Mayer, G.; Heckel, A. Biologically active molecules with a "light switch". *Angew. Chem. Int. Ed.*, **2006**, *45*, 4900-4921.
35. Liu, D.; Karanicolas, J.; Yu, C.; Zhang, Z.; Woolley, G. A. Site-specific incorporation of photoisomerizable azobenzene groups into Ribonuclease S, *Bioorg. Med. Chem. Lett.* **1997**, *7*, 2677-2680.

36. Willner, I.; Rubin, S.; Shatzmiller, R.; Zor, T. Photoregulation of α -chymotrypsin by its immobilization in a photochromic azobenzene copolymer, *J. Am. Chem. Soc.*, **1993**, 115, 8690-8694.
37. Willner, S.; Rubin, A.; Riklin, J. Photoregulation of Papain activity through anchoring photochromic azo groups to the enzyme, *J. Am. Chem. Soc.*, **1991**, 113, 3321-3325.
38. Schierlinga, B.; Noëla, A.; Wendea, W.; Hienb, L.H.; Volkovb, E.; Kubarevab, E.; Oretskaya, T.; Kokkinidis, M.; Römpf, A.; Spengler, B.; Pingoud, A.; Controlling the enzymatic activity of a restriction enzyme by light, *PNAS*, **2010**, 107, 1361-1366.
39. a) Yamana, K.; Yoshikawa, A.; Nakano, H. Synthesis of a new photoisomerizable linker for connecting two oligonucleotide segments, *Tetrahedron Lett.*, **1996**, 37, 637-640. b) Yamana, K.; Yoshikawa, A.; Kan, K.; Nakano, H. Synthesis of oligonucleotides containing a new azobenzene fragment with efficient photoisomerizability, *Bioorg. Med. Chem. Lett.*, **1999**, 7, 2977-2983.
40. Asanuma, H.; Ito, T.; Yoshida, T.; Liang, X.; Komiyama, M. Photoregulation of the formation of and dissociation of a DNA duplex by using the *cis-trans* isomerization of azobenzene, *Angew. Chem.* **1999**, 111, 2547-2549; *Angew. Chem. Int. Ed.*, **1999**, 38, 2393-2395.
41. Asanuma, H.; Liang, X.; Yoshida, T.; Yamazawa, A.; Komiyama, M. Photo-control of triplex formation by azobenzene-bearing oligo(thymidine), *Angew. Chem.*, **2000**, 112, 1372-1374. *Angew. Chem. Int. Ed.*, **2000**, 39, 1316-1318.
42. Asanuma, H.; Tamaru, D.; Yamazawa, A.; Liu, M.; Komiyama, M. Photo-regulation of transcription reaction by T7 RNA polymerase by tethering an azobenzene in the promoter, *Chem. Bio. Chem.*, **2002**, 3, 786-789.
43. Liu, M.; Asanuma, H.; Komiyama, M. Azobenzene-tethered T7 promoter for efficient photoregulation of transcription, *J. Am. Chem. Soc.*, **2006**, 128, 1009-1015.
44. Matsunaga, D.; Asanuma, H.; Komiyama, M. Photoregulation of RNA digestion by RNase H with azobenzene-tethered, *J. Am. Chem. Soc.*, **2004**, 126, 11452-11453.
45. a) Yoshino, J.; Kano, N.; Kawashima, T. Synthesis of the most intensely fluorescent azobenzene by utilizing the B-N interaction, *Chem. Commun.*, **2007**, 559-561. b) Yoshino, J.; Furuta, A.; Kame, T.; Itoi, H.; Kano, N.; Kawashima, T.; Ito, Y.;

- Asashima, M. Intensely fluorescent azobenzenes: synthesis, crystal structures, effects of substituents, and application to fluorescent vital stain, *Chem.-Eur. J.*, **2010**, 16, 5026-5035.
- 46.** a) Siewertsen, R.; Neumann, H.; Buchheim-Stehn, B.; Herges, R.; Nather, C.; Renth, F.; Temps, F. Highly efficient reversible Z-E photoisomerization of a bridged azobenzene with visible light through resolved s(1)(n-pi*) absorption bands, *J. Am. Chem. Soc.*, **2009**, 131, 15594-15595. b) Siewertsen, R.; Schonborn, J.B.; Hartke, B.; Renth, F.; Temps, F. Superior Z → E and E → Z photoswitching dynamics of dihydrodibenzodiazocine, a bridged azobenzene, by S₁(nπ*) excitation at λ = 387 and 490 nm, *Phys. Chem. Chem. Phys.*, **2011**, 13, 1054-1063.

Chapter 2

Chapter 2

2 Synthesis and Photophysical Studies of Azo-Based Quencher for PNA-Molecular beacon

Using fluorescent probes for nucleic acid detection has attracted much attention due to its efficiency, ease of synthesis and availability of commercial reporters that facilitate the probe synthesis. Nucleic acid detection takes place by changing either the intensity of the reporters fluorescent signal or the colour of its fluorescence. In this chapter, we describe the synthesis of a peptide nucleic acid monomer carrying an azobenzene unit and evaluation of its photoisomerization and quenching properties. In the following section a brief overview on the origin of fluorescence and mechanism of fluorescence generation in different types of fluorescent hybridization probes will be given.

2.1 Fluorescence

Luminescence is a spectrochemical process that involves the emission of light as a result of irradiating a molecule at certain wavelength. This process is due to the molecule absorbing photons and consequently being excited to higher electronic states. When relaxing back to the ground state, it accompanied with emission of light. Light emission usually takes place at longer wavelength due to loss of some of its energy as heat. The difference between the maximum absorption and maximum emission is known as "Stokes shift" referred to *Sir. G. G. STOKES* who described this phenomena.¹

Luminescence is divided into two major types, fluorescence and phosphorescence depending on the electronic states that photons are relaxing from as singlet (S) or triplet (T) states, respectively, as shown in simplified Jablonski diagram (Fig. 2-1). There are two important features that distinguish fluorophores: 1) fluorescence quantum yield and 2) life time. Fluorescence quantum yield (Φ_F), is the ratio of absorbed photons to emitted photons. In other words, fluorescence efficiency is determined by the fraction of excited molecules that can emit light when relaxing from excited state by fluorescence rather than any of non-radiative mechanism.

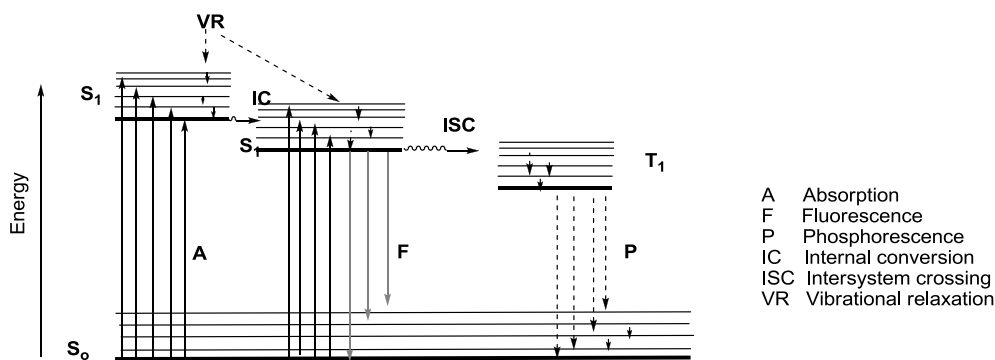


Figure 2-1: Jablonski diagram illustrated luminescence origin.

2.2 Fluorescence resonance energy transfer (FRET) theory and fluorescent hybridization probes

Several types of fluorescent probes have been reported and they are all labelled with at least one fluorophore. Upon excitation of that fluorophore at an appropriate wavelength, it will be excited from the ground state to a higher excited singlet state. Relaxation of fluorophore back to lowest singlet state is accompanied by the emission of light. Most fluorescent detection protocols are based on the ability of nearby molecule, another fluorophore or non-fluorescent molecule, to decrease the intensity of fluorescence.

Mainly, there are two mechanisms for fluorescent signal quenching, contact quenching and fluorescence resonance energy transfer (FRET). In contact quenching mechanism, an interaction between the donor (fluorophore) and the acceptor (fluorophore or nonfluorescent molecule) is mediated through hydrogen bonding “called proton-coupled electron transfer” forming non-fluorescent complex. The characteristic feature of contact quenching mechanism is the absorption spectral change of the donor and acceptor at the time of complex formation.

Fluorescence resonance energy transfer (FRET) mechanism, also called (Förster resonance energy transfer),² involves the transfer of the excitation energy to a nearby acceptor in non-radiative fashion through energy exchange of the donor oscillating dipole with an acceptor dipole that has similar resonance frequency.

There are two main strategies behind the design of FRET probes for biological studies. One is by designing the probe by using two fluorescent dyes. In this type a donor fluorescent dye is irradiated at its excitation wavelength and by FRET, the excitation energy is transferred to the acceptor fluorescent dye and consequently it is excited and emits light at its characteristic emission wavelength. Alternatively, a probe can carry a donor fluorescent dye at one terminus and nonfluorescent molecule which acts as acceptor, called a "quencher", at the other end. Quenchers are molecules capable of quenching the fluorescent signal without emitting light. The efficiency of FRET relies on the distance between the donor and acceptor and the extent of spectral overlapping between absorption spectra of acceptor with the emission spectra of the donor as shown in (Fig. 2-2). The effective distance between the donor and acceptor is in the range of 10-100Å³ which is roughly equal to the distance between 3-30 nucleotides in DNA duplex. The extent of spectral overlap is determined by Förster radius (R_o) and FRET efficiency (E) can be determined from equation (Eq. 2-1).

$$E = (1 + R^6/R_o^6)^{-1} \quad (\text{Eq. 2-1})$$

Where R is the distance between the donor and acceptor, Förster radius for a given donor-acceptor pair, is conducted from equation (Eq.2-2).

$$R_o = 8.8 \times 10^{-28} \Phi_F k^2 n^{-4} J(v) \quad (\text{Eq. 2-2})$$

Where Φ_F is fluorescence quantum yield of the donor in the absence of the acceptor, n is the refractive index of the medium, K^2 is a parameter that depends on the relative orientation of the donor and acceptor transition moment and $J(v)$ is the spectral overlap between the donor emission and the acceptor absorption.

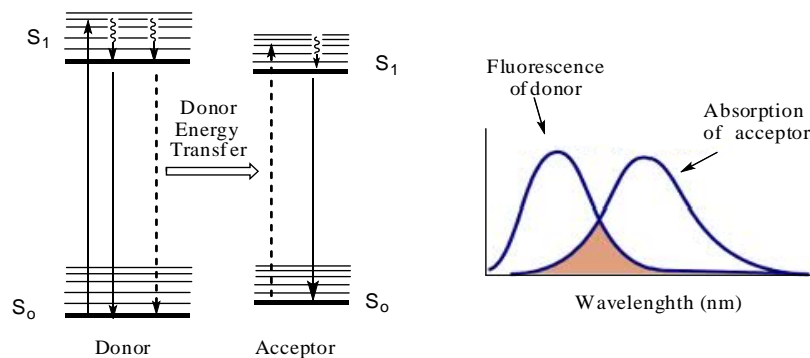


Figure 2-2: Resonance energy transfer Jablonski diagram and spectral overlap donor emission spectra with acceptor absorption spectra.

2.2.1 Examples of fluorescent hybridization probes using FRET mechanism

2.2.1.1 Adjacent probes or (Light Cycler™ hybridization probe)

In this technique, two single-stranded hybridization probes are designed in a way that they bind to neighboring sites on the target nucleic acid. The donor is attached to one probe at the 3`end while the other probe is labeled with acceptor at 5`end. Upon hybridization with the target, the donor and acceptor are located at a distance allows FRET to take place (Fig. 2-3).

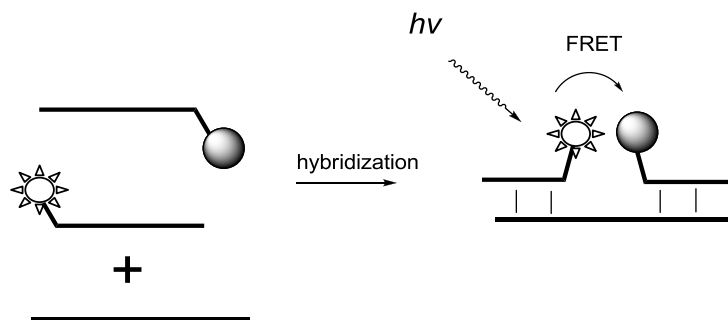


Figure 2-3: Schematic representation for adjacent probes.

2.2.1.2 5`-Nuclease probes or (TaqMan® probes)

A 5`-Nuclease probe is single-stranded probe labeled with a donor at one end and an acceptor at the other end and is amenable to 5`-nuclease digestion. This probe is

designed as polymerase chain reaction primer in addition to the complementary sequence for the target DNA. Upon hybridization to the target, DNA polymerase extends the primer and consequently digestion of the probe by 5'-nuclease is obtained. As a result of the cleavage, the donor and acceptor are separated and consequently the fluorescence signal intensity is increased as shown in (Fig. 2-4)

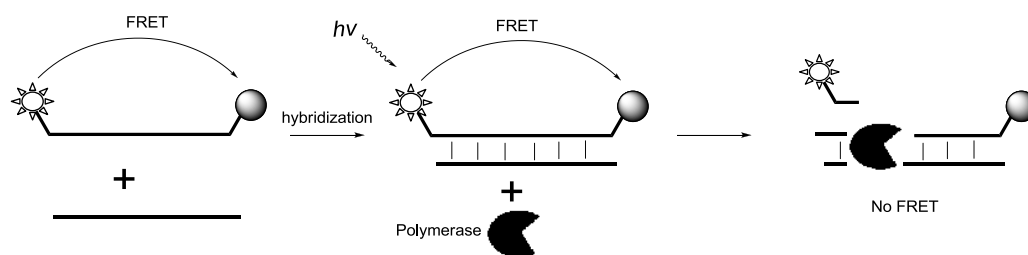


Figure 2-4: Schematic representation for 5'-nuclease probes.

2.2.1.3 Strand-displacement probes (or Yin-Yang probes)

In this technique, two complementary sequences are used whereas one sequence is labeled with donor and the other is labeled with quencher (nonfluorescent molecule). When the two probes are hybridized to each other forming a duplex, the fluorescence signal is quenched. In the presence of the target DNA, it binds with one of the two probes forming more stable hybrid and consequently the two labeled probes being separated leading to increase in fluorescence intensity (Fig. 2-5).

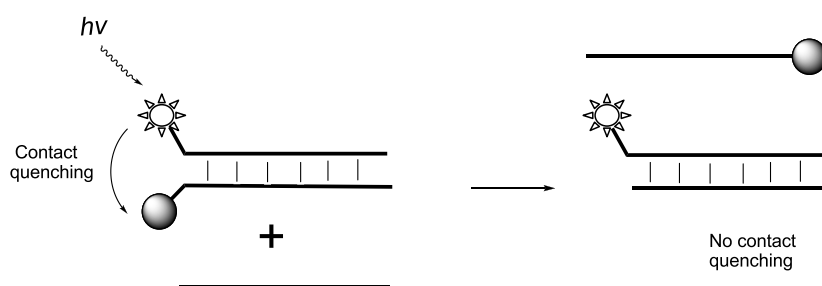


Figure 2-5: Schematic representation for strand-displacement probes.

2.2.1.4 Molecular beacon

Molecular (MB) beacon technology,⁴ one of the applications that used fluorescent probes in nucleic acid detection. A MB is a single stranded nucleic acid probe labelled with a

fluorescent dye (donor) in one end and a dye (acceptor) at the other end. MB probe design consists of three main domains: stem, loop and fluorophore/quencher pair. This design forces the fluorescent dye to be in close proximity to the quencher as illustrated in (Fig. 2-6). It was found that for PNA, a MB hairpin structure is not required to bring the quencher in close proximity to the fluorophore,⁵ therefore it is called a stemless PNA-MB. The probe sequence is chosen to be complementary to a specific target sequence that is present in the nucleic acid to be detected. When the fluorescent dye is excited the energy is transferred to the quencher through fluorescence resonance energy transfer (FRET) and therefore no emission is observed. Upon hybridization with the complementary single-stranded DNA target, the quencher is located farther from the fluorescent dye and as consequence the fluorescence signal is produced. Most MB probes are between 25 and 40 nucleotides long in which the recognition sequence (loop) usually consists of 15-30 nucleotides and the stem is formed by 5-10 base pairs.

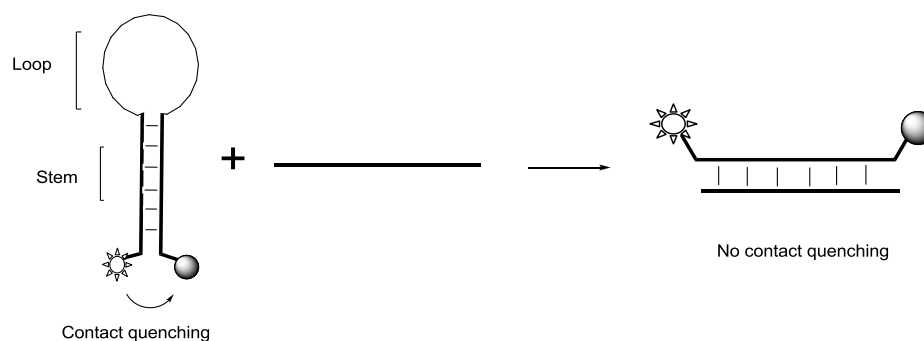


Figure 2-6 : Schematic representation for molecular beacon.

There are a plethora of commercially available fluorophores that are commonly used for labeling fluorescent hybridization probes such as fluorescein derivatives: 5-carboxyfluorescein (F) and 2',7'-dimethoxy-4',5'-dichloro-6-carboxyfluorescein (JOE) and rhodamine derivatives as : N,N,N',N'-tetramethyl-6-carboxyrhodamine (TAMRA); 6-carboxy-X-rhodamine (ROX) and 6-carboxyrhodamine (R6G). For example, quenchers that are commonly used are DDQ-1, Black hole quenchers (BHQ), Eclipse and Dabcyl (Fig. 2-7). The choice of fluorophore quencher combinations is mainly based on the emission range of the fluorophore that should overlap with the absorption range of the

quencher to facilitate the transfer energy from the fluorophore to the quencher via FRET and consequently quench the fluorescence of the fluorophore

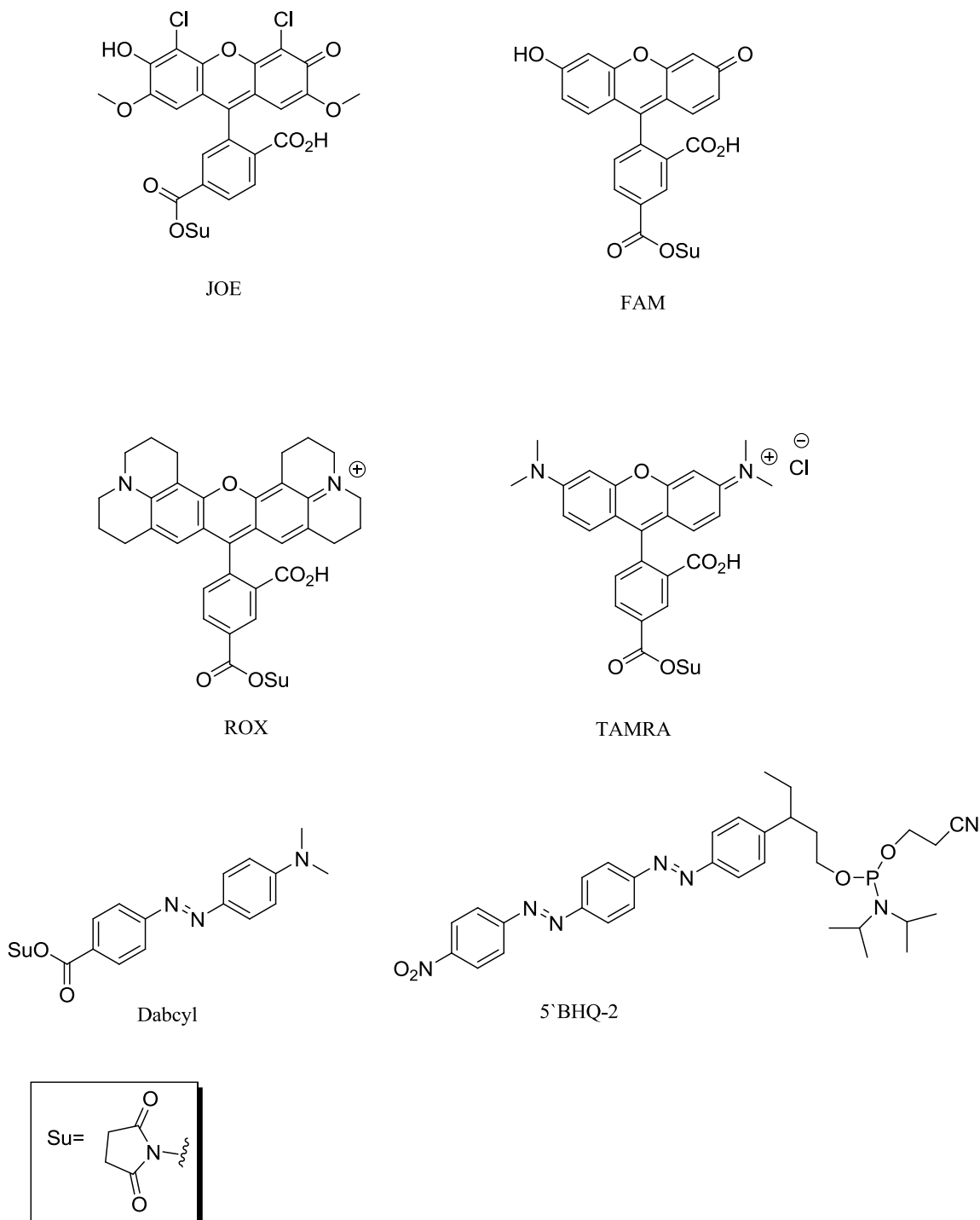


Figure 2-7: Examples of fluorophores and quenchers have been used in fluorescent probes.

2.3 Peptide nucleic acid (PNA)

Since many human diseases are related to genetic perturbations, detection of mutations has become an essential mission for scientists to accomplish. There are many causes contributing to the differences in sequences such as single nucleotide polymorphisms (SNP) or other sequence alterations such as point mutations, insertion and deletions. SNPs are considered the most common type of genetic variation among people, and their detection has attracted much attention.

Several techniques have been developed to detect SNPs based on nucleic acid probes tagged with a fluorescent moiety as a reporter. Currently, the utility of the fluorescent-based probes in SNP detection is the most common strategy due to their safety.⁶ A remarkable example of probes that have been used is peptide nucleic acids (PNAs). PNA, a DNA analog, was invented 20 years ago by Nielsen.⁷ It consists of a pseudo polypeptide backbone that is comprised of repeating *N*-(2-aminoethyl)glycine units and nucleobases are attached to the backbone via a methylene-carbonyl linker as illustrated in (Fig. 2-8). Unlike natural nucleic acids, PNA does not contain phosphate groups and therefore it possess a neutral character which provide stronger binding between PNA and its complementary nucleic acid than that between DNA: DNA and DNA: RNA at low to medium ionic strength.

The PNAs are depicted like peptide, from the *N*-terminus to the *C*- terminus, when the *N*-terminus of the PNA faces the 5'end of the DNA or RNA the complex is termed parallel. Formation of duplexes can be obtained in both parallel and anti-parallel orientations but the anti-parallel is strongly preferred. In addition, due to PNA's artificial character they show the ability to resist nuclease or protease degradation and consequently possess extended lifetime both *in vivo* and *in vitro*.⁸

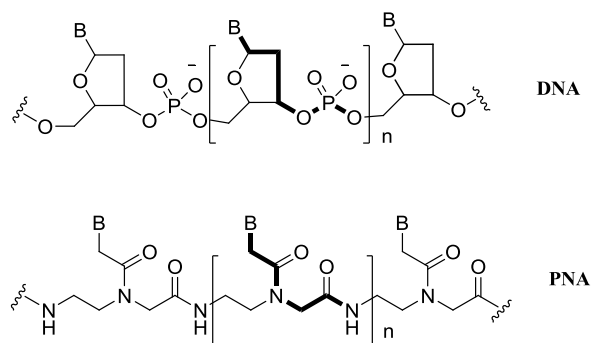


Figure 2-8: Comparison between DNA and PNA structures.

2.3.1 PNA binding modes with nucleic acids (NAs)

PNA forms stable duplexes with single stranded-nucleic acids similar to DNA:DNA and DNA: RNA obeying Watson-Crick base pairing rules. PNA may bind to the double stranded-DNA through different types of binding modes⁹ as illustrated in (Fig. 2-9). PNA binds with double stranded-DNA forming classical triplexes via Hoogsteen base pairing and this type of binding requires a high cytosine content of the PNA^{10a,b} (Fig. 2-9. A). Homopyrimidine PNAs bind to the complementary DNA forming (PNA)₂:DNA via triplex invasion^{10a,b} through opening the DNA double helix and one PNA strand binds to DNA obeying Watson-Crick base pairing rules and the other PNA binds through Hoogsteen base pairing (Fig. 2-9B).

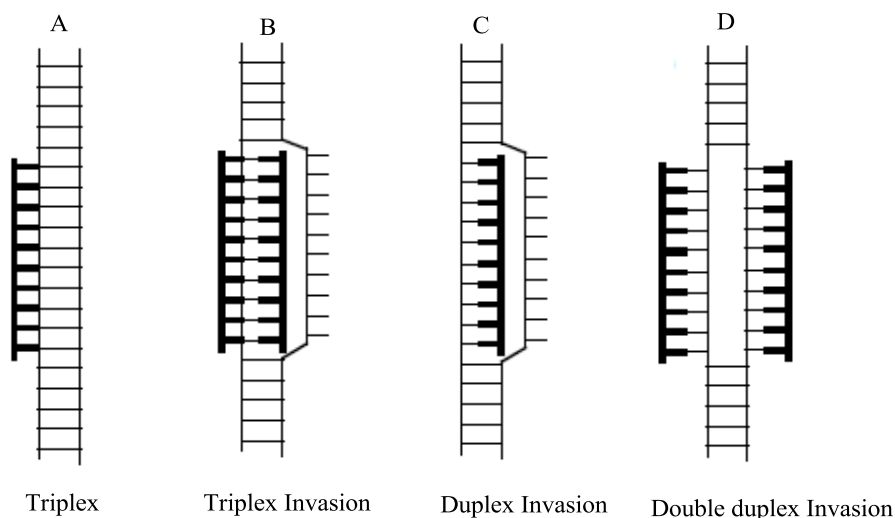


Figure 2-9: Binding modes of PNA with double-stranded DNA.

Thymine is able to engage with adenine by Hoogsteen pairing, while cytosine requires protonation which occurs below physiological pH to form stable Hoogsteen base pair with guanine. Such pH dependence limits this binding and this limitation can be avoided by replacing cytosine with pseudoisocytosines (ψ IC) "J-base"¹² or N⁷-guanine.¹³ PNA with high purine content can bind with double-stranded DNA forming duplex invasion via opening the DNA duplex helix followed by invasion of PNA (Fig. 2-9C). Finally, it was found that PNA has the ability to bind to DNA duplex via double duplex invasion by using modified nucleobases in the PNA strands "pseudo complementary PNAs" In this type of binding, the DNA target should contain at least 50% of AT and all A/T base pairs in PNA strand are replaced with 2,6-diaminopyrimidine/2-thiouracil base pair. The presence of 2,6-diaminopyrimidine/2-thiouracil base pairs in PNA prevents binding of the two PNA strands to each other due to the steric hindrance. Thusly, they bind only to the target DNA (Fig. 2-11). PNA has shown a high binding affinity and specificity for nucleic acids, therefore, it is considered a very interesting and potentially useful tool in molecular biology, and may have both diagnostic and therapeutic applications.^{14a-c}

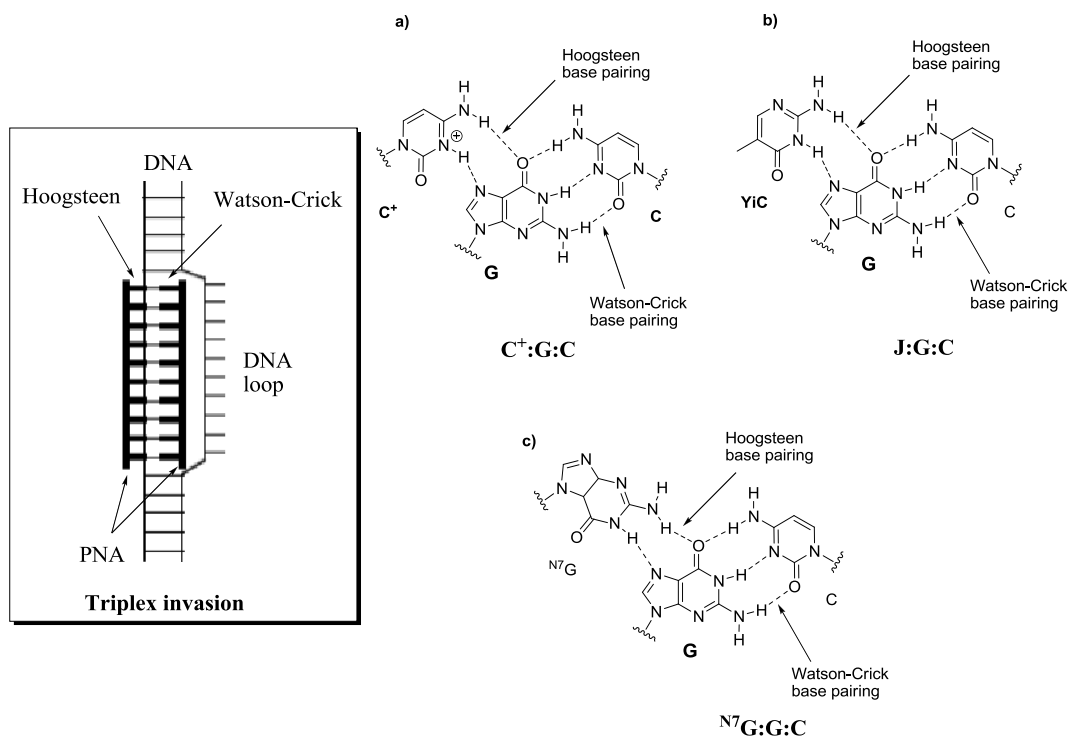


Figure 2-10: Triplex invasion of double helix DNA by homopyrimidine PNA oligomers. a) Protonated cytosine for Hoogsteen base pairing, replacing all cytosines with b) pseudoisocytosines (J) or c) N^7 -guanines in the Hoogsteen strand to avoid low pH required for N3 protonation.

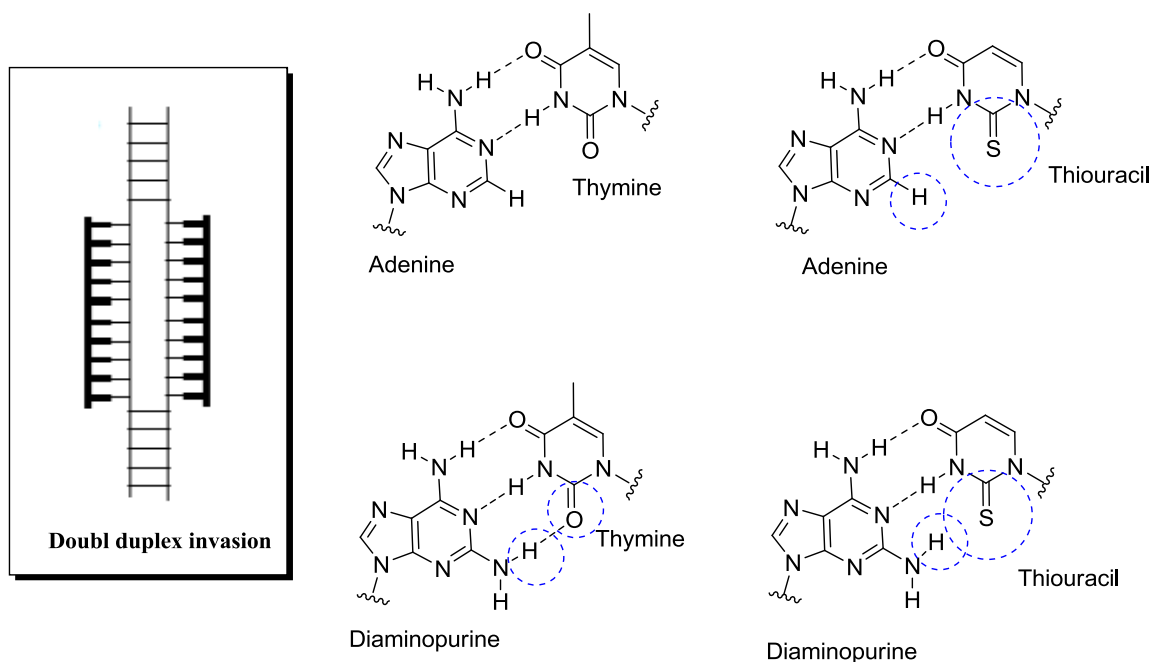


Figure 2-11: Double duplex invasion of DNA by pseudo complementary PNAs.

2.3.2 PNA modifications

Despite the attractive and interesting properties of PNA, a number of drawbacks have been observed such as poor solubility,¹⁵ tendencies to self aggregation and poor cell permeability.¹⁶ These limitations motivated researchers to modify the aminoethylglycine (*aeg*) PNA structure. A large number of PNA analogues have been synthesized through different types of modification on the backbone and/or nucleobases. A numerous chemical modifications on the aminoethylglycine backbone have been obtained,¹⁷ only few have shown a practical interest such as the lysine derived backbone (Fig. 2-12). Introduction of few lysine based monomer provides the PNA with cationic charges and thus increase the aqueous solubility of the PNA. In addition, different chemical modifications on nucleobase have been carried out to introduce a new functional group to the PNA and thus new properties as luminescence, potential-helix stabilization.^{18a-c} Furthermore, some of non natural nucleobases have been incorporated in PNA oligomers, as pseudoisocytosines (ψ IC) as mentioned before it mimics the N3-protonated cytosine (Fig. 2-13).

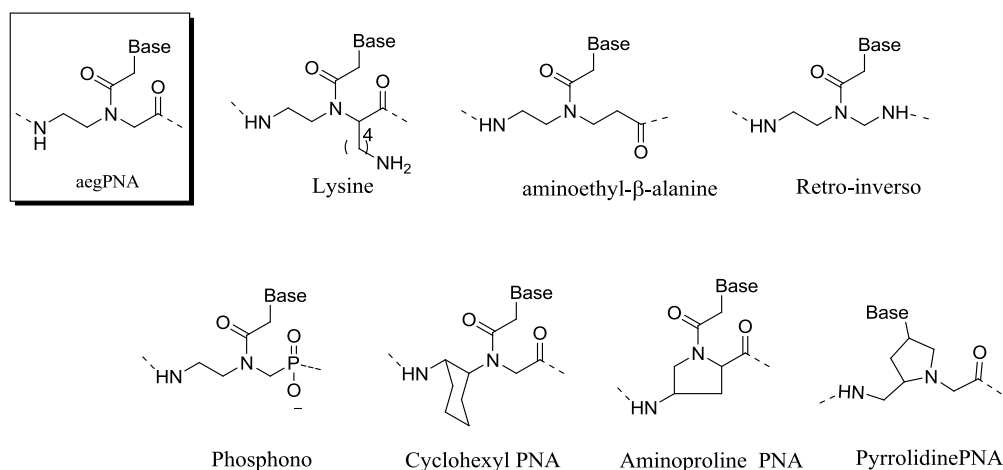


Figure 2-12: Selected examples of modified PNA backbone.

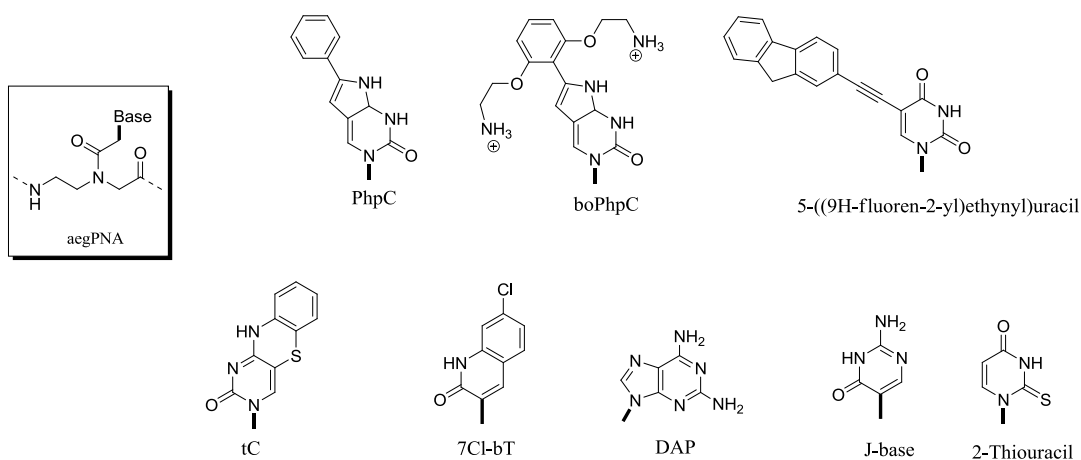


Figure 2-13: Selected examples of modified PNA nucleobases.

2.3.3 Synthesis of PNA oligomers

The synthesis of PNA oligomers relies on traditional solid phase peptide synthesis protocols (SPPS). Solid phase methodology has many advantages over the conventional synthesis as: 1) utility of excess reagents drives reactions to completion and resulting in increasing the reaction yield, 2) removal of reagents simply carried out by washing, 3) due to the product is synthesized on the resin, the handling loss of the product was minimized, 4) can be automated. On the basis of these remarkable advantages of solid

phase, the synthesis of polypeptides on support through a repetitive synthesis cycles was possible.

The synthesis of first PNA was reported by using Boc strategy that was heavily used in peptide synthesis. This protocol relies on using *tert*-butyloxycarbonyl (*t*Boc) group to protect the free amino group of PNA monomer backbone and benzyloxycarbonyl (Z) group to protect the exocyclic amino group of A, C and G nucleobases. The differential acid liability between *t*Boc and (Z) group facilitates the PNA synthesis whereas *t*Boc group is removed by trifluoroacetic acid (TFA) and Z groups are removed using trifluoromethane sulphonic acid (TFMSA). Cleavage of PNA oligomer from the solid support usually carried out with hydrogen fluoride (HF). In Boc protocol, usually acid labile resins as PAM (name is derived from the linker 4-(oxymethyl)phenyl-acetamidomethyl) which produces carboxylic C-terminal or MBHA (methylbenzhydrylamine) that produces amide C-terminal.

Some drawbacks were observed in this protocol such as during the deprotection of *t*Boc with TFA neither remove of side-chain protective groups nor a cleavage of the peptide from the resin was observed and therefore reducing the yield of the desired oligomer. Another disadvantage of *t*Boc protocol is the need for hazardous chemicals such as HF and the harsh condition for removal of Z group, that highlighted the need for new methodology to avoid such limitations. To avoid the repetitive acid treatment of the growing peptide in *t*Boc protocol, a milder method for the synthesis of the peptide with the solid phase technique was developed. This method based on introduction of base labile N-protecting group. Atherton and Shepard¹⁸ developed a convenient solid phase protocol for peptide synthesis based on using fluorenylmethoxycarbonyl group (Fmoc) for N-protection.

In Fmoc methodology, the free amino group of PNA monomer backbone is protected with Fmoc group and benzhydryloxycarbonyl (Bhoc) group is used to protect the nucleobase exocyclic amino group. Deprotection of Fmoc group carried out under mild conditions using 20% piperidine in DMF forming 9-(1-piperidinylmethyl)fluorene and piperidine carbamate salt by-products which are easily detectable spectrophotometrically

at 300-320 nm²⁰ or via measuring the conductivity respectively, which enables the automated monitoring of each deprotection step. At the end of the automated synthesis, the quality of the synthesis can be assessed by inspection of the chromatogram of all Fmoc groups removed during the synthesis cycles. Deprotection of Bhoc group is carried out at the end of the synthesis cycle by TFA at the same time with the cleavage of the peptide from the resin. Fmoc-based solid phase peptide synthesis protocol has been greatly enhanced by the introduction of a variety of solid supports, linkages, and side chain protecting groups. The cleavage of the peptide from the resin depends on the type of support and linker that have been chosen. Mainly, acid sensitive supports are used for Fmoc-mediated protocols as Wang resin also called HMP (4-(hydroxymethyl)-phenoxyethyl)polystyrene-1% divinylbenzene resin (produces carboxylic C-terminal) or Rink amide (produces amide C-terminal). The release of the peptide from the support usually carried out using TFA and purification of the synthesized PNA oligomer usually takes place via RP-HPLC and analyzed by mass spectrometry. There are two main side reactions that may occur during PNA synthesis as shown in (Fig. 2-14) firstly, acyl migration of the nucleobase acetyl moiety to the *N*-terminal leaving the secondary amine amenable to subsequent coupling giving a PNA with undesired sequence. Secondly, intramolecular attack of the primary amine at the *N*-terminal on the carbonyl group of the amide resulting in the lose of the *N*-terminal as ketopiperazine derivative. Cleavage of peptide from resin by TFA and side-chain deprotection can lead to side reactions due to reaction of the generated carbocations with the peptides. To overcome this problem, scavenger is used to avoid alkylation of the peptide. The choice of scavenger is depending on the type of side chain protective groups present. The strategy of solid phase synthesis for peptide nucleic acid oligomer using Fmoc or Boc is illustrated in (Fig. 2-15).

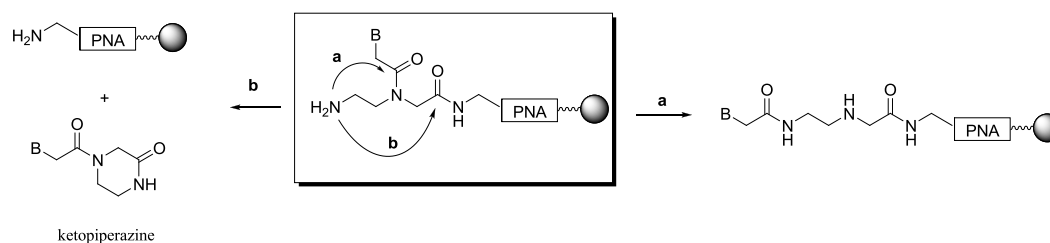


Figure 2-14: Side reactions in PNA synthesis

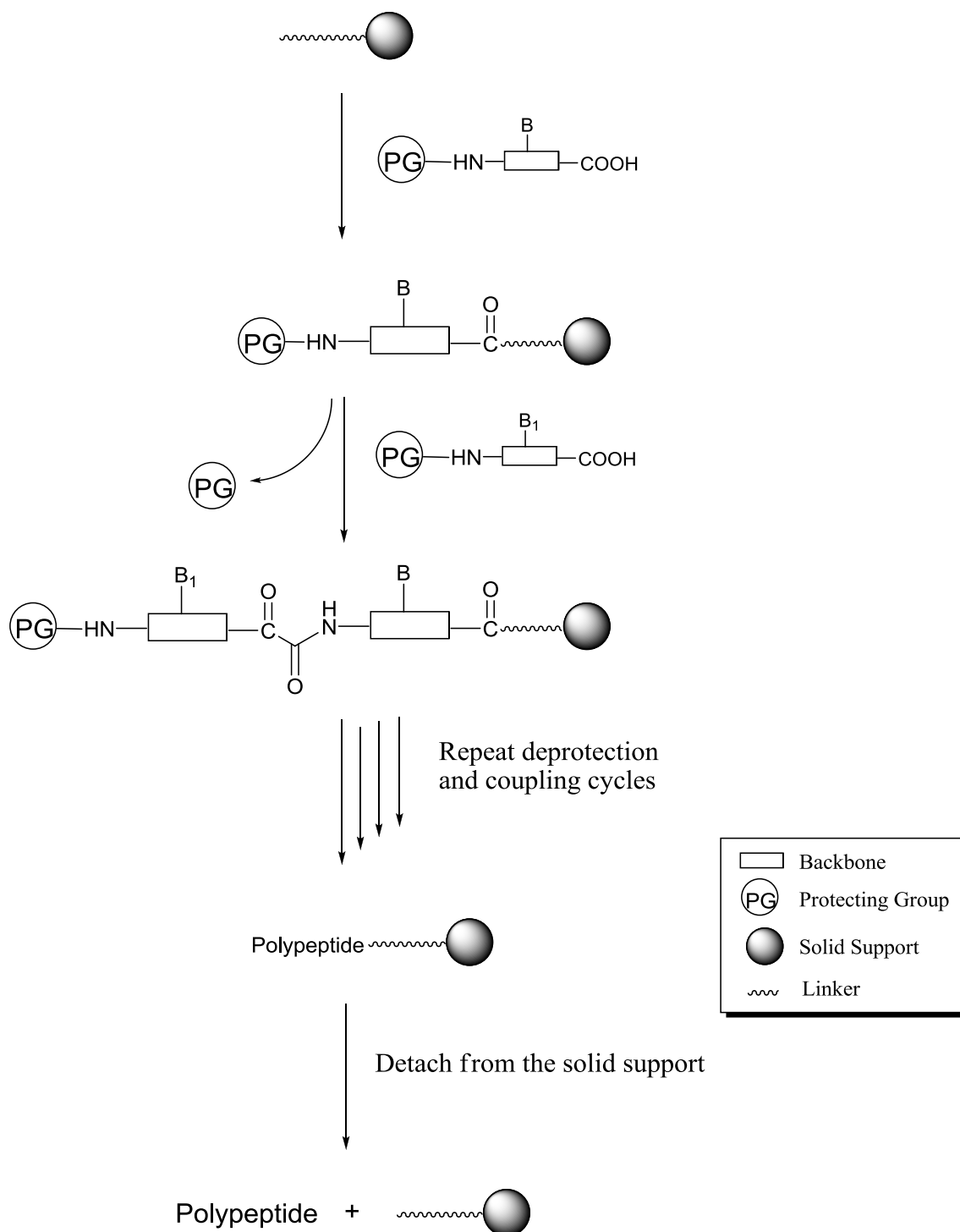


Figure 2-15: General strategy for solid phase peptide nucleic acid synthesis.

Currently, there are two types of commercially available PNA monomers for peptide nucleic acid synthesis. The structures of the protected PNA monomers are illustrated in (Fig. 2-16 and 2-17).

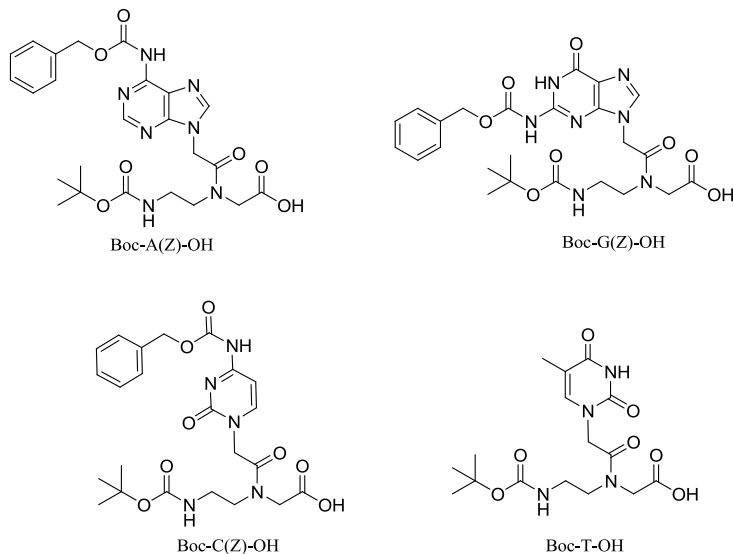


Figure 2-16: Structures of commercially available tBoc/Z PNA monomers.

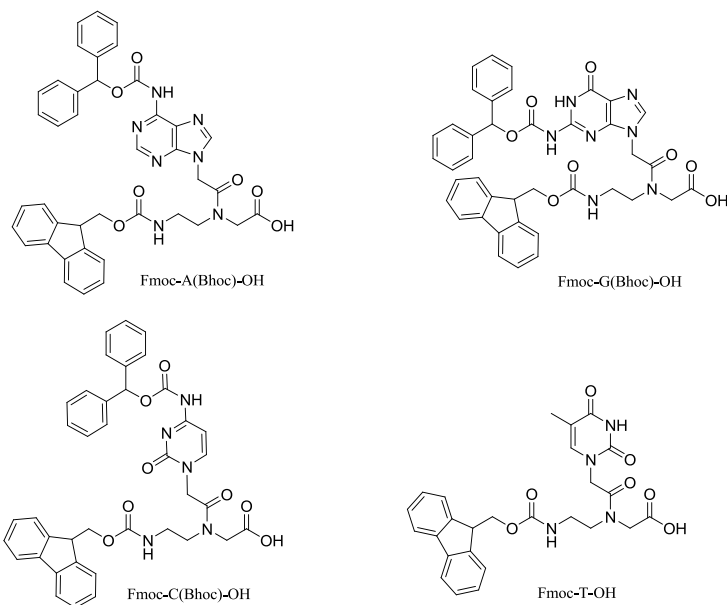


Figure 2-17: Structures of commercially available Fmoc/Bhoc monomers.

Several protecting group combinations have been investigated for the synthesis of PNA-oligonucleotide conjugates as Fmoc/Acy1,²¹ Mmt/Acy1^{22a,b} while Fmoc/Mmt²³ and Fmoc/Z

Protecting group strategies were used in the synthesis of PNA-peptide conjugates (Fig. 2-18). The utility of these protecting groups is limited due to they do not allow orthogonal synthesis with commercially available amino acid monomers. Bradley²⁴ introduced 1-(4,4-dimethyl-2,6-dioxacyclohexyl)ethylidene (Dde) group for protecting the terminal amino group of the backbone and monomethoxytrityl group (Mmt) for the exocyclic amino group of the nucleobases. The Dde group is usually cleaved by hydrazine in DMF which also deprotects the Fmoc group. A milder condition for Dde protection was developed by Bradley using a mixture of hydroxylamine hydrochloride and imidazole under slightly acidic conditions which would be fully orthogonal to the Fmoc group.²⁴ *o*-Nitroveratryloxycarbonyl group (NVOC)/Acyl²⁵ strategy in which NVOC group protects the amino group of the backbone was introduced by Liu and it is easily photolytically cleaved with irradiation at wavelength > 300nm. Some examples of different protecting groups combinations is shown in (Fig. 2-18).

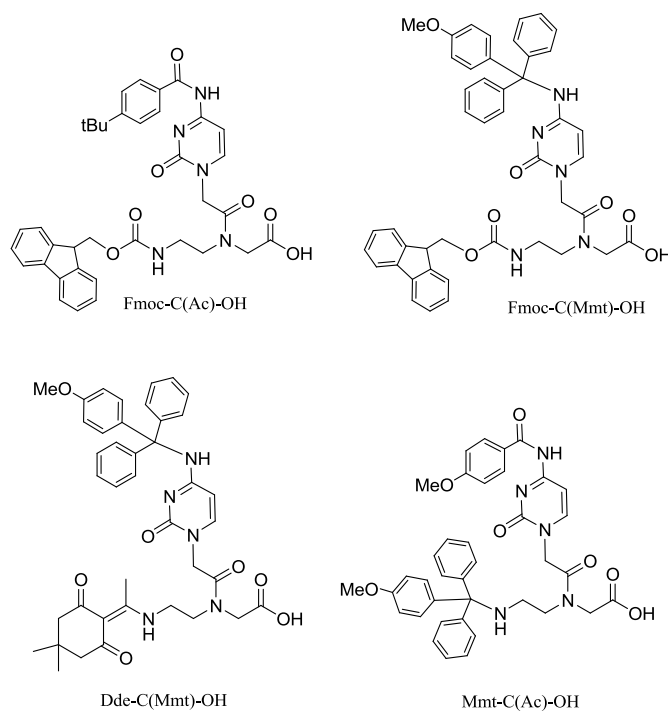


Figure 2-18: Examples of various protecting groups in PNA synthesis, protection of exocyclic amino group in A, G and C (only cytosine is shown for illustration).

2.4 PNA applications

On the basis of the remarkable high binding and high specificity properties of PNA with nucleic acids, PNAs have been employed in various biological applications as diagnostic or detection tools in addition to its utility for controlling gene expression.

2.4.1.1 PNA as therapeutic drug

As described in section 1-1, There are basically two strategies for therapeutic drug namely antigene and antisense. Relying on the ability of PNAs to bind with double-stranded DNA via strand invasion, PNAs have been shown to be a good candidate as antigene or antisense agents.²⁷ PNAs as antigene tools have been demonstrated its ability to arrest transcription processes through formation of triplex complex with DNA via strand invasion that confer a structural hindrance and consequently block the activity of RNA polymerase.²⁸ *In vivo*, plasmid DNA replication has been blocked by PNA.²⁹ *In vitro*, several studies have been demonstrated the ability of PNAs to inhibit DNA replication via triplex structure by strand-invaded complexes.³⁰

PNAs as antisense drug, relies on the recognition and binding to the complementary sequence of m-RNA through the formation of double helix complex and thus inhibit translation of the target gene to protein. Several reports have been introduced to illustrate the ability of PNAs as antisense. PNA was able to block liver-specific microRNA (miR-122) activity in human and rat liver cells.^{31a,b} However, utility of PNAs as tools for regulating gene expression was hampered by the slow cellular uptake of PNA by the living cells due to its uncharged character. Numerous strategies have been explored to improve the efficiency of PNA cellular uptake such as conjugation of PNA with DNA oligomers,³² ligands as antibodies, steroids,^{33a,b} or peptides such as cell penetrating peptides as penetratine.³⁴ Incorporation of positively charged residues as lysine or arginine into PNA sequence enhanced the PNA delivery. Dragulescu and coworkers showed that replacing the glycine side chains in PNA backbone with D-arginines forming guanidine-based PNA (GPNA) as shown in (Fig. 2-19) improves the PNA cellular uptake³⁵ and inhibit protein translation.³⁶

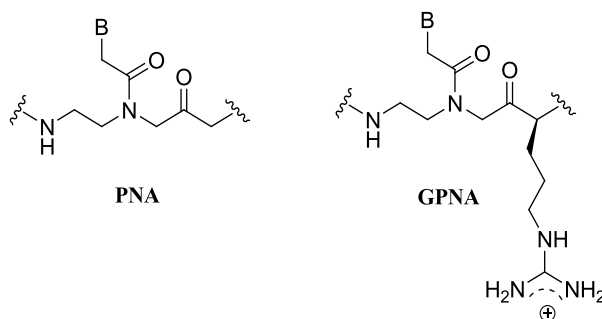


Figure 2-19: Comparison between the structure of GPNA and *aeg*-PNA.

2.4.1.2 PNA for diagnostics and detection

The excellent hybridization properties of PNAs with nucleic acids have allowed the use of PNA in a variety of genetic diagnostic techniques. For example, PNA-fluorescence *in situ* hybridization (FISH) technique. In this technique, a fluorescently labelled PNA is used to visualize the complementary nucleic acid target inside the cell. PNA-FISH have been used for quantitative telomere analysis,^{37a,b} chromosome painting, bacterial and viral diagnostics.^{38a,b} In 2006, advanDx' PNA FISH probes product for *in vitro* diagnosis of blood was a proved by Food and Drug Administration (FDA) of United States.

Another powerful application of PNA is PNA directed PCR clamping. In this strategy, PNA probes are employed in detection of single base pair mutations or single-nucleotide polymorphism (SNPs) by polymerase chain reaction technique (PCR). PNA probe was designed to bind to one of the PCR primer sites forming PNA:DNA complex which is effectively blocked this sites and hence inhibit amplification of the PCR product.^{39a,b} Furthermore, PNA used in molecular beacon design,⁴⁰ a description of molecular beacon design is introduced in details in (section 2-2.1.4).

2.5 Results and discussion

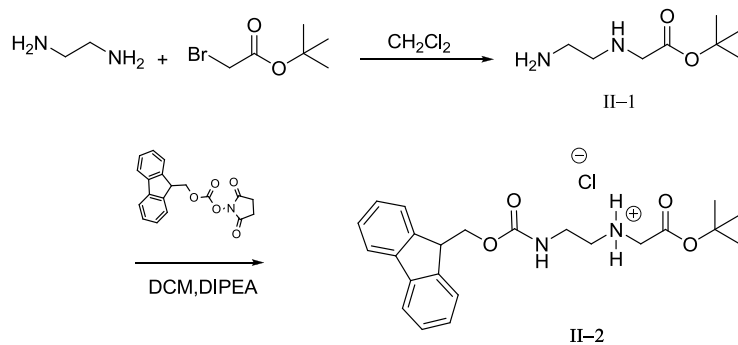
Relying on the aforementioned remarkable properties of both azobenzene (as photoswitch and quenching tool) and PNA as diagnostic tools, we have decided to pursue the synthesis of PNA-MB bearing azobenzene moiety and assess the quenching ability of appended azobenzene moiety against different types of fluorophores that used in fluorescence studies.

4-(*N,N*-Dimethylamino)azobenzene has been chosen as azobenzene analog for many reasons, azobenzene moiety allows the photoisomerization study for the synthesized PNA monomer. The presence of dimethylamino group which is susceptible to protonation facilitates the study of pH effect. Finally, the structure of 4-(*N,N*-dimethylamino)azobenzene PNA monomer mimics the structure of universal quencher. 4-(*N,N*-dimethylamino)-azobenzene-4'-carboxylic acid (DABCYL) and thus may have potential quenching effect.

2.5.1 Synthesis of the backbone

The synthesis of PNA monomers relies on the assembly of the protected 2-aminoethyl glycine backbone and protected nucleobase substituted acetic acid structural units.⁴¹ We aim to synthesize the PNA oligomer using Fmoc protocol for solid phase peptide synthesis and therefore synthesis of Fmoc protected PNA monomer is required.

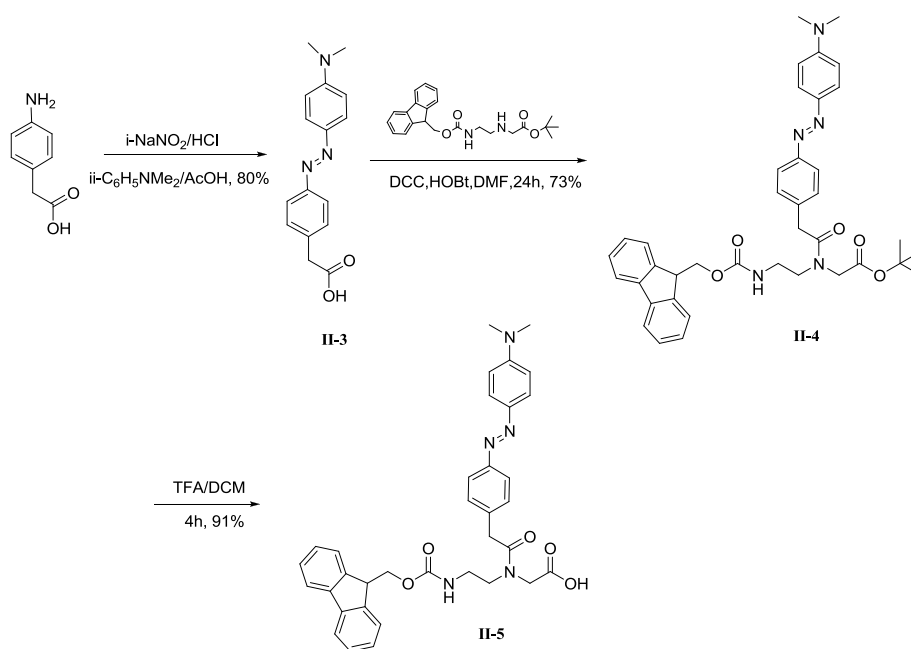
The synthesis of 4-(*N,N*-dimethylamino)azobenzene PNA monomer was carried out in two steps, synthesis of the *tert*-butyl-1-(2-(Fmoc)aminoethyl)glycinate backbone and nucleobase acetic acid derivative. The Fmoc(aeg)*tert* butyl ester backbone was obtained according to the synthetic route outlined in (Scheme 2-1) following the method reported in the literature.⁴² *tert*-Butyl-1-(2-aminoethyl)glycinate **II-1** was obtained by reaction of ethylenediamine with *tert*-butyl bromoacetate in dichloromethane followed by protecting the free amino group by *N*-(9-fluorenylmethoxycarbonyloxy) succinimide (Fmoc-OSu) to afford the backbone as oil. Fmoc backbone **II-2** was isolated as the hydrochloride salt by acidifying the solution with HCl/ether solution.



Scheme 2-1: Synthesis of 2-Fmoc(aeg)-*t*-butyl ester backbone.

2.5.2 Synthesis of the dimethylaminoazobenzene PNA monomer

The synthesis of PNA monomer carrying 4-(*N,N*-dimethylamino)azobenzene as shown in (Scheme 2-2) was obtained via series of chemical transformations started with diazotization of *p*-aminophenylacetic acid followed by coupling with *N,N*-dimethylaniline to give 4-(*N,N*-dimethylamino)azobenzene-4'-acetic acid **II-3** in 80% yield. **II-3** was coupled with *tert*-butyl-*N*-[2-(Fmoc)aminoethyl]glycinate by dicyclohexylcarbodiimide (DCC) mediated coupling to give the *tert*-butyl ester derivative **II-4** in 73% yield. Finally, the *tert*-butyl group was removed by trifluoroacetic acid in dichloromethane to afford the azobenzene PNA monomer **II-5** in 91% yield.



Scheme 2-2: Synthesis of azo-based PNA monomer.

2.5.3 Effect of acid on dimethylaminoazobenzene PNA monomer

The presence of the dimethylamino group imparts a susceptibility to protonation which facilitates the study of pH effects on the azo-based PNA monomer **II-5** (halochromism). The behavior of 4-(*N,N*-dimethylamino)azobenzene moiety under acidic conditions have been investigated. An ethanol solution of **II-5** was titrated with trifluoroacetic acid (0.005 M). Upon addition of trifluoroacetic acid, a decrease in the $\pi\text{-}\pi^*$ absorption band for non-

protonated form at 409 nm with an increase in π - π^* absorption band for protonated form at 524 nm was observed with isosbestic point at 465 nm as shown in (Fig. 2-20). This spectral change is explained with the aid of (Scheme 2-3). Although there are two basic sites in azo-PNA monomer **II-5**, dimethylamino and azo groups,⁴³ protonation in ethanol favors the lower energy, resonance-stabilized azonium ion over the ammonium ion.

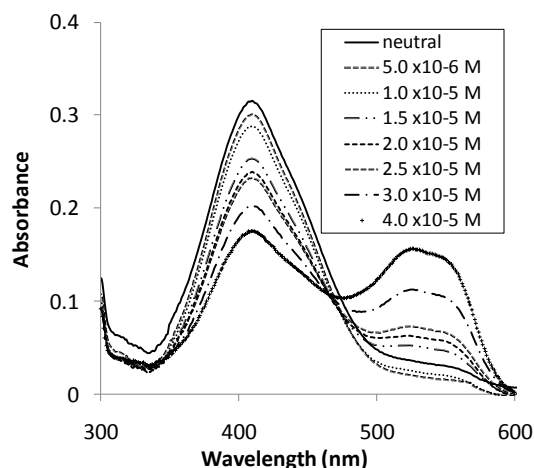
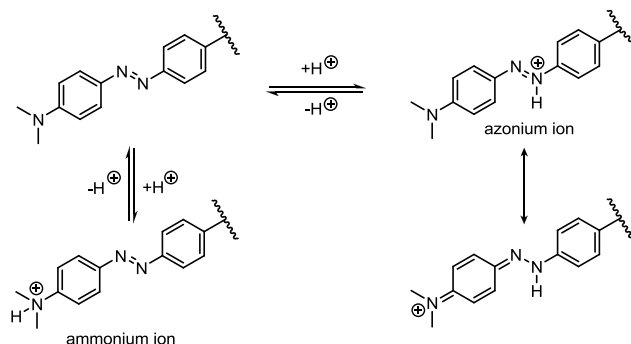


Figure 2-20: Changes in the UV-vis absorption spectrum of II-5 in EtOH at 1.66×10^{-5} M during titration with trifluoroacetic acid, from 0.3 to 2.4 equivalents.



Scheme 2-3: Ammonium/azonium protonated ions of dimethylaminoazobenzene.

2.5.4 Photoisomerization studies

Photoisomerization of azobenzene is well established, azobenzene can readily undergo conformational change about the azo bond between the *trans* and *cis* geometrical isomers by light. The *trans*-isomer can be photoisomerized to the *cis*-isomer upon illumination with UV light ($300 < \lambda < 400\text{nm}$), while *cis* isomers can be converted back to the *trans*

isomer again either by irradiation with visible light ($\lambda > 400\text{nm}$) or thermally. The isomerization is completely reversible.

By using UV/Vis spectroscopy for monitoring the photoisomerization of azo-based PNA monomer **II-5** in dichloromethane, It was observed that with irradiation of **II-5** with UV-light at 366 nm from hand held source, a decrease in the absorption band centered at 411 nm with appearance of unexpected large peak at 525 nm similar to the peak observed in effect of acids of **II-5** study (Fig. 2-20), this may attributed to generation of acid under irradiation condition. To circumvent the effect of acid, the irradiation was necessarily obtained in the presence of base. Under basic condition, upon illumination of **II-5** UV-light at 366 nm for a period of time, a decrease in the intensity of π - π^* band at 411 nm was observed. Recovery of *trans*-isomer was obtained by heat and it was confirmed by growth of the absorption band at 411 nm. (Fig. 2-21)

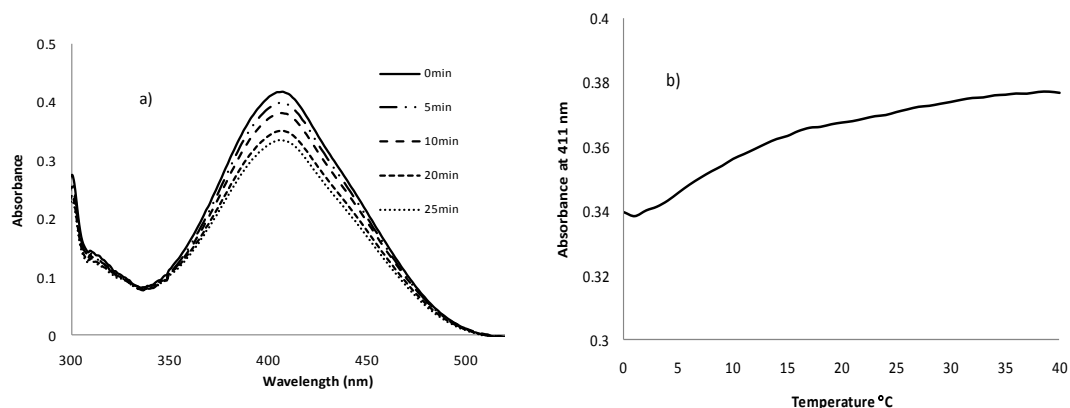


Figure 2-21: UV-Vis spectral change of **II-5 in dichloromethane. a) under irradiation at 366 nm, monitored at the time points shown. b) Recovery of the *trans* absorption band at 411nm by heat at rate 1°C/min.**

2.5.5 Quenching ability of dimethylaminoazobenzene PNA monomer

A preliminary, qualitative study to assess the ability of the 4-(*N,N*-dimethylamino)azobenzene PNA monomer to quench the emission of fluorescein, pyrene and sulforhodamine luminophores was made. PNA monomer **II-5** is an analog of the well-established FRET quencher DABCYL. PNA monomer **II-5** has a strong, broad absorption the spanning the near UV and visible region centered at approximately 410

nm in ethanol. This absorbance overlaps with the emission of several commonly used fluorophores, when in close proximity, may quench the fluorescence via (FRET). The ability of the **II-5**, to effect intermolecular quenching of representative appropriate fluorophores was observed for fluorescein ($\lambda_{\text{excitation}} = 488 \text{ nm}$; $\lambda_{\text{emission}} = 525 \text{ nm}$) and pyrene ($\lambda_{\text{excitation}} = 330 \text{ nm}$; $\lambda_{\text{emission}} = 377, 395 \text{ and } 418 \text{ nm}$) as demonstrated in (Fig. 2-22).

The authenticity of the quenching effect observed for fluorophores that matched their emission to the absorption band of **II-5** was confirmed by using a dye that is not a suitable FRET partner: sulforhodamine. The sulforhodamine dye is a longer wavelength emitting dye ($\lambda_{\text{excitation}} = 550 \text{ nm}$; $\lambda_{\text{emission}} = 595 \text{ nm}$) and is not suitable for use with DABCYL. The results shown in (Fig. 2-22) also indicate that the PNA monomer **II-5** behaves in an analogous fashion as free DABCYL, and does not cause any significant fluorescence quenching) The small (overall 7%) decrease in fluorescence intensity is likely due to dilution or screening effects. These results provide a direct evidence of the quenching ability of the synthesized 4-(*N,N*-dimethylamino)azo-PNA monomer.

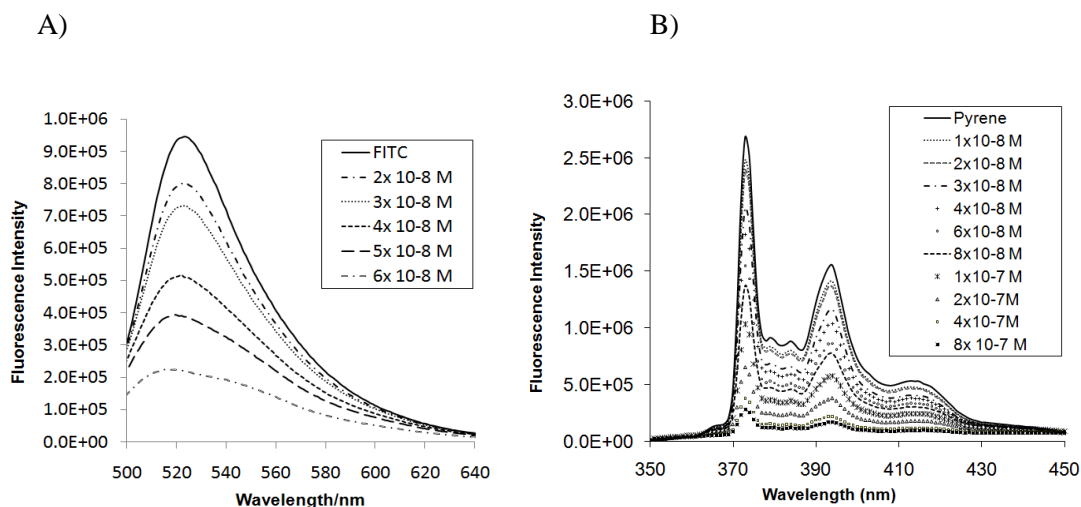


Figure 2-22: The effect of increasing amounts of II-5 on the emission spectra of A) fluorescein and B) pyrene, 5 μmol of each. Spectra were recorded in absolute EtOH and room temperature, $\lambda_{\text{excitation}}$ (fluorescein) = 488 nm and, $\lambda_{\text{excitation}}$ (pyrene) = 330 nm.

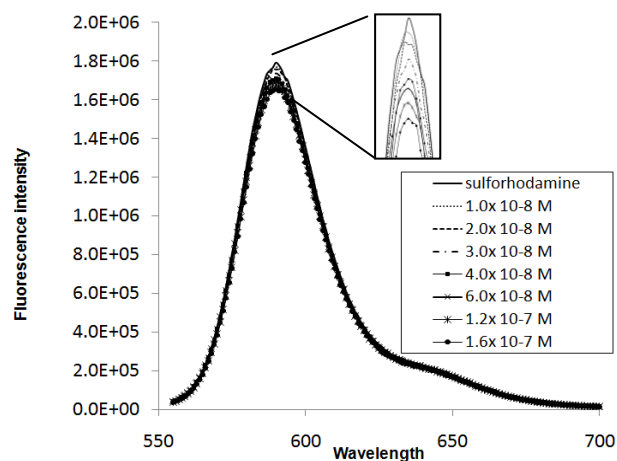


Figure 2-23: The effect of increasing amounts of II-5 on the fluorescence emission spectra of sulforhodamine 640 dye, $\lambda_{\text{excitation}}$ = 550 nm. Inset, expansion of the peak centered at ~590 nm.

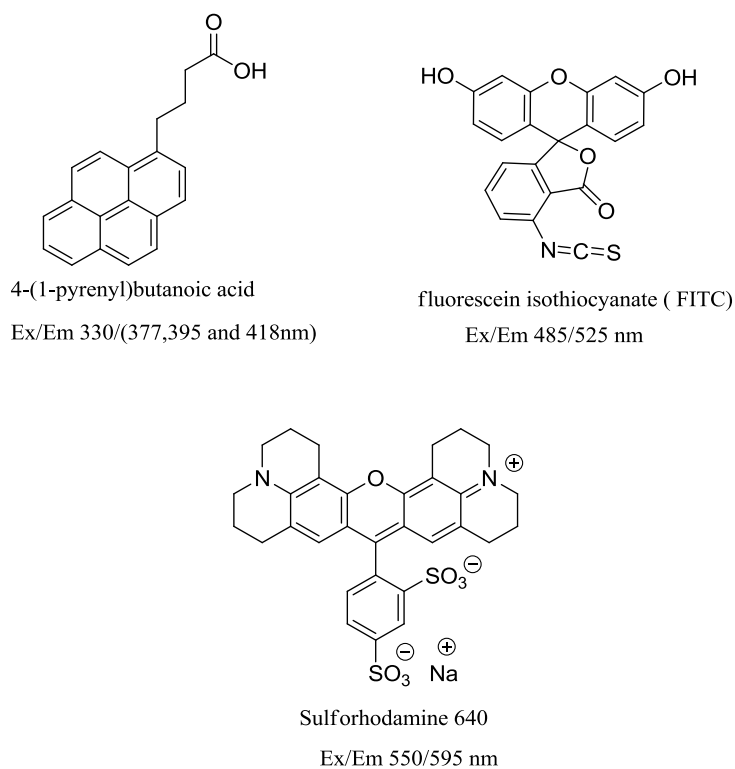


Figure 2-24: Structures of the fluorophores used in the study.

2.5.6 Design and synthesis of dual-labeled PNA molecular beacon

In order to assess the quenching ability of the azo-based PNA monomer in biological environment, 4-(*N,N*-dimethylamino)azobenzene unit was incorporated into short 8-mer PNA sequence **FCTTTTTC**Az**** (**II-6**), **Az** is azo-based monomer at *C*-terminus and **F** is the fluorescein moiety at *N*-terminus of a molecular beacon design using standard solid-phase PNA synthetic protocols using Fmoc protected monomers on a lysine-functionalized Rink amid resin (Nova Syn® TGR). Once the PNA oligomer synthesis with uncapped *N*-terminus was achieved, the resin was divided into two portions, first portion was treated with TFA to release the oligomer (**II-6**) which will be used later for hybridization studies to assess the effect of the presence of azobenzene on the stability of the triplex formation with the complementary DNA sequence. Fluorescein isocyanate

(FITC) was coupled manually to the uncapped *N*-terminus oligomer-bound resin (second portion). The completion of FITC coupling was confirmed by Kaiser test⁴⁴ and the PNA-MB (**II-7**) was purified by reversed phase-HPLC and characterized by MALDI-TOF mass spectrometry as shown in (Fig. 2-25 and 2-26).

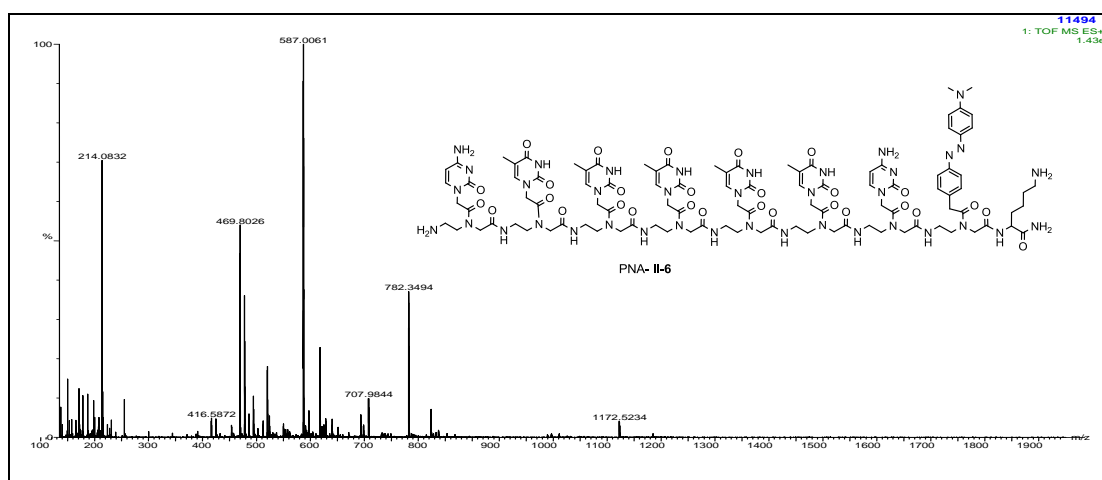


Figure 2-25: Mass spectrum of azo-based PNA oligomer II-6, calculated 2345.0335, found 2345.0468 [MH⁺]

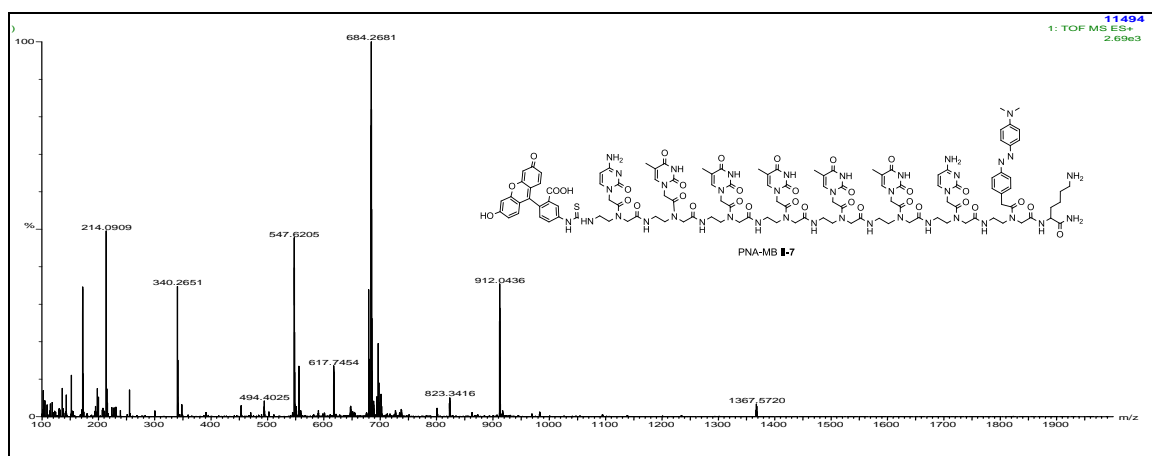


Figure 2-26: Mass spectrum of PNA-MB II-7, Calculated 2735.0772, found 2735.1440 [MH⁺]

On the basis of the quenching results that 4-(*N,N*-dimethylamino)azobenzene PNA monomer has proven. Molecular beacon design allows the presence of the azobenzene moiety in close proximity to the fluorophore and as a result the fluorescence signal of the

fluorescein should be turned off or decreased due to FRET. As illustrated in figure (Fig. 2-27), upon duplex formation between the PNA-MB (**II-7**) and the cDNA 5'-TCGAAAAGCT-3' at 2 μ M scale the fluorophore is located in a distance from the 4-(*N,N*-dimethylamino)azobenzene unit and as consequence the fluorescence intensity was increased by over 100 fold.

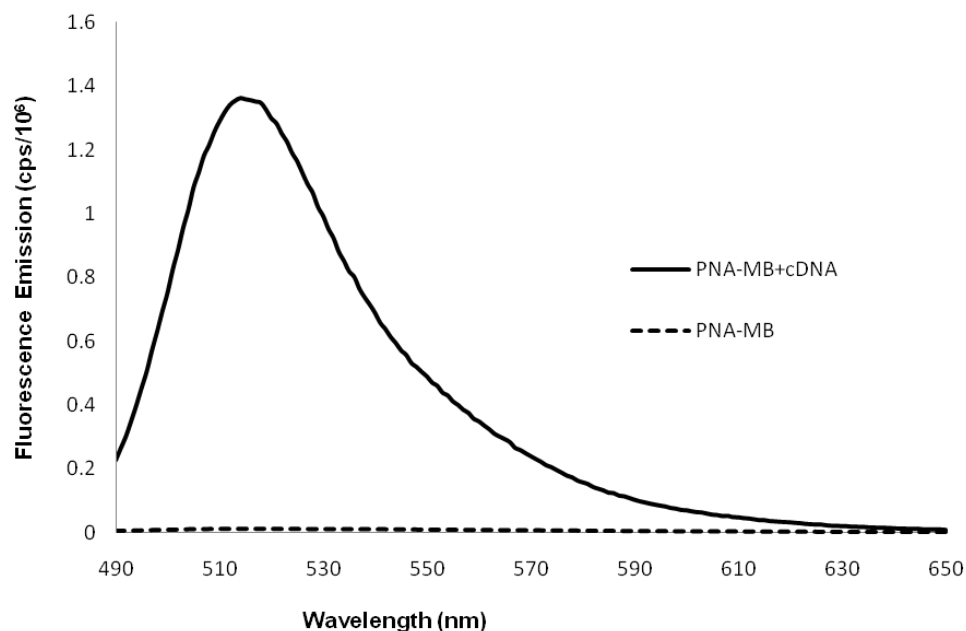


Figure 2-27: Fluorescence emission spectra ($\lambda_{\text{excitation}} = 488 \text{ nm}$) of 4-(*N,N*-dimethylamino)azobenzene based PNA-MB at 2 μ M scale under ionic condition 100 mM NaCl, 10 mM Na_2HPO_4 , 0.1 mM EDTA, pH 7.0, PNA-MB-cDNA (solid line) and PNA-MB (dotted line).

2.5.6.1 Hybridization properties of dimethylaminoazobenzene-PNA sequence

To evaluate the influence of 4-(*N,N*-dimethylamino)azobenzene moiety in the stability of the duplex formed between the azo-based PNA oligomer (**II-6**) and the complementary counterpart sequence “5'-TCGAAAAGCT-3'”. The hybridization properties were studied by temperature dependent UV absorbance in 2:1 ratio at (6 μ M PNA: 3 μ M

cDNA) was evaluated near physiological ionic conditions (100 mM NaCl, 10 mM Na₂HPO₄, 0.1 mM EDTA at pH 7.0). It was found that incorporation of 4-*N,N*-dimethylaminoazobenzene moiety into PNA oligomer resulted in an increase of melting temperature ΔT_m (+11 °C, with DNA) comparing to a control PNA oligomer. This increase in stability is may ascribed to the presence of hydrophobic azobenzene moiety at the end of the triplex structure that expected to stack well and therefore preventing end fraying.

cDNA: 5'-TCGAAAAAGCT-3'		
	T_m °C	ΔT_m
II-6, CTTTTTCX	52	+11
Control PNA, CTTTTTC	41	-----

Table 2-1: Melting Temperature

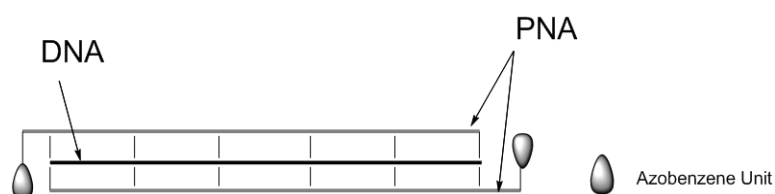


Figure 2-28: Schematic representation for formation of triplex PNA₂:DNA stabilized by azobenzene units.

2.6 Conclusion

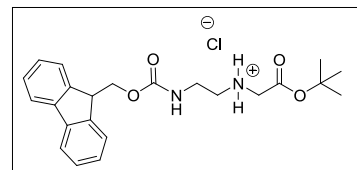
We have described the synthesis of an Fmoc-PNA monomer possessing an integral 4-*(N,N*-dimethylamino)azobenzene moiety as a nucleobase surrogate. This PNA monomer showed the ability to undergo a light-driven configurational change which might be beneficial for photoregulation of duplex stability between the PNA and

complementary nucleic acid. The azo-based PNA monomer also showed the ability to quench the fluorescence of fluorescein and pyrene and would be compatible with the same panel of dyes for which DABCYL is an effective quencher. The azo-based PNA monomer was successfully incorporated into oligomer using standard Fmoc-based oligomerization in a molecular beacon design with fluorescein as the optical label. As a result of hybridization of the azo-based PNA-MB to its complementary DNA, an increase of the fluorescence signal by 100 fold was observed.

2.7 Experimental

tert*-Butyl-*N*-[2(-((9H-fluoren-9-yl)methoxy)carbonyl)amino]ethyl]amino]acetate HCl salt **II-2*

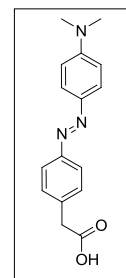
To a stirred solution of ethylenediamine (20 mL, 0.3 mol) in CH₂Cl₂ (150 mL) at 0 °C, *tert*-butyl bromoacetate (4 mL, 0.03 mol) in CH₂Cl₂ (20 mL) was added with slowly



addition over 5 h. The mixture was allowed to warm to r.t. and was stirred for 16 h. The mixture was washed with water (3 x 200 mL) and the combined organic solvent was collected, dried over Na₂SO₄ and filtered. A sample (1 mL) of the organic was evaporated and was dried to give product **II-2** as oil: ¹H NMR (CDCl₃) δ: 3.29 (s, 2 H), 2.77 (t, *J* = 7.0 Hz, 2H), 2.65 (t, *J* = 7.0 Hz, 2H), 1.51 (s, 3H), 1.45 (s, 9H). To the filtered solution (4.35 g, 0.025 mol) DIEA (10.6 mL, 0.075 mol) was added followed by dropwise addition of FmocOSu (8.43 g, 0.025 mol) in CH₂Cl₂ (25 mL) over 5 hr and the mixture was stirred for 12 h. The mixture was washed with water (3 x 200 mL) and was dried over Na₂SO₄ and filtered then was concentrated under reduced pressure to (50 mL). A solution of saturated HCl/diethylether (8 mL) was added to the reaction mixture till the solution turned turbid, cooled at 0° C for 3 h and the resulted white solid was collected, dried to give the hydrochloride salt of the backbone (6.5 g, 60 %). ¹H NMR (DMSO-*d*₆) for **II-2** δ: 9.27 (s, 2 H), 7.88 (d, *J* = 7.4 Hz, 2H), 7.68 (d, *J* = 7.4 Hz, 2H), 7.56 (t, *J* = 5.8 Hz, 1H), 7.41 (t, *J* = 7.3 Hz, 2H), 7.32 (t, *J* = 7.3 Hz, 2H), 4.33 (d, *J* = 6.8 Hz, 2H), 4.22 (t, *J* = 6.6 Hz, 1H), 3.86 (s, 2H), 3.32 (m, 2H), 2.98 (t, *J* = 6 Hz, 2H), 1.44 (s, 9 H).

4-[4'-(*N,N*-Dimethylamino)phenyl]diazenyl]phenylacetic acid **II-3**.

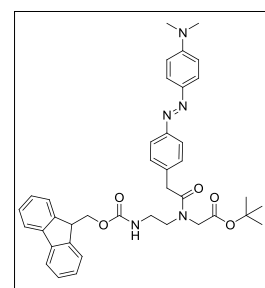
To an ice-cooled stirred solution of 4-aminophenylacetic acid (1.0 g, 6.62 mmol) in 1 M HCl (30 mL), a cold solution of sodium nitrite (0.685 g, 9.93 mmol) in H₂O (3 mL) was added dropwise. The mixture was stirred for 30 min and the resultant solution of diazonium salt was transferred to dropping funnel then was added to a solution of *N,N*-dimethylaniline



(1 mL, 7.94 mmol) in a mixture of glacial acetic acid and water (30 mL, 2:1, v/v). The mixture was stirred for 3 h. A brown solid precipitated after the pH was adjusted to 8 by use of an aqueous solution of 2 M sodium acetate. The solid was collected by filtration and was washed sequentially with cold water and ether and then dried to give product **II-3** in pure form (1.49 g, 80%), ¹HNMR (400 MHz, CDCl₃) δ : 7.78 (d, *J* = 8.9 Hz, 2H), 7.72 (d, *J* = 8.2 Hz, 2H), 7.40 (d, *J* = 8.2 Hz, 2H), 6.76 (d, *J* = 8.6 Hz, 2H), 3.7 (s, 2H), 3.07 (s, 6H); ¹³C NMR (100 MHz, CDCl₃) δ : 177.1, 152.3, 143.6, 134.4, 129.8, 124.9, 122.4, 111.5, 40.8, 40.3. HRMS (EI): calcd. For C₁₆H₁₇N₃O₂ [M⁺] 283.1321, found 283.1323.

tert-Butyl-2-[*N*-(2-((9H-fluoren-9-yl)methoxy)carbonylamino)ethyl]-2-[4-((4'-(*N,N*-dimethylamino)phenyl)diazenyl)phenyl]acetamido] acetate **II-4**.

To a solution of **II-3** (0.5 g, 1.76 mmol) in dry DMF (7 mL), DCC (0.366 g, 1.76 mmol) and HOBT (0.238 g, 1.76 mmol) was added. The reaction mixture was degassed for 15 min and then was stirred for 1 h followed by the dropwise addition of a solution of the Fmoc-backbone ester, *tert*-butyl 2-(2-(((9H-fluoren-9-yl)methoxy)carbonylamino)ethylamino)acetate, (0.635 g, 1.6 mmol) in (5 mL)

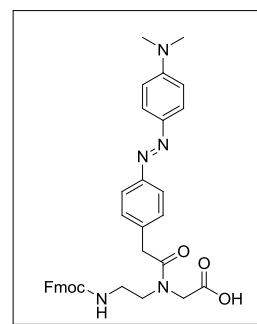


of dichloromethane. The mixture was stirred at r.t. for 36 h. The formed DCU was filtered; the filtrate was poured into ice-water with stirring which produced a brown precipitate. The solids were collected by filtration and then subjected to column chromatography using hexane/CH₂Cl₂ (70:30 v/v) as the eluent to afford **II-3** (0.852 g, 73%). Compound **II-3** exists in solution as a pair of slowly exchanging rotamers; signals attributed to major (ma.) and minor (mi.) rotamers are designated: ¹HNMR (400 MHz, CDCl₃) δ : 7.82 (d, *J* = 8.2 Hz, 2H), 7.79-7.74 (m, 4H), 7.58 (d, *J* = 7.4 Hz, 2H), 7.38-

7.27 (m, 6H), 6.74 (d, $J = 8.2$ Hz, 2H), 4.38 (d, $J = 7.1$ Hz, 2H), 4.22 (m, 1H), 3.95 (s, mi., 0.6H), 3.91 (s, ma., 1.4H), 3.75 (s, ma., 1.3H), 3.67 (s, mi., 0.7H), 3.58-3.48 (m, 2H), 3.39-3.31 (m, 2H), 3.07 (s, 6H), 1.48 (s, 9H); ^{13}C NMR (100 MHz, CDCl_3) δ : 156.5, 152.4, 143.7, 141.2, 129.5, 127.6, 127.1, 125.0, 119.9, 112.6, 83.1, 82.3, 49.9, 47.1, 40.8, 28.0. HRMS (ESI): calcd. For $\text{C}_{19}\text{H}_{44}\text{N}_5\text{O}_5$ $[\text{MH}^+]$ 662.3342, found 662.3328.

2-(*N*-(2-(((9H-fluoren-9-yl)methoxy)carbonylamino)ethyl)-2-(4-((4'-*N,N*-dimethyl amino)-phenyl)diazenyl)phenyl)acetamido)acetic acid II-5.

To an ice-cooled suspension of compound **II-4** (0.5 g, 0.75 mmol) in dichloromethane (2 mL), TFA (2 mL) was slowly added and the reaction mixture was stirred for 1 hr in ice bath and for 3 h at r.t. The mixture was evaporated in vacuo to dryness and the remaining residue was coevaporated with dichloromethane (3 x 10 mL), was dissolved in dichloromethane (2 mL) and precipitated with the



addition of diethyl ether (30 mL). The mixture was cooled to 0 °C for 12 h, filtered, washed with cold ether and dried to give the title compound as red solid (0.416 g, 91 %). ^1H NMR (400 MHz, DMSO) δ : 8.11 (s, 1H), 7.89 (d, $J = 7.4$ Hz, 2H), 7.77 (d, $J = 8.6$ Hz, 2H), 7.69-7.66 (m, 4H), 7.40-7.30 (m, 6H), 6.83 (d, $J = 8.6$ Hz, 2H), 4.31 (m, 1H), 4.20 (d, $J = 6.6$ Hz, 2H), 3.85 (s, ma., 0.5H), 3.75 (s, mi., 1.5H), 3.63 (s, 2H), 3.40 (m, 2H), 3.19 (m, 2H), 3.05 (s, 6H); ^{13}C NMR (100 MHz, $\text{DCM}-d_2$) δ : 161.1, 157.4, 144.4, 141.7, 136.5, 131.1, 128.2, 127.6, 125.6, 120.4, 119.9, 115.8, 76.3, 67.5, 47.6, 42.1, 40. HRMS (ESI): calcd. For $\text{C}_{35}\text{H}_{36}\text{N}_5\text{O}_5$ $[\text{MH}]^+$ 606.2716, found 606.2739

PNA Oligomer and PNA-MB synthesis

PNA 8-mer was synthesized on a 5 μmol scale using the standard FastMoc module on an Applied Biosystems 433A synthesizer using Nova SynTGR (Rink amide) resin. After the PNA synthesis was completed with uncapped *N*-terminus, the resin (40 mg, ~ 2 μmol) was transferred to a reaction vessel and was washed and drained with dry CH_2Cl_2 and DMF several times, DMF (1mL), FITC (6 equiv.) and DIEA (10 equiv.) were added and the reaction mixture was shaken in the dark for 6 h. The resin was washed with CH_2Cl_2 and DMF, completion of FITC coupling was confirmed by Kaiser test.

Cleavage of the PNA-MB from the resin

The PNA was cleaved from the resin with of TFA (1mL) for 90 min and the reaction mixture was filtered, the filtrate was evaporated with nitrogen stream and was treated with cold anhydrous diethyl ether (1 mL) to precipitate the crude PNA. The crude PNAs were dissolved in 0.05% TFA-H₂O (300 μ L), filtered, and purified by RP-HPLC using a 250 mm x 4.6 mm, C18-bonded phase, 100 pore, 5 μ m particle size column. Column was eluted at a flow rate of 1mL/ min with the solvent system: A) TFA (0.05%, v/v) in H₂O and B) TFA (0.05%, v/v) in CH₃CN with a binary gradient elution 0-5 min, 100% A; 5-20 min, 100% to 60% A; 20-30 min, 60% to 40% A; 30-40 min, 40% to 0% and were characterized by MALDI-TOF mass spectrometry, for **II-6** found 2345.0468 [MH⁺] , (2345.0335. calcd. for C₁₀₁H₁₃₆N₃₈O₂₉) and for **II-7** found 2735.1440 [MH⁺] , (2735.0772. calcd. for C₁₂₂ H₁₄₈ N₃₉O₃₄S).

PNA stock solutions were prepared in deionized water and stored at -4°C. Concentrations of PNA oligomer were determined by measuring UV absorbance at 260 nm at 80 °C and the extinction coefficients were calculated by summing the values for the individual nucleobases, FITC (70000 M⁻¹ cm⁻¹), and 4-(*N,N*-dimethylamino)azobenzene (32600 M⁻¹ cm⁻¹).

Photoisomerization study

UV-Vis spectra were measured with a Varian Cary 300 Bio spectrophotometer. A solution of **II-5** (2.06×10^{-5} M) in dichloromethane with 7.08×10^{-2} M of NEt₃ was irradiated in a quartz cuvette at room temperature using a UVGL-58 hand held lamp (6 watt, 366 nm) at a distance of approximately 4 cm. At given time points, a UV-visible spectrum was collected. The time course for spontaneous reversion was monitored at the wavelength of maximum change (411 nm).

Fluorescence studies

Fluorescence measurements were carried out on a Photon Technologies International Quanta Master 7/2005 spectrophotometer, excited at 488 nm and detected at 490-650nm. First, the fluorescence intensity was measure for a sample of 2 μ M of azo-based PNA-

MB under ionic conditions (100 mM NaCl, 10 mM Na₂HP0₄, 0.1 mM EDTA at pH 7.0) in 1 cm-quartz cuvette. The cDNA at 2 μM concentration was added to the PNA-MB and incubated for 1 hr to form duplex with the PNA-MB (**II-7**) and followed by measuring the fluorescence intensity of fluorescien.

Hybridization studies:

Hybridization and UV melting experiments were carried on a Varian Cary III under the same buffer condition used previously, melting experiments were performed at 6 μM concentration for PNA-MB and 3 μM concentration for cDNA (2:1) ratio for triplex formation. Sample was heated to 95 °C for 2-3 min, cooled to room temperature over 45 min. Denaturation was performed from 10 °C to 85 °C at a scan rate of 0.5 °C/min. The T_m values are an average of three measurements and are rounded to the nearest 0.5 °C. The error in T_m values was ± 0.5 °C. T_m values were estimated for cooperative transitions by the first derivative method. ΔT_m values are the difference between the melting temperature T_m of azo-based PNA oligomer (**II-6**) and the PNA control sequence [without 4-(*N,N*-dimethylamino)azobenzene monomer]

2.8 References

1. Guilbault, G.G. **1990**. Practical Fluorescence, 2nd Ed., Marcel Dekker, Inc., New York
2. Förster, T. Intermolecular energy migration and fluorescence. Translated by R.S. Knox. *Ann. Phys. (Leipzig)*, **1948**, 2, 55-75.
3. Haugland, R.P.; Yguerabide, J.; Stryer, L. Dependence of the kinetics of singlet-singlet energy transfer on spectral overlap. *Proc. Natl Acad. Sci. USA*, **1969**, 63, 23-30.
4. Youngmi, K.; Dosung, S.; Weihong, T. Molecular beacons in biomedical detection and clinical diagnosis, *Int. J. Clin. Exp. Pathol.*, **2008**, 1, 105-116.
5. Svanvik, N.; Nygren, J.; Westman, G.; Kubista, M. Free-probe fluorescence of light-up probes, *J. Am. Chem. Soc.* **2001**, 123, 803-809.
6. Nath, J.; Johnson, K. L. A review of fluorescence in situ hybridization (FISH): current status and future prospects, *Biotechnol. Histochem.*, **2000**, 75, 54-78.
7. Nielsen, P.E.; Egholm, M.; Berg R.H.; Buchardt, O. Sequence-selective recognition of DNA by strand displacement with a thymine substituted polyamide, *Science*, **1991**, 254, 1497-1500.
8. Demidov, V.V.; Potaman, V.N.; Frank-Kamenetskii, M.D.; Egholm, M.; Buchard, O.; Sonnichsen, S.H.; Nielsen, P.E. Stability of peptide nucleic acids in human serum and cellular extracts, *Biochem. Pharmacol.*, **1994**, 48, 1310-1313.
9. Nielsen, P.E.; Egholm, M. An introduction to peptide nucleic acid, *Current Issues Molec. Biol.*, **1999**, 1, 89-104.
10. a) Praseuth, D.; Grigoriev, M.; Guieysse, A. L; Pritchrd, L.L.; Harel-Bellan, A.; Nelsien, P.E.; Hellen, C. Peptide nucleic acid directed to the promoter of the chain of the interleukin-2-receptor, *Biochim. Biophys. Acta.*, **1997**, 1309, 226-238. b) Wittung, P.; Nielsen, P.E.; Norden, B. Extended DNA-recognition repertoire of PNA. *Biochem.*, **1997**, 36, 7973-7979.
11. a) Nielsen, P.E.; Egholm, M.; Bauchardt, O. Evidence for (PNA)₂/DNA triplex structure upon binding of PNA to dsDNA by strand displacement, *J. Mol. Recogn.*, **1994**, 7, 165-170. b) Cherny, D.Y.; Belotserkovskii, B.P.; Frank-Kamenetskii, M.D.; Egholm, M.; Bauchardt, O.; Berg, R.H.; Nielsen, P.E. DNA unwinding

upon strand-displacement binding of a thymine substituted polyamide to double-stranded DNA, *Proc. Natl. Acad. Sci. USA*, **1993**, 90, 1667-1670.

12. Nielsen, P.E. Peptide nucleic acid targeting of double-stranded DNA, *Methods Enzymol.*, **2001**, 340, 329-340.
13. Porcheddu, A.; Giacomelli, G. Peptide nucleic acids (PNAs), a chemical overview, *Curr. Med. Chem.*, **2005**, 12, 2561-2599.
14. a) Nielsen, P.E. PNA Technology, *Mol. Biotechnol.* **2004**, 26, 233-248. b) Brandt, O.; Hoheisel, J.D. Peptide nucleic acids on microarrays and other biosensors, *Trends Biotechnol.* **2004**, 22, 617-622. c) Ray, A.; Norden, B. Peptide nucleic acid (PNA): its medical and biotechnical applications and promise for the future, *FASEB J.* **2000**, 14, 1041-1060.
15. Vernille, J.P.; Kovell, L.C.; Schneider, J.W. Peptide nucleic acid (PNA) amphiphiles: synthesis, self-assembly and duplex stability, *Bioconjugate Chem.* **2004**, 15, 1314-1321.
16. Wittung, P.; Kajanus, J.; Edwards, K.; Nielsen, P.E.; Norden, B.; Malmstrom, B. G. Phospholipid membrane permeability of peptide nucleic acid, *FEBS Lett.* **1995**, 365, 27-29.
17. Ganesh, K.N.; Nielsen, P.E. Peptide nucleic acids: analogs and derivatives. *Curr. Org. Chem.* **2000**, 4, 931-943.
18. a) Wojciechowski, F.; Hudson, R.H.E. Fluorescence and hybridization properties of peptide nucleic acid containing a substituted phenylpyrrolocytosine designed to engage guanine with an additional H-bond, *J. Am. Chem. Soc.*, **2008**, 130, 12574-12575. b) Haaima, G.; Hansen, H. F.; Christensen, L.; Dahl, O.; Nielsen, P.E. Increased DNA binding and sequence discrimination of PNA oligomers containing 2,6-diaminopurine, *Nucleic Acids Res.* **1997**, 25, 4639-4643. c) Eldrup, A.; Nielsen, B.B.; Haaima, G.; Rasmussen, H.; Kastrup, J.S.; Christensen, C.; Nielsen, P.E. 1,8-Naphthyridin-2(1H)-ones. Novel bi- and tricyclic analogues of thymine in peptide nucleic acids (PNA), *Eur. J. Org. Chem.* **2001**, 1781-1790.
19. Atherton, E.; Hübscher, W.; Sheppard, R.C.; Woolley, V.; *Hooper-Seyler's Z. Physiol. Chem.*, **1981**, 362, 833-839.

20. Kruijtzter, J.A.W.; Hofmeyer, L.J.F.; Heerma, W.; Versluis, C.; Liskamp, R.M. J. ; Solid-phase syntheses of peptoids using Fmoc-protected *n*-substituted glycines: the synthesis of (retro) peptoids of Leu-enkephalin and substance P, *Chem. Eur. J.*, **1998**, 4,1570-158.
21. Kovacs, G.; Timar, Z.; Kupihar, Z.; Kele, Z.; Kovacs, L.; Kovacs, L. Synthesis and analysis of peptide nucleic acid oligomers using Fmoc/acyl-protected monomers, *J. Chem. Soc., Perkin Trans. 1*, **2002**, 1266-1270.
22. a) Breipohl, G.; Will, D. W.; Peyman, A.; Uhlmann, E. Novel synthetic routes to PNA monomers and PNA-DNA linker molecules, *Tetrahedron*. **1997**, 53, 14671-14686. b) Musumeci, D.; Roviello, G.N.; Valente, M.; Sapio, R.; Pedone, C.; Bucci, E.M.; New synthesis of PNA-3`DNA linker monomers, useful building blocks to obtain PNA/DNA Chimeras , *Biopolymers*, **2004**, 76, 535-542.
23. Breipohl, G.; Knolle, J.; Langner, D.; Omalley, G.; Uhlmann, E. Synthesis of polyamide nucleic acids (PNAs) using a novel Fmoc/Mmt protecting-group combination, *Bioorg. Med. Chem. Lett.* **1996**, 6, 665-670.
24. Bialy, L.; Diaz-Mochon, J. J.; Specker, E.; Keinicke, L.; Bradley, M.; Dde-Protected PNA monomers, orthogonal to Fmoc, for the synthesis of PNA-peptide conjugates. *Tetrahedron*, **2005**, 61, 8295-8305.
25. Diaz-Mochon, J.J.; Bialy, L.; Full orthogonality between Dde and Fmoc: the direct synthesis of PNA-peptide conjugates, *Org. Lett.* **2004**, 6, 1127-1129.
26. Liu, Z. C.; Shin, D.S.; Lee, K.T.; Jun, B.H.; Kim, Y.K.; Lee, Y.S., Synthesis of photolabile *o*-nitroveratryloxycarbonyl (NVOC) protected peptide nucleic acid monomers, *Tetrahedron*, **2005**, 61, 7967-7973.
27. Hanvey, J.C.; Peffer, N. J.; Bisi, J. E, Thomson, S. A; Cadilla, R.; Josey, J.A.; Ricca, D.J.; Hassman, C.F.; Bonham, M. A.; Au, K. G. Antisense and antigene properties of peptide nucleic acids, *Science*, **1992**, 258,1481-1485.
28. Larsen, H. J.; Nielsen, P.E. Transcription-mediated binding of peptide nucleic acid (PNA) to double-stranded DNA: sequence-specific suicide transcription, *Nucleic Acids Res.***1996**, 24,458-463.

29. Diviacco, S.; Raozzi, V.; Xodo, L.; Helene, C.; Quadrifoglio, F.; Giovannangieli, C. Site-directed inhibition of DNA replication by triple helix formation *FASEB J.*, **2001**, 15, 2660-2668.
30. Vickers, T.A.; Griffity, M.C.; Ramasamy, K.; Risen, L.M.; Freier, S.M. Inhibition of NF-kappaB specific transcriptional activation by PNA strand invasion, *Nucleic Acids Res.* **1995**, 23, 3003-3008.
31. a) Fabani, M.M.; Gait, M.J. miR-122 Targeting with LNA/2'-O-methyl oligonucleotide mixmers, peptide nucleic acids (PNA), and PNA-peptide conjugates. *RNA* **2008**, 14, 336-346. b) Ivanova, G.D.; Fabani, M.M.; Arzumanov, A.A.; Abes, R.; Yin, H.; Lebleu, B.; Wood, M.; Gait, M.J.; PNA-peptide conjugates as intracellular gene control agents. *Nucleic Acids Symposium Series*, **2008**, 52, 31-32.
32. Nastruzzi, C.; Cortesi, R.; Esposito, E.; Gambari, R.; Borgatti, M.; Bianchi, N.; Feriotto, G.; Mischiati, C.; Liposomes as carriers for DNA-PNA hybrids, *J. Controlled Release*, **2000**, 68, 237-249.
33. a) Simmons, C.G.; Pitts, A.E.; Mayfield, L.D.; Shay, J.W.; Corey, D.R. Synthesis and permeability of PNA-peptide conjugates, *Bioorg. Med. Chem. Lett.* **1997**, 7, 3001-3007. b) Rebuffat, A.G.; Nawrocki, A.R.; Nielsen, P.E.; Bernasconi, A.G.; Bernal-Mendez, E.; Frey, B.M.; Frey, F.J. Gene delivery by a steroid-peptide nucleic acid conjugate, *FASEB J.* **2002**, 16, 1426-1428.
34. Diaz-Mochon, J.J.; Bialy, L.; Watson, J.; Sanchez-Martin, R.M.; Bradley, M. Synthesis and cellular uptake of cell delivering PNA-peptide conjugates, *Chem. Commun.* **2005**, 26, 3316-3318.
35. Dragulescu-Andrasi, A.; Rapireddy, S.; He, G.; Bhattacharya, B.; Hyldig-Nielsen, J.J.; Zon, G.; Ly, D.H. Cell-permeable Peptide nucleic acid designed to bind to the 5'-untranslated region of e-cadherin transcript induces potent and sequence-specific antisense effects, *J. Am. Chem. Soc.* **2006**, 128, 16104-16112.
36. Dragulescu-Andrasi, A.; Zhou, P.; He, G.; Ly, D.H. Cell-permeable GPNA with appropriate backbone stereochemistry and spacing binds sequence-specifically to RNA, *Chem. Commun.* **2005**, 2, 244-246.

37. a) Lansdorp, P.M.; Verwoerd, N.P.; van de Rijke, F.M.; Dragowska, V.; Little, M.T.; Dirks, R.W.; Raap, A. K.; Tanke, H. J. Heterogeneity in telomere length of human chromosomes, *Hum. Mol. Genet.* **1996**, 5, 685-691. b) Mathioudakis, G.; Storb, R.; McSweeney, P. A.; Torok-Storb, B.; Lansdorp, P. M.; Brummendorf, T. H.; Gass, M.J.; Bryant, E.M.; Storek, J.; Flowers, M.E.; Gooley, T.; Nash, R.A. Polyclonal hematopoiesis with variable telomere shortening in human long-term allogeneic marrow graft recipients. *Blood*, **2000**, 96, 3991-3994.
38. a) Perry-O'Keefe, H.; Stender, H., Broomer, A.; Oliveira, K.; Coull, J.; Hyldig-Nielsen, J.J. Filter based PNA in situ hybridization for rapid detection, identification and enumeration of specific micro-organisms. *J. Appl. Microbiol.* **2001**, 90, 180-189. b) Stender, H.; Kurtzman, C.; Hyldig-Nielsen, J.J.; Sørensen, D.; Broomer, A.; Oliveira, K.; Perry-O'Keefe, H.; Sage, A.; Young, B.; Coull, J. Identification of *dekkera bruxellensis* (*Brettanomyces*) from wine by fluorescence in situ hybridization using peptide nucleic acid probes. *Appl. Environ. Microbiol.*, **2001**, 67, 938-941.
39. a) Ørum, H.; Nielsen, P.E.; Egholm, M.; Berg, R.H.; Bruchardt, O.; Stanley, C.; Single base pair mutation analysis by PNA directed PCR clamping. *Nucleic acid Res.* **1993**, 21, 5332-5336. b) Thiede, C.; Bayerdörffer, E.; Blasczyk, R.; Wittig, B.; Neubauer, A. Simple and sensitive detection of mutations in the ras proto-oncogenes using PNA-mediated PCR clamping, *Nucleic Acids Res.* **1996**, 24, 983-984.
40. Seitz, O.; Köhler, O. Convergent strategies for the attachment of fluorescing reporter groups to peptide nucleic acids in solution and on solid phase, *Chem. Eur. J.* **2001**, 7, 3911-3925.
41. Uhlmann, E.; Peyman, A.; Breipohl, G.; Will, D.W. PNA: Synthetic polyamide nucleic acids with unusual binding properties, *Angew. Chem., Int. Ed.* **1998**, 37, 2796-2823.
42. a) Thomson, S.A.; Josey, J.A.; Cadilla, R.; Gaul, M.D.; Hassman, C.F.; Luzzio, M. J.; Pipe, A.J.; Reed, K.L.; Ricca, D.J.; Wiethe, R.W.; Noble, S.A. Fmoc mediated synthesis of peptide nucleic acids, *Tetrahedron*, **1995**, 51, 6179-6194. b)

- Hudson, R.H.E.; Goncharenko, M.; Wallman, A.P.; Wojciechowski, F. PNA-directed triple-helix formation by N7-xanthine, *Synlett*, **2005**, 9, 1442-1446.
- 43.** Yeh, S.J.; Jaffé, H.H., Tautomeric equilibria. VI. The structure of the conjugate acid of *p*-dimethylaminoazobenzene, *J. Am. Chem. Soc.* **1959**, 81, 3283-3287.
- 44.** Kaiser, E., Colescot, R. L., Bossinge, C.D.; Cook, P.I. Color test for detection of free terminal amino groups in solid-phase synthesis of peptides., *Anal. Biochem.*, **1970**, 34, 595-598.

Chapter 3

Chapter 3

3 Synthesis and Photophysical Studies of Novel Quencher for PNA

3.1 Introduction

To the best of our knowledge introduction of azobenzene derivatives into peptide nucleic acid was accomplished by inclusion of azobenzene residues as a replacement for the nucleobases. (Fig. 3.1).^{1a-c} In this chapter, we are interested in the synthesis of a novel azo-based PNA monomer that possess the azophenyl moiety which provides the photoswitching property in addition to its potential quenching effect with maintaining hydrogen bonding ability with the complementary nucleobase. To achieve this goal, uracil nucleobase has been chosen as starting point, by simple chemical modifications to introduce phenylazo moiety at C-5 position which is characterized by it does not interfere with the hydrogen bonding sites of uracil.

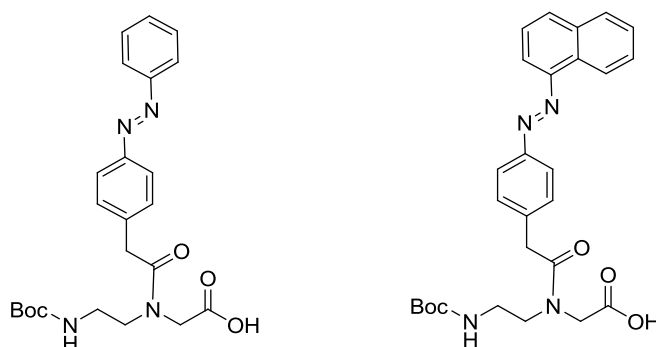


Figure 3-1: Examples of azo-based PNA monomers.

We are interested in the synthesis of 4-(*N,N*-dimethylamino)phenylazouracil analog (DMA) because it structurally mimics the universal 4-(*N,N*-dimethylamino)azobenzene-4'-benzoic acid quencher (DABCYL) that is widely used in Fluorescence Resonance Energy Transfer (FRET) applications as shown in (Fig. 3-2), and this may leads to a new PNA-quencher.

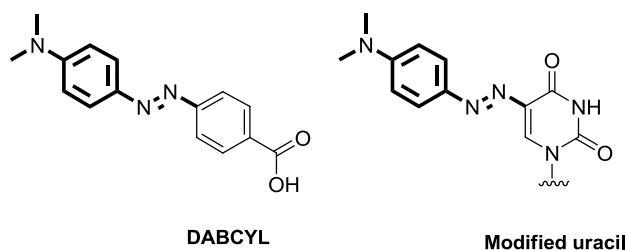
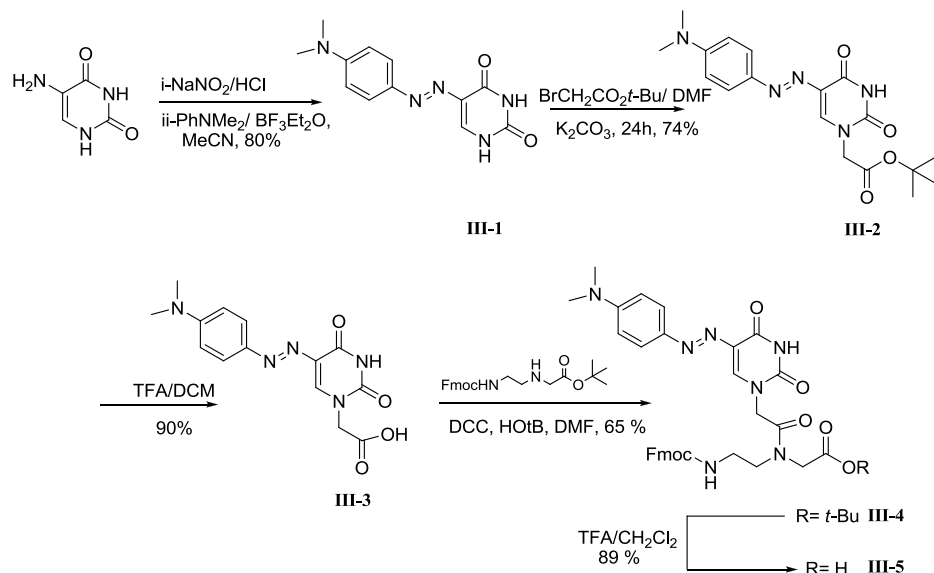


Figure 3-2: Similarity in structure between DABCYL and the modified uracil

3.2 Results and discussion

The synthesis of azo-based PNA monomer is outlined in (Scheme 3-1). Starting with diazotization of commercially available 5-aminouracil affords the corresponding diazonium salt solution followed by coupling with *N,N*-dimethyl aniline following the reported procedure² to give 4-(*N,N*-dimethylamino)phenylazouracil **III-1** in 80% yield. Alkylation of compound **III-1** with *t*-butyl bromoacetate under basic conditions at N-1 to afford the corresponding ester **III-2** which underwent removal of *t*-butyl group by TFA treatment to obtain the acid derivative **III-3** in 90% yield. Carbodiimide mediated condensation of **III-3** with *N*-[2-(Fmoc)aminoethyl]glycine-*t*-butyl ester gave the desired monomer ester **III-4**. Finally, removal of *t*-butyl group was carried out by acidolysis using TFA to give the azo-based PNA monomer **III-5** in 89% yield.



Scheme 3-1: Synthesis of 4-(*N,N*-dimethylamino)phenylazouracil PNA monomer.

Azobenzenes are known to have two configurational isomers which are *trans* and *cis*. The *trans* isomer is the most thermally stable due to lack of steric clash that was found in *cis* isomer. Similarly, 4-(*N,N*-dimethylamino)phenylazouracil derivatives are expected to exist in *trans* form. To confirm this assumption, a crystal structure of *tert*-butyl-4-(*N,N*-dimethylamino)phenylazo-5-uracil-1-yl acetate **III-2** was obtained that confirmed the *trans* configuration as shown in (Fig. 3-3). Selected bond distances (Å) and angles (°), with estimated standard deviations in parentheses is shown in Table 3-1.

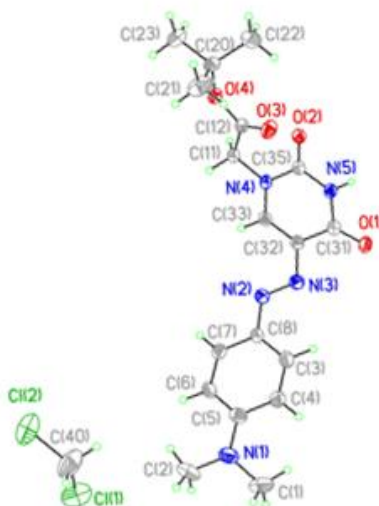


Figure 3-3: The X-ray crystal structure of **III-2** showing the phenylazouracil unit is existing in *trans*-configuration.

	Bond lengths [Å]		Angles [°]	
N3-N2	1.268(4)	N2-N3-C32	110.6(3)	
N3-C32	1.424(4)	C33-C32-N3	122.6(3)	
N2-C8	1.408(4)	N3 C32 C31	117.6(3)	
N4-C11	1.454(4)	C35-N4-C11	117.5(3)	
N5-C35	1.364(4)	C35-N5-C31	127.5(3)	
N4-C11	1.454(4)	C33-N4-C11	120.4(3)	

Table 3-1: Selected bond distances (Å) and angles (°) for **III-2**

3.2.1 Photoisomerization of azo-based uracil derivative and solvent effect on its absorption spectrum

Similarly to azobenzene, 4-(*N,N*-dimethylamino)phenylazouracil derivatives are expected to undergo a transformation from the thermally stable *trans* isomer to the *cis* form by irradiation with UV light, while the reverse transformation *cis*-to-*trans* can be achieved either by illumination with visible light or thermally.^{3a,b}

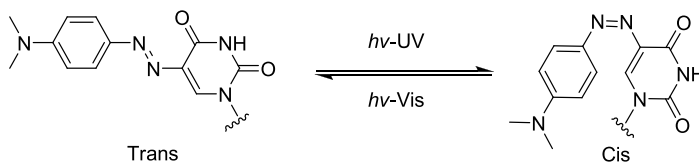


Figure 3-4: Photoisomerization of 4-(*N,N*-dimethylamino)phenylazouracil derivatives.

4-(*N,N*-Dimethylamino)phenylazouracil acetic acid **III-3** has been chosen as a model to investigate its photoisomerization ability due to it showed good solubility in water and various organic solvents. The maximum absorption band and molar extinction coefficient of **III-3** under different solvent is reported in (Table 1).

Solvent	H ₂ O	EtOH	CH ₃ CN	MeOH	Acetone	DCM
λ_{\max}/nm	465	436	439	441	437	459
$\epsilon(\text{L}/\text{Mol}\cdot\text{cm}^{-1})$	14480	32474	24855	27087	28982	-----

Table 3-2: Maximum absorption wavelength and molar extinction coefficient of compound III-3 in various solvents.

As shown in (Table 3-2), compound **III-3** showed positive solvatochromic effect, in other words, the absorption maximum wavelength is increased with the increase of solvent polarity. As demonstrated in (Fig. 3-5), UV-Vis absorption spectrum of **III-3** in acetonitrile exhibited a characteristic broad absorption band centered at 439 nm corresponding to π - π^* transition of azophenyl moiety. Upon illumination with 366 nm light, compound **III-3** underwent *trans*-to-*cis* isomerization accompanied with decrease

in the intensity of π - π^* band at 439 nm which is derived mainly from the azo moiety. Recovery of *trans* isomer was achieved by thermal relaxation.

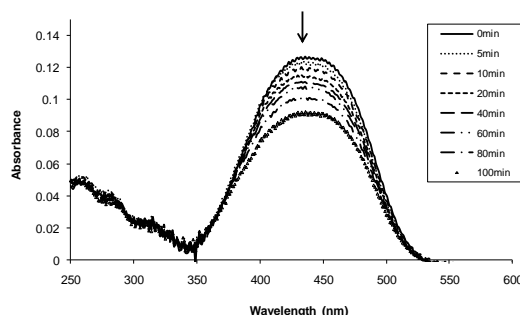


Figure 3-5: Absorption spectrum of III-3 in CH₃CN at 3.78 μ M. The arrow indicates the direction of change in peak at 439 nm upon irradiation with 366 nm light.

3.2.2 pH-Sensitivity of azo-based uracil

Similar to the acid effect study that was carried out on the azobenzene PNA monomer (discusses in chapter 2), on the basis of structural similarity between 4-(*N,N*-dimethylamino)azobenzene and 4-(*N,N*-dimethylamino)phenylazouracil, we have investigated the effect of acids on compound **III-3** using UV-Vis spectroscopy.

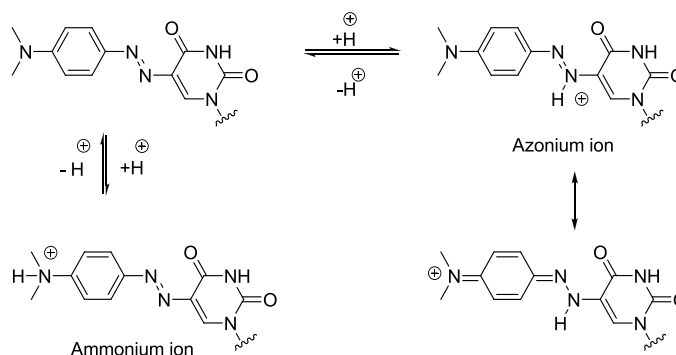


Figure 3-6: Schematic representation of azonium and ammonium ions.

As shown in (Fig. 3-6), there are two sites, dimethylamino- and azo groups, susceptible for protonation. Interestingly, upon addition aqueous solution of 3 mM HCl to compound **III-3** in different solvents, in nonpolar solvents as benzene and toluene only azonium ion band (usually appears at > 500 nm) was observed while with the increase of solvent

polarity both azonium and ammonium ions (usually appears at < 400)⁴ bands were observed (Fig. 3-7).

Solvent	DMSO	H ₂ O	EtOH	CH ₃ CN	MeOH	Acetone	DCM	Toluene	Benzene
λ_{\max}/nm (Neutral)	453	469	436	439	441	437	459	452	452
λ_{\max}/nm (protonated)	351	349	585/359	595	593/351	587	612	607	605

Table 3-3: Effect of addition of 3 mM HCl on absorption maximum wavelength (λ_{\max}) of III-3, λ_{\max} of ammonium ion is shown in bold.

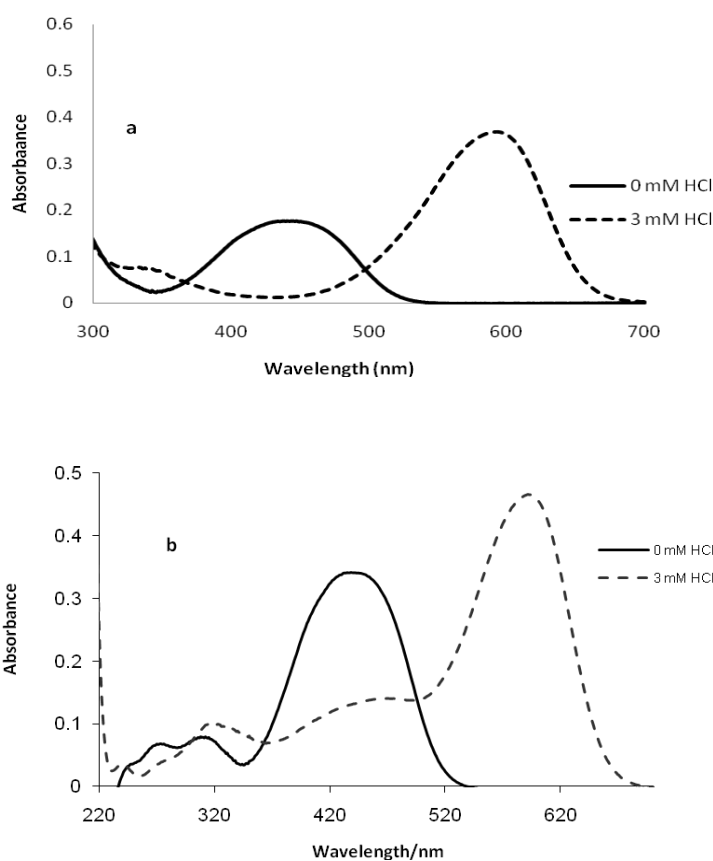


**Figure 3-7: Spectral change of III-3 at a) 10.5 μM concentration in CH_3COCH_3
b) 8 μM concentration in CH_3CN upon addition of 3 mM HCl.**

As demonstrated in (Fig. 3-8), we monitored the effect of TFA on **III-3** spectroscopically. Upon addition of small aliquots of TFA in acetonitrile (0.005 M) to **III-3** in acetonitrile, a noticeable decrease of the non-protonated π - π^* absorption band centered at 439 nm was observed, similar to the effect of HCl, with appearance of a new absorption band at 595 nm for the protonated form with clear isosbestic point at 504 nm. Comparing these results with that carried out in ethanol, nonprotonated form appeared at 436 nm, while after protonation with ethanolic solution of TFA, two new absorption bands at 352 nm and 585 nm were observed. This phenomenon can be explained based on the fact that due to the presence of two sites dimethylamino- and azo groups which are amenable for protonation with the acid producing ammonium ion and azonium ion, respectively.

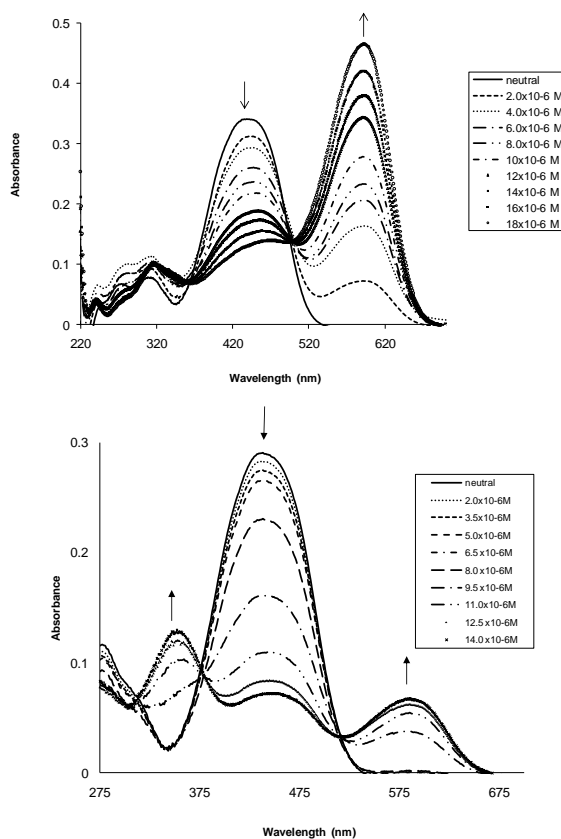


Figure 3-8: Effect of TFA on III-3 at a) 10.5 μ M concentration in CH_3CN at range (0-18 μ M) (0-1.7 equivalent), b) at 6 μ M concentration in EtOH at range (0-14 μ M) (0-2.3 equivalent), arrow directions indicates the spectral change upon addition of TFA.

Interestingly, azo-nucleobase derivative **III-3** displayed intriguing halochromism property. It was observed that treatment of **III-3** in various solvents with halogenated acids, as trifluoroacetic acid, gave dramatically different colours. Halogenated solvents as chloroform or dichloromethane produced a deep blue colour. While under basic conditions the reversible change to deep yellow/orange was observed (Fig. 3-9 and 3-10).

Surprisingly, mineral acids did not effect this colour change, nor was the colour change observed in oxygenated solvents (H_2O , alcohols, Et_2O , EtOAc , and THF). The blue colour in halogenated solvents was not quenched by shaking against water either. These perplexing phenomena continue to be investigated which may lead to its use as a non-aqueous pH indicator.



Figure 3-9: Compound III-3 in a) various solvents: from left to right: dioxane, dichloromethane, chloroform, diethyl ether, methanol, ethanol and H_2O . b) after addition of TFA., c) after basification.

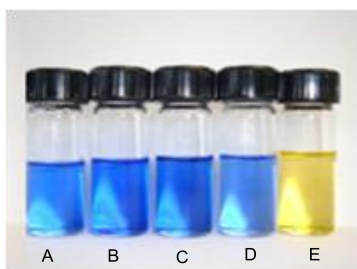


Figure 3-10: Compound III-3 in DCM with A) Trifluoroacetic acid, B: Dichloroacetic acid, c: fluorodichloroacetic acid, D: trichloroacetic acid, E: AcOH.

To assess the quenching ability of the azo-based PNA monomer **III-3**, a preliminary study using similar protocol that has been used in chapter 2, two fluorophores: fluorescein and pyrene were used. As shown from the absorption spectra of **III-3** in ethanol, it has absorption range 350-525 nm with maximum wavelength 436 nm which is expectedly overlap with emission spectra of fluorophores that used in the study. A solution of fluorophores in ethanol was titrated with aliquots of compound **III-3**. As illustrated in (Fig. 3-11 and 3-12), upon addition of small portions of **III-3** to the fluorophore, a subsequent fluorescent signal is quenched with the increase of **III-3** concentrations.

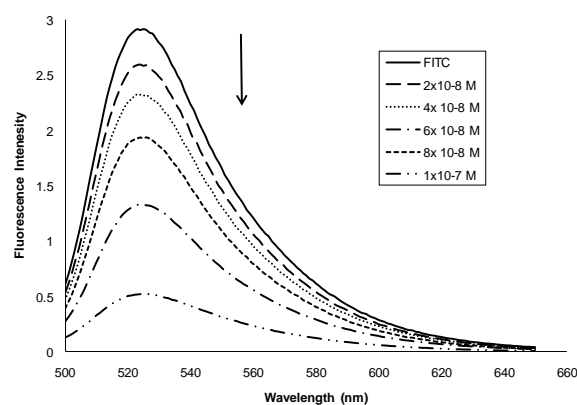


Figure 3-11: Fluorescence changes of 8 μM fluorescein upon addition of various amount of **III-3 in EtOH at the range (0-0.1 μM) with excitation wavelength 488 nm.**

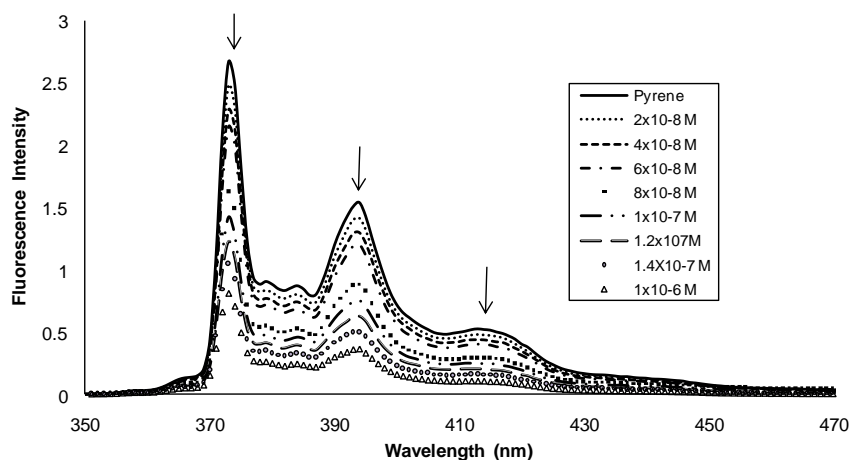


Figure 3-12: Fluorescence spectra of 5 μM concentration of pyrene in ethanol recorded upon addition of varied amount of **III-3 in EtOH at the range (0-1 μM) with excitation wavelength 330 nm.**

3.2.3 Design and synthesis of dual peptide for quenching study

We have designed and synthesized a FRET-peptide MB containing the azo-based PNA monomer. FRET peptides are peptides labeled with fluorescent dye (donor) at one terminal and a non fluorescent dye (acceptor) at the other terminal, due to presence of the donor and acceptor in close proximity no fluorescence emission is observed due to fluorescence energy transfer (FRET). FRET peptides are widely used mainly for detection of proteases and protein kinases activities.⁵ The choice of both donor and acceptor is very crucial to have a good FRET peptide. The donor should have high fluorescence quantum yield and the acceptor should have the ability to quench the emission of the donor. In other words, the emission spectrum of the donor must overlap with the excitation spectrum of the acceptor. As illustrated in (Fig 3-13), when the acceptor is close enough, excitation is transferred from the donor to the acceptor without emission of photons and as a result the fluorescence of the donor is quenched. By the effect of enzymatic degradation on a specific site of peptide sequence, the donor separates from the acceptor and subsequently the quenching effect is lost and leading to increase of the emission intensity of the donor.

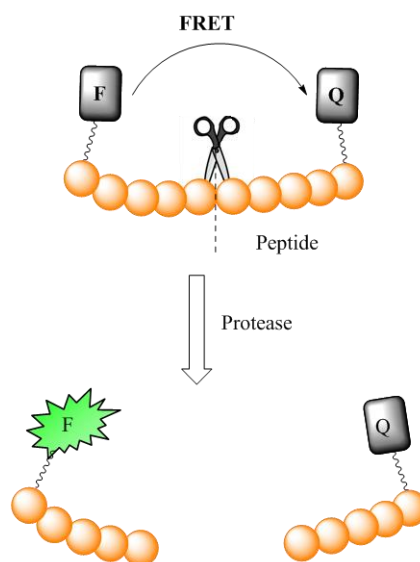


Figure 3-13: Schematic representation on the mechanism of FRET-Peptide.

The peptide sequence is determined based on the given protease; in this study we have used Cathepsin D (Cat D), lysosomal aspartyl endopeptidase. Cat D is known to cleave peptide bonds mainly between hydrophobic amino acids units.^{6a,b} As shown in (Fig. 3-14), we have designed a peptide sequence, contains core cleavage sequence (ILFFRL) based on literature report⁷ showed that Cat D was effectively cleaved the peptide bond between the two phenylalanine units. The synthesized PNA was labelled with fluorescein as optical tag at the *N*-terminal.

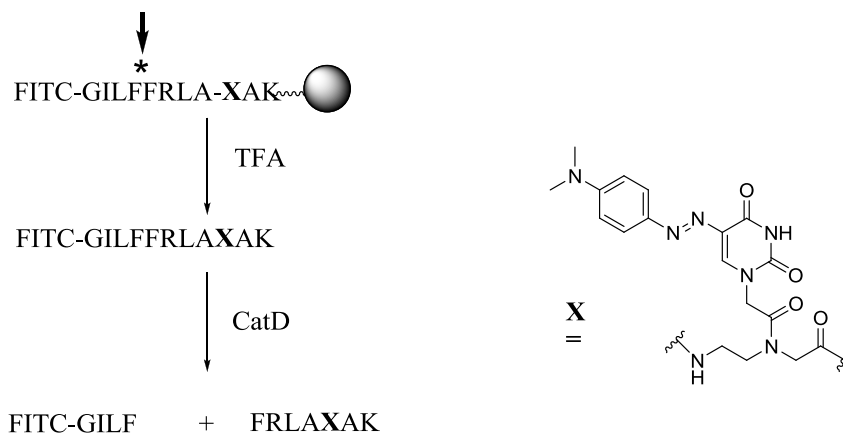
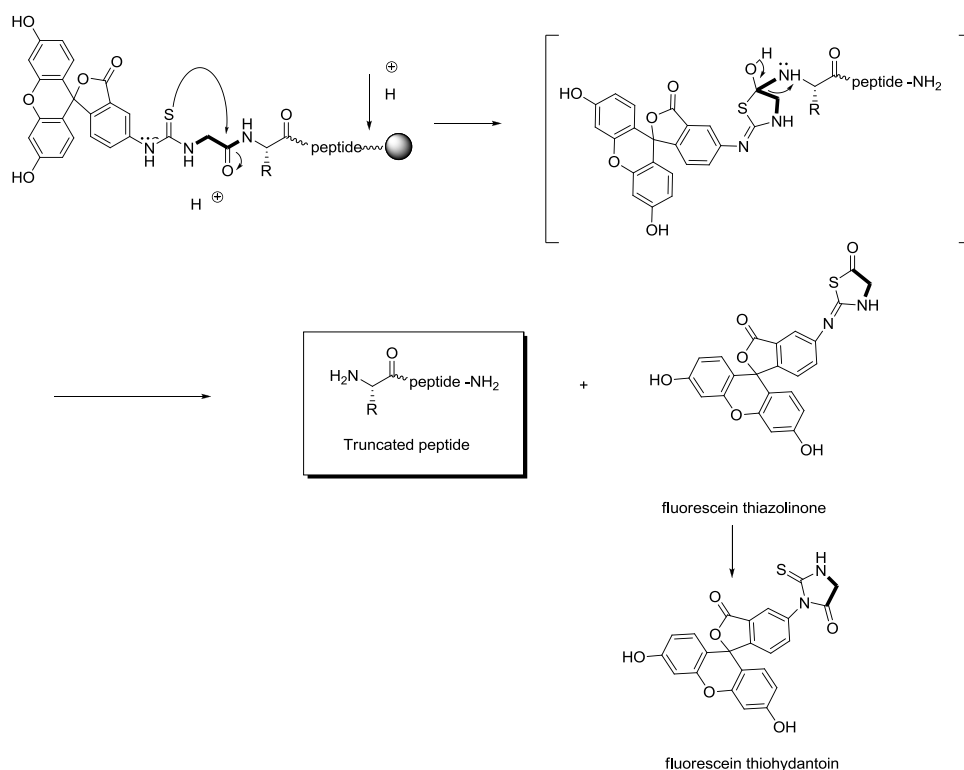


Figure 3-14: Designed FRET Peptide having azo-based PNA monomer as quencher and FITC as fluorophore.

The desired FRET peptide was synthesized by Fmoc mediated solid peptide phase strategy. After the completion of the sequence synthesis, fluorescein was introduced manually to the uncapped *N* terminal and completion of the fluorescein labelling was confirmed by Kaiser test. The peptide was cleaved from the resin by TFA and was purified by reversed phase high pressure liquid chromatography. To confirm the formation of the synthesized peptide by mass spectrometry, unfortunately, the expected mass for the desired dual labelled peptide cannot be observed. The mass spectrum has shown a peak at m/z 1478.8732. It was found that this mass peak is attributed to the peptide sequence "ILFFRLA-XAK" with no evidence of the presence of fluorescein moiety or the last amino acid "glycine". By reviewing the literatures, a similar case was reported by Jullian and coworkers,⁸ they postulated that this type of degradation could occurred during the cleavage of the peptide from the resin by TFA through a cyclization

leading to the formation of a fluorescein thiohydantoin with subsequent removal of the last amino acid following a mechanism similar to Edman degradation⁹ (Scheme 3-2).



Scheme 3-2: Degradation mechanism of FITC labelled peptide by the effect of TFA.

As illustrated in the mechanism, formation of five-membered ring is only possible when the last residue is α -amino acid. Simply to avoid such degradation, this can be achieved by using resin that susceptible to non-acidic cleavage of the targeted peptide or by using longer spacer as β -alanine or amino hexanoic acid.

To circumvent the degradation of the peptide, we have modified the design of the peptide by replacing glycine residue with β -alanine (Fig. 3-16) and the desired peptide sequence was built at the peptide synthesizer followed by coupling of fluorescein manually. The synthesis of the FRET-peptide was confirmed primarily from UV-Vis spectra as shown in (Fig. 3-15) absorption band at 465 nm attributed to 4-(*N,N*-dimethylamino)

phenylazouracil and at 485 nm for fluorescein and by mass spectrometry a peak at m/z 1938.0471 $[MH^+]$ was observed for the desired dual peptide.

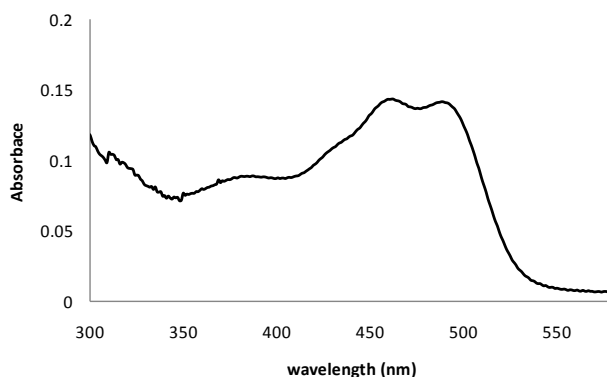


Figure 3-15: UV-Vis spectra of FRET-Peptide showed bands at 462 nm for DMAzo unit and at 485 nm for FITC.

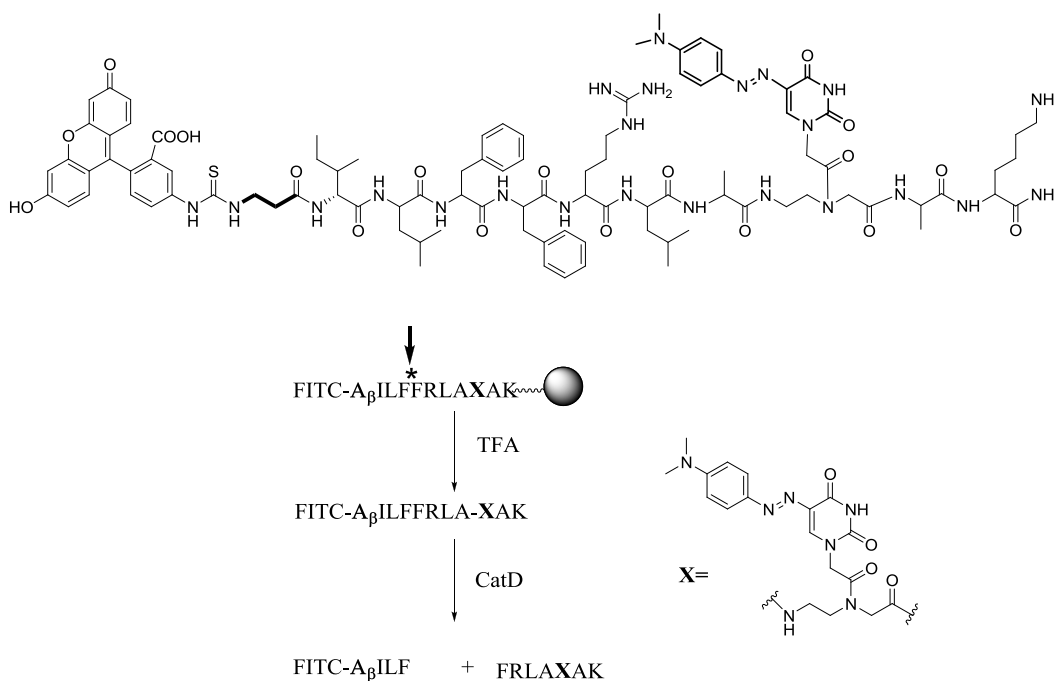


Figure 3-16: Schematic representation of the modified dual labeled peptide design.

To assess the quenching ability of the azo-based modified uracil, the fluorescence of fluorescein in dual labeled peptide was measured at emission wavelength at 520 nm with excitation at 488 nm. The FRET-Peptide was subjected to Cat D digestion for 30 min and

the fluorescence intensity was measured again as shown in (Fig. 3-17), it was found that the emission intensity was increased by 3.5 fold due to cleavage of the peptide at the bond between F-F. The digested products were analyzed by MALDI-MS, there was no sign of undigested substrate peak at m/z 1938.0471 which indicates that the digestion had gone for completion and moreover a peak at m/z 1103.0483 was observed for the cleavage product attributed to sequence FRLAXAK as a result of cleavage between the F-F (Fig. 3-19).

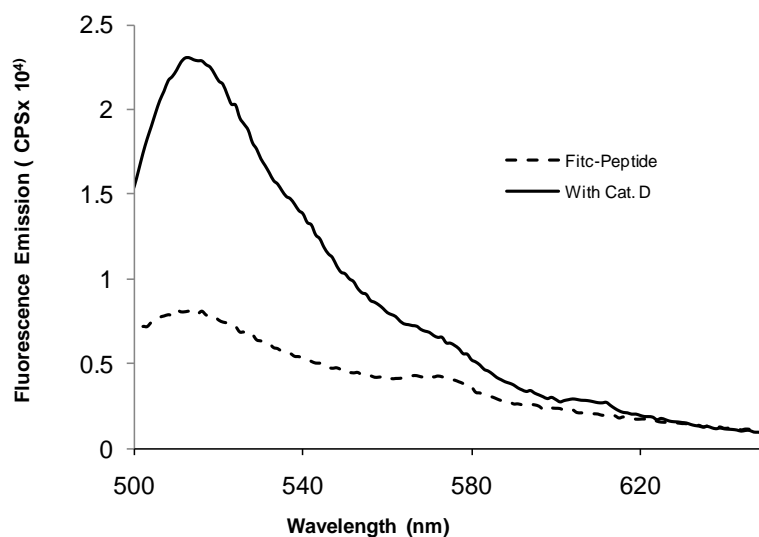
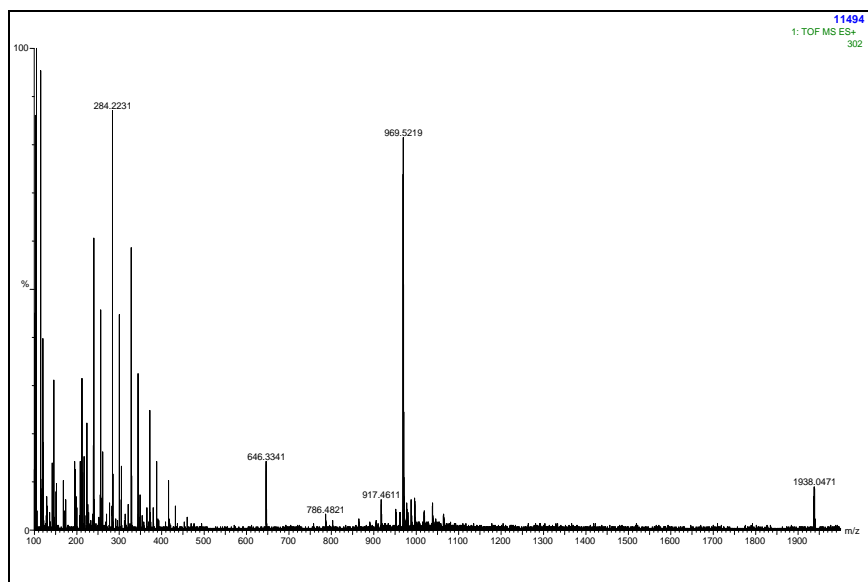
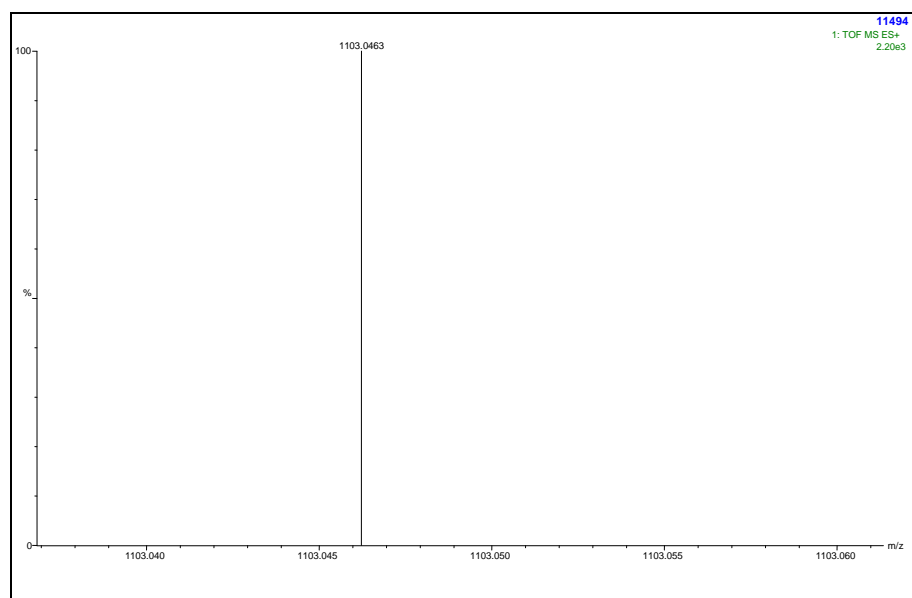


Figure 3-17: Fluorescence emission spectrum of dual peptide with excitation at 488 nm upon hydrolysis by Cat. D



**Figure 3-18: Mass spectrum of FRET-peptide, Calc. 1938.9478, found 1938.0471
[MH⁺]**



**Figure 3-19: Mass spectrum of FRET-peptide after digestion , Calc. 1103.6627,
found 1103.0463 [MH⁺]**

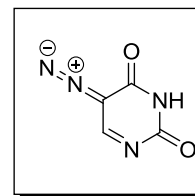
3.3 Conclusion

We have synthesized a novel modified azo-based uracil PNA monomer for the utility as a quencher for PNA-MB design. The synthesized monomer has shown the ability to quench fluorescein and pyrene emissions. In addition, it was incorporated into a dual peptide sequence that was used in the evaluation of the activity of Cathepsin D. The azo-based PNA monomer may have potential application in photoregulation of hybridization due to it showed *trans*-to-*cis* photoisomerization upon illumination with UV-light (366 nm) and *trans* isomer was recovered thermally. The synthesized PNA monomer has showed a characterized spectral change upon changing the pH, this may lead to a new type of pH-indicator based on modified nucleobase.

3.4 Experimental

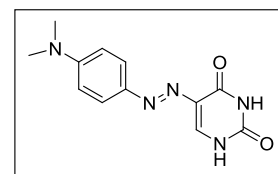
5-Diazouracil¹⁰

To a cold solution of 5-aminouracil (3.0 g, 23.62 mmol) in hydrochloric acid 1N (45 mL), a solution of 6.9 % NaNO₂ (18 mL) was added dropwise over a period of 15 min. a pal yellow solid was precipitated. The reaction mixture was stirred for further 30 min for complete precipitation. Solid was collected by filtration, wash with iced water and was dried under vacuum to give (3.12 g, 84%) and used for the next step without further purification.



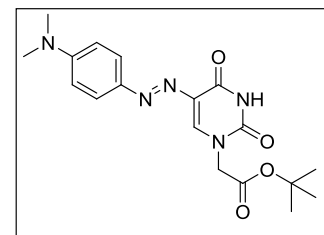
5-[4'(*N,N*-Dimethylamino)phenyl]diazonyl)-(1*H*,3*H*)-pyrimidine-2,4-dione **III-1**.

A suspension of 5-diazouracil (2.0 g, 12.8 mmol) in anhydrous acetonitrile (160 mL) was purged with N₂ for 10 min, borontrifluoride etherate (1.64 mL, 12.8 mmol) and *N,N*-dimethylaniline (1.53 mL, 12.8 mmol) were added to the mixture and was stirred for 2 h. The separated solid was filtered and refluxed in EtOH (150 mL) for 1 h. The solid was collected and dried to afford (2.58 g, 80%) of **III-1**. ¹H NMR (400 MHz, DMSO-d₆) δ : 11.42 (s, 1H), 11.28 (s, 1H), 7.66 (s, 1H), 7.61 (d, *J* = 8.9 Hz, 2H), 6.79 (d, *J* = 8.7 Hz, 2H), 3.01 (s, 6H); ¹³C NMR (100 MHz, DMSO-d₆) δ : 161.8, 152.7, 151.3, 143.5, 130.7, 129.5, 124.9, 112.2, 47.6. HRMS (EI): calcd. for C₁₂ H₁₃ N₅O₂ [M⁺] 259.1069 found 259.1062



tert-Butyl 2-(5-[(4'(*N,N*-dimethylamino)phenyl)diazonyl]-2,4-dioxo-3,4-dihydro pyrimidin-1(2*H*)-yl)acetate **III-2**.

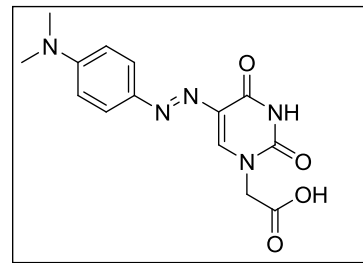
To a solution of **III-1** (1.0 g, 3.86 mmol) in dry DMF (8 mL), *tert*-butyl-2-bromoacetate (0.93 g, 3.86 mmol) and anhydrous K₂CO₃ (0.54 g, 3.9 mmol) were added. The reaction was stirred for 24 h under N₂, the solid was filtered through celite, and the solvent was removed under reduced pressure. The residue was dissolved in dichloromethane (100 mL) and washed with aqueous saturated Na₂CO₃ (2 x



50 mL), brine (50 mL) and dried over Na₂SO₄. The combined organic solvent was concentrated under pressure to obtain a yellow oil which was purified via flash chromatography using ethyl acetate/ hexane as eluting solvents (7: 3, v/v) to yield **III-2** as a yellow solid (0.98 g, 74%). ¹H NMR (400 MHz, DMSO-d₆) δ : 11.8 (s, 1H), 8.06 (s, 1H), 7.65 (d, *J* = 8.4 Hz, 2H), 6.79 (d, *J* = 8.4 Hz, 2H), 4.52 (s, 2H), 3.02 (s, 6H), 1.41 (s, 9H); ¹³C NMR (100 MHz, DMSO-d₆) δ : 167.7, 161.8, 152.8, 150.9, 143.5, 134.6, 129.6, 125.3, 112.2, 82.6, 50.51, 28.3. HRMS (EI): calcd. for C₁₈ H₂₃ N₅O₄ [M⁺] 373.1750 found 373.1732.

***tert*-Butyl 2-(5-[(4'(N,N-dimethylamino)phenyl)diazenyl])-2,4-dioxo-3,4-dihydro pyrimidin-1(2H)-yl) acetic acid **III-3**.**

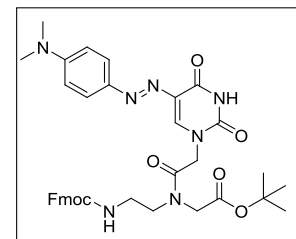
To a cold solution of **III-2** (0.90 g, 2.41 mmol) in dry dichloromethane (3 mL), TFA (3 mL) was added dropwise, the reaction mixture was stirred for 4 h at r.t. under N₂. A cold diethylether (15 mL) was added and the mixture kept overnight at 4 °C. The resultant solid was collected by



filtration, washed with cold diethylether and dried to give **III-3** (0.69 g, 90%) as yellowish brown solid. ¹H NMR(400 MHz, DMSO-d₆) δ : 13.22 (s, br, 1H), 11.78 (s, 1H), 8.07 (s, 1H) 7.65 (d, *J* = 8.9 Hz, 2H), 6.81 (d, *J* = 8.9 Hz, 2H), 4.55 (s, 2H), 3.03 (s, 6H); ¹³C NMR (100 MHz, DMSO-d₆) δ : 170.1, 161.4, 152.8, 150.9, 143.5, 134.7, 129.6, 125.0, 112.2, 49.8. HRMS (EI): calcd. for C₁₄ H₁₅ N₅O₄ [M]⁺ 317.1124 found 317.1121.

***tert*-Butyl-2-(N-(2-(((9H-fluoren-9-yl)methoxy)carbonylamino)ethyl)-2-(5-[(4-N,N-dimethylamino)phenyl)diazenyl])-2,4-dioxo-3,4-dihydropyrimidin-1(2H)-yl)acetamido)acetate **III-4**.**

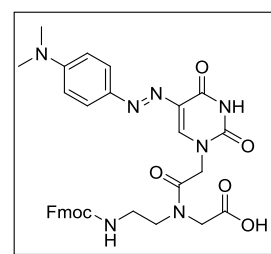
To a cold solution of compound **III-3** (0.50g, 1.57 mmol) in dry DMF (7 mL), DCC (0.32 g, 1.57 mmol) and HOBt (0.21 g, 1.57 mmol) were added. The reaction purged with N₂ for 15 min then was stirred for 1h under ambient atmosphere, followed by dropwise addition of a solution of N-[2-(Fmoc)aminoethyl]



glycine-*t*-butyl ester (0.63 g, 1.57 mmol) in dichloromethane (5 mL). The reaction was stirred under N₂ for 24 h, filtered through celite to remove the formed DCU and the solvent was removed under reduced pressure. The residue was dissolved in dichloromethane (50 mL), washed with aqueous 5% NaHCO₃ (50 mL) (2 x 50 mL), and brine (50 mL) and dried over Na₂SO₄. The organic solvents were removed under pressure and the residue was subjected to flash chromatography using ethylacetate/hexane (7:3, v/v) as the eluting solvents. The combined fractions were evaporated to give **III-4** as yellow solid (0.72 g, 65%). Compound **III-4** exists in solution as a pair of slowly exchanging rotamers; signals attributed to major (ma.) and minor (mi.) rotomers are designated: ¹H NMR (400MHz, DMSO-d₆) δ: 11.76 (s, 1H), 8.09 (s, 1H) 7.89 (d, *J* = 7.5, 2H), 7.69-7.60 (m, 4H), 7.42-7.32 (m, 4H), 6.78 (d, *J* = 7.6 Hz, 2H), 4.86 (s, ma., 1.2H), 4.67 (s, mi., 0.8H), 4.34-4.18 (m, 4H), 3.95 (s, 1H), 3.70 (s, 1H), 3.42-3.39 (m, 2H), 3.27-3.26 (m, 2H), 3.01 (s, 6H), 1.46 (s, mi., 3H), 1.36 (s, ma., 6H); ¹³C NMR (100 MHz, DMSO-d₆) δ: 161.1, 156.2, 155.6, 150.7, 143.9, 142.8, 140.7, 130.1, 128.9, 127.6, 126.8, 125.1, 124.3, 120.1, 111.5, 77.6, 72.47, 65.3, 46.7, 36.9, 28.2. HRMS (ESI-TOF): calcd for C₃₇H₄₂N₇O₇ [MH⁺] 696.3146 found 696.3107.

2-(N-(2-(((9H-fluoren-9-yl)methoxy)carbonylamino)ethyl)-2-(5-[(4-N,N-dimethylamino)phenyl]diazenyl)-2,4-dioxo-3,4-dihydropyrimidin-1(2H)-yl)acetamido)acetic acid **III-5.**

To a cold solution of ester **III-4** (0.35 g, 0.5 mmol) in dichloromethane (2 mL), TFA (2 mL) was added over 10 min. The reaction mixture was stirred under N₂ for 6 h. The solvent was evaporated in *vacuo*. The residue was coevaporated with dichloromethane (4 x 10 mL). The residue was dissolved in



dichloromethane (2 mL), diethylether (5 mL) was added, and the mixture was stored at 4 °C overnight, the resulting solid was filtered and dried to afford **III-5** as yellow solid (0.29 g, 89%). Compound **III-5** exists in solution as a pair of slowly exchanging rotamers; signals attributed to major (ma.) and minor (mi.) rotomers are designated: ¹H NMR (400MHz, DMSO-d₆) 11.67 (s, 1H), 8.07 (s, 1H) 7.84 (s, ma, 0.6 H), 7.87 (d, *J* = 7.4 Hz, 2H), 7.83 (s, mi., 0.4 H) 7.65-7.50 (m, *J* = 7.4 Hz, 4H), 7.38-7.20 (m, *J* = 7.6 Hz,

2H), 7.30 (m, $J = 7.6$ Hz, 2H), 6.76-6.64 (m, $J = 7.6$ Hz, 2H), 4.84 (s, 1H), 4.65 (d, $J = 7.6$ Hz, 1H), 4.31 (d, $J = 7.8$ Hz, 2H), 4.18-4.11 (m, $J = 7.6$ Hz, 1H), 3.93 (s, 1H), 3.86 (s, 1H), 3.39 (t, $J = 7.8$ Hz, 1H), 3.25 (t, $J = 7.8$ Hz, 1H), 3.01 (s, 6H). HRMS (ESI-TOF): calcd for $C_{33}H_{34}N_7O_7$ [MH^+] 640.2520 found 640.2514.

Fluorescence-quenching studies

Fluorescence measurements were carried out on a Photon Technologies International Quanta Master 7/2005 spectrophotometer. All the fluorescence titrations are carried out in ethanol containing 5 μ M concentrations for pyrene and 8 μ M for fluorescein. 1 ml of ethanolic solution of fluorophore was placed in 1cm-fluorescence cell and a small portion (10 μ L) of **III-3** at 5 μ M concentration was added. The emission spectrum was recorded with excitation wavelength set at 488 nm and monitoring emission signal of fluorescein at 520 nm and of pyrene at (337, 395 and 418 nm).

Crystallography

Crystals of **III-2** were grown from a concentrated dichloromethane solution by slow diffusion of hexane. An orange plate was mounted on a glass fiber. Data were collected at low temperature (-123 °C) on a Nonius Kappa-CCD area detector diffractometer with COLLECT (Nonius B.V., 1997-2002). The unit cell parameters were calculated and refined from the full data set. Crystal cell refinement and data reduction were carried out using HKL2000 DENZO-SMN (Otwinowski & Minor, 1997). The absorption correction was applied using HKL2000 DENZO-SMN (SCALEPACK). The crystal data and refinement parameters for **III-2**• CH_2Cl_2 are listed in (Table 3-3).

The SHELXTL/PC V6.14 for Windows NT (Sheldrick, G.M., 2001) suite of programs was used to solve the structure by direct methods. Subsequent difference Fourier syntheses allowed the remaining atoms to be located. Distinct molecules were formed. The molecule was very well ordered. The solvent was located on a symmetry element and was modeled as an anisotropic C and Cl atom. All of the non-hydrogen atoms were refined with anisotropic thermal parameters. The hydrogen atom positions were calculated geometrically and were included as riding on their respective carbon atoms.

Crystal	III-2
Empirical formula	C ₁₉ H ₂₅ Cl ₂ N ₅ O ₄
Formula weight	458.34
Crystal system	Monoclinic
Crystal dimensions	0.20 x 0.18 x 0.15(mm ³)
Space group	P 2 ₁ /n
Z	4
Unit cell dimensions	$a = 13.151(3) \text{ \AA}$ $b = 10.740(2) \text{ \AA}$ $c = 17.188(3) \text{ \AA}$ $\alpha = 90^\circ$ $\beta = 112.31(3)^\circ$ $\gamma = 90^\circ$
Collection ranges	-16<= <i>h</i> <=16; -13<= <i>k</i> <=13; -20<= <i>l</i> <=20
Density(calculated)	1.356 Mg/m ³
Temperature	150(2) K
Volume	2245.7(8) Å ³
Denisty (calculated)	1.355(Mg m ⁻³)
Radiation	Mo K α ($\lambda = 0.71073 \text{ \AA}$)
Absorption coeff.	0.324 mm ⁻¹
Absorption correction	Multi-Scan
<i>F</i> (000)	960
Theta range for data collection	1.68to 27.12°
Observed reflections	17227
Data/restraints/parameters	4945/1/271
Final R indices (<i>l</i> > 2 σ (<i>l</i>))	$R_1 = 0.1145$, $wR_2 = 0.2453$
R indices (all data)	$R_1 = 0.0769$, $wR_2 = 0.2124$
Goodness-of-fit on <i>F</i> ²	1.036

Table 3-4: X-ray crystallographic structural parameters for compound III-2.

Synthesis of dual labeled peptide:

Synthesis of the peptide sequence was obtained using preloaded NovaSyn TGR resin with loading 0.0655 mmol/g on 5 μ mol scale using the standard FastMoc module on an Applied Biosystems 433A synthesizer. After synthesis completion, the last Fmoc protecting group was removed and fluorescein isothiocyanate (FITC) coupling to the N-terminal of the last amino acid was performed manually.

Peptide labeling with FITC

After completion of the peptide synthesis with uncapped *N*-terminal, 30 mg (~ 2 μ mol) of the resin was transferred to a peptide vessel and resin was washed with dry CH_2Cl_2 (3 mL), and drained followed by DMF wash (3 mL), and drained. A solution of FITC (3equiv.) and DIEA (6 equiv) in of dry DMF (1 mL) was added to the resin. Vessel was shaken for 12 h in the dark at r.t. Completion of FITC coupling was confirmed by Kieser test. The dual-labeled peptide sequence was cleaved off and was purified by RP-HPLC. The solvent was drained, the resin was washed with dry CH_2Cl_2 (3 mL) and DMF (3 mL) and dried.

Cleavage of the peptide from resin

To 20 mg (~ 1.3 μ mol) of the resin-bound peptide, in a glass vial, of TFA (1 mL) was added and the mixture was purged with nitrogen and was shaken for 1.5 h. The mixture was filtered and the resin was rinsed with of TFA (0.5 mL). The combined TFA was evaporated with a stream of nitrogen to obtain a sticky residue to the glass vial. By the addition of cold ether (3 mL), an orange precipitate was formed and was collected through decantation of the ether. The solid was dissolved in 0.05% TFA- H_2O (300 μ L), filtered, and purified by RP-HPLC using a 250 mm x 4.6 mm, C18-bonded phase, 100 pore, 5 μ m particle size column. Column was eluted at a flow rate of 1.1 mL/min with the solvent system: A) TFA (0.05%, v/v) in H_2O and B) TFA (0.05%, v/v) in CH_3CN with a binary gradient elution 0-5 min, 100% A; 5-20 min, 100% to 60% A; 20-40 min, 60% to 0%. The collected fractions was lyophilized and was dried to give yellowish-white pellet which was dissolved in mili-Q water (100 μ L) and was stored at -4 $^\circ\text{C}$.

Hydrolysis of FRET-peptide by Cat D.

The emission spectrum was measured for a sample of the dual peptide (0.1 μ mol) in 20 mM citrate-phosphate buffer at a pH 4.5 followed by addition of Cathepsin D (0.01 units, ~0.7 μ g) from bovin spleen, sigma, for digestion. The reaction mixture was incubated at 40 $^\circ\text{C}$ for 30 min then was left to cool to room temperature followed by measuring the emission of fluorescien signal after digestion.

3.5 References

1. a) Shan, S.Y.; Du, J.L.; Yan, J.Z.; Jun, J.L.; Miao, C. Synthesis and photo-activity of peptide nucleic acids containing an azobenzene unit, *Chinese sci. Bull.*, **2009**, 54, 4753-4755. b) Sheng, L.; Miao, C.; Du, j.; HaoBo, Z.; JinQing, W.; Sheng Rong, W. Application of peptide nucleic acids containing azobenzene self-assembled electrochemical biosensors in detecting DNA sequences, *Sci. China Ser. B-Chem.* **2009**, 52, 1009-1013. c) Du, J.L.; Miao, C.; Liu, S.; HaoBo, Z.; Liu, L.Z. Synthesis and photo-activity of phenylazonaphthalene peptide nucleic acid monomers, *Chinese Chemical Letters*, **2008**, 19, 807-810.
2. Tsupak, E.B.; Shevchenko, M.A.; Tkachenko, Y.N.; Nazarov, D.A. 5-Diazouracils in azo coupling reactions, *Russ. J. Org. Chem.*, **2002**, 38, 923-930.
3. a) Griffiths, J. Photochemistry of azobenzene and its derivatives, *J. Chem. Soc. Rev.*, **1972**, 1, 481-493. b) Loudwig, S.; Bayley, H. Photoisomerization of an individual azobenzene molecule in water :an on-off switch triggered by light at a fixed wavelength, *J. Am. Chem. Soc.*, **2006**, 128, 12404-12405.
4. Kuwabara, T.; Nakamura, A.; Ueno, A.; Toda, F. Inclusion complexes and guest-induced color changes of pH-indicator-modified - β -cyclodextrins, *J. Phys. Chem.* **1994**, 98, 6297-6303.
5. a) Kelly, J.; Cuerrier, D.; Graham, L.; Campbell, R.; Davies, P. Profiling of calpain activity with a series of FRET-based substrates, *Biochimica et Biophysica Acta*, **2009**, 1794, 1505-1509. b) Fischer, R.; Bächle, D.; Fotin-Mleczek, M.; Jung, G.; Kalbacher, H., Brock, R.; A targeted protease substrate for a quantitative determination of protease activities in the endolysosomal pathway , *Chem. Bio. Chem.*, **2006**, 7, 1428-1434.
6. a) Fortenberry, S.C., Chirgwin J.M. The propeptide is nonessential for the expression of human cathepsin D. *J. Biol. Chem.* **1995**, 270, 9778-9782. b) Scarborough, P.E.; Dunn, B.M. Redesign of the substrate specificity of human cathepsin D: the dominant role of position 287 in the S2 subsites. *Protein Eng.* **1994**, 7, 495-502.
7. Suchy, M.; Ta, R., Li, X.A.; Wojciechowski,F.; Pasternak, H.S.; Bartha, R.; Hudson, H. E. R. A paramagnetic chemical exchange-based MRI probe metabolized by

Cathepsin D: design, synthesis and cellular uptake studies, *Org. Biomol.Chem.*, 2010, 8, 2560-2566

8. Jullian, M.; Hernandez, A.; Maurras, A.; Puget, K.; Muriel Amblard, M.; Martinez, J.; Subra, G. N-terminus FITC labeling of peptides on solid support: the truth behind the spacer, *Tetrahedron Lett.*, 2009, 50, 260-263.
9. Edman, P. V. Mechanism of the phenyl *isothiocyanate* degradation of peptides, *Nature*, **1956**, 177, 667-668.
10. Thurber, T.C.; Townsend, L.B. A reinvestigation of the structures for 5-diazouracil, 5-diazouridine, 5-diazo-2'-deoxyuridine and certain related derivatives by proton magnetic resonance spectroscopy, *J. Heterocyclic Chem.*, 1972, 9, 629-636.

Chapter 4

Chapter 4

4 Synthesis and Photophysical Studies of Novel photochromic Phosphoramidite for DNA and RNA

4.1 Introduction

Hybridization of nucleic acids is considered the cornerstone for many biomedical applications as antigene and antisense. Recently, much effort has been devoted to controlling DNA functions through external stimuli as light, pH, electric field and heat. Light is preferred over all other external stimuli due to reasons such as light is efficient, clean and does not produce any contaminants to the biological system. Light is a powerful tool to control several bioactive species such as protein, peptides and nucleic acids.

Photoregulation of nucleic acids is based on covalent attachment of a photoresponsive molecule to the single-stranded DNA. This process can be achieved by i) introduction of photolabile protecting groups called caging groups. *ortho*-Nitrobenzyl group (ONB) is an example for caging groups that have been widely used in photoregulation of oligonucleotide and peptides.¹ Recently the ONB group has been used for photocontrol of several biological processes such as gene expression, ribozyme cleavage and RNA polymerase activity.^{2a-c} In these processes, the ONB group is able to cage substrates and then release them upon photoirradiation. ONB groups are removed under mild irradiation with long-wavelength UV radiation (>345 nm) without damaging the biological system. In this strategy, regulation occurs only once and in one direction. Alternatively, ii) a photoswitchable molecule as azobenzene may be used.^{3a,b}

Photoisomerization of azobenzene has been used to photo-control several molecular processes. Azobenzene residues were introduced to oligonucleotides via two approaches: as a side chain on the oligonucleotide phosphate backbone;^{4a-c} and/or as a linker between two oligonucleotide segments in the main chain of an oligonucleotide.^{5a,b} Incorporation of azobenzene as a side chain of the oligonucleotide backbone induces *trans*-to-*cis* isomerization and therefore exerts notable effects on the physicochemical properties and

on the duplex formation abilities of oligonucleotides. Although, the utility of azobenzene as a linker has been demonstrated an efficient *trans*-to-*cis* photoisomerization, no successful application has yet been reported.

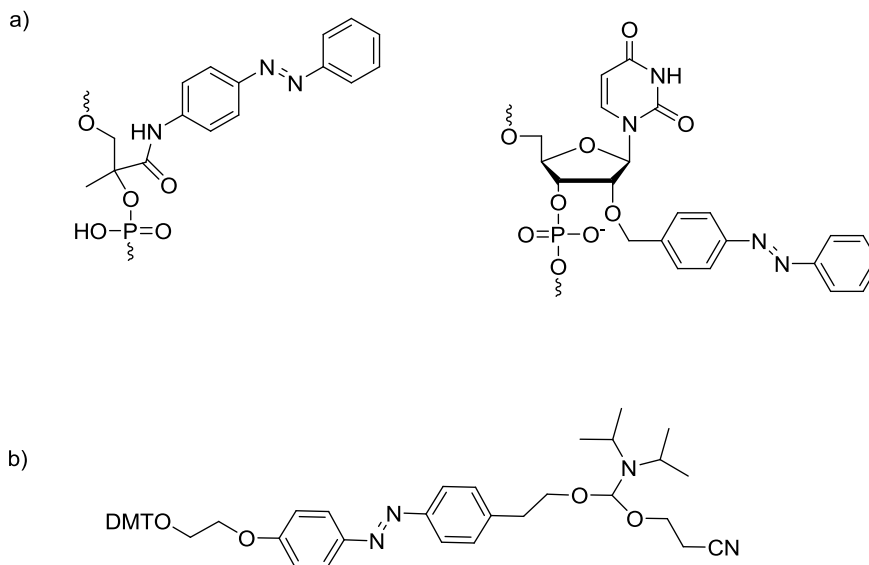


Figure 4-1: Modified oligonucleotides carrying azobenzene a) in the side chain, b) as linker.

Introduction of several azobenzene residues to oligonucleotides led to an increase in melting temperature difference ΔT_m corresponding to the photo-induced isomerization. For example, incorporation of one azobenzene residue into a short 8-mer oligonucleotide forming a duplex, upon *trans*-to-*cis* photoisomerization caused a decrease in ΔT_m by 14.3 °C, while when two azobenzene residues were incorporated, a decrease in ΔT_m by 21.5°C was observed. Incorporation of large numbers of azobenzene residues to duplex structure resulted in deviation of the duplex structure far from the B-form and thusly lost its ability to interact with proteins.⁶

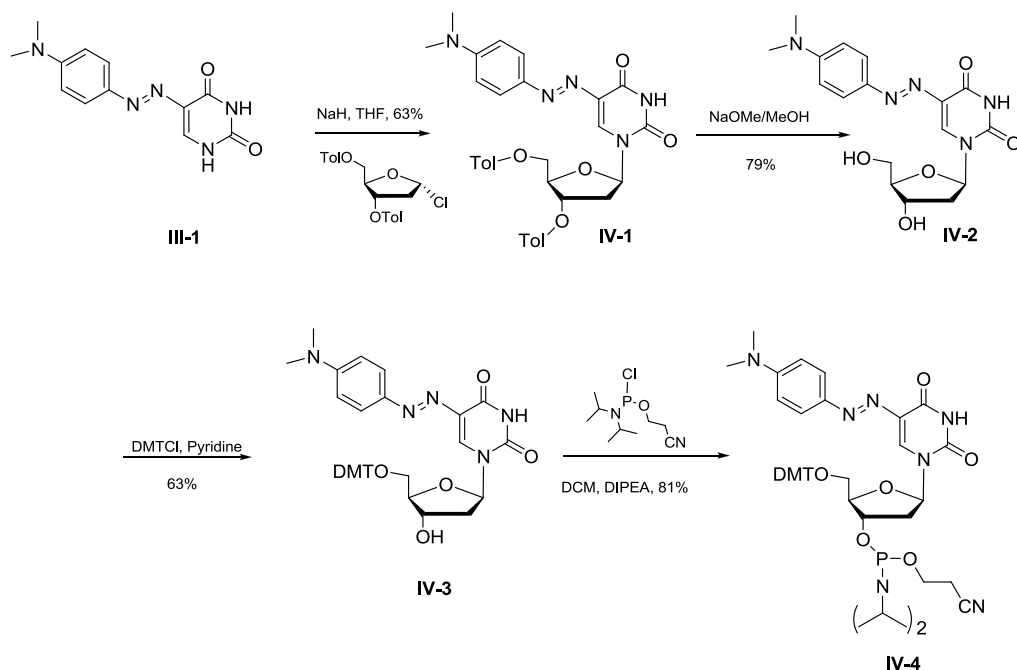
Despite the remarkable properties of azobenzenes and its utility in reversible photoswitching of nucleic acid-related activities, there are some drawbacks arising from the non-nucleosidic nature of the attached azobenzene. In other words, azobenzene is not able to form hydrogen bonding with nucleobases and it undergoes stacking interactions

with the nucleotides that differ from the stacking interaction that occurs among the natural nucleotides and consequently led to change in its structural features. Recently, it was reported that incorporation of azobenzene into DNAzymes and ribozymes lead to loss of its catalytic activity due to interfering with the active site.⁷

4.2 Result and discussion

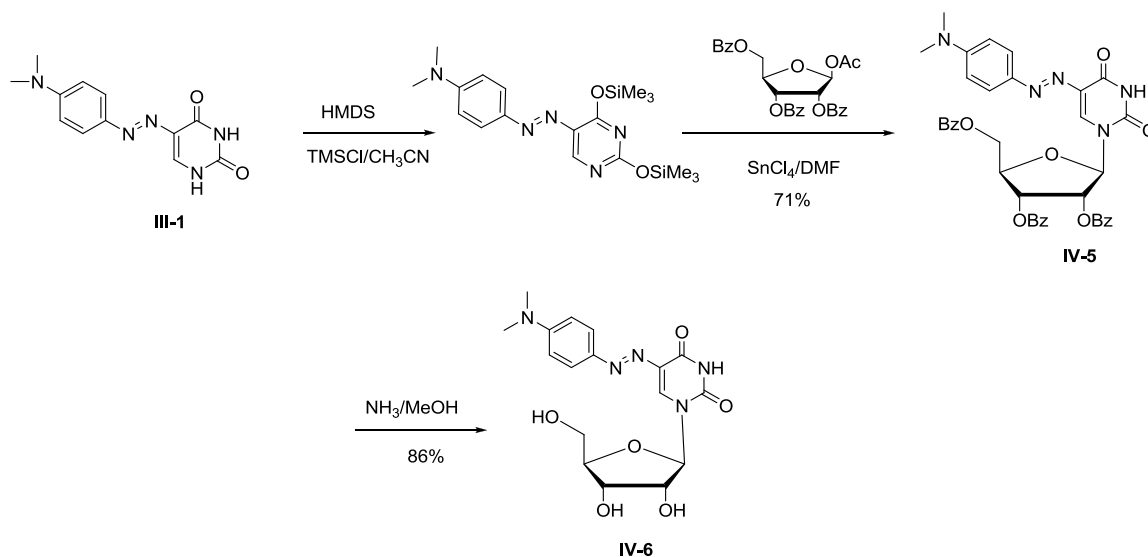
In this work we aimed to synthesize novel photochromic nucleosides for DNA and RNA synthesis bearing azo-moiety as a solution to circumvent the aforementioned limitations observed in azobenzene-based oligonucleotides. The synthesized photochromic nucleosides are characterized by their ability to form hydrogen bonding with nucleosides obeying Watson-Crick base pairing rules with potential quenching properties based on the results shown in chapter 3. This goal was achieved by utilizing the naturally occurring uracil as starting material to maintain hydrogen bonding ability with the complementary nucleobase adenine (A), and via chemical transformations to introduce phenylazomoiety to uracil.

As outlined in (Scheme 4-1), the synthetic route to synthesize the azo-uracil phosphoramidite **IV-4** was started with reaction of azo-modified uracil **III-1** with 1-chloro-3,5-di-*O*-*p*-toluoyl-1,2-dideoxy- α -D-ribofuranose under basic conditions to yield the corresponding protected deoxyriboside **IV-1** in 63% yield. Removal of the toluoyl protecting groups was carried out with sodium methoxide in methanol giving the 2-deoxyriboside **IV-2** in 79% yield. Standard methods were used to convert the unprotected nucleosides to 5'-dimethoxytrityl-protected derivative **IV-3** by using dimethoxytrityl chloride (DMTCl) in pyridine giving the product in 63% yield. This was followed by conversion to the corresponding cyanoethyl phosphoramidite derivative **IV-4** in 81 % yield after column chromatography purification.



Scheme 4-1: Synthesis of uracil phosphoramidite possesses phenylazo moiety for photoswitching.

To get an access for RNA chemistry, ribonucleoside **IV-5** was synthesized as outlined in (Scheme 4-2) following Vorbrüggen procedure⁸ starting with refluxing **III-1** with hexamethyldisilazane (HMDS) and trimethylsilyl chloride (TMSCl) to form the corresponding silylated nucleoside followed by coupling with 1-*O*-acetyl-2,3,5-tribenzoyl- β -D-ribofuranose in dimethylformamide (DMF) in the presence SnCl_4 to afford **IV-5** in 71% after column chromatography purification. Removal of benzoyl groups was carried out by ammonia in methanol to yield azo-based riboside **IV-6** in 86% yield.



Scheme 4-2: Synthesis of photochromic riboside.

4.2.1 Photoisomerization studies

Azobenzene is well known to photoisomerize from its planar *trans* isomer to the non-planar *cis* isomer after UV-light irradiation (300nm ~ 400nm), and back to the *trans*-isomer upon irradiation with visible light (> 400nm) or thermally. This process is completely reversible under UV and visible irradiations. Based on this observation, the synthesized nucleosides carrying 4-(*N,N*-dimethylamino)azophenyl moiety are expected to follow the same behavior that azobenzene follows as demonstrated in (Fig. 4-2).

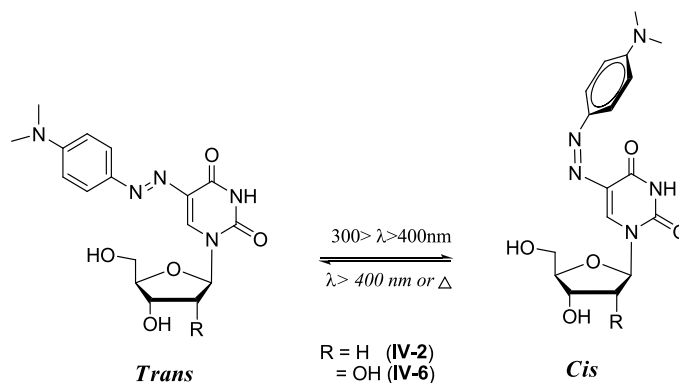


Figure 4-2: Schematic representation of reversible *trans-cis* photoisomerization of the photochromic nucleoside IV-2 and IV-6.

To assess the photochromic behaviour of the synthesized nucleosides **IV-2** and **IV-6** by monitoring the changes that may occur at their absorption with response to irradiation. As can be seen from (Fig. 4-3), the absorption spectrum of *trans* isomer has a major peak centered at 454 nm (in dichloromethane for **IV-2**) and at 443 nm (in acetonitrile for **IV-6**) attributed to strong π - π^* transition which overlapped with the weak peak attributed to weak n - π^* transition. By irradiating with UV-light at 366 nm, a decrease in the intensity of the absorption band was observed along with the irradiation time due to *trans*-to-*cis* isomerization, while the reverse *cis*-to-*trans* isomerization was achieved via thermal relaxation.

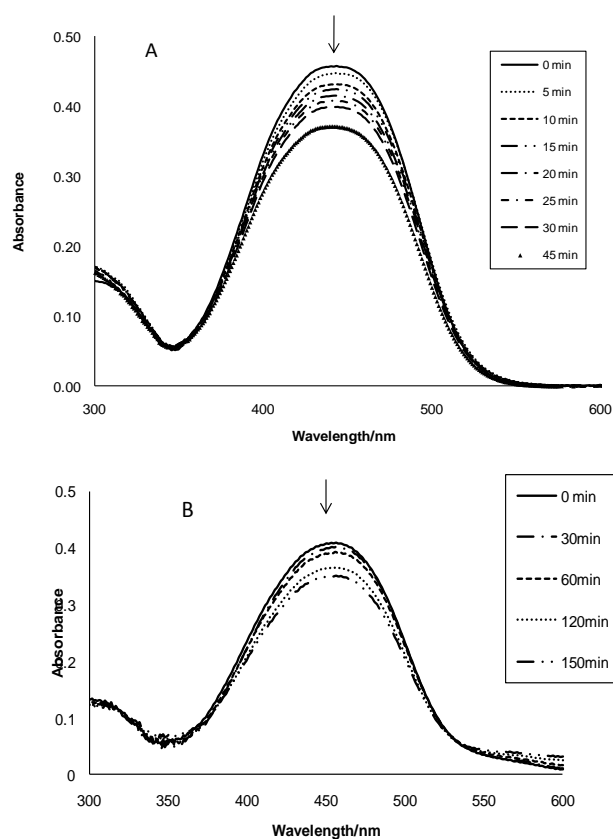


Figure 4-3: Absorption spectra of A) **IV-2** in ethanol and B) **IV-6** in acetonitrile at 10 μ M concentrations for *trans*-to-*cis* photoisomerization upon illumination with UV-light at 366 nm.

4.2.2 pH-Sensitivity

Azobenzenes derivatives especially aminoazobenzene and 4-(*N,N*-dimethylamino)azobenzene attracted much attention due to their ability to change colour in solution with the changing of the pH. It is well established that protonation of aminoazobenzene derivatives led to the formation of two tautomeric azonium and ammonium forms.^{9a,b} The azonium ion is obtained by protonation on azo-nitrogen leading to delocalized of the lone-pair electrons of the aromatic ring and as consequence a red shift in absorption maximum was occurred. Ammonium ion is obtained by protonation at amino-nitrogen resulting in prevention the conjugation of electrons lone-pairs and thusly the UV-Vis spectrum looks similar to that of unsubstituted azobenzene due to diminish the effect of amino substituent.

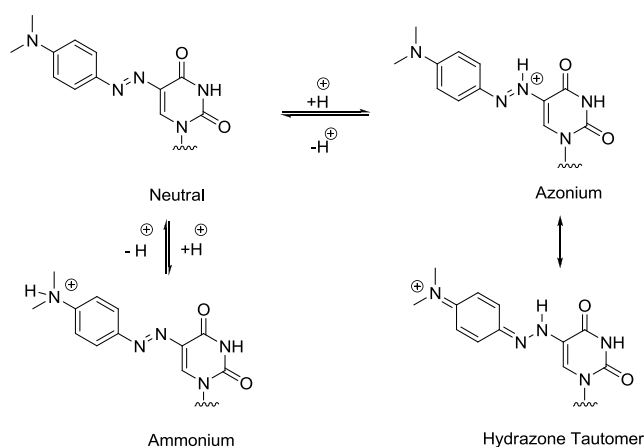
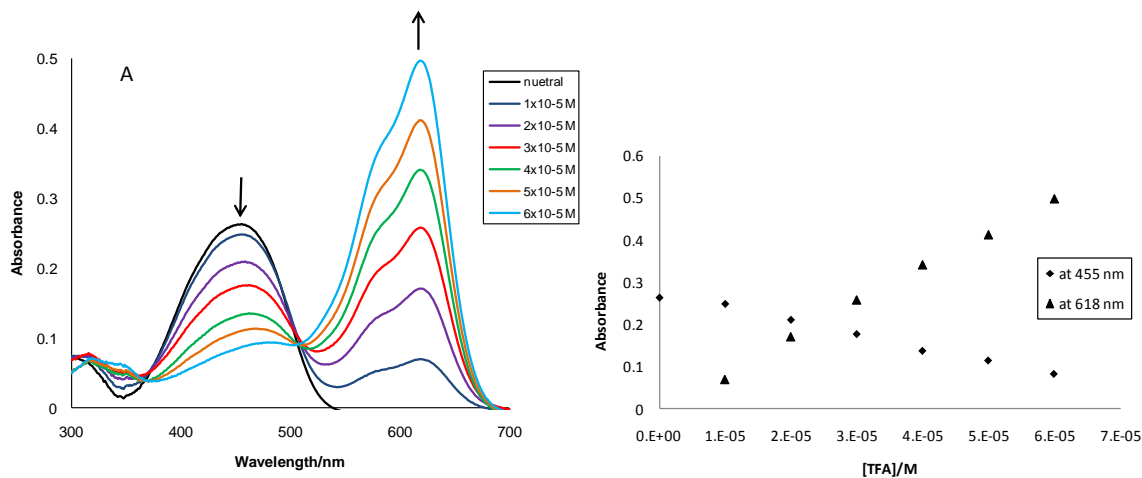


Figure 4-4: Structure of 4-(*N,N*-dimethylamino)azophenyl(deoxy)uridine and its protonated forms. Sugar was removed for simplicity.

As mentioned in chapter 3, the presence of an azo- and dimethylamino groups in the synthesized nucleosides promoting us to study the effect of acid. We investigated the effect of trifluoroacetic acid solution (0.005 M) in dichloromethane and ethanol on the nucleosides **IV-2** and **IV-6** respectively. Matazo and coworkers¹⁰ have studied the effect of acid on 4-(*N,N*-dimethylamino)azobenzene, they observed that absorption band appears at λ_{\max} 411 nm in acetonitrile which is attributed to neutral *trans* 4-(*N,N*-dimethylamino)azobenzene, upon protonation this band was red shifted to λ_{\max} 535 nm with appearance of absorption band at λ_{\max} 318 nm. They have assigned the two bands

to the azo-protonated (azonium) and amino protonated (ammonium) of *trans*-4-(*N,N*-dimethylamino)azobenzene, respectively, based on quantum-chemical calculations and resonance Raman spectra.

Similarly, as can be seen in (Fig. 4-5), upon addition of TFA solution to deoxyriboside **IV-2** in dichloromethane leads to a decrease in the π - π^* absorption band at λ_{\max} 455 nm which is attributed to the neutral form with an increase in π - π^* absorption bands centered at 618 and 350 nm attributed to azonium and ammonium ions respectively. There are two isosbestic points were observed at 376, 507 nm indicate that **IV-2** exists either as non-protonated or protonated species in tautomeric equilibrium. While, upon titrating of **IV-6** with small aliquots of TFA in ethanol, the π - π^* absorption band for neutral form at λ_{\max} 436 nm was decreased with appearance of new absorption bands centered at 623 and 342 nm attributed to the protonated forms azonium and ammonium ion respectively. These results are in excellent agreement with the aforementioned study. Surprisingly, subjecting solutions of **IV-2** and **IV-6** in halogenated solvents as dichloromethane or chloroform to TFA leads to colour change from yellow to deep blue colour while using solvents as ethanol, methanol, and ethyl acetate instead this colour change was not observed.



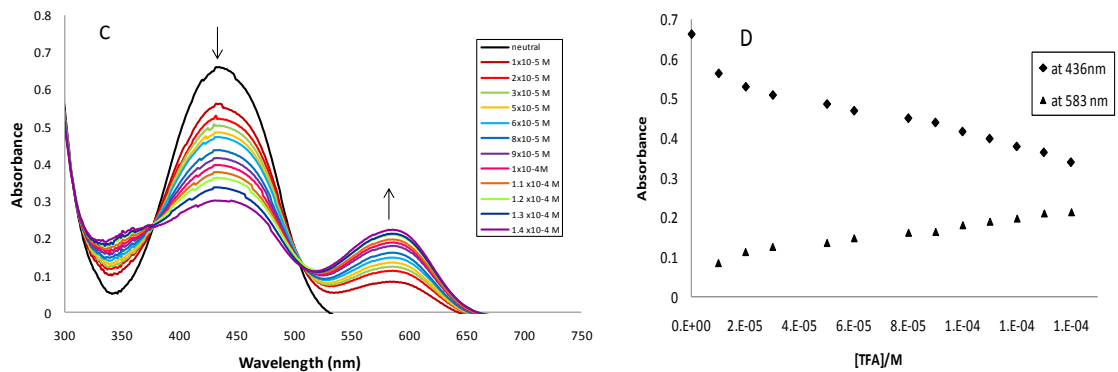


Figure 4-5: Changes in UV-Vis spectra of A) IV-2 and C) IV-6 upon addition of increasing concentrations of TFA, arrows indicate the progressive decrease of absorption band for neutral form and the growth of protonated form. B, D) Variation of absorbance vs TFA concentration for the respective absorption bands.

4.3 Conclusion

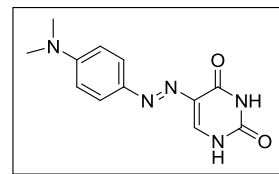
We have successfully designed and synthesized novel photochromic azo-based nucleosides. These nucleosides showed the ability to undergo *trans*-to *cis* isomerization upon irradiation with visible light at 366 nm and reversibly the *trans* configuration was recovered thermally in the dark. In addition, the synthesized photochromic nucleotides showed halochromic effect upon acid treatment. Therefore, they may be contributing in photoregulation of nucleic acids. To the best of our knowledge, this is the first example of azo-based (deoxy)uridine derivatives possess intrinsic photoswitching property.

4.4 Experimental

General consideration. All solvents and chemicals were commercially available and were used as purchased. Reactions were monitored by thin layer chromatography (TLC) on pre-coated 0.2 mm Merck Kieselgel 60 TLC plates. Silica gel 60 F254 (Merck) plates and visualized with an ultraviolet light source at 254 nm. Silica gel (Merck Kieselgel 60, 15-40 mm) was used for column chromatography. ^1H NMR, ^{13}C NMR and ^{31}P NMR spectra were recorded at a Varian Mercury Plus spectrometer (400.09 MHz, 100.61MHz and 242.9 MHz respectively) at room temperature. Chemical shifts are reported in parts per million (δ), were measured from tetramethylsilane (0 ppm) and are referenced to the residual proton in the deuterated solvent: CDCl_3 (7.26 ppm), $\text{DMSO-}d_6$ (2.48 ppm), CD_3OD (2.04 ppm) for ^1H NMR and CDCl_3 (77.0 ppm), $\text{DMSO-}d_6$ (39.5 ppm) and CD_3OD (49.1) for ^{13}C NMR. Multiplicities are described as s (singlet), d (doublet), m (multiplet), and br s (broad singlet). Coupling constants (J) are reported in Hertz (Hz).

5-[4'-(*N,N*-Dimethylamino)phenyl]diazenyluracil III-1

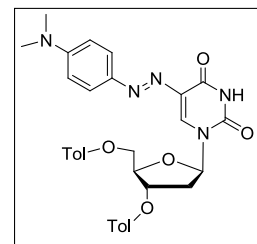
To a cold solution of 5-aminouracil (1.0 g, 7.87 mmol) in hydrochloric acid 1N (15 mL), a solution of 6.9% NaNO_2 (6 mL) was added dropwise over a period of 15 min. a pal yellow solid was precipitated. The reaction mixture was stirred for further 30



min for complete precipitation. Solid was collected by filtration, wash with iced water and was dried under vacuum to give 5-diazouracil (1.04 g, 84%) and used for the next step without further purification. A suspension of 5-diazouracil (0.5 g, 3.2 mmol) in anhydrous acetonitrile (50 mL) was purged with N_2 for 10 min, borontrifluoride etherate (0.41 mL, 3.2 mmol) and *N,N*-dimethylaniline (0.38 mL, 3.2 mmol) were added to the mixture and was stirred for 2 h. The separated solid was filtered and refluxed in EtOH (100 mL) for 1 h The solid was collected and dried to afford (1.38 g, 80%) of **IV-1**. ^1H NMR ($\text{DMSO-}d_6$) δ : 11.42 (s, 1H), 11.28 (s, 1H), 7.66 (s, 1H), 7.61 (d, J = 8.9 Hz, 2H), 6.79 (d, J = 8.7 Hz, 2H), 3.01 (s, 6H); ^{13}C NMR ($\text{DMSO-}d_6$) δ : 161.8, 152.7, 151.3, 143.5, 130.7, 129.5, 124.9, 112.2, 47.6. HRMS (EI): calcd. for $\text{C}_{12}\text{H}_{13}\text{N}_5\text{O}_2$ [M^+] 259.1069 found 259.1062.

**5-[(4'-(*N,N*-dimethylamino)phenyl)diazenyl]-3'', 5''-di-*O*-(*p*-toluoyl)-2''-deoxyuridine
IV-1**

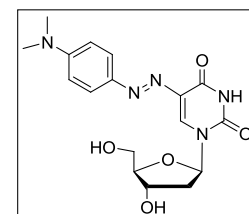
To a suspension of 5-((4'-(*N,N*-dimethylamino)phenyl)diazenyl) uracil (0.44 g, 1.72 mmol) in dry THF (20 mL), NaH (60% dispersion in mineral oil, 82 mg, 3.44 mmol) was added and stirred at r.t. for 2 h. A solution of 1- α -Chloro-3,5-di-*O*-toluoyl)-2-deoxyribose (0.69 g, 2.23 mmol) in dry THF (5 mL) was added to



the mixture in one portion and the reaction mixture was stirred for 24 h under an atmosphere of N₂. Solvent was evaporated under vacuum and the residue was dissolved in dichloromethane (30 mL), was washed with saturated aqueous sodium Na₂CO₃, brine and dried over anhydrous Na₂SO₄. The solution was filtered, concentrated, and the residue was subjected to purification by flash chromatography with CH₂Cl₂/CH₃OH (20:1, v/v) as eluent to give bis-toluoyl ester **IV-1** as red solid. The product was obtained as a mixture of two isomers (0.65 g, 63%). ¹H NMR (DMSO-d₆) δ : 11.78 (br s, 1H), 8.02 (s, 1H), 7.92-7.89 (m, 2H), 7.80 (d, *J* = 7.8 Hz, 1H), 7.68 (d, *J* = 8.2 Hz, 1H), 7.50 (d, *J* = 8.9 Hz, 1H), 7.37-7.33 (m, 3H), 7.16 (d, *J* = 8.2 Hz, 1H), 6.91 (d, *J* = 8.2 Hz, 1H), 6.75 (d, *J* = 8.9 Hz, 1H), 6.69 (d, *J* = 9.3 Hz, 1H), 6.32 (m, 1H), 5.57 (d, *J* = 5.8, 1H), 5.01 (m, 1H), 4.57 (m, 1H), 4.41 (m, 1H), 3.02 (s, 6H), 2.97 (m, 1H), 2.61 (m, 1H), 2.37 (s, 3H), 2.26 (s, 3H); ¹³C NMR (CDCl₃) δ : 166.1, 165.7, 152.2, 144.3, 143.5, 129.8, 129.6, 129.1, 126.5, 126.6, 126.3, 125.7, 111.2, 87.9, 77.3, 74.6, 64.1, 40.1, 27.96. HRMS (ED): calcd. 611.2380 for C₃₃H₃₃N₅O₇ [M⁺] found 611.2391.

5-[4'-(*N,N*-dimethylamino)phenyl)diazenyl]-2''-deoxyuridine IV-2.

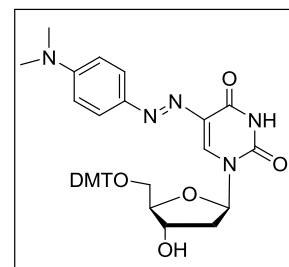
To a cold solution of the toluoyl ester **IV-1** (0.5 g, 0.82 mmol) in dry CH₂Cl₂ (5 mL), NaOMe solution (0.2 M in MeOH) (9.8 mL, 1.96 mmol) was added dropwise over 15 min. The reaction mixture was stirred at r.t. for 1 h. An aqueous solution of 5% NH₄Cl was added to the mixture till the pH was 8 and the mixture was extracted with ethylacetate (3 x 30 mL). The combined organics were washed with brine, dried over anhydrous Na₂SO₄ and concentrated under reduced pressure to afford red oil residue. The



residue was subjected to flash chromatography using hexane/ CH₂Cl₂ (70:30, v/v) as the eluent to yield the deoxyriboside **IV-2** as red powder (0.25 g, 79%). ¹H NMR (CD₃OD) δ: 8.50 (s, 1H), 7.79 (d, *J* = 7.8 Hz, 1H), 6.77 (d, *J* = 7.8 Hz, 1H), 6.33 (t, *J* = 6.5 Hz, 1H), 4.43 (m, 1H), 3.96 (m, 1H), 3.83 (m, 1H), 3.75 (m, 1H), 3.20 (dd, *J* = 3.3 and 7.3 Hz, 1H), 3.03 (s, 6H), 2.40 (m, 2H); ¹³C NMR (CD₃OD): δ 163.5, 154.3, 151.5, 131.2, 126.4, 112.7, 89.3, 87.4, 72.1, 62.7, 41.8, 40.5. HRMS (EI): calcd. 375.1543 for C₁₇H₂₁N₅O₅ [M⁺] found 375.1535.

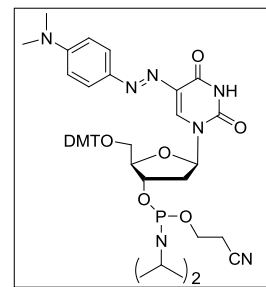
5-[4'-(*N,N*-dimethylamino)phenyl]diazenyl]-2''-deoxy-5''-O-(*p,p'*-dimethoxytrityl)uridine **IV-3**

The free nucleoside **IV-2** (0.2 g, 0.54 mmol) was dried by coevaporation with dry pyridine (3 x 5 mL) and then was dissolved in dry pyridine (10 mL). A solution of 4,4'-dimethoxytritylchloride (0.269 g, 0.69 mmol) in dry pyridine (5 mL) and DIPEA (7.0 mmol, 1 mL) was added and the mixture was stirred at r.t. for 3 h. The reaction mixture was quenched by the addition of methanol (2 mL), was diluted with CH₂Cl₂ (75 mL) and then was washed with saturated aqueous solution of NaHCO₃ (3 x 50 mL). The organics were combined, dried over anhydrous Na₂SO₄ and filtered. The solvent was removed under reduced pressure to give red oil. The crude product was purified by flash column chromatography using CH₂Cl₂/ MeOH/ Et₃N (85: 10: 5, v/v) as elution solvent afforded the tetritylated derivative **IV-3** as red solid (0.28 g, 63%). ¹H NMR (CDCl₃) δ: 8.25 (s, 1H), 7.65 (d, *J* = 8.9 Hz, 2H), 7.38 (d, *J* = 7.4 Hz, 2H), 7.27 (d, *J* = 7.4 Hz, 4H), 7.22 (d, *J* = 7.0 Hz, 2H), 7.14 (m, 2H), 6.78 (d, *J* = 8.5 Hz, 3H), 6.51 (d, *J* = 8.5 Hz, 2H), 6.18 (m, 1H), 4.57 (m, 1H), 4.39 (m, 1H), 3.69 (s, 6H), 3.20 (m, 1H), 3.25 (m, 1H), 2.90 (s, 6H), 2.80 (m, 1H), 2.47 (m, 1H); ¹³C NMR (CDCl₃) δ: 161.4, 158.3, 152.0, 149.7, 144.5, 143.3, 135.6, 135.39, 130.4, 129.8, 127.9, 127.7, 126.6, 125.0, 113.0, 111.1, 89.1, 86.2, 71.9, 64.1, 55.0, 45.6, 40.0. HRMS (ESI): calcd. 678.2928 for [MH⁺] C₃₈H₄₀N₅O₇ found 678.2906.



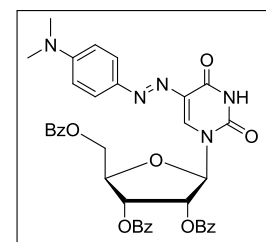
5-[4'-(*N,N*-dimethylamino)phenyl]diazenyl]-2''-deoxy-3''-(2-cyanoethyl)diisopropyl phosphoramidite)-5''-O-(*p,p'*-dimethoxytrityl)uridine **IV-4**

To a solution of DMT-deoxyuridine **IV-3** (0.16 g, 0.24 mmol) in dry CH₂Cl₂ (5 mL), DIPEA (340 μL, 2.4 mmol), 2-cyanoethyl-(*N,N'*-diisopropylamino) chlorophosphite (105 μL, 0.47 mmol) was added. The reaction mixture was stirred at r.t. under ambient atmosphere for 3 h until deemed complete by TLC. Solvent was removed and the resultant residue was dissolved in CH₂Cl₂ (25 mL), washed with aqueous solution of 5% NaHCO₃ (25 mL), brine (20 mL) and was dried over anhydrous Na₂SO₄. After removal of solvent the crude product was subjected to flash chromatography using hexane/ ethylacetate/ Et₃N (80:15: 5 to 50:45:5, v/v) to yield the phosphoramidite derivative **IV-4** (0.169 g, 81%). ¹H NMR (CDCl₃) δ : as two diastereomers: 8.19 and 8.17 (2s, 1H), 7.77 (d, *J* = 7.6 Hz, 2H), 7.38 (d, *J* = 7.6 Hz, 2H), 7.21 (m, 7H), 6.79 (d, *J* = 6.7Hz, 4H), 6.63 (d, *J* = 6.5 Hz, 2H), 6.29 (m, 1H), 4.80 (m, 1H), 4.54-4.46 (m, 2H), 3.75 (s, 6H), 3.57-3.48 (m, 2H), 3.03 (s, 6H), 3.38 (m, 1H), 3.11 (m, 1H), 2.85 (m, 2H), 2.38-2.17 (m, 2H), 1.20 (s, 12H); ¹³C NMR (CDCl₃) δ : 160.8, 158.5, 152.3 149.5, 144.3, 143.5, 135.5, 129.9, 128.0, 126.9, 125.1, 113.2, 111.2, 88.7, 85.5, 74.1, 67.1, 55.0, 43.0, 40.2, 32.2, 29.6, 26.3, 24.4, 23.38; ³¹P NMR (CDCl₃): δ two diastereomeric peaks at 149.2 and 148.6. HRMS (ESI): calcd. 878.3880 for [MH⁺] C₄₆H₅₅N₈O₈P, found 878.3889.



5-[(4'-(*N,N*-dimethylamino)phenyl)diazenyl]-1-(2'', 3'', 5''-tri-*O*-benzoyl-β-D-ribofuranosyl)]uridine **IV-5**

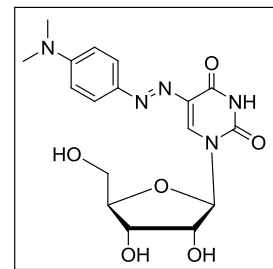
A suspension of 5-((4'-(*N,N*-dimethylamino)phenyl)diazenyl)uracil **III-1** (0.26 g, 1 mmol) in of 1,1,1,3,3,3-hexamethyldisilazane (HMDS) (20 mL) and of trimethylsilyl chloride (1 mL) was refluxed until a clear solution was obtained. The solution was allowed to cool, and excess HMDS was removed under reduced pressure. The silylated uracil derivatives were dissolved in CH₃CN (5 mL) and the solution was purged with nitrogen for 15 min prior to addition of SnCl₄ (10% excess)



(127 μL , 1.2 mmol) to the reaction mixture with vigorous stirring. A solution of 1-*O*-acetyl-2,3,5-tri-*O*-benzoyl- β -D-ribofuranose (0.56 g, 1.1 mmol) in CH_2Cl_2 (20 mL) was added dropwise to the reaction mixture. The solution was stirred at r.t. for 6 h at which the reaction came to completion as determined by TLC. The reaction mixture was quenched by aqueous saturated NaHCO_3 solution (100 ml) and was extracted with CH_2Cl_2 (3 x 50 ml) and was dried over anhydrous Na_2SO_4 . The solvent was removed under reduced pressure leaving brown residue. The crude product was purified by flash column chromatography using elution with a gradient of hexane/ CH_2Cl_2 (from 100:0 to 60:40, v/v). Compound **IV-5** was isolated as a red solid (0.5 g, 71%). ^1H NMR (CDCl_3) δ : 9.86 (br s, 1H), 8.05 (s, 1H), 7.96 (d, $J = 7.4$, 2H), 7.91 (d, $J = 7.0$, 2H), 7.70 (d, $J = 7.4$, 3H), 7.49 (m, 4H), 7.32 (m, 6H), 6.66 (d, $J = 7.0$, 2H), 6.29 (m, 1H), 4.82 (m, 1H), 4.72 (m, 3H), 3.06 (m, 1H), 3.03 (s, 6H); ^{13}C NMR (CDCl_3) δ : 166.2, 165.3, 160.6, 152.7, 149.4, 143.4, 133.8, 133.4, 129.9, 129.8, 128.5, 125.5, 111.2, 88.6, 80.9, 74.2, 71.5, 64.2, 40.2. HRMS (ESI): calcd. for $\text{C}_{38}\text{H}_{34}\text{N}_5\text{O}_9$ [MH^+] 704.2357 found 704.2358.

5-[(4'-(*N,N*-dimethylamino)phenyl)diazenyl]uridine **IV-6**

Compound **IV-5** (0.4 g, 0.57 mmol) was dissolved in saturated solution of ammonia in methanol (20 mL) and was stirred for 4 h at r.t. The solution was evaporated under pressure to give the crude product which was purified by flash column chromatography using $\text{CH}_2\text{Cl}_2/\text{MeOH}$ (90: 10,v/v) yielding 0.19 g (86%). ^1H NMR (DMSO-d_6) δ : 7.73 (s, 1H), 7.64 (d, $J = 8.9$, 2H), 6.78 (d, $J = 8.9$, 2H), 6.14 (m, 1H), 5.07 (m, 1H), 4.90 (m, 1H), 4.62 (m, 1H) (Exchangeable 3OH), 4.52 (m, 1H), 4.12 (d, $J = 5.4$, 1H), 3.69 (m, 1H), 3.62 (m, 2H), 3.44 (m, 1H), 3.01 (s, 6H); ^{13}C NMR (DMSO-d_6) δ : 160.8, 152.5, 143.2, 124.8, 111.9, 94.9, 84.9, 71.4, 70.6, 63.7, 62.79, 40.5. HRMS (ESI): calcd. for $\text{C}_{17}\text{H}_{21}\text{N}_5\text{NaO}$ [M^+] 414.1390 found 414.1382.



UV-Vis measurements:

All UV-Vis spectra were measured with a Varian Cary 300 Bio spectrophotometer using quartz cuvette cells of 1 mm of optical path.

Photoisomerization.

Trans-to-cis photoisomerization of nucleosides **IV-2** and **IV-6** were monitored by UV-Vis spectroscopy. A solution of the nucleosides at 1.06×10^{-5} M concentration (**IV-2** in dichloromethane) and (**IV-6** in acetonitrile) were irradiated with UV-light at room temperature using a UVGL-58 hand held lamp (6 watt, 366 nm) at A distance of approximately 5 cm. The spectral change for absorption maximum peak at 455 nm (for **IV-2**) and 436 nm (for **IV-6**) were monitored with the time course of irradiation. While the *cis-to-trans* isomerization was achieved and confirmed by retrieving the maximum absorption bands at 455 nm (for **IV-2**) and 436 nm (for **IV-6**) thermally by leaving the samples at the dark at room temperature.

Effect of acids

The spectral change of the synthesized photochromic nucleosides at concentration 6.2×10^{-6} M (in dichloromethane for **IV-2**) and 1.5×10^{-5} M (in ethanol for **IV-6**) were monitored upon addition of small aliquots of TFA solution (0.005 M).

4.5 References

1. Mayer, G., Heckel, A. Biologically active molecules with a "Light Switch", *Angew. Chem.*, **2006**, 118, 5020-5042, *Angew. Chem. Int. Ed.* **2006**, 45, 4900-4921.
2. a) Young, D.D.; Garner, A.R.; Yoder, A.J.; Deiters, A. Light-activation of gene function in mammalian cells via ribozymes, *Chem. Commun.* **2009**, 568-570. b) Chou, C.; Young, D.D.; Deiters, A. Photocaged T7 RNA polymerase for the light activation of transcription and gene function in pro- and eukaryotic cells. *Chem. Bio. Chem.*, **2010**, 11, 972-977. c) Shi, Y.; Koh, T.J. Light-activated transcription and repression by using photocaged SERMs, *Chem. Bio. Chem.*, **2004**, 5, 788-796.
3. a) Shao, Q.; Xing, B. Photoactive molecules for applications in molecular imaging and cell biology, *Chem. Soc. Rev.* **2010**, 39, 2835-2846. b) Ogasawara, S.; Maeda, M. Straightforward and reversible photoregulation of hybridization by using a photochromic nucleoside, *Angew. Chem.* **2008**, 120, 8971-8974, *Angew. Chem. Int. Ed.*, **2008**, 47, 8839-8843.
4. a) Asanuma, H.; Yoshida, T.; Ito, T.; Koniya, M. Photo-responsive oligonucleotides carrying azobenzene at the 2'-position of uridine, *Tetrahedron Lett.* **1999**, 40, 7995-7998. b) Asanuma, H.; Ito, T.; Yoshida, T.; Liang, X.; Koniya, M. Photoregulation of the Formation and Dissociation of a DNA Duplex by Using the cis-trans Isomerization of Azobenzene, *Angew. Chem. Int. Ed.*, **1999**, 38, 2393-2395. c) Asanuma, H.; Ito, T.; Koniya, M. Photo-responsive oligonucleotides carrying azobenzene in the side-chains, *Tetrahedron Lett.* **1998**, 39, 9015-9018.
5. a) Yamana, K.; Kan, K.; Nakano, H. Synthesis of oligonucleotides containing a new azobenzene fragment with efficient photoisomerizability, *Bioorg. Med. Chem.*, **1999**, 7, 2977-2983. b) Yamana, K.; Yoshikawa, A.; Noda, R.; Nakano, H.; synthesis and binding properties of oligonucleotides containing an azobenzene linker, *Nucleosides, Nucleotides and Nucleic Acids* , **1998**, 17, 233-242.

6. Asanuma, H.; Matsunaga, D.; Komiyama, M. Clear cut photo-regulation of the formation and dissociation of DNA duplex by modified oligonucleotide involving multiple azobenzenes. *Nucleic Acids Symp. Ser.*, **2005**, 49, 35-36.
7. Liu, Y.; Sen, D. Light-regulated catalysis by an RNA cleaving deoxyribozyme. *J. Mol. Biol.*, **2004**, 341, 887-892.
8. Niedballa, U.; Vorbrüggen, H. A general synthesis of N-glycosides. On the mechanism of the stannic chloride catalyzed silyl Hilbert-Johnson reaction, *J. Org. Chem.*, **1976**, 41, 2084-2086.
9. a) Swasicki, E. Physical properties of the aminoazobenzene dyes., *J. Org. Chem.* **1957**, 22, 365-367. b) Kumar, S. K.; Patnaik A. Tunable Electronic Properties of a Proton-Responsive *N,N*-Dimethyl aminoazobenzene Fullerene (C₆₀) Dyad. *Chem. phys. chem.*, **2010**, 11, 3645-3655.
10. Matazo, D.R.C.; Ando, R.A.; Borin, A.C.; Santos, P.S. Azo-Hydrazone tautomerism in protonated aminoazobenzenes: resonance Raman spectroscopy and quantum-chemical calculations. *J. Chem. Phys. A*, **2008**, 112, 4437-4443.

Chapter 5

Chapter 5

5 Synthesis of Acridine-Based PNA Monomer Suitable for PNA-Fluorescent Probes.

It is well known that the stability of nucleic acid double helical structure (DNA:DNA, DNA:RNA, PNA:DNA, PNA:RNA and PNA:PNA) relies on many intermolecular interactions such as hydrogen-bonding between nucleotides, π -stacking interactions, solvent effect.

5.1 Hydrogen bonding

Generally, a hydrogen bond is formed between hydrogen atom covalently attached to an electronegative atom (donor atom) and an electronegative atom (acceptor). In nucleobases H-bonds mainly form between N-H \cdots N or/and N-H \cdots O of complementary nucleotide base pairs. H-bond formation mechanistically can be described by interactions of lone-pair orbitals on O or N of one nucleobase with σ^* orbital of N-H.¹ Despite the H-bond being very weak compared to covalent bonds, formation of many H-bonds between complementary nucleotides in two DNA strands is sufficiently strong enough to keep the two DNA strands in duplex structure.

Several reports show that the stability of the nucleic acid structures benefit from increasing the number of hydrogen bonds sites in nucleobases. Simply, this can be achieved by modifying naturally occurring nucleobases. Diaminopurine (DAP), an adenine analogue, is characterized by its ability to pair with thymine by three hydrogen bonds (only two hydrogen bonds between A:T) (Fig. 5-1).

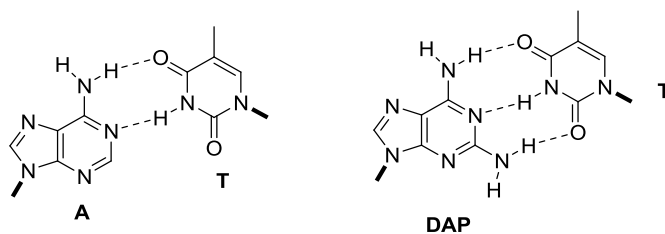


Figure 5-1: Base pairing between DAP:T comparing to A:T .

Another example was introduced from our lab is (mono-*ortho*-(aminoethoxy)phenyl) pyrrolocytosine (moPhpC). This modified cytosine is able to base pairing with guanine by formation of four hydrogen bonds. The design of moPhpC is characterized by the extending aromatic ring system of pyrrolocytosine that will improve π -stacking in addition to presence of aminoethoxy linker that provides a new site for formation of H-bonds with O(6) of guanine via Hoogsteen base pairing. Incorporation of **moPhpC** into a 10-mer PNA with the sequence GTAGAT**X**ACT-Lys (X= **moPhpC**) resulted in an increase in the stability of DNA and RNA duplexes by (+10.5°C) and (+4 °C), respectively, which was rationalized by the formation of an additional hydrogen bond to guanine (Fig. 5-2).²

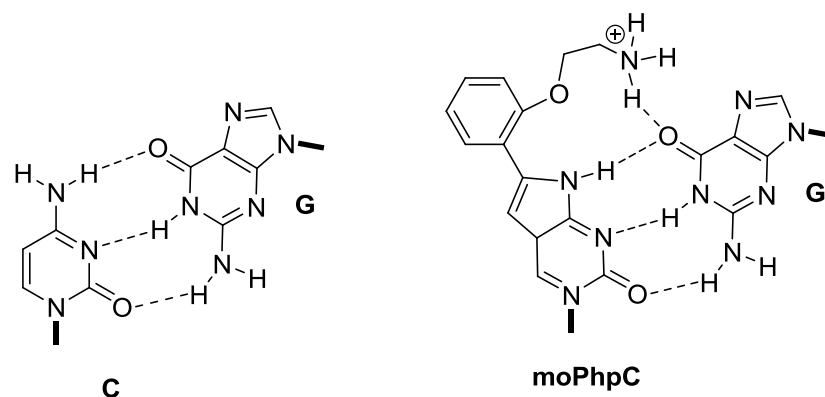


Figure 5-2: Hybridization of cytosine (left) and its modification moPhpC (right) with guanine to demonstrate the effect of increasing of H-bonds on the stability of duplex.

5.2 Base-stacking

In base stacking there are no covalent interactions between the nucleobases in a dsDNA structure. In most of all known DNA structures the bases are found to have face-to-face interaction due to their planar structure. There are many factors affecting π -stacking such as Van der Waals dispersive forces between bases, permanent electrostatic effects of interacting dipoles and solvation effects.³ A number of studies have proved base-stacking contributes significantly to the stabilization of DNA and RNA helical structure. For

example, Turner and coworkers⁴ have found that double-helical structure of short RNA is stabilized by introducing unpaired base at the end. This study was based on the "dangling-end effect".

5.3 Fluorescent nucleobases

Since 1980's, much effort has been devoted to exploit using fluorescence techniques in detection of nucleic acids. Aromatic-based amino acids (phenylalanine, tyrosine and/or tryptophan) are characterized by their intrinsic fluorescence that may be used in fluorescent studies; but natural nucleic acids are known to be nonfluorescent.^{5a,b} Due to the promising results shown for detection of nucleic acid using fluorescent probes, intensive research has been devoted to design and synthesize nucleobases possessing fluorescent properties. There is a great demand for such nucleobases, especially ones that are fluorescent while maintaining the hydrogen bonding ability to the complementary nucleobases.

Fluorescent nucleobases are classified by Tor⁶ into five major families as 1) isomorphous base analogues, 2) pteridines, 3) Expanded nucleobases, 4) chromophoric base analogues and 5) conjugated base analogues. In the following paragraphs a brief details are given for each family.

1) Isomorphous base analogues, heterocyclic compounds characterized by its similarity to the natural nucleobases in overall dimension and their ability to Watson-Crick base pairing. The most common example of this class is 2-aminopurine (2-AP). 2-AP is an analog of guanine and adenine and therefore it can pairs with thymine and uracil obeying Watson-Crick⁷ base pairing and with cytosine by Wobble base pairing⁸ as shown in (Fig.5-3). 2-AP is distinguished by its high fluorescence quantum yield ($\Phi_F = 0.68$ in aqueous solution) and high sensitivity to the local environment. Upon incorporation of 2-AP into nucleic acid, the fluorescence intensity of 2-AP was drastically reduced ~ 100 times due to stacking interactions with nearest neighbor nucleobases. This reduction in 2-AP quantum yield is highly dependent on base sequence.⁹ Owing to 2-AP sensitivity to microenvironment, it has been widely used in several studies of nucleic acid structure and dynamics within DNA,¹⁰ and RNA.¹¹

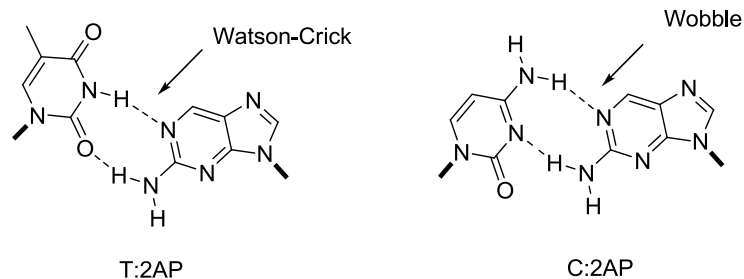


Figure 5-3: Representation of hybridization of 2AP with natural base complements thymine and cytosine.

2) Pteridines, purine analogues, are bicyclic planar compounds formed from two condensed six membered rings and are distinguished by their ability to form hydrogen bonds with complementary bases in addition to their intensive emission quantum yield ($\Phi_F = 0.77-0.88$ for adenosine analogues and $0.39-0.48$ for the guanosine)¹² (Fig. 5-4). Pteridines have been employed in numerous applications as hybridization probes which are used in measuring the cleavage activity of the retrovirally coded protein, human immunodeficiency virus-1 (HIV-1) integrase (IN).¹³ Another example of using pteridine probes (using 6MAP as replacement of A-residues) in detection of A-tract structure.¹⁴

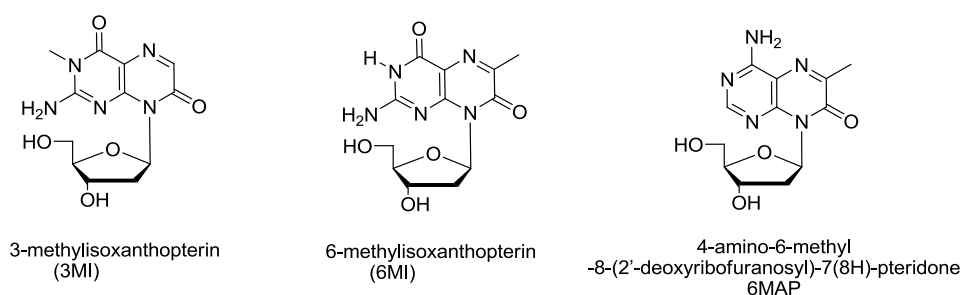


Figure 5-4: Structures of some pteridine derivatives.

3) Expanded nucleobases, are natural nucleobases that have been extended with fused aromatic rings. Etheno-A,¹⁵ the simplest example of fluorescent extended nucleobases with quantum yield = 0.54 (in dioxane-H₂O 1:1), it was prepared by reaction of chloroacetaldehyde with adenosine. Despite the fluorescence property of Etheno-A, it can not engage in hydrogen bonding. Much work has been done to extend the nucleobases

structures while retaining their ability to hydrogen bond with complementary nucleobases (Fig.5-5).¹⁶

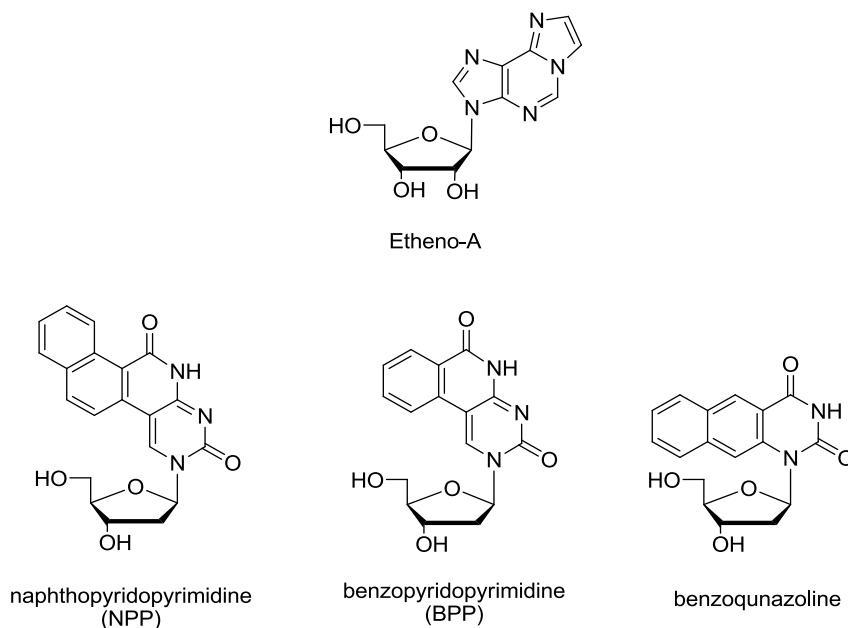


Figure 5-5: Examples of expanded nucleobases.

4) Chromophoric base analogues, are produced when the natural nucleobases are replaced by hydrocarbons and heterocyclic residues that are characterized by their emission such as pyrene, phenanthrene, terphenyl, terthiophene, benzoterthiophene and coumarin (Fig. 5-6).¹⁷ Using multiple dyes as replacement of DNA bases in adjacent position in a DNA sequences can be used in detection of genetic sequence. For example, pyrene is a well-characterized excimer-forming fluorophore. When it is used alone it emits blue light while using two units of pyrene leads to emission of green light ascribed to the formation of an excimer complex through energy transfer from one pyrene unit to the other. Kool and coworkers¹⁸ have exploited this colour change of pyrene upon excimer complex formation in detection of a portion of a gene. This was achieved by synthesis of two single pyrene-labeled strands at 3' and 5' ends and these strands were designed to be a complementary to a portion of the gene under study. Upon hybridization, the two pyrene units are located in adjacent position and thusly change fluorescence colour due to formation of excimer.

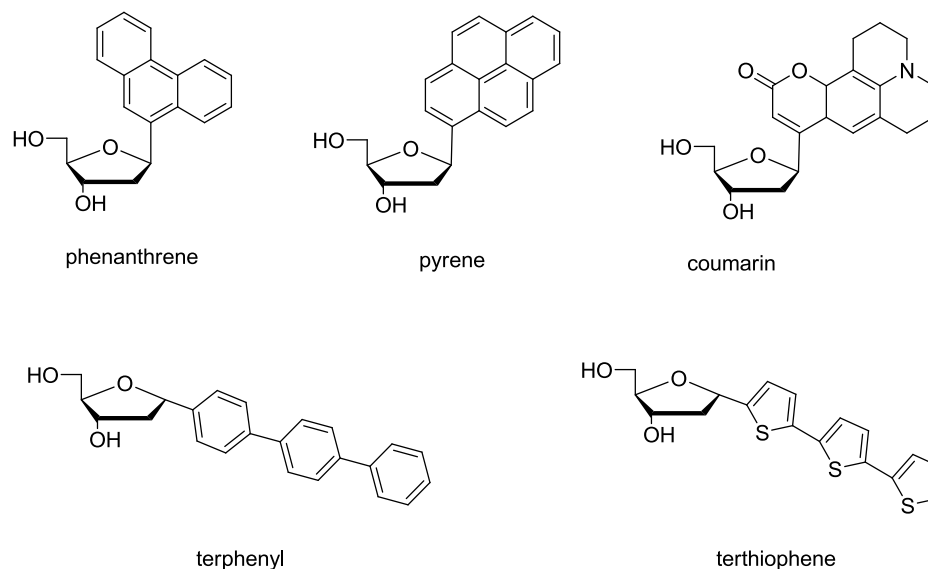


Figure 5-6: Examples of hydrocarbons and heterocycle DNA base replacement.

5) Conjugated base analogues, are the fluorescent aromatic residues that are conjugated to the nucleobases via a linker. This class is characterized by introducing fluorescent property from the aromatic residue and maintaining the hydrogen bond ability with their complementary nucleobase. 5-alkynyluracil derivatives^{19a-f} are good examples of this class were reported by several groups their synthesis is based on Sonogashira cross coupling reaction. Hudson and coworkers^{19a} have exploited mismatch detection by 5-ethynyldeoxuridine derivatives, it was found that the greatest fluorescence response (6 fold increase in fluorescence intensity with matching sequence) was observed for the oligomer containing *p*-methoxyphenylethynyluracil unit (Fig. 5-7).

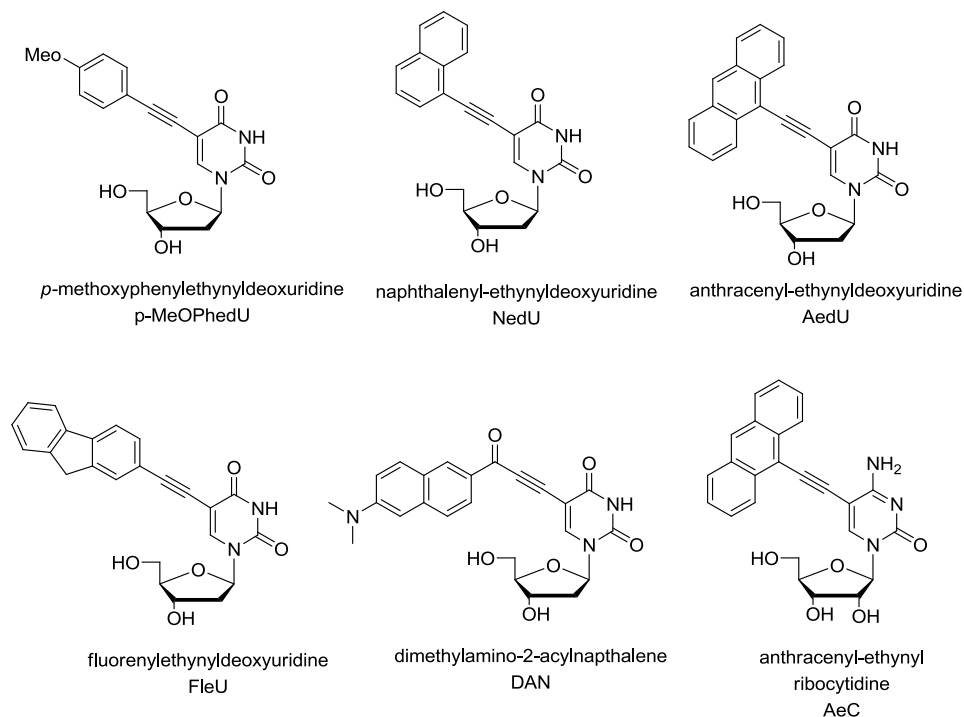


Figure 5-7: Structures of some conjugated base analogues used in DNA and RNA probe.

5.4 Acridine

Acridine is a heterocyclic analog of anthracene where the central CH group is replaced by nitrogen atom as shown in (Fig 5-8). Acridine derivatives have been known since 19th century but they have attracted much interest after World War I when they were used as antibacterial and antimalarial agents.^{20,21}

Acridine derivatives have been employed for targeting several biological targets as topoisomerases I and II, telomerase/telomere and protein kinases.²² The biological activity of the acridines is mainly ascribed to their planar configuration that allow them to intercalate within the double-stranded DNA structure leading to interference with the cellular machinery.

Several acridine-based drugs are reported in literature proved their ability as anticancer, antibacterial and antimalarial agents. For example, Amsacrine (*m*-AMSA), was designed by Denny and coworkers²³ and it was the first drug has been proved to bind with topo II-

DNA complex by intercalation.²⁴ Chourpa and coworkers²⁵ confirmed by using surface-enhanced Raman scattering (SERS) spectroscopy that the side chain located at the *meta*-position participates in an additional specific interaction with topo II-DNA complex. It is well established that acridine derivatives can bind to DNA and RNA through intercalation of the acridine ring between adjacent base pairs in the DNA duplex.^{26-a-c} Acridine units are held in their positions by: 1) strong ionic bonds between the protonated acridine-nitrogen atoms and the phosphate ions of DNA backbone and 2) van der Waals forces between acridine unit and the base pairs.

Acridine derivatives have been extensively used for labeling oligonucleotide probes, acridine orange (AO) is an example of fluorescent acridine derivative which is also characterized by its affinity to nucleic acids. In aqueous solution, AO has been shown to exist in two forms: 1) one is distinguished by an absorption maximum band at 494 nm and green fluorescence maximum band at 530 nm this form was found in highly-diluted solutions (10^{-7} M) attributed to presence of acridine as single monomers. 2) the other form is characterized by an absorption maximum band at 465 nm and red fluorescence maximum band at 640 nm this form was found in highly-concentrated solutions ($> 10^{-2}$ M) this is ascribed to presence of acridine as dimers.²⁷ AO was used for discriminate between dsDNA and ssDNA through enhancement of fluorescence upon dsDNA binding whereas AO intercalates into dsDNA while it binds to ssDNA electrostatically.²⁸

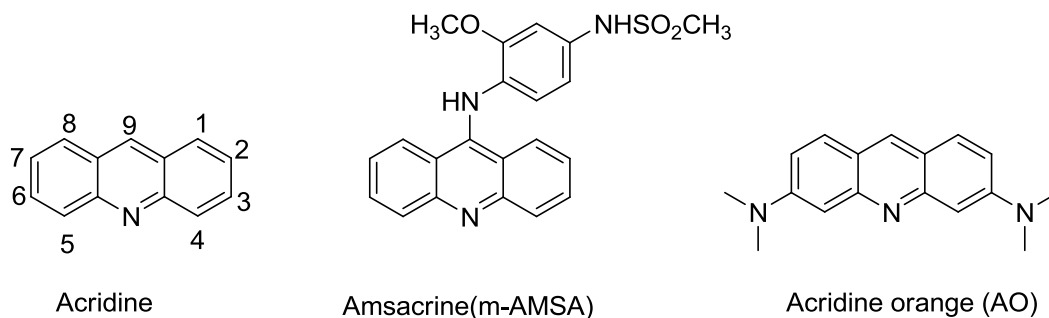


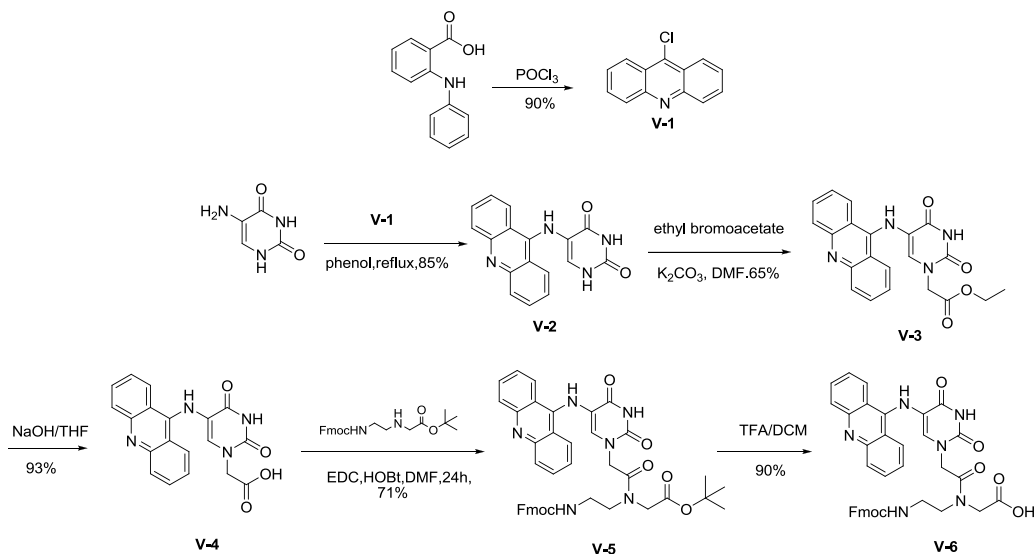
Figure 5-8: Structure of acridine, m-AMSA and acridine orange (AO).

Based on the aforementioned properties of either acridine as a fluorogenic molecule or peptide nucleic acid (PNA) as artificial nucleic acid analog with remarkable binding

ability, we interested in synthesis of PNA monomer possessing acridine moiety. Incorporation of acridine-based PNA monomer in PNA oligomer may be used as reporter probe for DNA detection in addition to its potential stabilization of duplex structure.

5.5 Results and discussion

The synthesis of the acridine-based PNA monomer is illustrated in (Scheme 5-1). Started with the synthesis of 9-chloroacridine (**V-1**) from *N*-phenylanthranilic acid and phosphoryl chloride according to the reported method.²⁹ In the next step, 9-chloroacridine was refluxed with 5-aminouracil in the presence of phenol to afford 5-(acridin-9-ylamino)uracil **V-2** in 85% yield. The ethyl ester derivative **V-3** was obtained in 65% yield by alkylation of **V-2** at N-1 position with 2-ethyl bromoacetate in DMF in the presence of anhydrous K₂CO₃. **V-3** underwent hydrolysis using aqueous NaOH (2.5 M) in THF to give the acetic acid derivative **V-4** in 93%. Carbodiimide mediated coupling of **V-4** with *N*-[2-(Fmoc)aminoethyl]glycine-*t*-butyl ester was accomplished using EDC/HOBt, to give the protected monomer ester **V-5** in 71 % yield. Finally, removal of *t*-butyl group was carried out by acidolysis using TFA to give the acridine-containing PNA monomer **V-6** in 90% yield.



Scheme 5-1: Synthesis of acridine-based PNA monomer.

5.5.1 Photophysical properties

UV-Vis spectra of acridine-based PNA monomer have been investigated under different solvents (Table 5-1), there is no clear trend between solvent polarities to the absorption maximum of **V-6**. It is well established that acridine moiety is amenable for protonation forming acridinium cation (AcH^+). The effect of acid on compound **V-6** has been investigated by UV-Vis as shown in (Fig 5-1). Treatment of **V-6** in various solvents with trifluoroacetic acid caused a red shift of the maximum absorption band, interestingly this shift was accompanied by an increasing of the absorption intensity.

Solvent	DCM	dioxane	Acetone	EtOH	CH ₃ CN
λ_{max} (Neutral) nm	404	406	412	409	402
λ_{max} (Protonated) nm	434, 443	427, 443	430, 453	417, 437	418, 433

Table 5-1: Photophysical properties of V-6

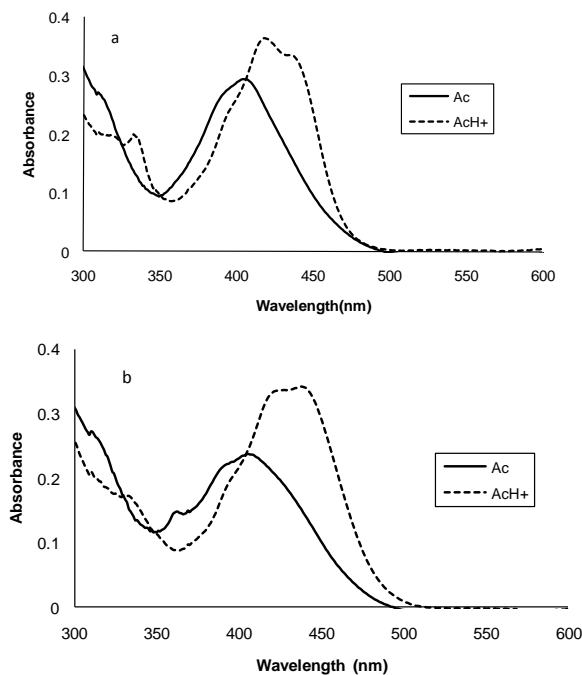


Figure 5-9: UV-Vis spectrum of V-6 (2.6 μM) neutral and acidic form in a) CH₃CN and b) Dioxane

5.5.2 Fluorescence properties of acridine-based monomer

A preliminary fluorescence study on compound **V-6** has been obtained, the acridine-based PNA monomer showed a high quantum yield of 0.32 in ethanol and 0.43 in dichloromethane. A drastic decrease in the fluorescence emission is observed upon increasing water content as shown in (Fig. 5-10). The quenching behaviour is a good indication for the potential use of PNA probe contacting acridine moiety in monitoring binding events.

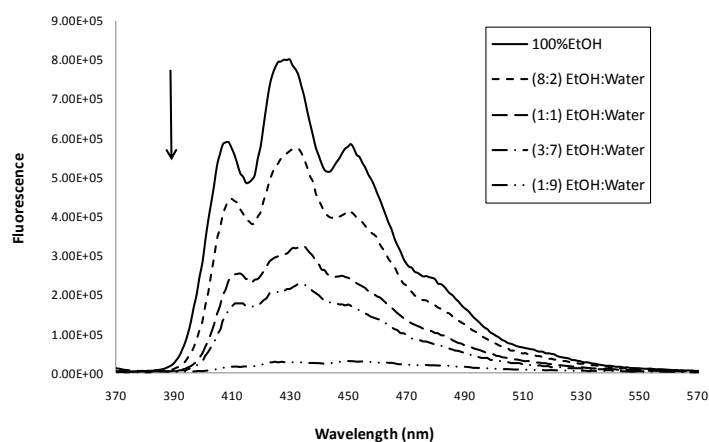


Figure 5-10: Quenching of fluorescence emission of V-6 in EtOH upon addition of water.

5.5.3 Future work

Incorporation of acridine-based PNA monomer into PNA oligomer is underway. This PNA oligomer may be used as reporter probe. Based on the fluorescence quenching of acridine upon subjecting to aqueous environment, the acridine containing PNA probe may be used to monitor the state of hybridization (single stranded or duplex structure)

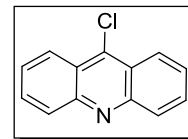
5.5.4 Conclusion

We synthesized PNA monomer carrying acridine moiety characterized by its high fluorescence quantum yield that may be used as reported in PNA probes with expected stabilization of the formed duplex structure. It was found that emission of acridine is sensitive to aqueous environment which indicates that PNA probe containing acridine moiety may be a good candidate for reporting binding events.

5.6 Experimental

9-Chloroacridine V-1

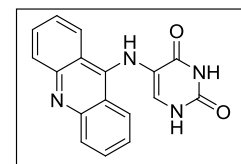
In a round bottom flask fitted with a water condenser, *N*-phenylanthranilic acid (2.0 g, 9.39 mmol) was suspended in POCl₃ (20.0 g, 47 mmol), the mixture was heated slowly for 15 min on water bath at 80 °C, the reaction



mixture was transferred to oil bath and heated for 2 h at 120 °C. The excess of POCl₃ was removed by distillation under vacuum leaving the residue. Cold water (200 mL) was added and the residue was basified with concentrated NH₄OH solution (28%, 15 mL) to afford the product as greenish gray solid (1.8 g, 90%). ¹H NMR (DMSO-d₆) δ: 8.40 (dd, *J* = 2.2 and 0.7, 1H), 8.38 (dd, *J* = 2.2 and 0.7, 1H), 8.21 (dd, *J* = 1.8 and 0.6, 1H), 8.19 (dd, *J* = 1.8 and 0.6, 1H), 7.95(d, *J* = 1.4, 2H), 7.92 (d, *J* = 1.8 and , 2H). HRMS (EI): calcd. for C₁₃H₈ClN [M]⁺ 213.0345, found 213.0339

5-(Acridin-9-ylamino)uracil V-2

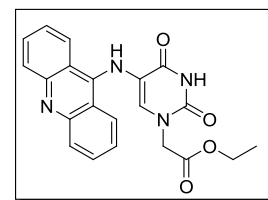
A mixture of 9-chloroacridine **V-1** (0.5 g, 2.35 mmol) and phenol (10.0 g, 0.11 mmol) was heated at 80 °C with stirring until phenol is melted, 5-aminouracil (0.28 g, 2.2 mmol) was added and the mixture



was heated at 120 °C for 2 h. The reaction mixture was cooled to room temperature and then was treated with dilute NH₄OH (50 mL) to precipitate an orange solid. The crude product was collected by filtration and was crystallized from ethanol to afford compound **V-2** (0.57 g, 85%). ¹H NMR (400 MHz, DMSO-d₆) δ: 11.82 (bs, 1H), 11.24 (s, 1H), 10.87 (s, 1H), 8.27 (d, *J* = 8.0, 2H), 7.57 (t, *J* = 7.6, 2H), 7.65 (d, *J* = 8.0, 2H), 7.22 (t, *J* = 7.6, 2H); ¹³C NMR: 177.5, 151.1, 141.5, 134.1, 131.9, 126.7, 121.7, 121.1, 117.9. HRMS (EI): calcd. for C₁₇H₁₂N₄O₂ [M]⁺ 304.0960, found 304.0971.

Ethyl-2-(5-(acridin-9-ylamino)-uracil-1-yl)acetate V-3.

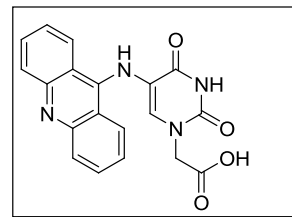
Compound **V-2** (0.5 g, 1.64 mmol) was dissolved in dry DMF (8 mL), anhydrous K₂CO₃ (0.68 g, 4.92 mmol) was added and the mixture was stirred on ice for 10 min followed by the dropwise



addition of ethyl-2-bromoacetate (0.3 g, 1.8 mmol) over 30 min and the reaction mixture was stirred for 24 h. The reaction mixture was filtered and the solvent was concentrated under pressure to leave yellow oil. The oil was dissolved in dichloromethane (100 mL) and was washed with saturated KHCO_3 (2 x 50 mL), H_2O (2 x 50 mL) and finally with brine (2 x 50 mL). The organic phase was collected and dried over anhydrous Na_2SO_4 , filtered and concentrated *in vacuo*. The crude product was purified by flash chromatography with hexane/ CH_2Cl_2 (8:2, v/v) to yield **V-3** as yellow solid (0.42 g, 65%). ^1H NMR (400 MHz, DMSO-d_6) δ : 11.42 (s, 1H), 10.97 (s, 1H), 8.25 (s, 1H), 7.94 (d, $J = 7.5$ Hz, 2H), 7.49 (d, $J = 7.4$ Hz, 7.5 2H), 7.31 (d, $J = 7.5$ Hz, 2H), 7.08 (t, $J = 7.5$ Hz, 2H), 4.51 (s, 2H), 4.16 (t, $J = 7.0$ Hz, 2H), 1.20 (q, $J = 7.0$ Hz, 3H); ^{13}C NMR (100 MHz, DMSO-d_6) δ ,177.4, 169.0, 161.9, 150.7, 150.0, 141.6, 134.1, 132.1, 126.7, 123.1, 121.6, 121.18, 117.9, 61.2, 49.2, 14.7. HRMS (EI) m/z : calcd. for $\text{C}_{21}\text{H}_{18}\text{N}_4\text{O}_4$ [M^+] 390.1328 found 390.1337.

2-(5-(Acridin-9-ylamino)-uracil-1-yl)acetic acid **V-4**.

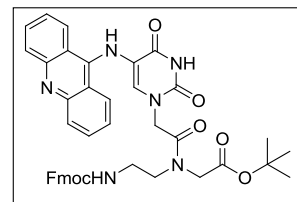
The ethyl ester **V-3** (0.35 g, 0.89 mmol) was dissolved in THF (25 mL) and was kept in an ice bath for 15 min followed by the dropwise addition of NaOH (2.5 M, 5 mL) over 5 min with stirring. The reaction mixture was removed from the ice bath and was



stirred at r.t. till completion of reaction. TLC analysis confirmed consumption of starting material after 20 min. The reaction mixture was transferred to separatory funnel containing KHSO_4 (1.0 M, 50 mL) and dichloromethane (100 mL). The aqueous layer was further extracted with dichloromethane (3 x 50 mL). The collected organics was dried over anhydrous Na_2SO_4 , filtered and concentrated *in vacuo* to afford the acid derivative **V-4** as orange solid (0.3 g, 93%). ^1H NMR (400MHz, DMSO-d_6) δ : 13.39 (br s, 1H), 11.93 (s, 1H), 11.01 (s, 1H), 8.67 (d, $J = 8.6$ Hz, 2H), 8.31 (s, 1H), 8.08 (d, $J = 8.1$ Hz, 2H), 7.99 (t, $J = 8.1$ Hz, 2H), 7.54 (t, $J = 8.1$ Hz, 2H) 4.59 (s, 2H); ^{13}C NMR (DMSO-d_6) δ : 170.1, 161.4, 152.8, 150.9, 143.5, 134.7, 129.6, 125.0, 112.2, 49.8. HRMS (ESI-TOF) m/z : calcd. for $\text{C}_{19}\text{H}_{15}\text{N}_4\text{O}_4$ [MH^+] 363.1093 found 363.1108.

***tert*-Butyl-2- *N*-(2-(9-fluorenylmethoxycarbonyl)aminoethyl)-2-(5-(acridin-9-ylamino)-uracil-1-yl)acetamido)acetate **V-5**.**

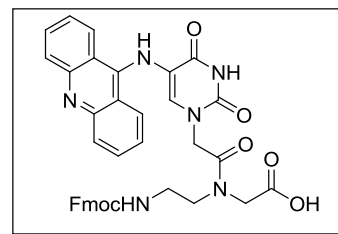
To a solution of **V-4** (0.20 g, 0.552 mmol) in DMF (5 mL), *N*-[2-(Fmoc)aminoethyl]glycine-*t*-butyl ester (0.20 g, 0.5 mmol), EDC (0.11 g, 0.6 mmol), and HOBt (0.09 g, 0.6 mmol) was added and the solution was stirred for 10 min at 4 °C and at r.t. for 24 h



under N₂. The mixture was poured into iced water (25 mL) and the suspension was placed at 4 °C for 2 h. The precipitated solid was collected by filtration, and was purified by column chromatography using CH₂Cl₂ /MeOH (9.5: 0.5, v/v) as the eluent to give the monomer ester **V-5** (0.29 g, 71%) as an orange solid. Compound **V-5** exists in solution as a pair of slowly exchanging rotamers; signals attributed to major (ma.) and minor (min.) rotomers are designated : ¹H NMR (400MHz, DMSO-d₆) δ : 10.9 (s, 1H), 10.5 (s, 1H), 8.24 (s, ma., 0.6H), 8.24 (s, mi., 0.4H), 7.89 (d, *J* = 7.4 Hz, 2H), 7.7 (t, *J* = 8.2 Hz, 2H), 7.6 (t, 7.3, 2H), 7.5 (m, 4H), 7.43 (t, *J* = 7.4 Hz, 2H), 7.34 (t, *J* = 7.4 Hz, 2H), 7.25 (t, *J* = 7.8 Hz, 2H), 4.37 (s, 2H), 4.32 (d, *J* = 6.4 Hz, 2H), 4.26-4.20 (m, 4H), 4.14 (m, 1H), 3.91 (s, 1H), 3.24-1.8 (m, 2H), 1.42 (s, mi., 2H), 1.39 (s, ma., 7H); ¹³C NMR (DMSO-d₆) δ : 176.8, 167.9, 166.5, 159.5, 156.4, 150.5, 143.9, 143.8, 140.9, 133.4, 131.3, 127.6, 126.0, 125.0, 121.0, 120.5, 120.1, 117.3, 115.3, 80.9, 65.5, 46.7, 42.0, 41.4, 27.6. HRMS (EI) *m/z*: calcd. for C₄₂H₄₀N₆O₇ [M⁺] 740.2958 found 740.2943.

2-(*N*-(2-(9-Fluorenylmethoxycarbonyl)aminoethyl)-2-(5-(acridin-9-ylamino)-uracil-1-yl)acetamido)acetic acid **V-6.**

To a suspension of compound **V-5** (0.20 g, 0.27 mmol) in dry CH₂Cl₂ (5 mL), Et₃SiH (40 μL, 0.2 mmol) was added and cooled to 0 °C followed by dropwise addition of TFA (5 mL) and The reaction was stirred for 30 min on ice and an



additional 2 h at r.t. The mixture was evaporated to dryness by nitrogen stream' the remaining volatiles were removed by coevaporation with CH₂Cl₂ and diethyl ether. The compound was dissolved in CH₂Cl₂ (3 mL), diethyl ether (50 mL) was added and cooled to 0 °C overnight. The precipitated product was collected by filtration and was dried under vacuum to obtain **V-6** as orange solid (0.167 g, 90%). Compound **V-6** exists in

solution as a pair of slowly exchanging rotamers; signals attributed to major (ma.) and minor (mi.) rotomers are designated : ^1H NMR (400MHz, DMSO- d_6) δ : 11.77 (br s, 1H), 11.45 (s, 1H), 10.77 (s, 1H), 8.61 (s, mi., 0.4H), 8.59 (s, ma., 0.6 H), 8.22 (d, J = 8.1, 1H), 8.06 (t, J = 6.2, 2H), 7.97 (d, J = 8.1, 1H), 7.90 (d, J = 8.1, 3H), 7.73 (t, J = 7.4, 1H), 7.65 (m, 4H), 7.43 (t, J = 7.0, 2H), 7.33 (t, J = 7.0, 2H), 4.41 (s, 2H), 4.33 (d, J = 6.4 Hz, 1H), 4.29 (d, 2H), 4.26-4.16 (m, 3H), 3.89 (s, 1H), 3.22-1.9 (m, 2H). (HRMS (ESI-TOF) m/z : calcd. for $\text{C}_{38}\text{H}_{33}\text{N}_6\text{O}_7$ [MH^+] 685.2411 found 685.2441.

Quantum Yield determination

Fluorescence quantum yields (Φ_F) of the acridine based monomer was determined using a Photon Technologies International Quanta Master 7/2005 spectrophotometer by the relative method³⁰ using anthracene ($\Phi_F = 0.32$) as a reference standard. The quantum yields were determined using emission wavelengths range between 370 and 600 nm with an excitation wavelength of 360 nm. The quantum yield of the unknown $\Phi(x)$ can be calculated by the following equation:

$$\Phi_{F(x)} = \Phi_{(ST)} (A_{ST}/A_X) (F_X/F_{ST}) (\eta_X^2/\eta_{ST}^2)$$

Where $\Phi_{(ST)}$ is the quantum yield of the standard, A is the absorbance at the excitation wavelength, F is the integrated area in the emission curve, the subscripts X and ST refer to unknown and standard respectively and η is the refractive index of the solvent. By measuring a series of diluted solutions with various absorbance readings the following equation may be used:

$$\Phi_{F(x)} = \Phi_{(ST)} (\text{Grad}_X/\text{Grad}_{ST}) (\eta_X^2/\eta_{ST}^2)$$

Where Grad is the gradient from the plot of integrated area in the emission curve versus absorbance at the excitation wavelength. The validity of the methodology was confirmed by measuring these characterized compounds: anthracene ($\Phi_F = 0.29$, in ethanol),³¹ dichloroanthracene ($\Phi_F = 0.58$, in ethanol)³⁰ and 9,10-Diphenylanthracene (DPA) ($\Phi_F = 0.95$ in ethanol),³² and gave the following values 0.27, 0.56, 0.91 that are in very good agreement with the literature values.

5.7 References

1. a) Fonseca, C.; Bickelhaupt, F.M.; Snijders, J.G.; Baerends, E.J. The nature of the hydrogen bond in DNA Base Pairs: the role of charge transfer and resonance assistance, *Chem. Eur. J.* **1999**, 5, 3581-3594. b) Fonseca, C.; Bickelhaupt, F.M. Charge transfer and environment effects responsible for characteristics of DNA Base pairing, *Angew. Chem.* **1999**, 111, 3120-3122; *Angew. Chem., Int. Ed.* **1999**, 38, 2942-2945.
2. Wojciechowski, F.; Hudson, R.H.E. Fluorescence and hybridization properties of peptide nucleic acid containing a substituted phenylpyrrolocytosine designed to engage guanine with an additional H-Bond, *J. Am. Chem. Soc.*, **2008**, 130, 12574-12575.
3. Guckian, K. M.; Schweitzer, B.A.; Ren, R.F.; Sheils, C. J.; Tahmassebi, D.C.; Kool, E.T. Factors contributing to aromatic stacking in water: evaluation in the context of DNA, *J. Am. Chem. Soc.* **2000**, 122, 2213-2222.
4. Petersheim, M.; Turner D. H. Base-stacking and base-pairing contributions to helix stability: thermodynamics of double-helix formation with CCGG, CCGGp, CCGGAp, ACCGGp, CCGGUp, and ACCGGUp, *Biochemistry*, **1983**, 22, 256-263.
5. a) Daniels, M.; Hauswirth, W. Fluorescence of the purine and pyrimidine bases of the nucleic acids in neutral aqueous solution at 300 °K, *Science*, **1971**, 171, 675-677. b) Pecourt, J. M. L.; Peon, J.; Kohler, B. Ultrafast internal conversion of electronically excited RNA and DNA nucleosides in water, *J. Am. Chem. Soc.* **2000**, 122, 9348-9349.
6. Greco, N. J.; Tor, Y. Furan decorated nucleoside analogues as fluorescent probes: synthesis, photophysical evaluation, and site-specific incorporation, *Tetrahedron*, **2007**, 63, 3515-3527.
7. a) Nordlund, T.M.; Andersson, S.; Nilsson, L.; Rigler, R.; Graeslund, A.; McLaughlin, L.W. Structure and dynamics of a fluorescent DNA oligomer containing the EcoRI recognition sequence: fluorescence, molecular dynamics, and NMR Studies, *Biochemistry*, **1989**, 28, 9095-9103. b) Law, S.M.; Eritja, R.; Goodman, M.F.; Breslauer, K.J. Spectroscopic and calorimetric characterizations

- of DNA duplexes containing 2-Aminopurine, *Biochemistry*, **1996**, 35, 12329-12337.
8. a) Fagan, P.A.; Fabrega, C.; Eritja, R.; Goodman, M.F.; Wemmer, D. E. NMR Study of the conformation of the 2-Aminopurine: cytosine mismatch in DNA, *Biochemistry*, **1996**, 35, 4026-4033. b) Sowers, L.C.; Boulard, Y.; Fazakerley, G. V. Multiple structures for the 2-aminopurine-cytosine mispair, *Biochemistry*, **2000**, 39, 7613-7620.
 9. Ward, D.C.; Reich, E.; Stryer, L. Fluorescence studies of nucleotides and polynucleotides. I. Formycin 2-aminopurine riboside 2,6-diaminopurine riboside and their derivatives, *J. Biol. Chem.*, **1969**, 244, 1228-1237.
 10. Stivers, J. T. 2-Aminopurine fluorescence studies of base stacking interactions at abasic sites in DNA: metal-ion and base sequence effects, *Nucleic Acids Res.*, **1998**, 26, 3837-3844.
 11. Ballin, J. D.; Bharill, S.; Fialcowitz-White, E. J.; Gryczynsky, I.; Gryczynsky, Z.; Wilson, G.M. Site-specific variations in RNA folding thermodynamics visualized by 2-aminopurine fluorescence, *Biochemistry*, **2007**, 46, 13948-13960.
 12. Hawkins, M.E. Fluorescent pteridine nucleoside analogs. A window on DNA interactions, *Cell Biochem. Biophys.*, **2001**, 34, 257-281.
 13. Hawkins, M.E.; Pfeleiderer, W.; Mazumder, A.; Pommier, Y.G.; Balis, F.M. Incorporation of a fluorescent guanosine analog into oligonucleotides and its application to a real time assay for the HIV-1 integrase 3'-processing reaction, *Nucleic Acids Res.* **1995**, 23, 2872-2880.
 14. Augustyn, K.E.; Wojtuszewski, K.; Hawkins, M.E.; Knutson, J. R.; Mukerji, I. Examination of the premelting transition of DNA A-tracts using a fluorescent adenosine analogue, *Biochemistry*, **2006**, 45, 5039-5047.
 15. Secrist, J. A.; Barrio, R. J.; Leonard, N. J.; Weber, G. Fluorescent modification of adenosine-containing coenzymes, biological activities and spectroscopic properties, *Biochemistry*, **1972**, 11, 3499-3506.
 16. a) Okamoto, A.; Saito, Y.; Saito, I. Design of base-discriminating fluorescent nucleosides, *J. Photochem. Photobiol.*, **2005**, 6, 108-122. b) Liu, H.; Gau, J.; Maynard, L.; Saito, Y.D.; Kool, E.T. Toward a new genetic system with expanded

- dimensions: size-expanded analogs of deoxyadenosine and thymidine, *J. Am. Chem. Soc.*, **2004**, 126, 1102-1109. c) Godde, F.; Toulme, J.; Moreau, S. Benzoquinazoline derivatives as substitutes for thymine in nucleic acid complexes. Use of fluorescence emission of benzo[g]quinazoline-2,4-(1H,3H)-dione in probing duplex and triplex formation, *Biochemistry*, **1998**, 37, 13765-13775.
- 17.** Kool, E.T. Replacing the nucleobases in DNA with designer molecules, *Acc. Chem. Res.* **2002**, 35, 936-943.
- 18.** Paris, P.L.; Langenhan, J.; Kool, E.T. Probing DNA sequences in solution with a monomersexcimer color change, *Nucleic Acids Res.* **1998**, 26, 3789-3793.
- 19.** a) Hudson, R.H.E.; Ghorbani-Choghamarani, A. Oligodeoxynucleotides incorporating structurally simple 5-alkynyl-2'-deoxyuridines fluorometrically respond to hybridization, *Org. Biomol. Chem.*, **2007**, 5, 1845-1848. b) Greco, N. J.; Tor, Y. Simple fluorescent pyrimidine analogues detect the presence of DNA abasic sites, *J. Am. Chem. Soc.*, **2005**, 127, 10784-10785. c) Xiao, Q.; Ranasinghe, R.T.; Tang, A.M.P.; Brown, T. Naphthalenyl- and anthracenyl-ethynyl dT analogues as base discriminating fluorescent nucleosides and intramolecular energy transfer donors in oligonucleotide probes, *Tetrahedron*, **2007**, 63, 3483-3490. d) Sessler, J.L.; Sathiosatham, M.; Brown, C.T.; Rhodes, T.A.; Wiederrecht, G. Hydrogen-bond-mediated photoinduced electron-transfer: novel dimethylanilineanthracene ensembles formed via Watson-Crick base-pairing, *J. Am. Chem. Soc.*, **2001**, 123, 3655-3660. e) Weber, G.; Farris, F.J. Synthesis and spectral properties of a hydrophobic fluorescent probe: 6-propionyl-2-(dimethylamino)naphthalene, *Biochemistry*, **1979**, 18, 3075-3078. f) Ryu, J. H.; Seo, Y.J.; Hwang, G.T.; Lee, J.Y.; Kim, B.H. Triad base pairs containing fluorene unit for quencher-free SNP typing, *Tetrahedron*, **2007**, 63, 3538-3547.
- 20.** Albert, A. *The Acridines*; Edward Arnold Publishers, Ltd.: **1966**, 2nd Ed., London.

21. Greenwood, D. Historical perspective: Conflicts of interest: the genesis of synthetic antimalarial agents in peace and war, *J. Antimicrob. Chemother.*, **1995**, 36, 857-872.
22. Belmont, P.; Bosson, J.; Godet, T.; Tiano, m. Acridine and acridone derivatives, anticancer properties and synthetic, methods: where are we now?, *Anticancer Agents in Medicinal Chemistry.*, **2007**, 7, 139-169.
23. Denny, W.A. In, "Chronicles of Drug Discovery. Volume 3 (E ds. D. Lednicer and J. Bindra), ACS Publications, Washington, **1993**, 381.
24. Denny, W.A. Chemotherapeutic effects of acridine derivatives, *Med. Chem., Rev.*, **2004**, 1, 257-266.
25. Chourpa, I.; Manfait, M. Specific molecular interactions of acridine drugs in complexes with topoisomerase II and DNA. SERS and resonance Raman study of *m*-AMSA in comparison with *o*-AMSA, *J. Raman Spect.* **1995**, 26, 813-819.
26. a) Lerman, S. L. The structure of the DNA-acridine complex, *Proc. Natl. Acad. Sci. U.S.A.*, **1963**, 49,94-102. b) Sakore, T.D.; Jain, S.C.; Tsai, C.; Sobell, H. M. Mutagen-nucleic acid intercalative binding: structure of a 9-aminoacridine: 5-iodocytidylyl(3'-5')guanosine crystalline complex, *Proc. Natl. Acad. Sci. U.S.A.* **1977**, 74,188-192. c) Waring, M. Variation of the supercoils in closed circular DNA by binding of antibiotics and drugs: evidence for molecular models involving intercalation, *J. Mol. Biol.*, **1970**, 54, 247-279.
27. Zelenin, A.V. "Acridine orange as a probe for molecular and cell biology. " Chapter 9 In: Mason, W.T., (Ed.), *Fluorescent and luminescent probes for biological activity. a practical guide to technology for quantitative real-time analysis.* Academic Press, London, **1999**, 114-135.
28. Mizuki, K., Sakakibara, Y., Ueyama, H., Nojima, T., Waki, M., Takenaka, S., Fluorescence enhancement of bis-acridine orange peptide, BAO, upon binding to double stranded DNA, *Org. Biomol. Chem.*, **2005**, 3, 578-580.
29. Roubaud, G.; Faure, R.; Galy, J.-P.¹H and ¹³C chemical shifts for acridines: Part XVIII. 9-Chloroacridine and 9-(*N*-allyl)- and 9-(*N*-propargyl)acridinamine derivatives, *Magn. Reson. Chem.* **2003**, 41, 549-553.

30. Fery-Forgues, S. Are fluorescence quantum yields so tricky to measure? a demonstration using familiar stationary products, *J. Chem. Educ.*, **1999**, 76, 1260-1264.
31. Guilbault, G.G. Practical Fluorescence, 2nd Ed., Marcel Dekker, Inc., New York, **1990**, 4-16.
32. Morris, J.V.; Mahaney, M.A.; Huber, J.R. Fluorescence quantum yield determinations. 9,10-Diphenylanthracene as a reference standard in different solvents, *J. Phys. Chem.* **1976**, 80, 969-974.

Chapter 6

Chapter 6

6 Future Outlook

We have achieved the synthesis of a PNA monomer bearing the 4-(*N,N*-dimethylamino)azobenzene unit as a nucleobase replacement and have successfully incorporated into an 8-mer PNA oligomer. Furthermore, we have demonstrated the utility of the 4-(*N,N*-dimethylamino)azobenzene unit to act as a quencher in a PNA-molecular beacon (PNA-MB) design utilizing fluorescein as the luminophore. The 4-(*N,N*-dimethylamino)azobenzene showed high quenching ability upon hybridization of the PNA-MB to the complementary deoxynucleic acid. Signalling of the hybridization event occurred by recovery of the fluorescence emission of fluorescein by over 100 fold.

The presence of an azobenzene unit in PNA oligomer caused an increase in the stability of the triplex structure formed between 2PNA containing thymine residues with the complementary DNA. These results encourage us to investigate the quenching ability, photoresponse and stability effect of some azobenzene derivatives with large fused ring systems such as phenanthrenyl and anthracenyl phenylazo derivatives as shown in (Fig. 6-1). These modifications may lead to increase the quenching range and stabilizing effect on the hybrid formed due to the good intercalation of the phenylazo derivatives into the helical structure.

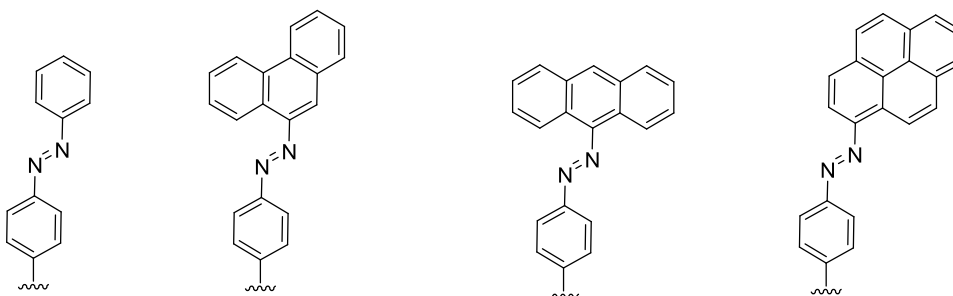


Figure 6-1: Structures of phenylazo derivatives.

We have also synthesized a modified uracil by introduction of phenylazo moiety at C5 to yield a uracil analogue that showed intrinsic quenching ability. A PNA monomer possessing the modified uracil was synthesized and it showed quenching ability to quench fluorescein emission in a short FRET-peptide design that was used as substrate for Cathepsin D enzyme. The advantage of this modification is that it provides the possibility to attach the modified azo-uracil at any position of the designed PNA oligomer and therefore may lead to increase the stability of the formed hybrid compared to the traditional azobenzene due to retaining its hydrogen bonding ability.

In addition, we aimed to introduce the azo-based uracil into DNA and RNA chemistry by formation of the corresponding phosphoramidites. Formation of DNA and RNA molecular beacon containing the azo-modified uracil may show quenching ability. Incorporation of several azo-modified uracil units into DNA may result in a photoresponsive oligomer, that is, the ability to photoregulate duplex formation with a complementary nucleic acid sequence through irradiation with light of a specific wavelength.

Incorporation of the modified azo-based uracil PNA monomer into PNA oligomer is underway to assess its ability to photoregulate the duplex structure that obtained with the complementary nucleic acid. We will investigate the effect of extending the ring size of phenylazo moiety on the quenching ability of the modified uracil as shown in (Fig.6-2).

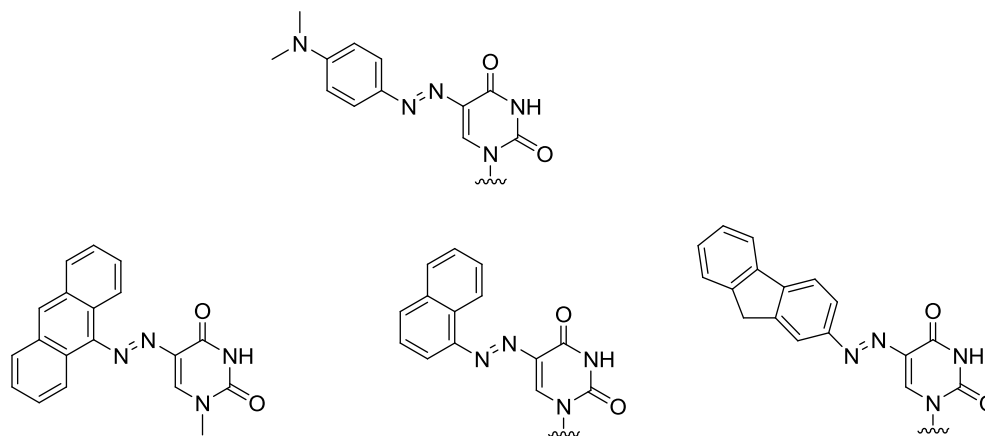
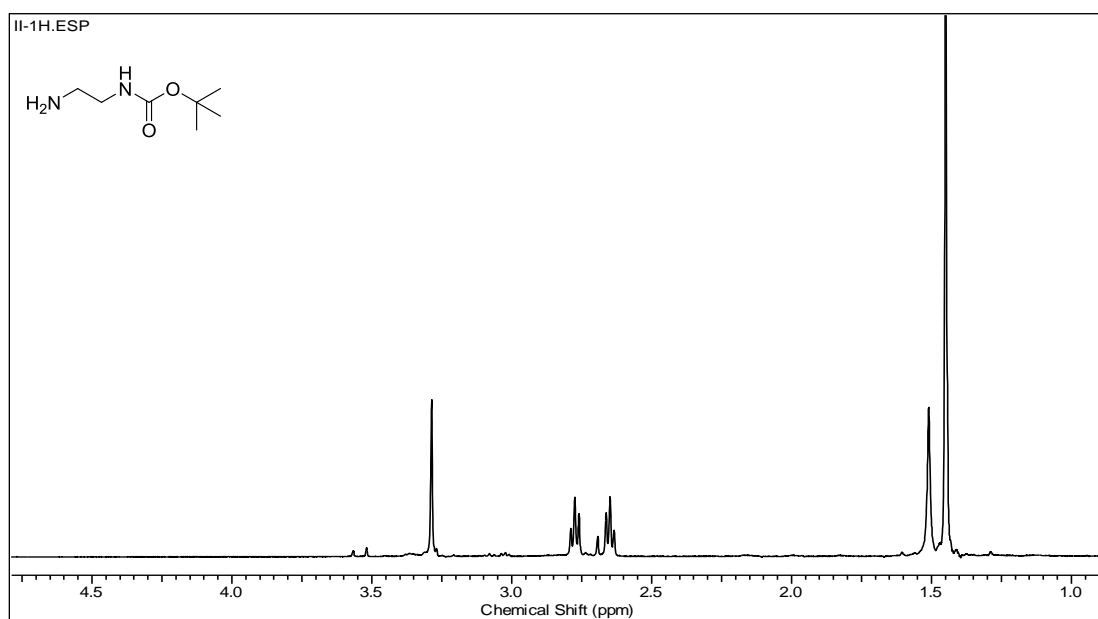


Figure 6-2: Structures of azo-based uracil derivatives.

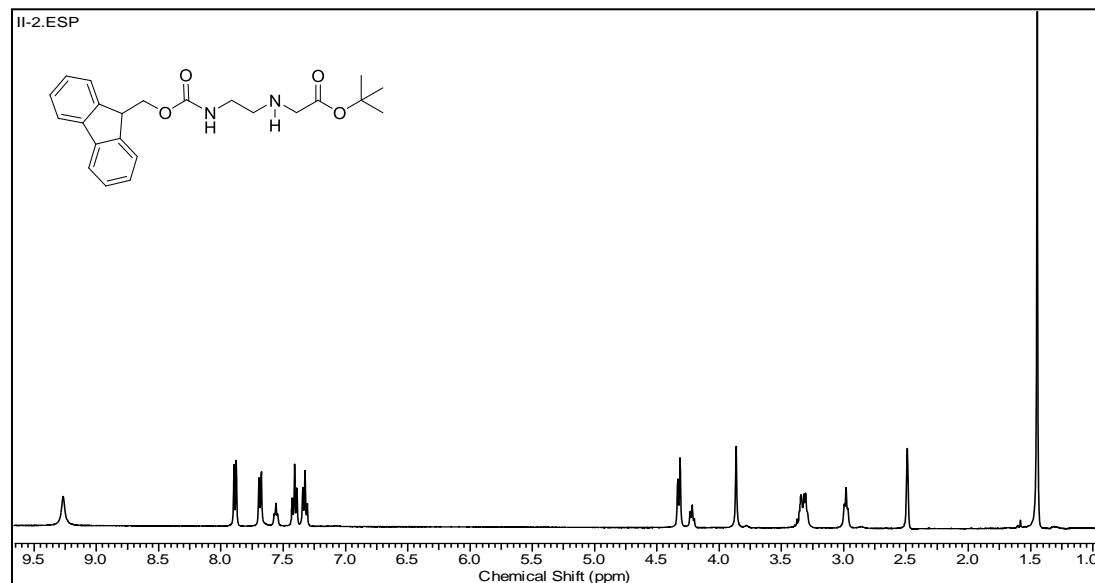
Appendices

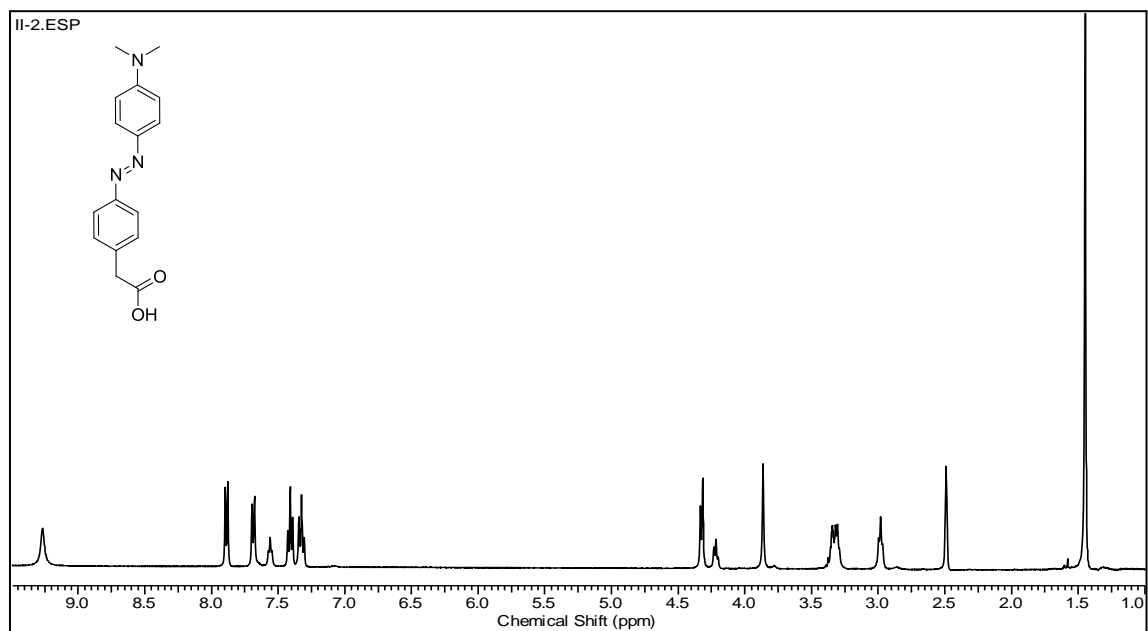
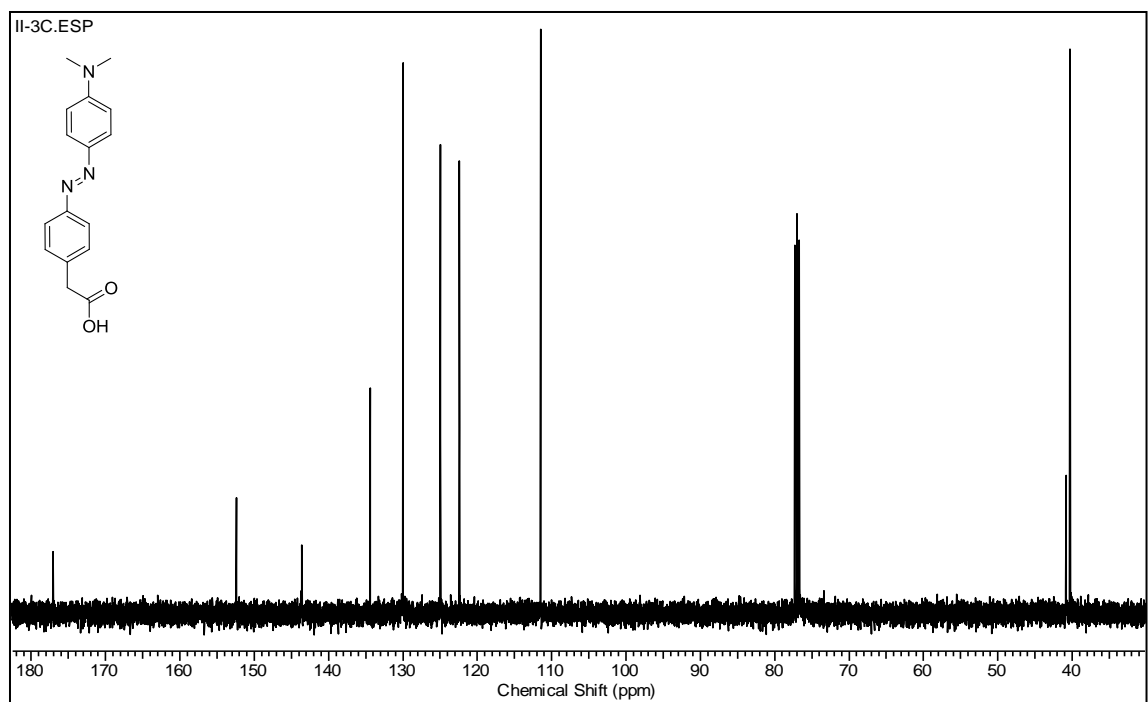
Selected NMR and MS spectra

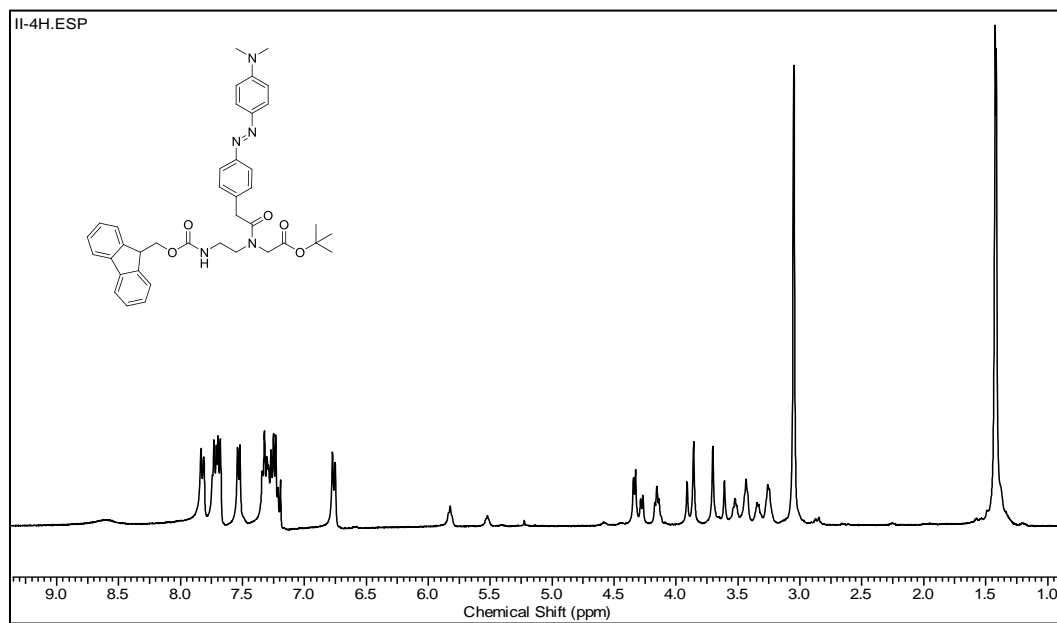
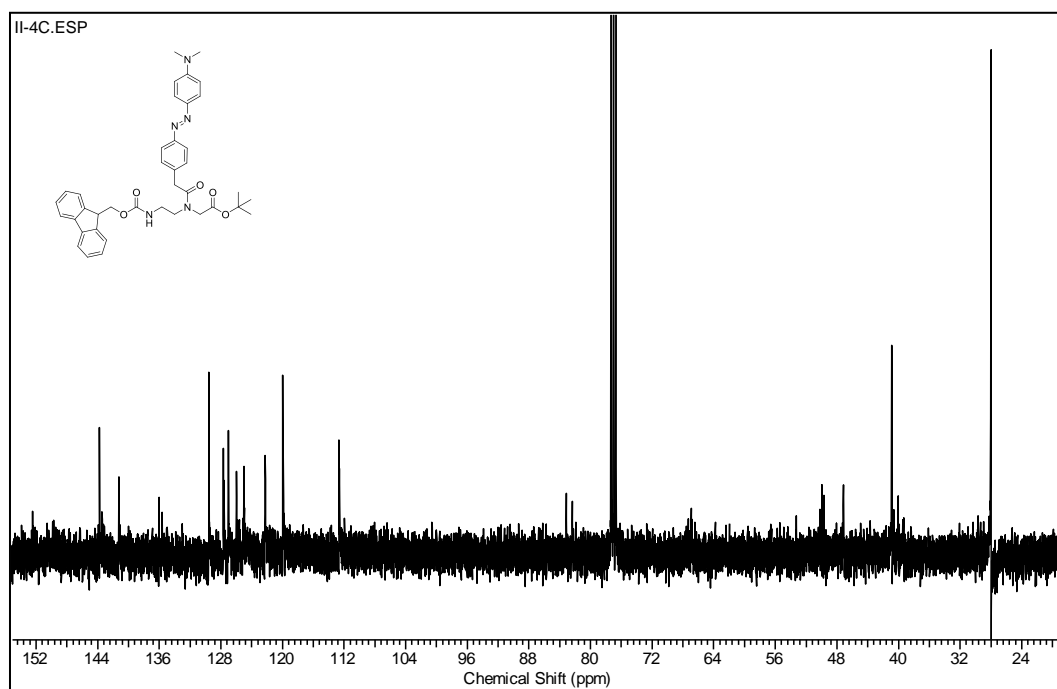
¹H NMR (400 MHz, CDCl₃) of II-1.

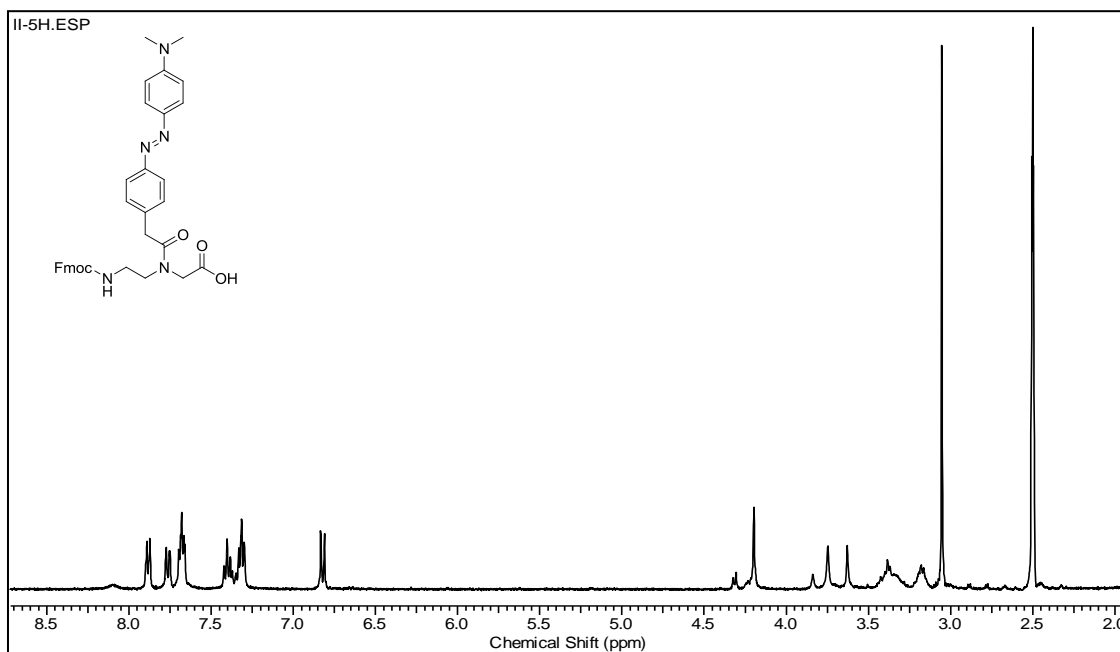
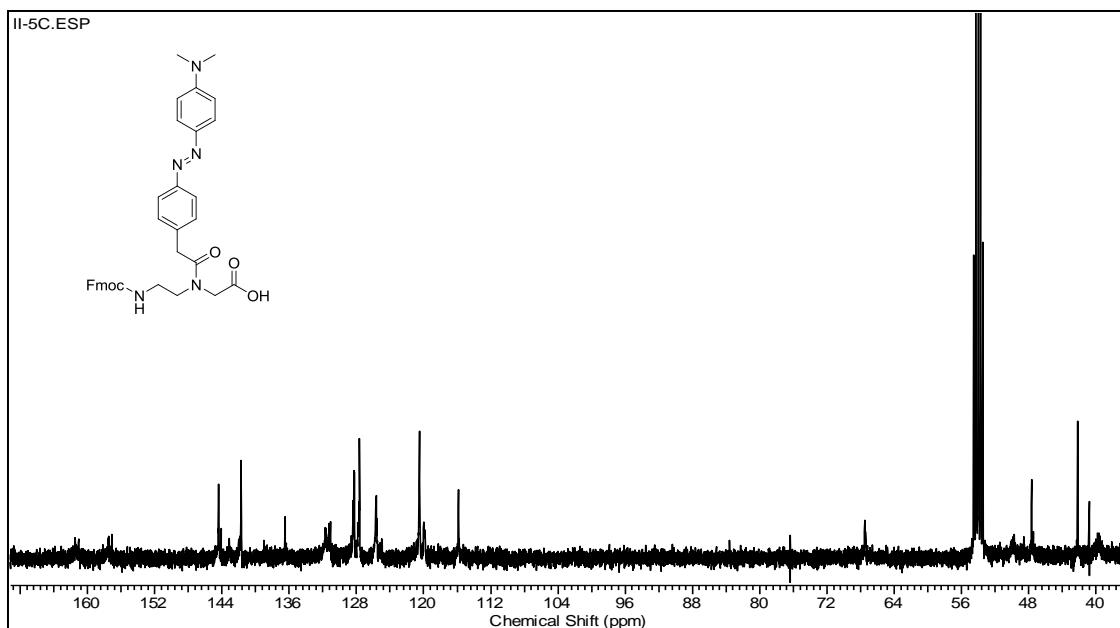


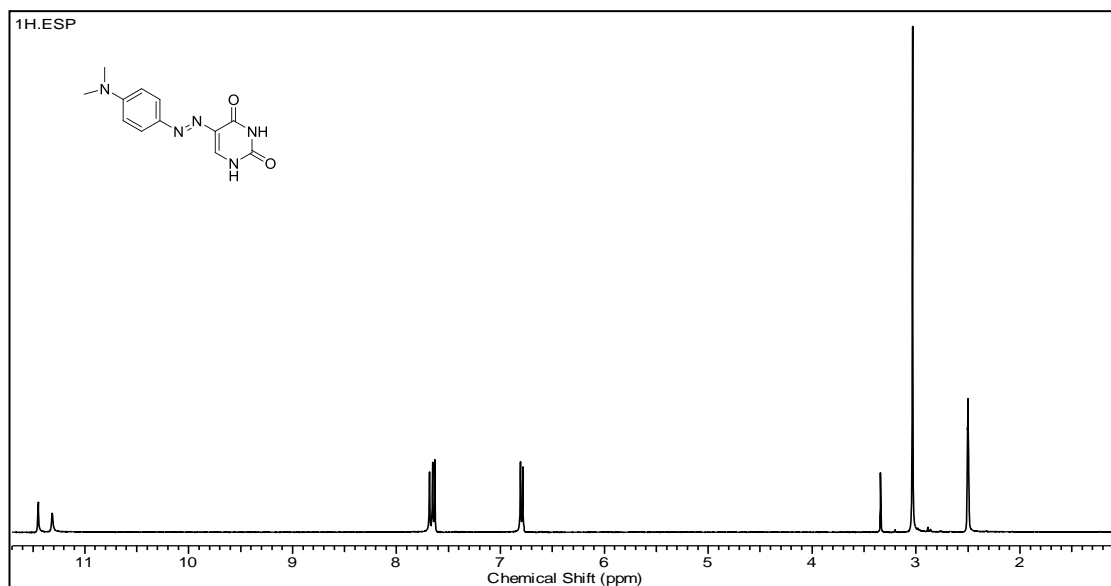
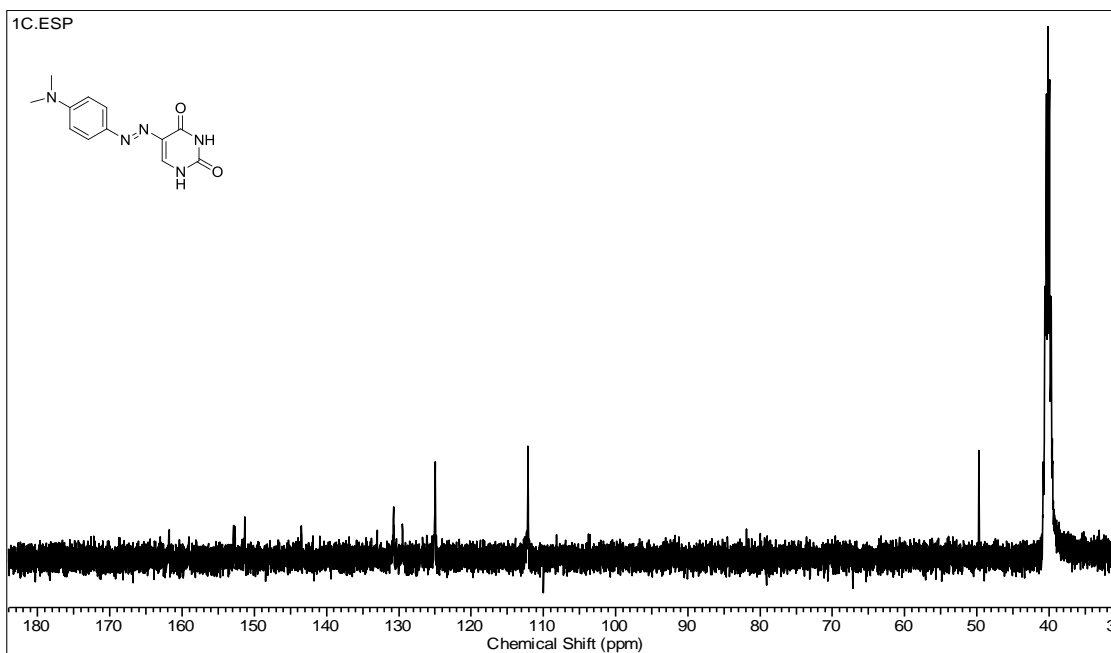
¹H NMR (400 MHz, DMSO-*d*₆) II-2.

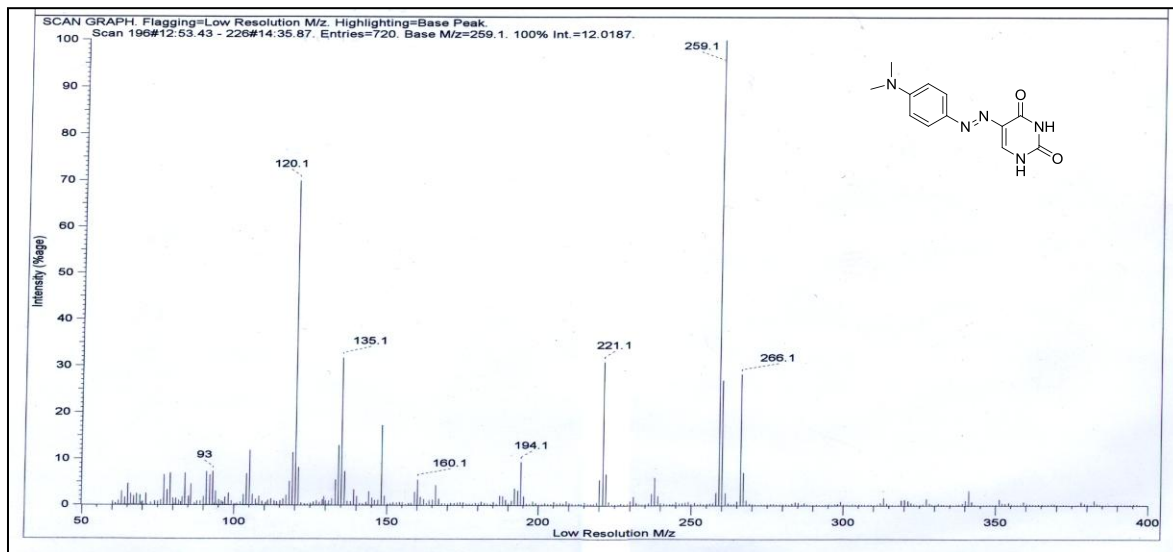
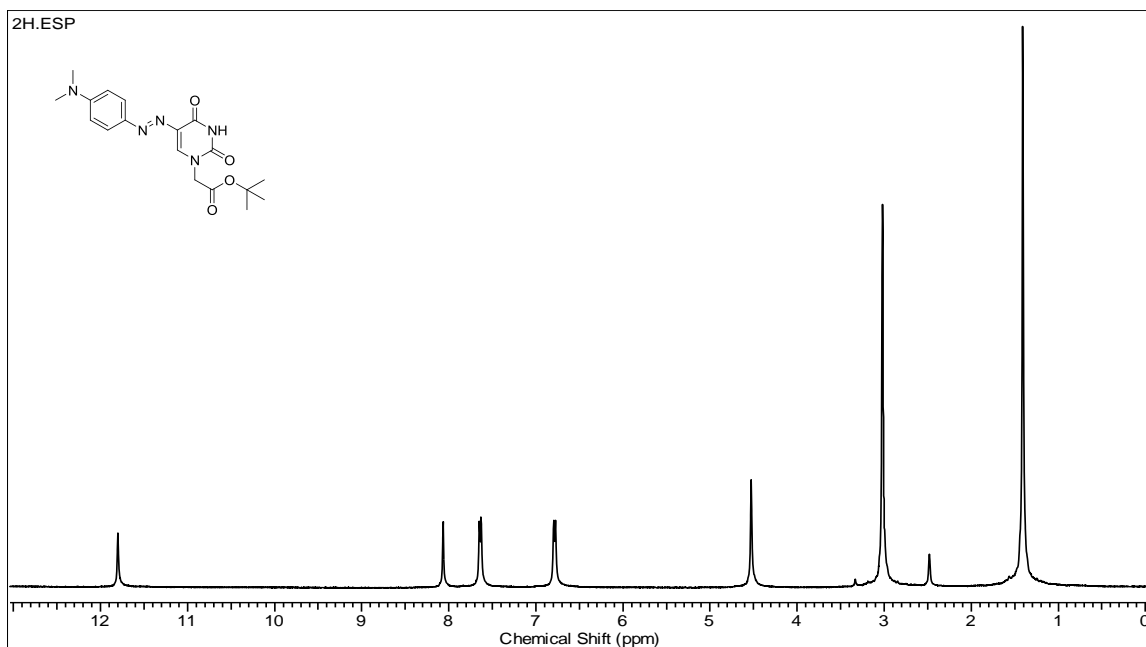


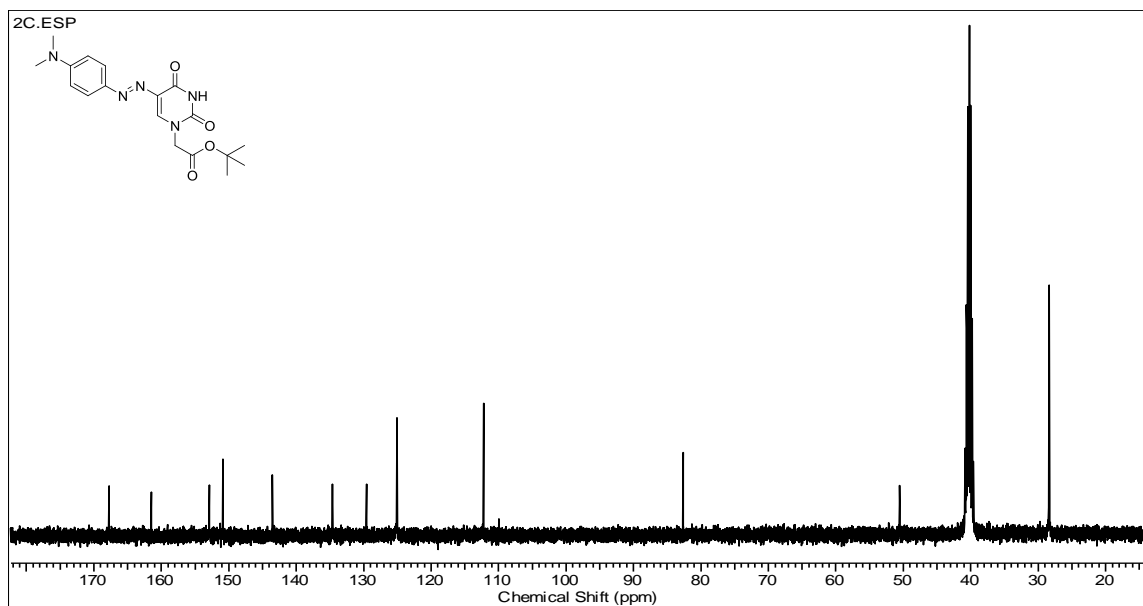
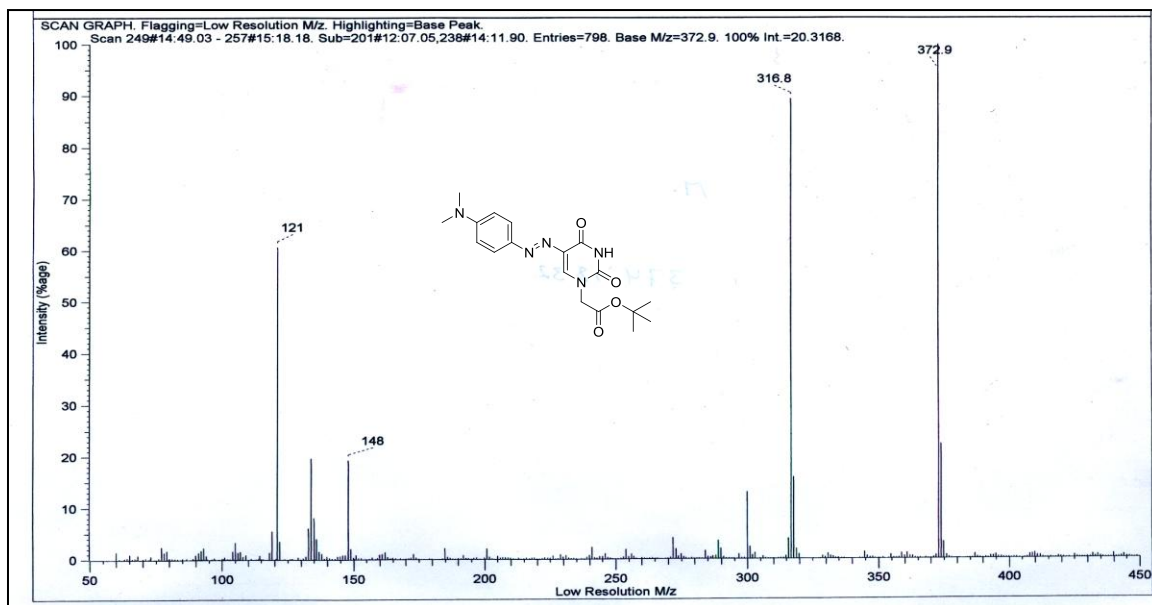
^1H NMR (400 MHz, $\text{DMSO-}d_6$) of II-3. **^{13}C NMR (100 MHz, CDCl_3) of II-3.**

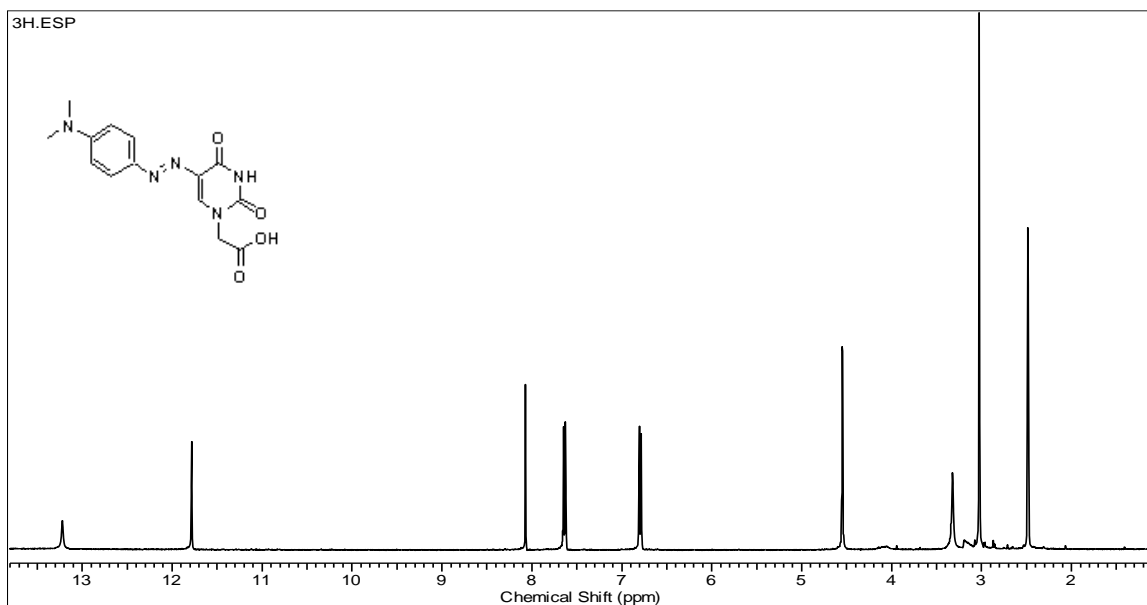
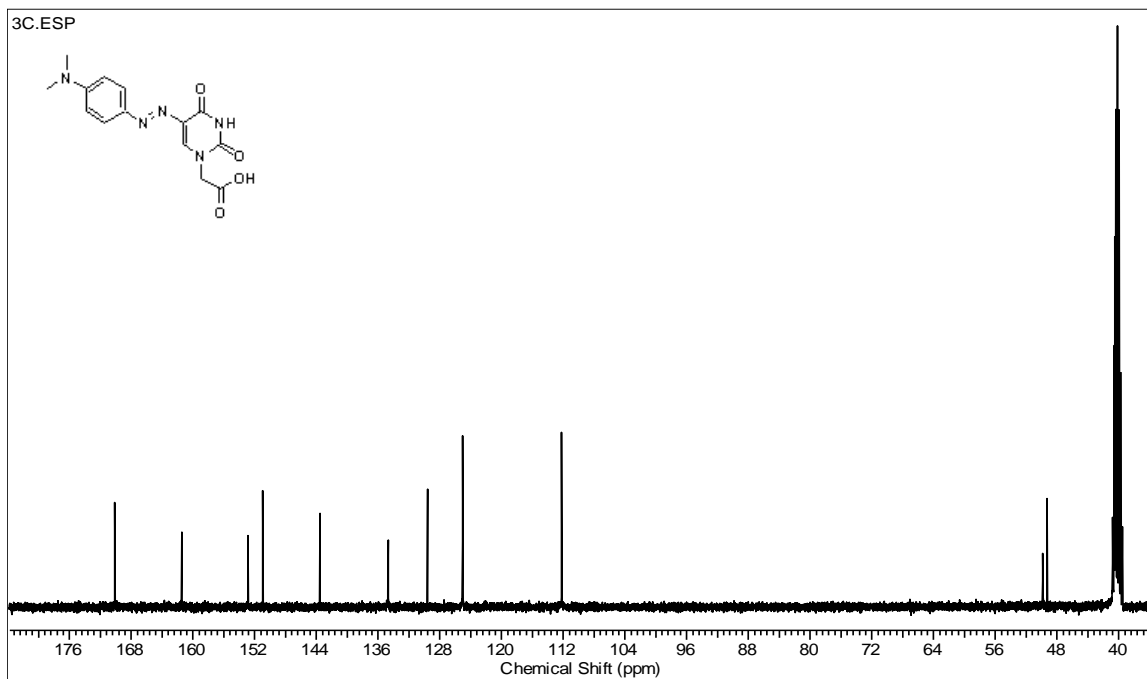
^1H NMR (400 MHz, CDCl_3) of II-4. **^{13}C NMR (100 MHz, CDCl_3) of II-4.**

^1H NMR (400 MHz, CDCl_3) of II-5. **^{13}C NMR (100 MHz, CDCl_3) of II-5.**

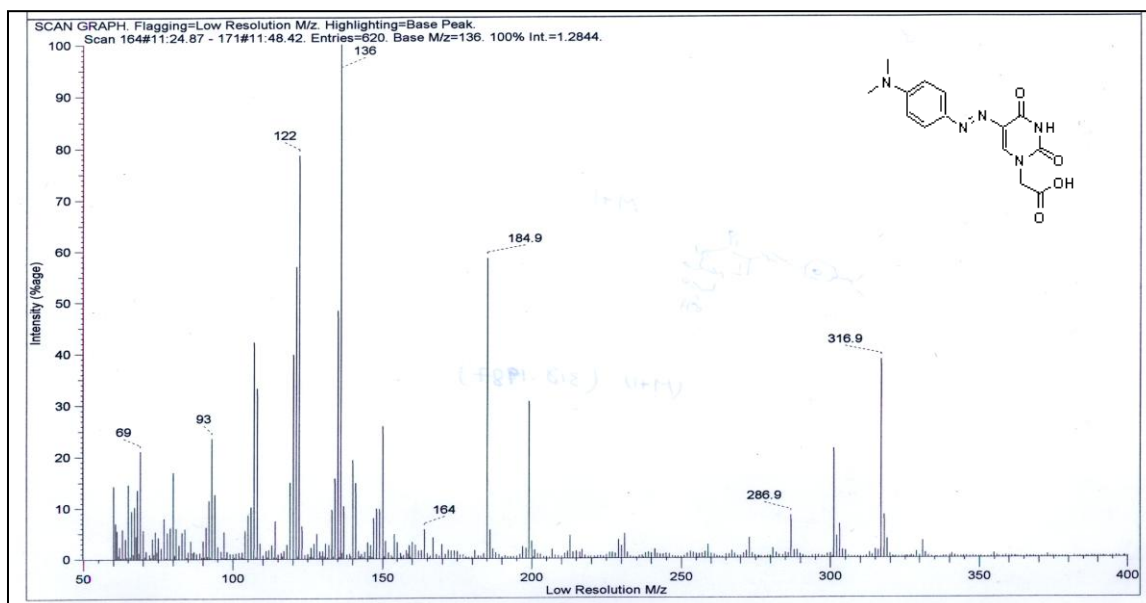
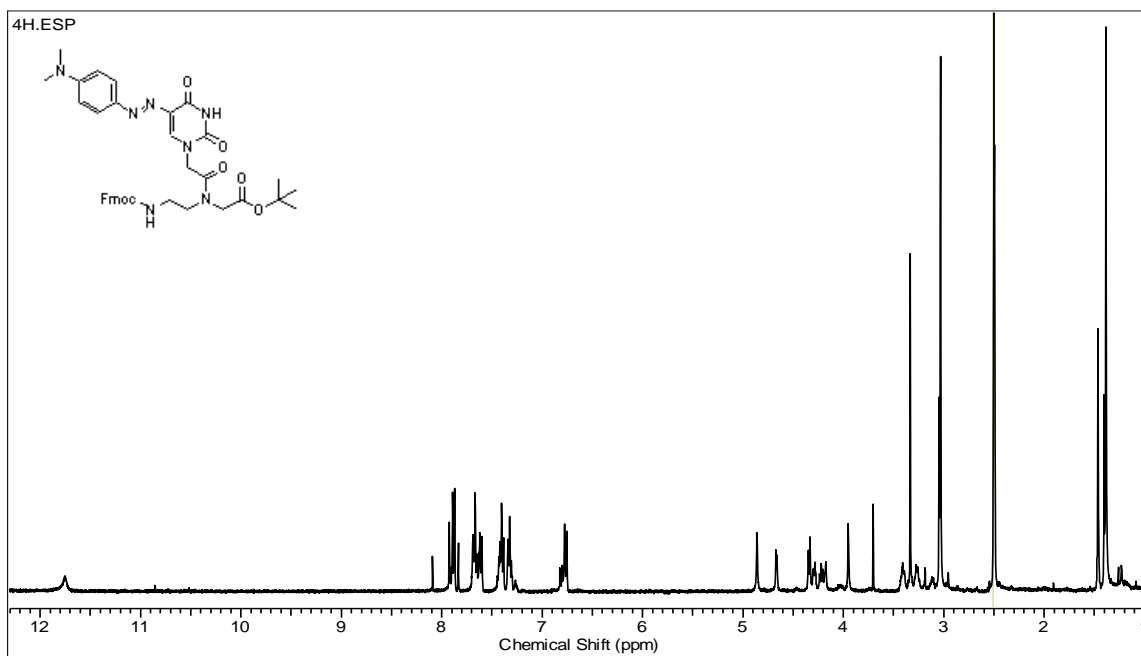
^1H NMR (400 MHz, DMSO- d_6) of III-1. **^{13}C NMR (100 Mz, DMSO- d_6) of III-1.**

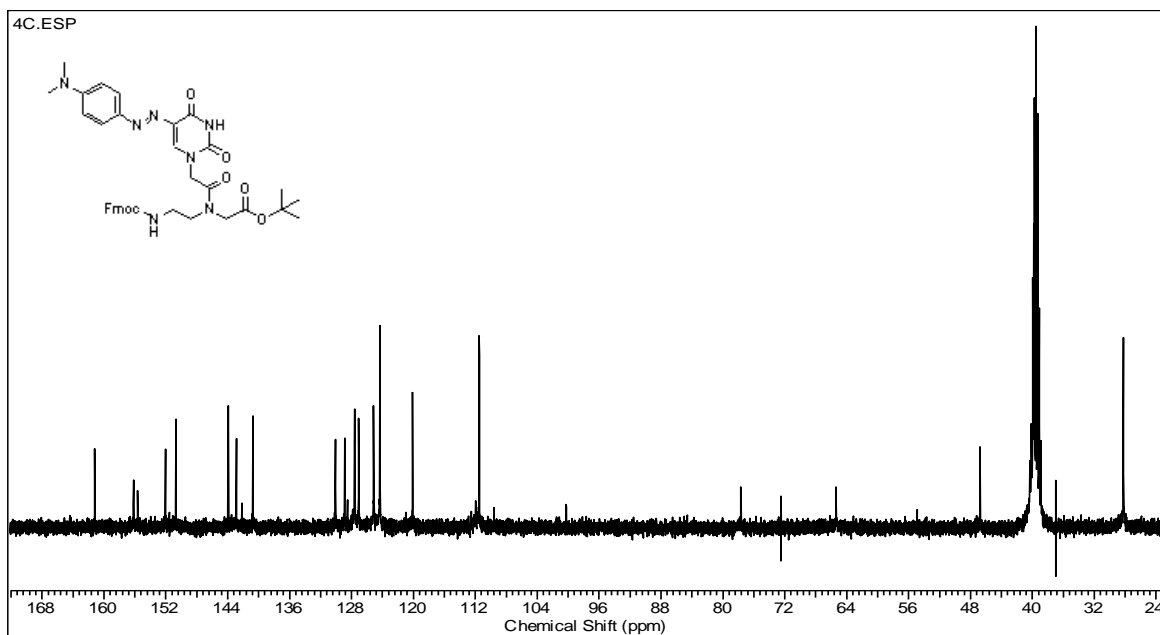
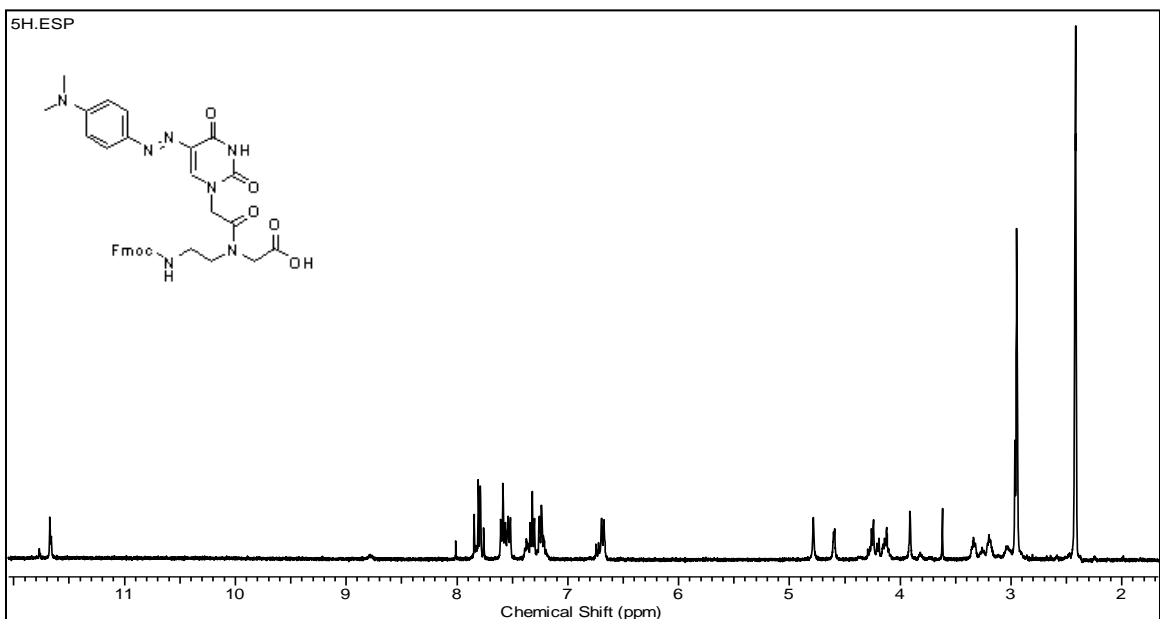
Ms of III-1.**¹H NMR (400 MHz, DMSO-d₆) of III-2.**

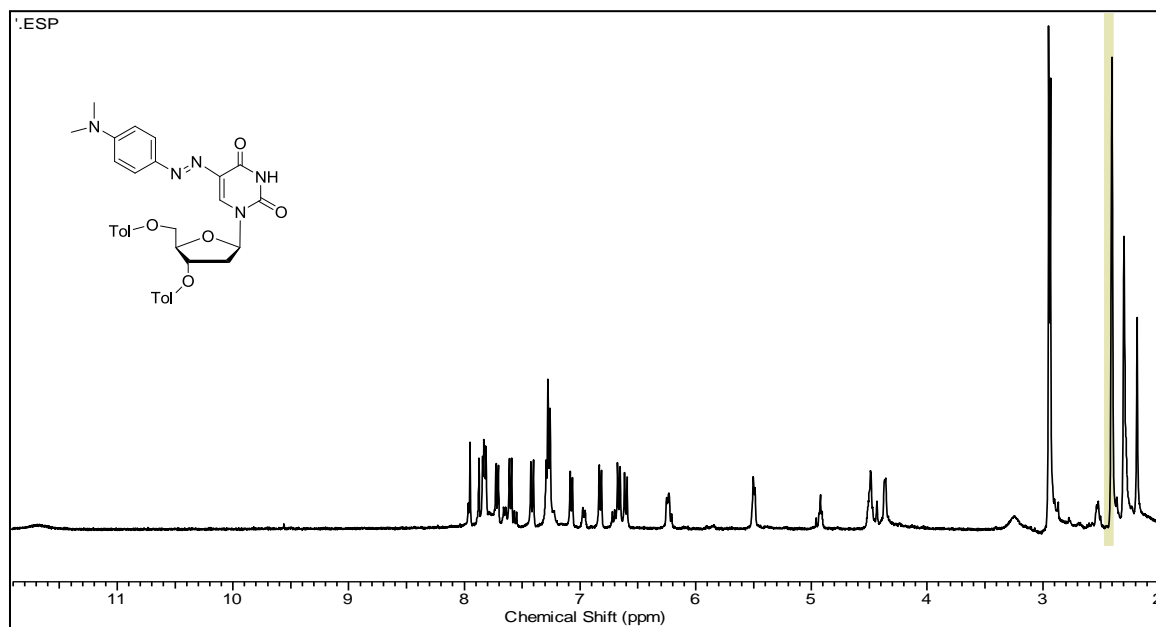
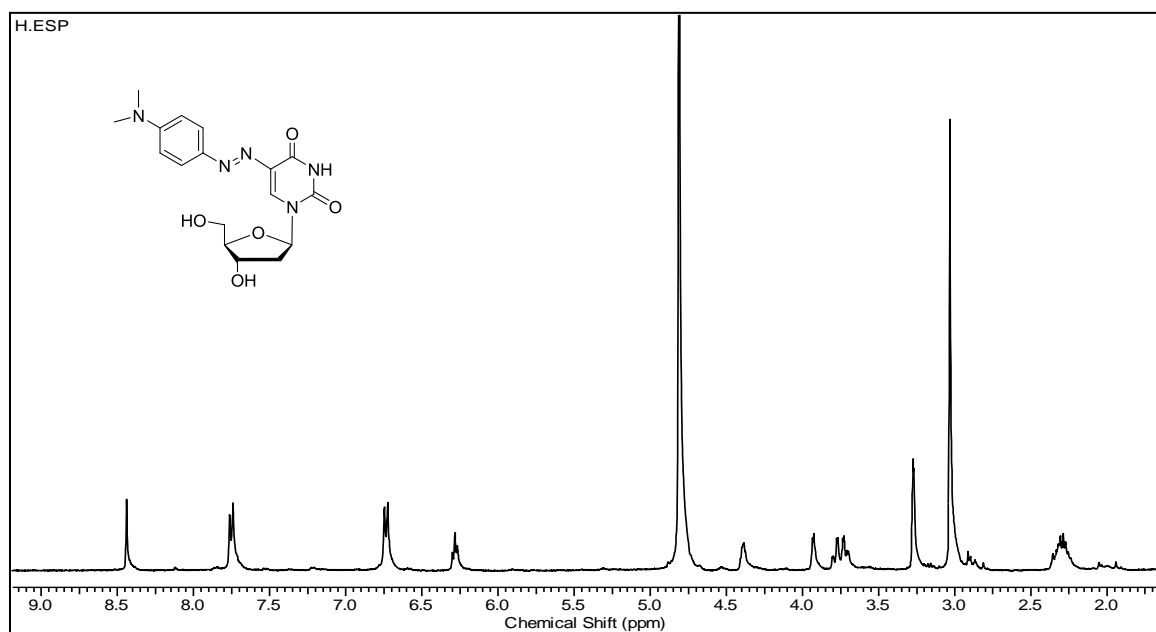
^{13}C NMR (100 MHz, DMSO- d_6) of III-2.**Ms of III-2.**

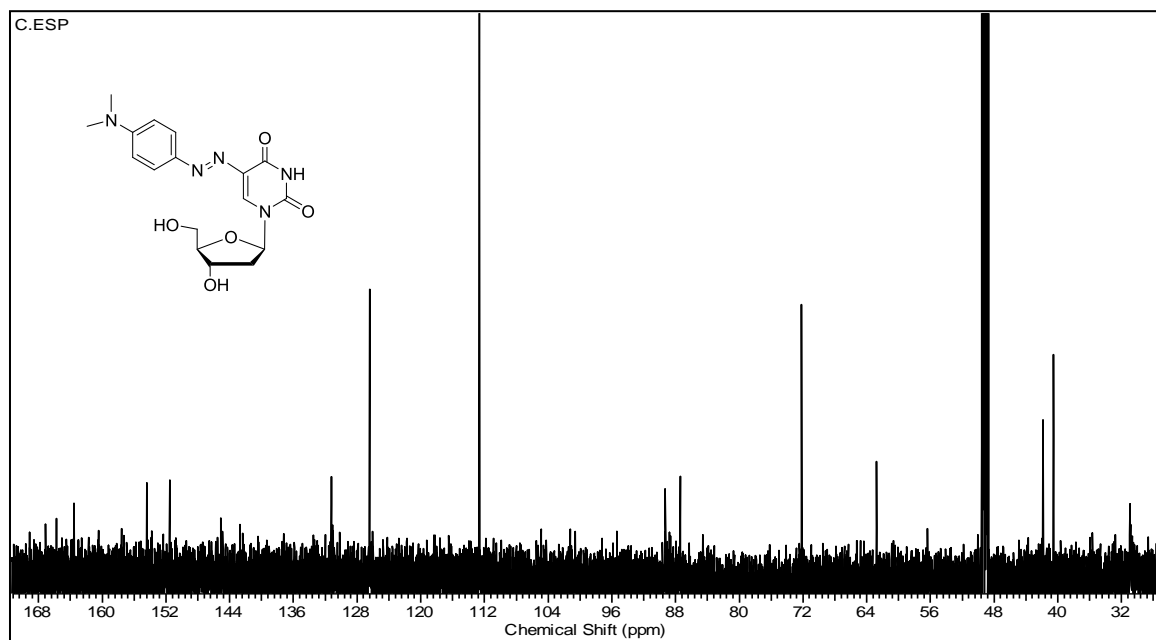
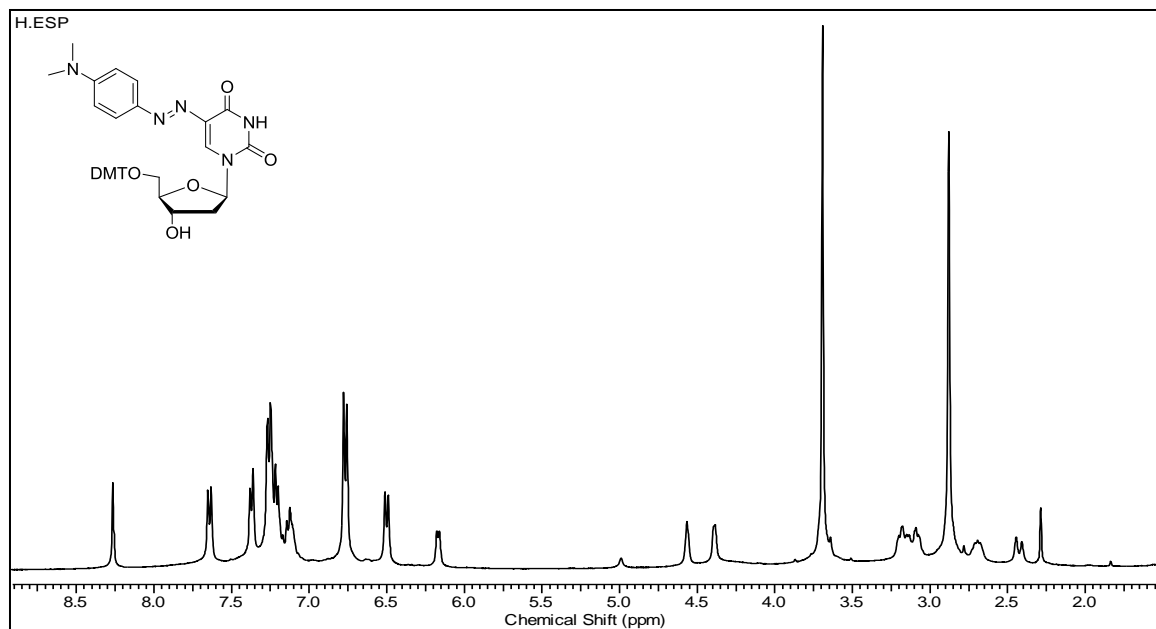
^1H NMR (400 MHz, $\text{DMSO-}d_6$) of III-3. **^{13}C NMR (100 MHz, $\text{DMSO-}d_6$) of III-3.**

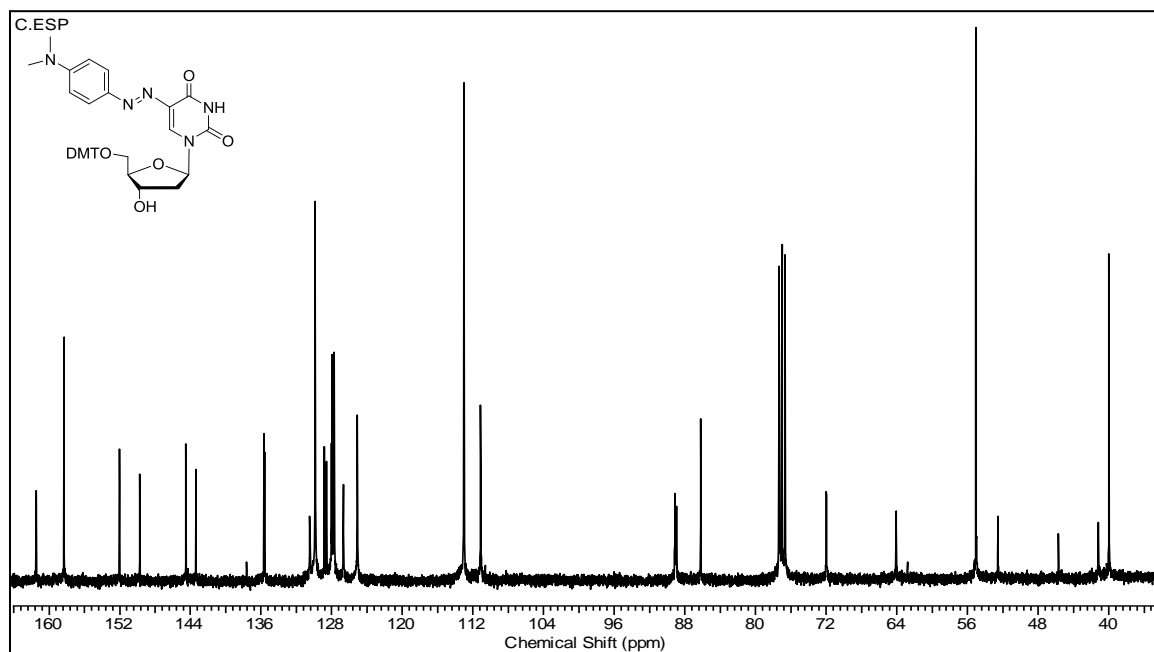
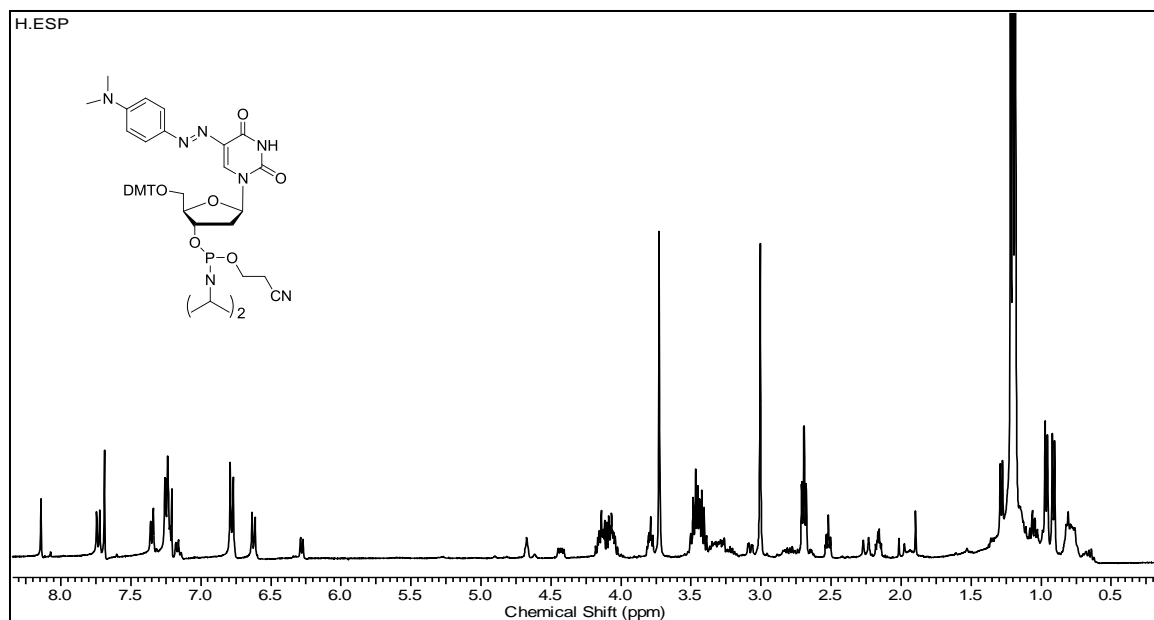
MS of III-3.

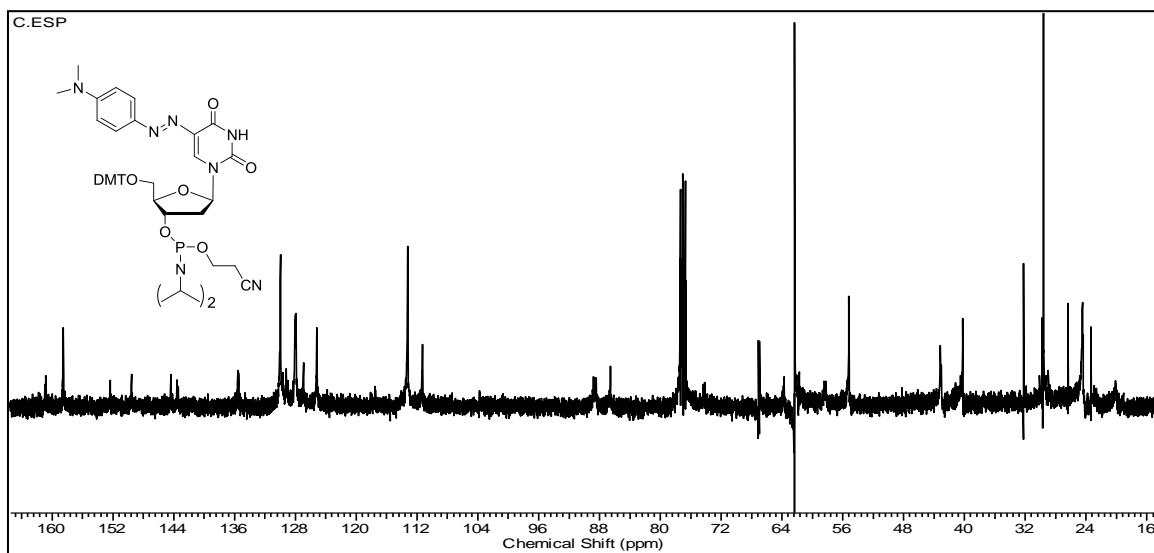
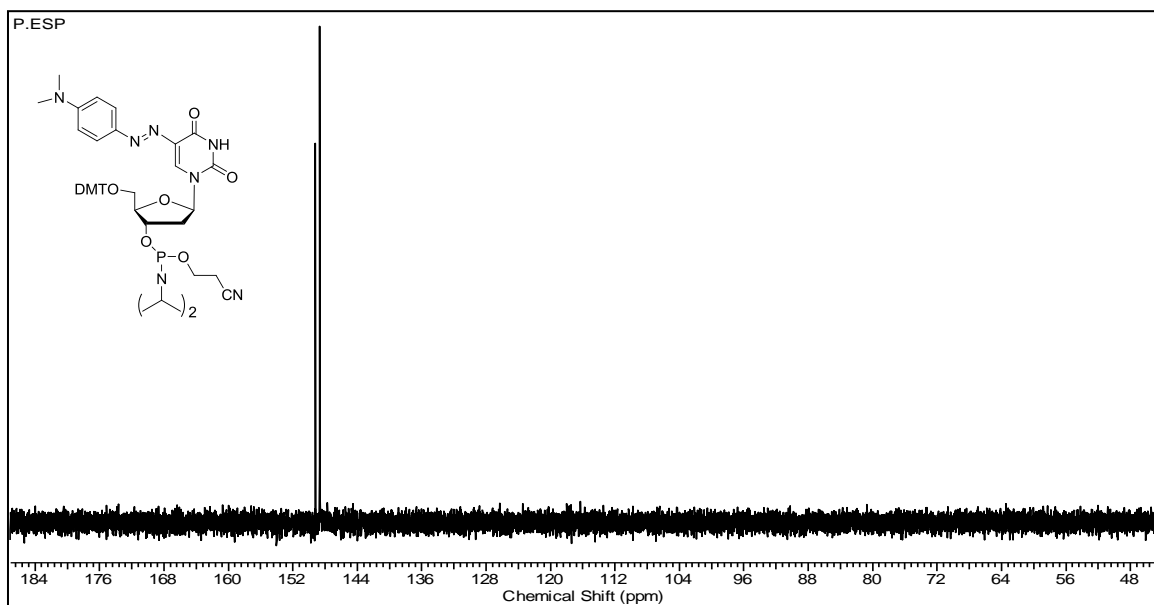
 ^1H NMR (400 MHz, DMSO- d_6) of III-4.

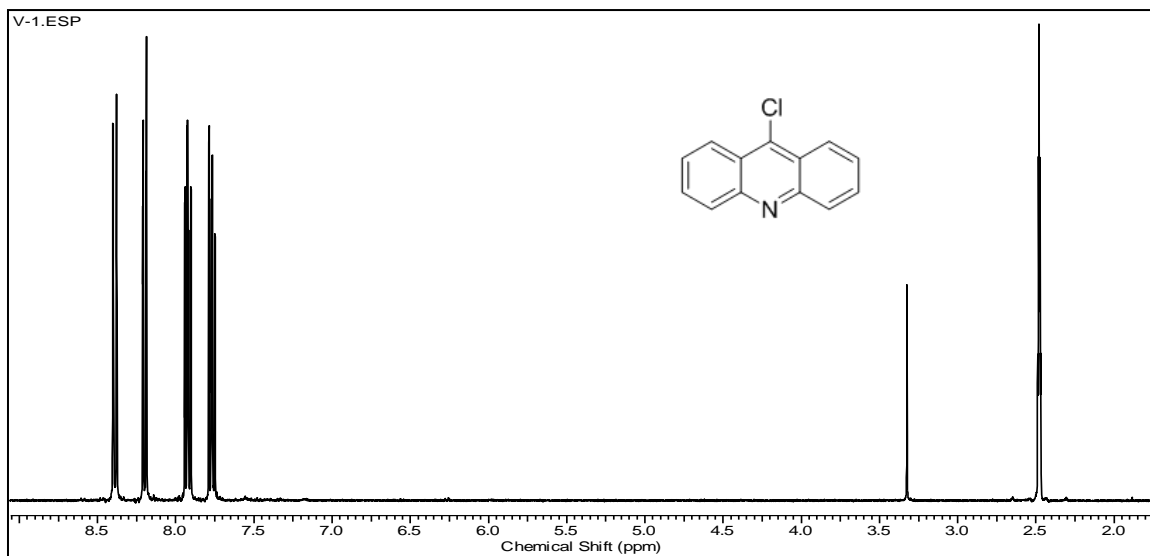
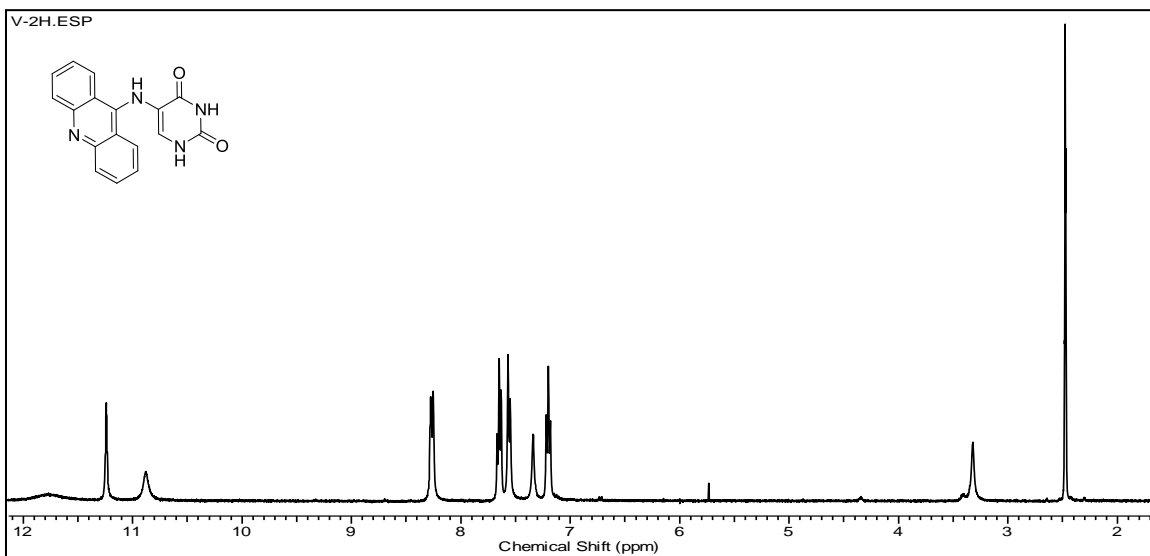
^{13}C NMR (100 MHz, $\text{DMSO-}d_6$) of III-4. **^1H NMR (400 MHz, $\text{DMSO-}d_6$) of III-5.**

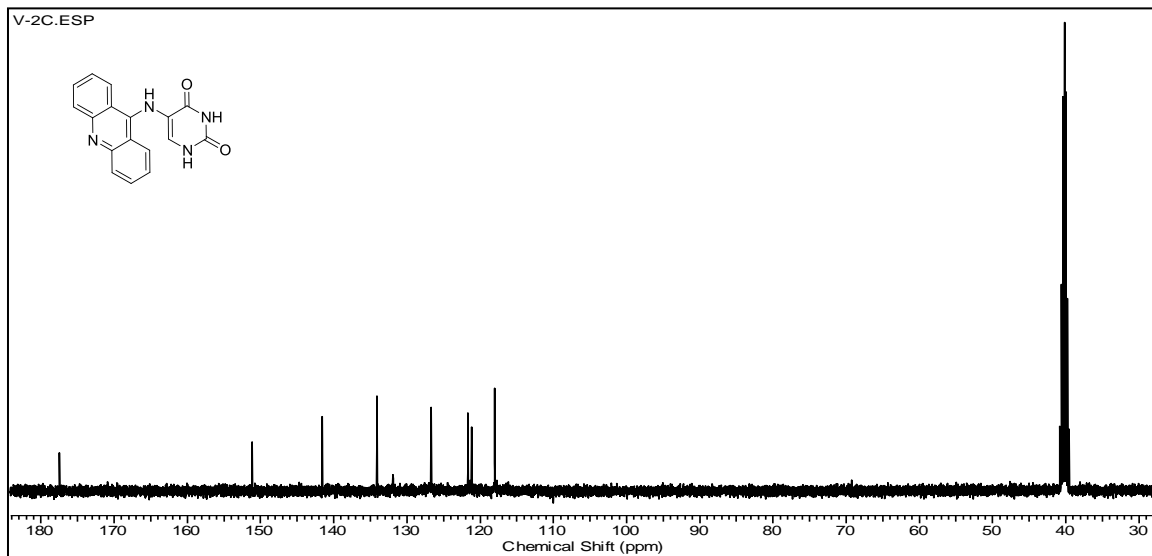
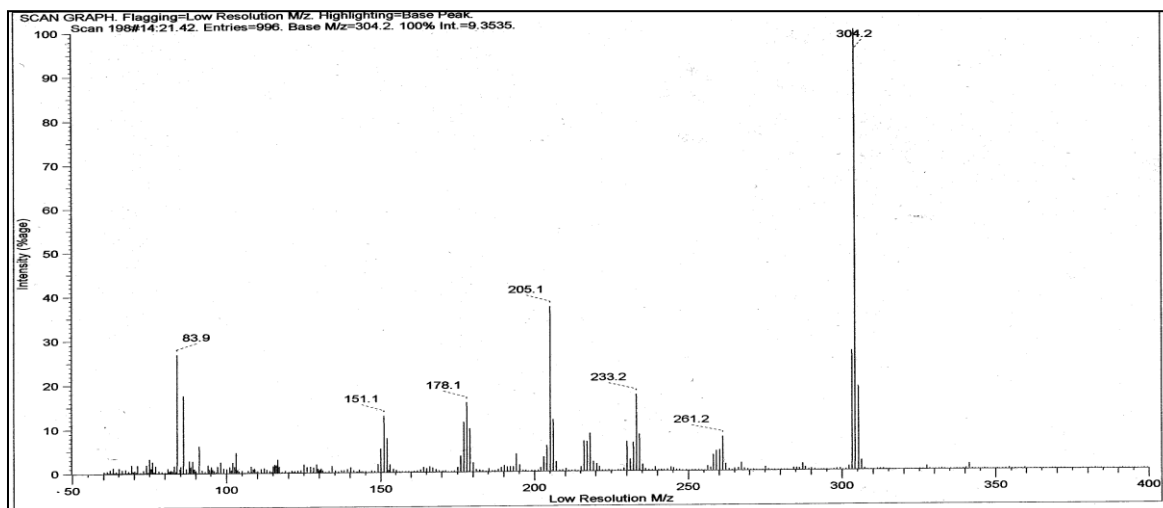
^1H NMR (400 MHz, $\text{DMSO-}d_6$) of IV-2. **^1H NMR (400 MHz, CH_3OD) of IV-2.**

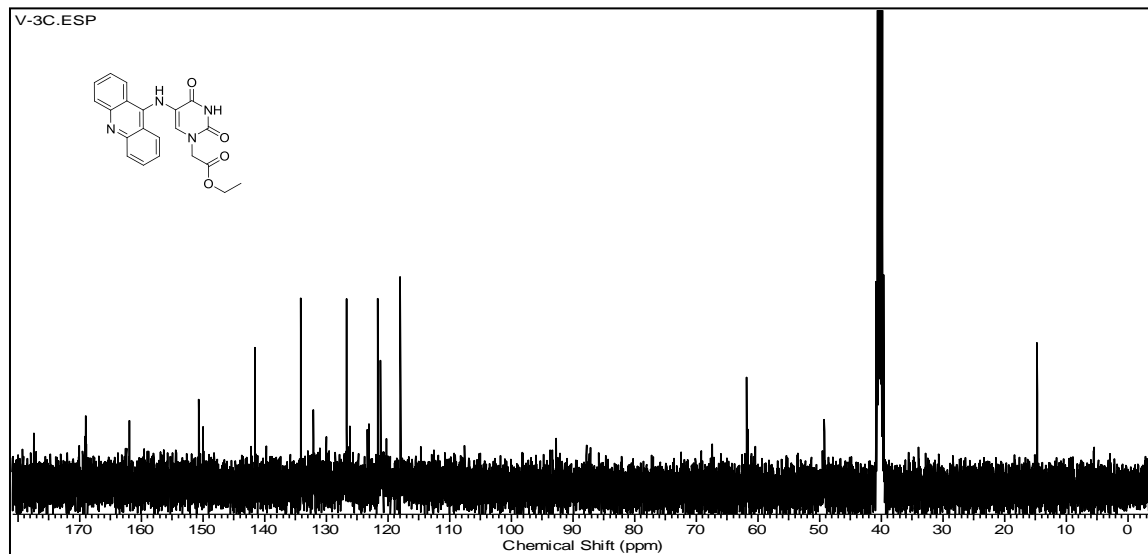
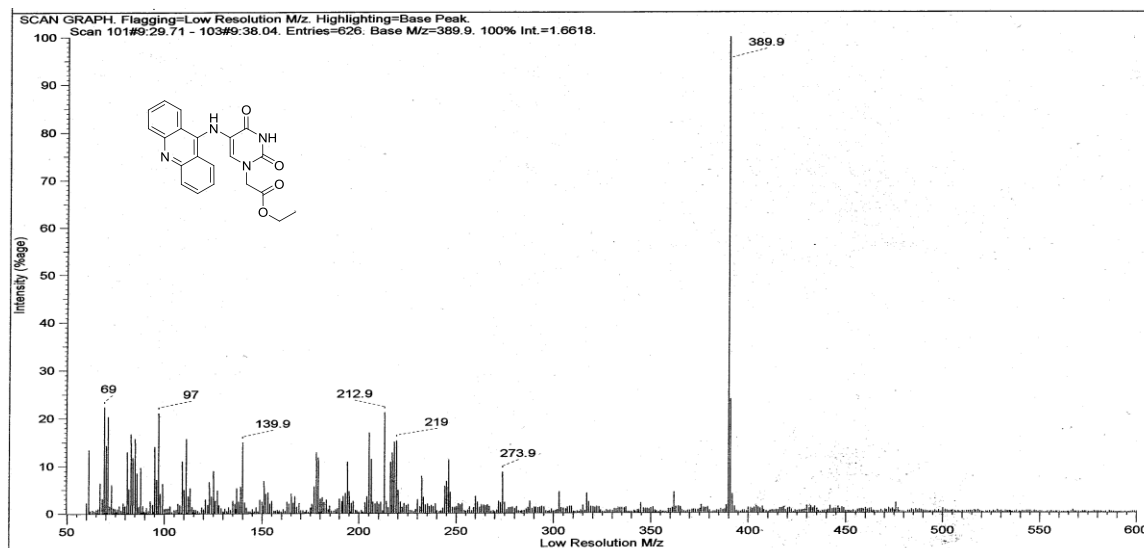
^{13}C NMR (100 MHz, CH_3OD) of IV-3. **^1H NMR (400 MHz, CDCl_3) of IV-3**

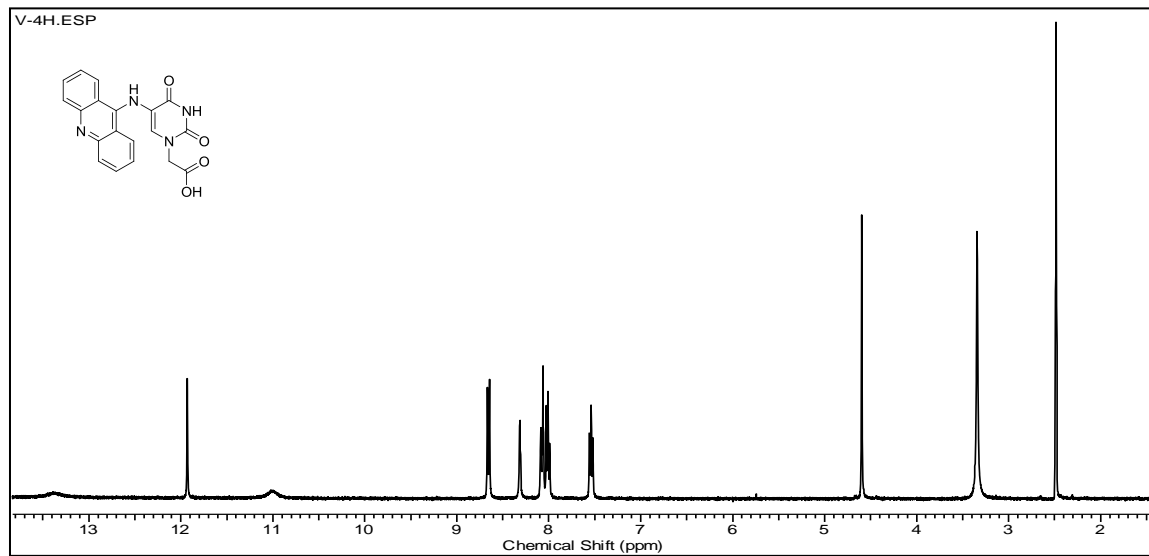
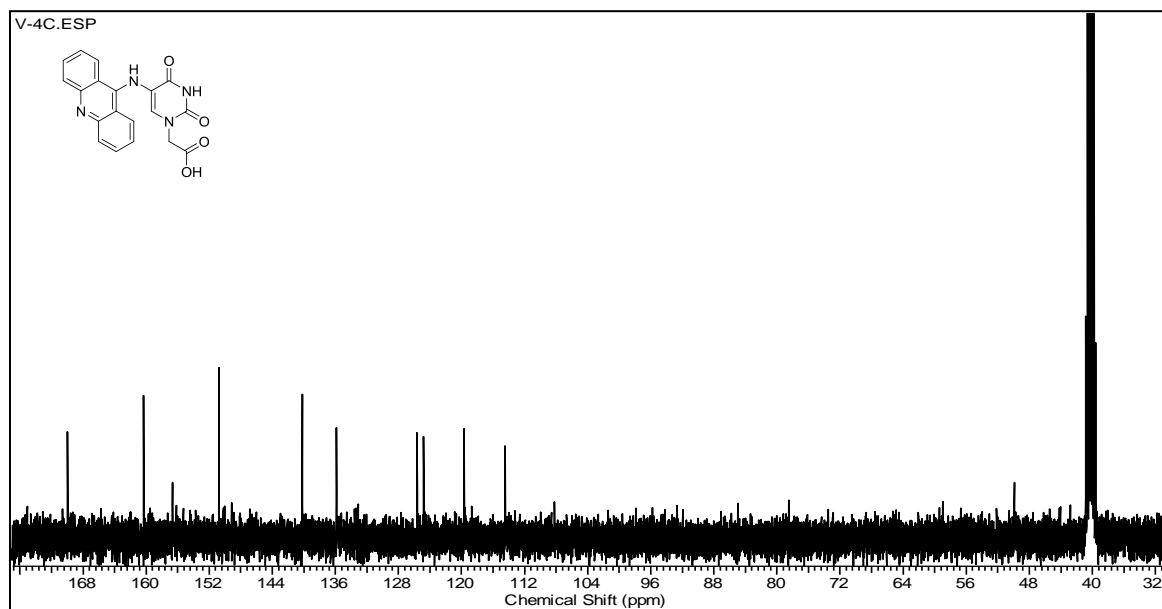
^{13}C NMR (100 MHz, CDCl_3) IV-3 **^1H NMR (400 MHz, CDCl_3) of IV-4.**

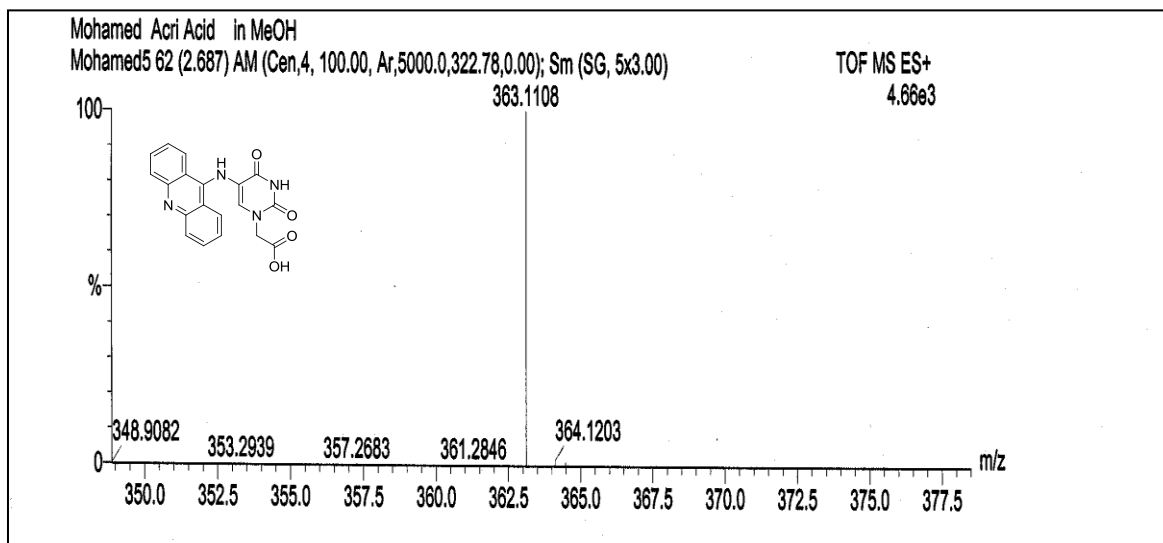
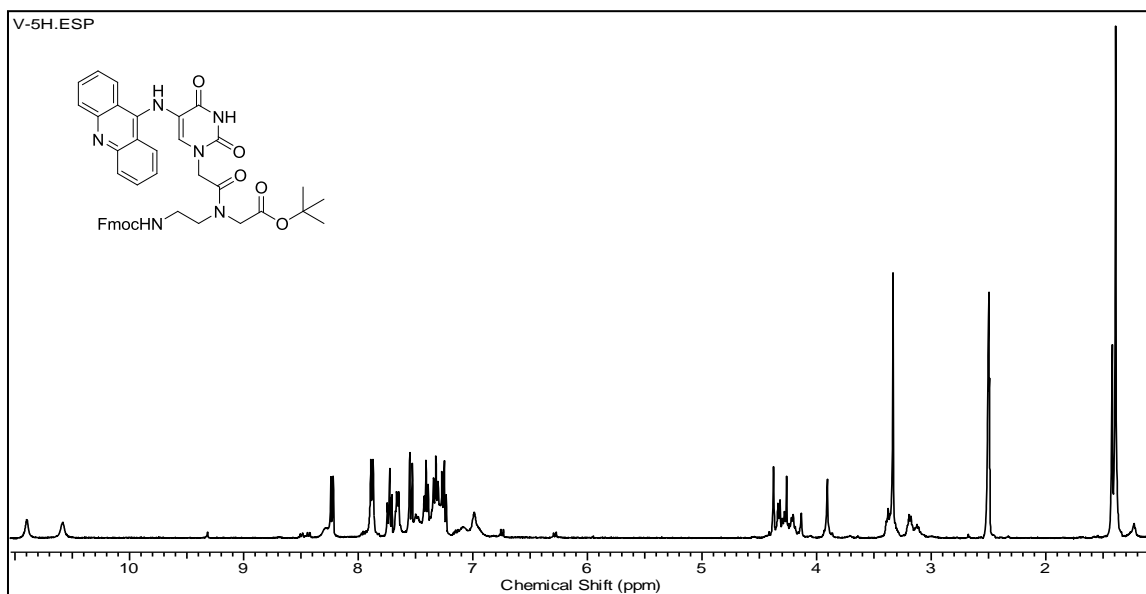
^{13}C NMR (100 MHz, CDCl_3) of of IV-4. **^{31}P NMR of of IV-4.**

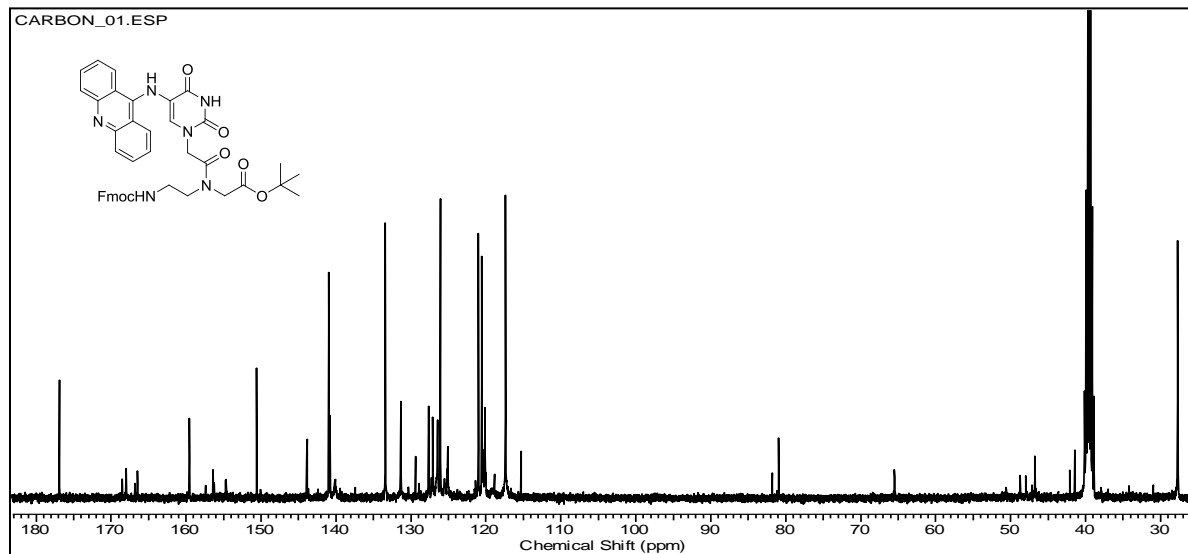
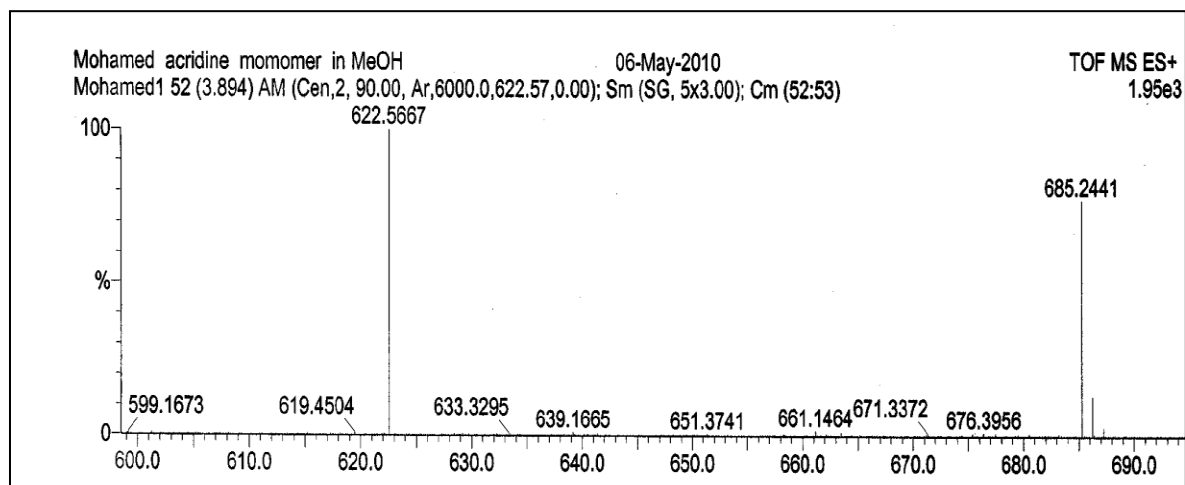
^1H NMR (400 MHz, $\text{DMSO-}d_6$) of V-1. **^1H NMR (400 MHz, $\text{DMSO-}d_6$) of V-2.**

^{13}C NMR (100 MHz, DMSO- d_6) of V-2.**MS of V-2.**

^{13}C NMR (100 MHz, DMSO- d_6) of V-3.**MS OF V-3.**

^1H NMR (400 MHz, $\text{DMSO-}d_6$) of V-4. **^{13}C NMR (100 MHz, $\text{DMSO-}d_6$) of V-4.**

MS OF V-4. **^1H NMR (400 MHz, DMSO- d_6) of V-5.**

^{13}C NMR (400 MHz, DMSO- d_6) of V-5.**MS of V-6.**

Curriculum Vitae

Name: Mohamed Moustafa

Post-secondary Education and Degrees: Suez Canal University -Faculty of Science, Ismailia-Egypt
1990-1994 B.Sc. Chemistry

Suez Canal University-Faculty of Science, Department of Chemistry
Ismailia-Egypt
1996-2003 M.Sc. Organic Chemistry

The University of Western Ontario
London, Ontario, Canada
2006-2011 Ph.D.

Suez Canal University-Faculty of Education
El-Arish Egypt
Lecturer start date 11/2011

Honours and Awards Oral Presentation Nucleic Acids Division, 92nd Canadian Chemistry Conference 2009.

Related Work Experience

- Teaching assistant (TA) September 2007 to present :
Department of chemistry, The University of Western Ontario, as lab TA for organic, general and medicinal chemistry courses (2213, 1050, 1024, 2223, and 3393)
- Lecturer assistant from 2003-2006:
Teaching organic lab courses for the 4th year students in chemistry department, faculty of Education- El-Arish branch, Suez Canal University, Egypt.
- Demonstrator from 1997-2003:
Teaching organic and bioorganic lab for the 2nd, 3rd and 4th year students in the department of chemistry, faculty of Education-El-Arish branch, Suez Canal University, Egypt.

Presentations

- Mohamed A. Moustafa and Robert H. E. Hudson “A Nucleobase Azo Compound as an Analog of DABCYL: A New Fluorescence Quencher.” Presented at the 92nd Canadian Chemistry Conference and Exhibition in Hamilton, Ontario, 2009. (Poster presentation).
- Mohamed A. Moustafa and Robert H. E. Hudson “Synthesis and Photo-Isomerization Studies on a Peptide Nucleic Acid Monomer Bearing The Dimethylaminophenylazobenzene Moiety.” Presented at the 93rd Canadian Chemistry Conference and Exhibition in Toronto, Ontario, 2010. (Poster presentation).
- Mohamed A. Moustafa and Robert H. E. Hudson “Synthesis and Photophysical Studies on an Azo-Modified Nucleobase and Nucleoside.” Presented at the International Roundtable on Nucleosides, Nucleotides and Nucleic acid (IRT-XIX) in Lyon, France, 2010. (Poster presentation).

Publications

- Mohamed A. Moustafa and Robert H. E. Hudson An Azo-Based PNA Monomer: Synthesis and Spectroscopic Studies, *Nucleosides, Nucleotides and Nucleic Acids*, *Accepted*.

Published Conference Proceedings

- Mohamed A. Moustafa and Robert H. E. Hudson “Synthesis and Photophysical Studies on an Azo-Modified Nucleobase and Nucleoside.” *Nucleic acids symposium series* 2010.

Volunteer Activity

- Served as Social officer of Egyptian Student Association in North America (*ESANA*) in the University of Western Ontario chapter for the academic year 2009
- Served as Social Officer of the Global Egyptian Student Association in North America (*ESANA*) for the academic year 2010.
- Served as Treasurer Officer of the Global Egyptian Student Association in North America (*ESANA*) for the academic year 2010.